Current Trends in Biotechnology and Pharmacy

KNOWLEDGE IS POWER

ASSOCIATION OF BIOTECHNOLOGY AND PHARMACY

www.abap.co.in

Current Trends in Biotechnology and Pharmacy
ISSN 0973-8916 (Print), 2230-7303 (Online)

Editors

Prof.K.R.S. Sambasiva Rao, India
krssrao@abap.co.in

Prof.Karnam S. Murthy, USA
skarnam@vcu.edu

Editorial Board

Assistant Editors

www.abap.co.in

KNOWLEDGE IS POWER

Association of Biotechnology and Pharmacy
(Regn. No. 28 OF 2007)

The Association of Biotechnology and Pharmacy (ABAP) was established for promoting the science of Biotechnology and Pharmacy. The objective of the Association is to advance and disseminate the knowledge and information in the areas of Biotechnology and Pharmacy by organising annual scientific meetings, seminars and symposia.

Members

The persons involved in research, teaching and work can become members of Association by paying membership fees to Association.

The members of the Association are allowed to write the title MABAP (Member of the Association of Biotechnology and Pharmacy) with their names.

Fellows

Every year, the Association will award Fellowships to the limited number of members of the   Association with a distinguished academic and scientific career to be as Fellows of the Association during annual convention. The fellows can write the title FABAP (Fellow of the Association of Biotechnology and Pharmacy) with their names.

Membership details

(Membership and Journal)		India	SAARC	Others
Individuals	– 1 year `	Rs. 600	Rs. 1000	$100
LifeMember		Rs. 4000	Rs. 6000	$500
Institutions	– 1 year	Rs. 1500	Rs. 2000	$200
(Journal only)	Life member	Rs.10000	Rs.12000	$1200

Individuals can pay in two instalments, however the membership certificate will be issued on payment of full amount. All the members and Fellows will receive a copy of the journal free.

Association of Biotechnology and Pharmacy
(Regn. No. 28 OF 2007)
#5-69-64; 6/19, Brodipet
Guntur – 522 002, Andhra Pradesh, India

Current Trends in Biotechnology and Pharmacy
ISSN 0973-8916

Volume 19 (2)	CONTENTS	April 2025

Information to Authors

The Current Trends in Biotechnology and Pharmacy is an official international journal of Association of Biotechnology and Pharmacy. It is a peer reviewed quarterly journal dedicated to publish high quality original research articles in biotechnology and pharmacy. The journal will accept contributions from all areas of biotechnology and pharmacy including plant, animal, industrial, microbial, medical, pharmaceutical and analytical biotechnologies, immunology, proteomics, genomics, metabolomics, bioinformatics and different areas in pharmacy such as, pharmaceutics, pharmacology, pharmaceutical chemistry, pharma analysis and pharmacognosy. In addition to the original research papers, review articles in the above mentioned fields will also be considered.

Call for papers

The Association is inviting original research or review papers and short comunications in any of the above mentioned research areas for publication in Current Trends in Biotechnology and Pharmacy. The manuscripts should be concise, typed in double space in a general format containing a title page with a short running title and the names and addresses of the authors for correspondence followed by Abstract (350 words), 3 – 5 key words, Introduction, Materials and Methods, Results and Discussion, Conclusion, References, followed by the tables, figures and graphs on separate sheets. For quoting references in the text one has to follow the numbering of references in parentheses and full references with appropriate numbers at the end of the text in the same order. References have to be cited in the format below.

Mahavadi, S., Rao, R.S.S.K. and Murthy, K.S. (2007). Cross-regulation of VAPC2 receptor internalization by m2 receptors via c-Src-mediated phosphorylation of GRK2. Regulatory Peptides, 139: 109-114.

Lehninger, A.L., Nelson, D.L. and Cox, M.M. (2004). Lehninger Principles of Biochemistry, (4th edition), W.H. Freeman & Co., New York, USA, pp. 73-111.

Authors have to submit the figures, graphs and tables of the related research paper/article in Adobe Photoshop of the latest version for good illumination and allignment.

Authors can submit their papers and articles either to the editor or any of the editorial board members for onward transmission to the editorial office. Members of the editorial board are authorized to accept papers and can recommend for publication after the peer reviewing process. The email address of editorial board members are available in website www. abap.in. For submission of the articles directly, the authors are advised to submit by email to krssrao@abap.co.in or krssrao@yahoo.com.

Authors are solely responsible for the data, presentation and conclusions made in their articles/research papers. It is the responsibility of the advertisers for the statements made in the advertisements. No part of the journal can be reproduced without the permission of the editorial office.

The Potential Impact of Probiotics Along with Prebiotic Against the Dermatic Pathogen *Staphylococcus aureus*: Isolation and Characterization

Nandini Sinhmar, Bindu Battan*, Surender Verma, Sulekha Chahal, Jitender Sharma

Department of Biotechnology, Kurukshetra University, Kurukshetra (136119), Haryana, India.
Department of Pharmaceuticals Science, Kurukshetra University, Kurukshetra (136119), Haryana, India.

*Corresponding Author: bbattan@kuk.ac.in

Abstract

In recent years, probiotics and prebiotics are now well known for their expanded clinical applications beyond the gut microbiome to the skin microbiome by managing several skin disorders from acne to skin cancer. *Lactobacilli* and *Bifidobacterium* were extracted from non-dairy origins such as honey, tomato, and banana. The obtained isolates, recognized as *Lactiplantibacillus pentosus*, *Lactiplantibacillus plantarum*, and *Bifidobacterium animalis*, underwent detailed analysis to assess their probiotic qualities. This assessment involved various morphological and biochemical tests, including the catalase test, pH tolerance, temperature resistance, salt sensitivity, antibiotic susceptibility, and antimicrobial activity. All three isolates showed increased growth under skin-like conditions including higher growth at pH 4 to 5, at wide range of temperature and at various salt concentrations. This research paper deals with the isolation of *Lactobacilli* and *Bifidobacterium* from non-dairy sources and further characterization to evaluate their antibiotic sensitivity against Ampicillin, Penicillin, Gentamycin, Ciprofloxacin, and Tetracycline and to study their antimicrobial effect against the main skin's opportunistic pathogen *Staphylococcus aureus,* that causes approx. 80% of skin diseases. Furthermore, research was undertaken to formulate optimal synbiotics. This involved assessing the preferential growth of isolated probiotics in the presence of prebiotics, specifically inulin, following an evaluation of the isolates' activity scores both with and without prebiotic supplementation.

Keywords: Probiotics, Prebiotics, Skin microbiome, Skin diseases.

Introduction

Nowadays, food is not only consumed for their taste and for nutrition, but also to improve overall health and well-being of recipients in health sector due to their therapeutic effects in preventing and treatment of many diseases (1,2). Lactic acid bacteria (LAB) constitute a diverse category of gram-positive rods or cocci, devoid of spores, with a heterogeneous nature. They thrive in various environments, including the gastrointestinal tracts of humans and animals, as well as in plants and non-living components of the environment. Notably, they are non-pathogenic and exhibit anaerobic or facultative aerobic characteristics, while being catalase negative (3,4). Because of the considerable role in animals and human diets as supplements, strains belonging to *Lactobacilli* are usually referred to as probiotics and are commercially available for human consumption

(5,6). In 2014, experts from ISAPP (International Scientific Association for Probiotics and Prebiotics) termed it as, "probiotics are referring to many types of microorganisms which demonstrate health benefits for the host, while remaining alive" [7].

Probiotics have garnered significant attention for their beneficial influence on human health, emerging healthy alternative therapeutics to mitigate drug resistance associated with the extensive use of antibiotics in combating infections (8,9). Present globally, these microorganisms have the capacity to enhance the native microbiota, bolstering and fortifying the immune system, while also impeding the proliferation of detrimental pathogens through the production of bacteriocins [10]. They can prevent and mend many health diseases including general digestion problems, *Helicobacter pylori* infection, Lyme diseases, Fever blisters, lowering liver lipids concentrations, atopic dermatitis or eczema, cardiovascular diseases, diabetes, allergic diseases, and even cancer (11,12,13).

Skin is the largest external organ in humans, and is remarkably inhospitable environment of rich and diverse communities of microorganisms, approximately one billion microbes per square centimetres including species of bacteria, fungi, mites, archaea that provides a primary protective barrier against infection causing microbes, also exerting several roles in addition to homeostasis and thermoregulation, immune responses, metabolic functions etc (14). The resident skin microbiome varies according to their respective location on the surface and are controlled by several extrinsic and intrinsic factors including age, temperature, moisture, gender, and environmental factors (15,16). However, cleansing practices and ethnicity may also be the secondary factors which determine cutaneous microbial composition as it was already revealed that increased exposure to skin's microbiota may lead to several conditions or diseases from acute to chronic (17,18). Any sudden disturbance in the maintained skin ecosystem changes microflora from beneficial

to pathogenic. The best example is *S. epidermidis* and *Staphylococcus aureus* as both are common and harmless members of the human skin ecosystem but when get disturbed can change phenotype and becomes pathogenic (19,20).

In accordance to Gibson and Roberfroid in 1995 and Roberfroid in 2007, Prebiotics one the other hand, are "selectively fermented ingredients belong to oligosaccharides, polysaccharides, and oligofructose that allows specific alterations, both in activity and composition of resident microflora of host that accord benefits on health and well-being" (21). The realm of prebiotics is multifaceted, comprising various oligosaccharides, polysaccharides, and inulin, specifically oligofructose, which can serve as a viable alternative or supplementary support to probiotics. In contrast to probiotics, which are live microorganisms, prebiotics function a kind of "fertilizers," fostering the selective growth and activity of probiotics while curbing the proliferation of harmful microbes. Presently, numerous scientists are delving into the significance of the microbiota as a pivotal tool in their respective research endeavours, aiming to develop novel biotherapeutics incorporating probiotics and prebiotics. These products hold promise for addressing skin disorders and diseases (22).

Researchers are starting to unravel the relationship between microbial communities and their associated diseases. Although understanding the skin's microbiome presents challenges, ample evidence already links dysbiosis in microbial composition to skin associated disorders from acute to chronic including acne, atopic dermatitis or eczema, seborrheic dermatitis, allergic inflammation, psoriasis, vitiligo, rosacea, UV-induced photodamage and photoaging, epidermolysis bullosa and skin cancer (23).

As our understanding of the influence of microbes on human health advances, there is a rapid emergence of probiotics-based dermal products for topical application. These products

may consist of probiotics alone, in the form of lysates or supernatants, or combined with pre-biotics to form synbiotics. Clinical data suggests that the use of probiotics-based biotherapeutic products can rebalance the skin microbiome, offering protection against and prevention of various skin conditions such as acne, eczema, atopic dermatitis, hypersensitive skin, UV-induced photodamage, and wound healing. Furthermore, these products contribute to mitigating signs of aging, thereby promoting overall skin health (24,25). Previous studies primarily explored the potential of gut-focused probiotics to elicit beneficial effects on the skin. However, recent research is shifting towards the direct application of probiotic and prebiotic-based products onto the skin. While the concept of improving skin health internally is commendable, a more practical and logical approach may involve addressing skin conditions directly at the site of concern, namely the skin surface. Gram-positive bacterial species such as *Lactobacillus* and *Bifidobacterium*, commonly used as probiotics, offers significant benefits to the skin microbiota due to their lack of proinflammatory lipopolysaccharides. This characteristic enables them to release bioactive molecules into the skin tissue, triggering signaling pathways that mitigate skin cell dysfunction (26,27). Consequently, recent research efforts are directed towards formulating topical synbiotics tailored for maintaining skin health.

Thus, this research endeavour stands to enrich our understanding of the identification and prevalence of potential probiotic bacteria in non-dairy sources, along with their relevance in promoting skin health. Key criteria such as antimicrobial activity, antibiotic susceptibility, acid and salt tolerance, and temperature stability are vital features in screening the probiotic potential of isolated strains for therapeutic applications. The primary aim of this study was to assess the antagonistic impact of *Lactobacilli* and *Bifidobacterium* strains isolated from non-dairy products against the standard strain of *Staphylococcus aureus*, sourced from the Regional Centre of Biotechnology in Faridabad, known as a major contributor to skin-related ailments.

Materials and Methods

Sources were collected from nearby area and the edible part of tomato and banana while honey as such was used for the isolation of LAB. The primary medium chosen for the isolation and selection of lactic acid bacteria (LAB) was deMan, Rogosa, and Sharpe (MRS) broth and agar medium. Approximately 1ml of liquid extract from each of the three samples was combined with a PBS buffer or sterile saline and inoculated into 100 ml of MRS broth. The samples were then incubated for 24-48 hours at 37°C, and turbidity in the MRS broth containing sample extracts was observed. Subsequently, serial dilutions of all three samples were prepared up to 10^-7 and plated onto MRS agar plates. Colonies with similar morphologies were streaked onto sterile MRS agar plates under aseptic conditions to obtain isolated and pure colonies, which were then incubated for 24 hours at 37°C. The resulting pure colonies were either stored at 4°C for immediate use or preserved in a 20% glycerol solution for future applications (28).

Identification and characterization of bacteria

Lactobacilli strains were extracted from non-dairy origins, specifically honey, tomato, and banana, through the enrichment of MRS (De Man, Rogosa, and Sharpe) broth (Hi-Media Pvt Ltd., India). The strains were confirmed through microscopic examination using Gram staining and catalase testing. Only strains exhibiting gram-positive characteristics and negative catalase reactions were chosen for subsequent use, classifying them as Lactic acid bacteria, as strains of *Lactobacilli* are rod shaped, gram-positive and catalase negative.

16s RNA sequencing

Fresh culture in the exponential growth phase was used to isolate the genomic DNA.

The resulting pellets obtained was resuspended in Tris EDTA buffer after being cleaned with ethanol. For isolates by PCR amplification 5' GGATGAGCCCGCGGCCTA 3' was used as 16S forward primer and 5' CGGTGTGTACAAG-GCCCGG 3'as the reverse primer. The result was integrated into sequencing programme at: http://blast.ncbi.nlm.nih.gov, where the isomers were determined and identified at a percentage > 90%. The identification and similarity of the strains was compared with the sequence of other *Lactobacilli* strains by using BLAST database. The strains were identified as *Lactiplantibacillus plantarum*, *Lactiplantibacillus pentosus*, and *Bifidobacterium animalis*. The selected cultures were identified from was performed by Bio kart Pvt. Ltd, Bangalore. The identified strain from banana had 99.92% similarity with *Bifidobacterium animalis*, strain from honey had 99.92% similarity with *Lactiplantibacillus plantarum* and from tomato the identified strain had 92.69% similarity with *Lactiplantibacillus pentosus.* (Table1)

Table 1. Identification of the isolates from different sources.

S. No.	Sources and designation of the isolates	Identified Strain	Accession number (NCBI)	Base length	% of similarity
1	Tomato SUB13507764	Lactiplantibacillus pentosus	OR105181	1446 bp	92.69% similarity with Lactiplantibacillus pentosus strain 124-2 16S ribosomal RNA NR_029133.1
2	Honey SUB13507721	Lactiplantibacillus plantarum	OR105053	1249 bp	99.92% with Lactiplantibacillus plantarum strain JCM 1149 16S ribosomal RNA NR_115605.1
3	Banana SUB13507546	Bifidobacterium animalis	OR105051	1271 bp	99.92% with Bifidobacterium animalis subsp. lactis strain YIT 4121 16S ribosomal RNA NR_040867.1
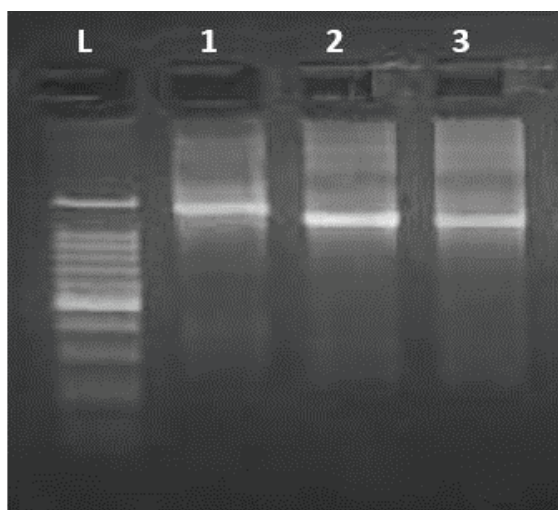
Figure 1. Gel image of PCR amplification.

Determination of optimal growth at pH

The optimal pH for the growth of all three isolated strains from non-dairy sources, namely *Lactiplantibacillus plantarum, Bifidobacterium animalis*, and *Lactiplantibacillus pentosus* was determined using MRS broth with pH values ranging from 2 to 7. Each broth was inoculated with 1% (v/v) of the respective isolates and then incubated at 37°C for 24-48 hours under anaerobic conditions. Bacterial growth was assessed by either measuring the optical density at 560 nm using a UV-visible spectrophotometer against a control or by spreading 0.1 ml of culture from the broth with varying pH onto MRS agar plates, with a control at pH 6.5, or observing colony formation after incubation at 37°C for 24 hours (29).

Assay for NaCl tolerance

The NaCl tolerance assay is useful to determine the optimal growth of isolated probiotics on varying salt concentration. For this 1% (v/v) of each sample were inoculated in 100 ml flasks containing MRS broth having varying concentration range of NaCl from 1% to 7% incubated at 37℃ for 24-48 h under anaerobic conditions. The growth was determined by optical density at 600 nm using UV-visible spectrophotometer (30).

Growth at various temperature

The temperature tolerance is done to determine both the refrigerated and shelf-stable varieties as many strains cannot tolerate certain range of temperature. The stability of various probiotic strains at different temperatures was measured by determining the viability of cells at different temperatures. For this, all isolates were inoculated in the flasks containing MRS broth and all the flasks were incubated at low to high range of temperature i.e., at 4℃, 25℃, 37℃, and 45℃ respectively. Growth was measured by taking optical density at 560 nm using UV-Spectrophotometer (31).

Antibiotic sensitivity test

To assess the antibiotic sensitivity of the bacteria, both disc diffusion and antibiotic strip diffusion methods were employed. Various antibiotics were tested on the isolated probiotic strains using Hi Comb™ MIC strips containing five different antibiotics. These MIC strips feature a comb-like structure with 15 extensions carrying porous material containing antibiotics of varying concentrations. Each strip encompasses 15 two-fold dilutions, ranging from the highest concentration at one end to the lowest at the other. Muller-Hinton agar (MHA) plates were prepared by pouring MHA media and allowing it to solidify at room temperature. Subsequently, 100 microliters of freshly grown cultures were spread onto the MHA plates, followed by the placement of appropriate antibiotic-impregnated strips over the surface. The zones of inhibition and minimum inhibitory concentration (MIC) values were then determined for each isolate. The antibiotic susceptibility pattern was evaluated using five antibiotic strips: Ampicillin (0.016-256 µg/ml), Penicillin (0.002-32 µg/ml), Ciprofloxacin (0.002-32 µg/ml), Gentamycin (0.016-256 µg/ml), and Tetracycline (0.016-256 µg/ml) for each of the three isolates obtained from banana, honey, and tomato pulp. When placed over the Muller-Hinton agar plates, these strips created a defined concentration gradient, allowing the antibiotics to diffuse into the porous agar bed. Consequently, zones of inhibition appeared in the form of ellipses. After 24 hours of incubation at 37°C, the zones of inhibition were examined to determine the sensitivity assay. Sensitivity was indicated by the presence of zones of inhibition, whereas resistance was characterized by the absence of such zones (32).

Antimicrobial activity

The antimicrobial activity against pathogen or conditional pathogen is one of the main requirements for probiotic strain as all probiotics show the strain-specific antimicrobial activity against pathogens. There is a necessity to examine the antimicrobial activity of each isolated strain against the selected pathogen i.e., *Staphylococcus aureus* via direct or indirect mechanisms of interactions. The existing methods belong to two major groups: *in- vitro* methods including well-diffusion method, disc-diffusion method, and co-culturing methods and *in- vivo* methods that directly involve animals or humans' trials. To assess the antimicrobial efficacy of the three isolates, the overnight cultures were centrifuged at 10,000 rpm at 4°C for 15-20 minutes. The resulting supernatants from each sample were then evaluated for their antibacterial properties against *Staphylococcus aureus*, which was inoculated onto Mannitol salt agar plates. Wells with a diameter of 8 mm were created in the agar plates, into which 50µl aliquots of each sample were added. Subsequently, the plates were incubated at 37°C for 24-48 hours, after which clear zones of inhibition surrounding the wells and discs were examined as indicators

of antimicrobial activity against the target micro-organisms (33-35).

Effects of inulin as *Prebiotic on growth of Probiotics*

Human skin acts as shield to external environment and harbours millions of microbes that are involved in developing immunity. Probiotic strains are very sensitive in nature and their growth and survival depend on external environment including oxygen, pH, moisture, heat etc. The prebiotics are defined as "non-digestible oligosaccharides that beneficially effects host health by selectively supporting or stimulating the growth or activity of probiotics." Including prebiotics promotes the proliferation of lactic acid bacteria through the facilitation of lactic acid fermentation. Inulin has garnered significant attention due to its ability to modulate microbial composition, favouring probiotic growth. Inulin is a polymeric compound composed of fructose units ranging from 2 to over 200, with the specific composition influenced by factors such as plant species, age, and extraction method. While over 30,000 plant species serve as potential sources of inulin, chicory roots and dahlia are commonly utilized as commercial sources for extraction (36).

Inulin as prebiotics, serves as food or fuel utilized by probiotics to optimize their functions. Derived from chicory root, it is an excellent ingredient in skincare products, aiding in balancing the skin's microbiome and thereby supporting the preservation of its healthy appearance.

Inulin is a naturally occurring anti-oxidant and humectant that draws moisture from the surrounding environment to the skin and keeps it hydrated. It also acts as a skin-conditioning agent by forming a protective thin layer over the skin surface that reduces dryness, redness, and aging thus makes the skin smooth and supple. Combination of Inulin as prebiotic and probiotics forms synbiotics when applied topically, inulin helps the probiotics to thrive thus maintains skin youthful, and subsequently, repair and restore the skin barrier (37).

Results and Discussion

Scientists are making sustained efforts to substitute chemical-based pharmaceutical drugs with natural biotherapeutic products. Recently, there has been renewed interest and investigation into the potential benefits of both probiotics and prebiotics. Hence, employing probiotics and prebiotics is believed to positively influence the normal functions of healthy skin and play a significant role in preventing and treating various skin conditions, such as acne, atopic dermatitis, psoriasis, photoaging, and wound healing. Collectively, they are believed to support skin health by hydrating, nourishing, and reducing inflammation, thus mitigating the risk of skin diseases. This paper aims to isolate and characterize probiotics sourced from non-dairy origins to assess their impact on the target bacteria *S. aureus,* which is implicated in dermatological conditions. Overall, this research advocates for the utilization of probiotics and prebiotics as a viable strategy for preventing and managing skin issues.

This study discovered that probiotics from the *Lactobacillus* and *Bifidobacterium* genera, sourced from non-dairy origins like fermented goods, fruits, and vegetables, exhibited resilience to acidity and salt, demonstrated resistance to antibiotics, and displayed antagonistic properties against pathogens associated with skin conditions. Numerous *Lactobacilli* species naturally inhabit the human body, including the gastrointestinal tract (GIT), oral cavity, and skin.

Hence, the objective of this study was to isolate and evaluate LAB strains from various environments, aiming to identify new probiotic candidates through in-vitro characterization. All three isolates underwent characterization for probiotic traits through morphological assessment via Gram staining and biochemical analyses, encompassing tests for catalase activity, pH tolerance, temperature resilience, salt tolerance, antibiotic susceptibility, and antimicrobial

efficacy. These attributes are crucial considerations when selecting probiotic strains for synbiotic formulations, offering an advantage in antimicrobial activity against harmful pathogens.

The majority of *Lactobacillus* and *Bifidobacterium* species identified from various origins have extensive records of safety for human consumption and have been designated as GRAS (38). Both strains have been extensively utilized as food supplements or in pharmaceuticals, or in both capacities. However, the primary criterion for selecting probiotics involves examining the behaviour of the isolated strains under conditions that mimic the skin environment and assessing their ability to endure harsh conditions, thereby establishing, and proliferating within the prevailing nutritional and ecological parameters.

Isolation and identification

Ample research has been conducted in the identification and isolation of probiotics from various biotic and abiotic sources including humans, fermented foods, dairy sources, air, and soil, but recent research has focused on isolates from varieties of non-dairy sources. As probiotics nowadays are not only used as diet supplements but also as therapeutic products, it is necessary to administer inflexible screening assays for the identification of new probiotic strains to discover their functional properties by different biochemical processes at varying pH, temperature, salt concentration, and safety properties such as antibiotic resistance, and antimicrobial activity for survival over skin surface under harsh conditions (39). The molecular identification of promising probiotic strains was conducted through 16S rDNA sequence analysis, following the 16S rRNA gene sequence and DNA-DNA hybridization analysis protocols. Strains obtained from honey, tomato, and banana were determined to be *Lactiplantibacillus plantarum, Lactiplantibacillus pentosus*, and *Bifidobacterium animalis*, respectively (40). The bacterial isolates were further characterized and screened for the confirmation of *Lactobacillus* species. The creamy colour gram-positive, rod-shaped bacterial isolates were observed by Gram-staining, and there was no bubble formation with hydrogen peroxide indicating that they were catalase negative.

pH tolerance

The acid tolerance of the isolates is a crucial trait, particularly given the acidic pH of the skin where many commensal organisms thrive. Hence, it is imperative for the isolated probiotic strains to endure acidic conditions and thrive within the pH range of 4-5, which is conducive to skin application. This study aimed to pinpoint probiotic isolates from non-dairy origins that exhibit stability within the skin's pH range of approximately 4 to 5. The viability assays demonstrated the pH stability of all three isolates *Lactiplantibacillus plantarum, Lactiplantibacillus pentosus* and *Bifidobacterium animalis*. It was observed that all three survived well at pH 4-5 after incubation at 37°C for 24 h, which is suitable for skin pH.

From the result obtained, it was interpreted that at pH 2 all showed less growth, at pH 3 the all isolates showed moderate growth, but at pH 4 and 5, all isolates showed the highest growth, which is the normal range of skin pH that supports microbial growth. (Table 2)

The pH of the skin plays a crucial role in maintaining homeostasis, ensuring proper barrier function, and preserving the integrity and cohesion of the stratum corneum. Additionally, it serves as a key component of the skin's antimicrobial defence system against external environmental factors. Typically, the skin maintains a slightly acidic pH, known as the acid mantle, ranging from 4 to 5. This pH varies according to the needs of specific skin regions, aiding in the regulation of the cutaneous microflora ecosystem. This balance helps safeguard the skin against harmful pathogens, contributing to overall skin health and well-being (41,42). There is a positive relationship between lower pH values ranging from 4 to 5 and preservation of the skin microbiome.

The Potential Impact of Probiotics along with Prebiotic against the Dermatic pathogen
Staphylococcus aureus: Isolation and Characterization

Table 2. Screening of all isolates at different pH levels.

S. No.	pH	Lactiplantibacillus pentosus	Lactiplantibacillus plantarum	Bifidobacterium animalis
Control	6.5	-	-	-
1	2	-	-	-
2	3	+	+	+
3	4	++	++	++
4	5	+++	+++	+++

Table symbols: '-' represents no growth, '+' less growth, '++' moderate growth, '+++' high growth.

Temperature tolerance

The surface temperature of the skin is an essential physiological indicator, reflecting the dynamics of heat exchange between the human body and its surroundings (43). Temperature is also a major factor that determines the stability and viability of probiotics when they are subjected to various harsh conditions during further refining methods, freeze-drying, nanoparticles, hydrogels or bio gels, and other pharmaceutical processes.

According to the results of the temperature tolerance assay indicated that, every isolate could withstand a broad range of temperatures and flourished at room temperature, both above and below it, and at higher temperatures relative to lower temperature. Isolated strains *Lactiplantibacillus plantarum* showed higher stability, as it grows well at different range of temperature followed by *Lactiplantibacillus pentosus* and *Bifidobacterium animalis.* (Figure 2)

Salt tolerance

Sweating diminishes bacterial load on healthy skin, and its generation directly impacts the salt levels within the skin. Research indicates that an excess of salt can influence the innate immune system by altering T cell responses (44,45).

The results of the assay showed that the viability of the isolates was reduced by high salt concentration. Tolerance to NaCl is required for controlling the skin's innate immune system. Species of *Lactobacilli* can thrive in conditions where the concentration of salt varies from 2% to 7%. The results of the assay showed that the viability of the isolates was reduced by high salt concentration. From the graph it was interpreted that *Lactiplantibacillus pentosus* was highly stable at 2% and 3% and least stable at 6% whereas, *Lactiplantibacillus plantarum* showed less stability at varying salt range as it was most stable at 2% and least stable at 6% and 7%. *Bifidobacterium animalis* was highly stable at 3% and 5% salt concentration. (Figure 3)

Figure 2. Effect of different temperature on *L. pentosus, L. plantarum*, and *B. bifidum*.

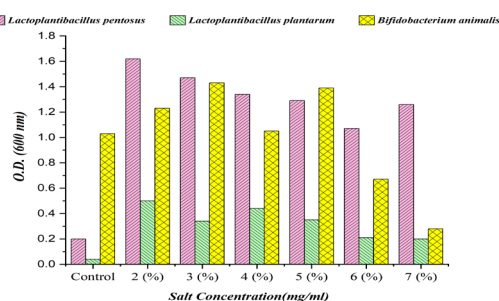Figure 3. Effect of different Salt concentration on *L. pentosus, L. plantarum*, and *B. bifidum*.

Antimicrobial assay

Antimicrobial efficacy stands as a vital criterion in probiotic culture selection, serving as natural adversaries against potentially harmful pathogens. Consequently, two *Lactobacillus* strains and one *Bifidobacterium* strain were assessed for their activity against *Staphylococcus aureus*, a primary culprit in skin infections. On agar plates, wells measuring 8 mm in diameter were created, and 50-100 µl of cell-free supernatant was introduced into these wells. The antimicrobial activity was gauged by the diameter of the inhibition zones surrounding the wells after an overnight incubation period at 37℃. Zones of inhibition measuring ≥10 mm were deemed positive. Varied sensitivities among the isolated probiotics resulted in distinct zones of inhibition against the target pathogens within the pH range of 4-5.

Many studies have accepted that *Lactobacilli* are bio conservatives as they exhibit a broad antimicrobial spectrum against diverse pathogens belonging to Gram-negative and Gram- positive microorganisms, including food-borne pathogens *E. coli, Pseudomonas*, and dermal pathogens including *Staphylococcus aureus*, the main culprit responsible for approx. 80% of skin diseases. Both lyophilized and concentrated cell-free substrates derived from the cultivation of isolated and selected *Lactobacilli* and *Bifidobacterium* in MRS broth underwent testing for antimicrobial activity (46). The primary cause of antimicrobial activity in *Lactobacilli* stems from the generation of organic acids, such as lactic and acetic acids, as well as the production of microbial metabolites, hydrogen peroxide, and various low molecular weight antimicrobial peptides like bacteriocins. Additionally, there is a decrease in pH because of competition with pathogenic bacteria (47,48,49). The antimicrobial impact is also attributed to the undissociated acid form and its ability to lower the intracellular pH, thereby inhibiting vital cell functions of pathogens (50,51).

The antimicrobial activity of the isolated *Lactobacillus* and *Bifidobacterium* strains was determined using the well diffusion method, which resulted in inhibition zones ranging from 0.9 to 1.5 cm or 9 to 15 mm in diameter against Staphylococcus aureus, the primary pathogen linked to various skin issues, particularly atopic dermatitis. From the antimicrobial assay performed, it was observed that the supernatants from all isolates showed activity against the pathogenic strain *Staphylococcus aureus.* Based on the findings, it was determined that *Lactiplantibacillus pentosus* had the largest inhibitory zone of 15mm, followed by *Lactiplantibacillus plantarum* of 13mm, and finally *Bifidobacterium animalis* of 9mm. It was determined that *Lactiplantibacillus plantarum*, *Bifidobacterium animalis*, and *Lactiplantibacillus pentosus* had the strongest antagonistic activity against *S. aureus.* (Table 3)

Table 3. Zone of inhibition of all isolates against *Staphylococcus aureus.*

S. No.	Name of the strain	Zones of inhibition against *Staphylococcus aureus* in mm.
1	*Lactiplantibacillus pentosus*	15 mm
2	*Lactiplantibacillus plantarum*	13 mm
3	*Bifidobacterium animalis*	9 mm

Antibiotic sensitivity assay

Antibiotic sensitivity assays for determining the sensitivity and resistivity against various antibiotics are of great importance in the human and veterinary fields. The safety assessment of strains intended for probiotic use necessitates an evaluation of their antibiotic susceptibility profiles and the presence of antibiotic-resistant genes. All three isolates displayed

comparable antibiotic susceptibility patterns with minor exceptions. None of them exhibited susceptibility to Penicillin and Ampicillin, while they demonstrated susceptibility to Ciprofloxacin, Gentamycin, and Tetracycline. The resistance of probiotic strains to certain antibiotics could serve both preventive and therapeutic purposes in combating skin-related ailments. This investigation unveiled that the intake of certain antibiotics, such as penicillin and ampicillin, would not affect the growth of the *Lactobacilli* population, whereas other antibiotics could significantly diminish *Lactobacillus* spp. populations. The antibiotic resistance data indicate differences among the isolates in terms of their antibiotic sensitivity patterns (52).

The tolerance of all three isolates to-ward ampicillin, tetracycline, ciprofloxacin, gentamycin, and penicillin was determined using antibiotic strips of different antibiotics with different ranges. We concluded that all the tested *Lactobacillus* and *Bifidobacterium* strains were resistant toward ampicillin and penicillin. *Lactiplantibacillus pentosus is s*ensitive to gentamicin and ciprofloxacin with MICs of 4.0 and 0.25, respectively. *Lactiplantibacillus plantarum* is sensitive to tetracycline, gentamicin, and ciprofloxacin with MICs of 1.0, 2.0 and 0.12, respectively. *Bifidobacterium animalis* is sensitive to Tetracycline, gentamicin, and ciprofloxacin with MICs of 32.0, 16.0 and 0.25, respectively. Generally, they are sensitive to broad-spectrum antibiotics including tetracycline and resistant to the beta-lactam antibiotic ampicillin and cell wall inhibitor antibiotic like penicillin. (Table 4)

Table 4. Antibiotic susceptibility profiles of the three probiotic bacteria to the selected antibiotics of Tetracycline, Ampicillin, Ciprofloxacin, Penicillin, and Gentamycin

Antibiotics	*Lactiplantibacillus pentosus*	*Lactiplantibacillus plantarum*	*Bifidobacterium animalis*
Tetracycline	R	S (MIC: 1.0)	S (MIC: 32.0)
Gentamycin	S (MIC: 4.0)	S (MIC: 2.0)	S (MIC: 16.0)
Ampicillin	R	R	R
Penicillin	R	R	R
Ciprofloxacin	S (MIC: 0.25)	S (MIC: 0.12)	S (MIC: 0.25)

MIC: minimum inhibitory concentration (µg/ml), R: resistant, S: susceptibility.

Prebiotics and their respective activity scores

Prebiotics function as promoters of probiotic growth, and their efficacy can be assessed through the calculation of a probiotic score, which evaluates the ability of prebiotics to support probiotic growth (53). The prebiotic score is determined by measuring the growth of bacterial cells from each isolate in the presence and absence of prebiotics and other saccharides, such as sucrose, using spread plate, pour plate, and optical density measurements at 560 nm. The impact of prebiotics on the growth of all three isolated probiotic strains was evaluated through the prebiotic activity score, represented as a percentage. A higher prebiotic score for inulin compared to sucrose indicates that the selected prebiotic molecule effectively supports the growth of the isolated probiotic bacterial strains.

Activity score of prebiotics on probiotics (%) = OD at 560 nm in absence of prebiotic/OD at 560 nm in presence of inulin.

Activity score of sucrose on probiotics (%) = OD at 560 nm in absence of sucrose/ OD at 560 nm in presence of sucrose.

Prebiotics, which are oligosaccharides resistant to digestion, stimulate the growth of probiotics when consumed in suitable quantities. Previous research has indicated that probiotics and prebiotics contribute positively to

skin health by enhancing skin moisture, elasticity, and radiance, as well as by improving skin barrier function and follicular structure through the regulation of keratinocyte differentiation. From the results, it was concluded that the inulin taken as prebiotic showed maximum activity score for *Lactiplantibacillus plantarum* isolated from honey followed by *Bifidobacterium anima-* *lis* from banana *and Lactiplantibacillus pentosus* from tomato as compared to sucrose taken as control carbohydrate as growth promoter in place of inulin. Also, inulin taken as prebiotic, showed higher activity than sucrose as a carbohydrate for promoting growth of isolated probiotics strains. (Table 5)

Table 5. Activity score of probiotics in presence and absence of prebiotics (inulin).

S. No.	Probiotic strain	Optical density at 560 nm in the absence of prebiotics	Optical density at 560nm in the presence of prebiotic (Inulin)	Optical density at 560 nm in the presence of control carbohydrate (Sucrose)	Activity score of probiotics in the presence and absence of Inulin	Activity score of probiotics in the presence and absence of Sucrose
1	*Lactiplantibacillus pentosus*	1.049	1.175	1.109	89.2%	73.9%
2	*Bifidobacterium animalis*	0.878	1.447	1.042	60.6%	59.16%
3	*Lactiplantibacillus plantarum*	1.083	1.112	1.663	97%	65.12%

Under in-vitro conditions, the isolates underwent assessment for their probiotic attributes, which encompassed tolerance to salt, acid, and temperature, as well as antagonistic activity against specific pathogens and antibiotic sensitivity. The isolated strains exhibit promising probiotic traits, such as tolerance to temperature, acidity, and salt, irrespective of their diverse origins. These favourable characteristics render the isolated strains viable for topical applications on the skin surface.

Conclusion

In recent times, there has been a surge in the exploration of probiotics, not only as supplements but also as therapeutic agents. Probiotics, which are live microorganisms that confer health benefits when consumed in adequate quantities, have gained considerable attention. Among the most widely utilized probiotics are species belonging to *Lactobacilli* and *Bifidobacterium*, which have been employed for many years. The skin cells and skin 's microbiome works synergistically to maintain homeostasis in daily routine. Employing probiotics and prebiotics, either independently or in an appropriate combination, could represent a fresh and efficient strategy for addressing a variety of skin disorders, spanning from acne to eczema. The sensitivity and resistance of numerous probiotic strains to commonly prescribed antibiotics render them safe for the formulation of diverse products for both animal and human use. Data analyse have already indicated that probiotics' antimicrobial properties against *Staphylococcus aureus* are beneficial for averting and managing skin conditions such as acne, inflammation, atopic dermatitis. In addition, it has been observed that the use of probiotic cultures and their lysates either alone or with prebiotics as cosmetic products and their ingredients moisturizes and exfoliates the skin, thus maintaining good skin health.

Conflicts of interest

The authors declare that there are no conflicts of interest.

References

1. Saarela M, L€ahteenm€aki L, Crittenden R, Salminen S, Mattila-Sandholm T. (2002). Gut bacteria and health foods the European perspective. *Int J Food Microbiol*,78 (12):99117

2. Smid Ej, Van Enckevort FJ, Wegkamp A, Boekhorst J, Molenaar D, Hugenholtz J, et al. (2005). Metabolic models for rational improvement of Lactic acid bacteria as cell factories. *J Appl Microbiol*, 98:1326-31.

3. Islam T, Sabrin F, Islam F, Billah M, Islam Didarul KM. (2012) Analysis of antimicrobial activity of *Lactobacillus paracasei* ssp paracasei-1 isolated from regional yogurt. *J Microbiol Biotechnol Food Sci*, 7:80-89.

4. Amin, M., Jorfi, M., Khosravi, A., Samarbafzadeh, A., Sheikh, A.F., (2009). Isolation and identification of *Lactobacillus casei* and *Lactobacillus plantarum* from plants by PCR and detection of their antibacterial activity. *J. Biol. Sci*, 9, 810–814.

5. Oyetayo V.O. (2012) Phenotypic characterisation and assessment of the inhibitory potential of *Lactobacillus* isolates from different sources. *African Journal of Biotechnology*, 3(7), 355-357.

6. TURGAY, Ö., & Erbilir, F. (2006). Isolation and characterization of *Lactobacillus bulgaricus* and *Lactobacillus casei* from various foods. *Turkish Journal of Biology*, *30*(1), 39-44.

7. Zielinska, Dorota, Danuta Kolozyn- Krajewska. (2018). Food -origin lactic acid bacteria may exhibit probiotic properties: Review, *Bio Med Research International*,1-15.

8. Del piano, M, Ballare, M, Montino, F, Orsello, M, Garello, E, Sforza, F. (2004) Clinical experience with probiotics in the elderly on total enteral nutrition. *J Clin Gastroenterol*,38: S111-S4.

9. Darbandi A, Ghanavati R, Asadi A, et al. (2021). Prevalence of bacteriocin genes in *Lactobacillus* strains isolated from fecal samples of healthy individuals and their inhibitory effect against foodborne pathogens. *Iran J Basic Med Sci*, 24(8):1117-1125. doi: 10.22038/ijbms.2021.53299.11998

10. Fuochi V, Coniglio MA, Laghi L, et al. (2019). Metabolic characterization of supernatants produced by lactobacillus spp. with in-vitro anti-legionella activity. *Front Microbiol*, 10:1403. doi: 10.3389/fmicb.2019.01403

11. Kaur M, Kaur G, Sharma A. (2018) Isolation of newer probiotic microorganisms from unconventional sources. *J Appl Nat Sci*, 10(3):847-852. doi: 10.31018/jans.v10i3.1724

12. Wu H, Xie S, Miao J, et al. (2020). *Lactobacillus reuteri* maintains intestinal epithelial regeneration and repairs damaged intestinal mucosa. *Gut Microbes* 11(4):997- 1014. doi: 10.1080/19490976.2020.1734423

13. Al-Yami AM, Al-Mousa AT, Al-Otaibi SA, Khalifa AY. (2022). *Lactobacillus* Species as Probiotic: Isolation Sources and Health Benefits. *J Pure Appl Microbiol*, 16(4):2270-2291. doi: 10.22207/JPAM.16.4.19.

14. Gallo RL. (2017). Human skin is the largest epithelial surface for interaction with microbes. *J Invest Dermatol,* 137(6):1213-1214. doi: 10.1016/j. jid.2016.11.045.

15. Si J, Lee S, Park JM, Sung J, Ko G. (2015). Genetic associations and shared environmental effects on the skin microbiome of Korean twins, *BMC Genomics,* 16;992.

16. Chen YE, Tsao H. The skin microbiome: current perspectives and future challenges. *J Am Acad Dermatol* 2013; 69: 143-155: e3.

17. Perez Perez GI, Geo Z, Jourdain R, Ramirez J, Gany F, Clavaud C, Demaude J, Breton L, Blaser MJ. (2016). Body site is a more determinant factors than human population diversity in the healthy skin microbiome, *PLoS One*: 11(4): e0151990.

18. Mukherjee S, Mitra R, Maitra A, Gupta S, Kumaran S, Chakrabortty A, Majumder PP. (2016). Sebum and hydration levels in specific regions of human face significantly predict the nature and diversity of facial skin microbiome, *Sci Re*; 27(6): 36062.

19. Christensen GJ, Bruggemann H. (2014). Bacterial skin commensals and their role as host guardians. *Benef Microbes*, 5: 201-215.

20. Haas BJ, Gevers D, Earl AM, Feldgarden M, Ward DV, Giannoukos G, Ciulla D, Tabbaa D, Highlander SK, Sodergren E, Methe´ B, DeSantis TZ, (2011). Human Microbiome Consortium, Petrosino JF, Knight R, Birren BW., Chimeric 16S rRNA sequence formation and detection in Sanger and 454-pyrosequenced PCR amplicons. *Genome Res,* 21:494–504 et al, 2011.

21. Glenn, G.; Roberfroid, M. (1995). Dietary modulation of the human colonic microbiota: Introducing the concept of prebiotics. *J. Nutr*, 125, 1401–1412.

22. Gibson, G.R.; Probert, H.M.; Van Loo, J.; Rastall, R.A.; Roberfroid, M.B. (2004). Dietary modulation of the human colonic microbiota: Updating the concept of prebiotics. *Nutr. Res. Rev*, 17, 259–275.

23. Schommer NN, Gallo RL. (2013). Structure and function of the human skin microbiome. *Trends Microbiol,* 12: 660-668.

24. Lebeer S, Oerlemans E, Claes I, et al. (2018). Topical cream with live lactobacilli modulates the skin microbiome and reduce acne symptoms. *Bio Rxiv*, doi: 10.1101/463307 et al, 2018

25. Higaki S. Lipase inhibitors for the treatment of acne. (2003). *J Mol Catal B Enzym* ,22(5-6):377-384. doi: 10.1016/S1381-1177(03) 00053-5 et al, 2003

26. Fuller R. (1989). Probiotics in man and animals. *J Appl Bacteriol*, 66: 365-378.

27. Ramsey MM, Freire MO, Gabrilska RA, Rumbaugh KP, Lemon KP. (2016). *Staphylococcus aureus* shifts towards commensalism in response to *Corynebacterium* species. *Front Microbiol*,17(7);1230.

28. Prasad, J., Gill, H., Smart, J., Gopal, P.K. (1998). Selection and Characterization of Lactobacillus and Bifidobacterium strains for use as probiotics. *Int. Dairy J*, 8,993-1002.

29. Shokryazdan P, Sieo CC, Kalavathy R, Liang JB, Alitheen NB, Jahromi MF & Ho YW. (2014). Probiotic potential of *Lactobacillus* strains with antimicrobial activity against some human pathogenic strains. *BioMed Res Int,* 10, (927268).

30. Handricks AJ, Mills BW, Shi VY. (2019). Skin bacterial transplant in atopic dermatitis: knows, unknowns, and emerging trends. *J Dermatol Sci*, 95(2): 56-61.

31. Gardini, F., Martuscelli, M., Caruso, M.C., Galgano, F., Crudele, M.A., Favati, F., Guerzoni, M.E., Suzzi,G . (2001). Effects of pH, temperature and NaCl concentra-

The Potential Impact of Probiotics along with Prebiotic against the Dermatic pathogen
Staphylococcus aureus: Isolation and Characterization

tion on the growth kinectics, proteolytic activity and biogenic amine production of Enterococcus faecalis. *Int J. Food Microbiol*, 64, 105-117.

32. Hassan, M.; Kjos, M.; Nes, I.F.; Diep, D.B.; Lotfipour, F. (2012). Natural antimicrobial peptides from bacteria: Characteristics and potential applications to fight against aantibiotic resistance. *J. Appl. Microbiol*, 113, 723-736.

33. Ahn, D.K.; Han, T.W.; Shin, H.Y.; Jin, I.N.; Ghim, S.Y. (2003). Diversity and antibacterial activity of lactic acid bacteria isolated from Kimchi. Korean *J. Microbiol. Biotechnol* 2003, 31, 191–196.

34. Rasika, D.M.D.; Vidanarachchi, J.K.; Luiz, S.F.; Azeredo, D.R.P.; Cruz, A.G.; Ranadheera, C.S. (2021). Probiotic Delivery through Non-Dairy Plant-Based Food Matrices. *Agriculture,* 11, 599. https://doi. org/10.3390/ agriculture11070599.

35. Ahn, K.B.; Baik, J.E.; Park, O.J.; Yun, C.H.; Han, S.H. (2018). *Lactobacillus plantarum* lipoteichoic acid inhibits biofilm formation of *Streptococcus* mutans. PLoS ONE, 13, e0192694.

36. Bhakti Prakash Mallik, Harshita Bhawsar, (2018). Evaluation of Prebiotic Score of Edible Mushroom Extract, *International Journal of Engineering Research & Technology (IJERT)*, Volume 07, Issue 10.

37. Teferra, T.F. (2021). Possible actions of inulin as prebiotic polysaccharide: A review. *Food Frontiers*, 2, 407-416. https://doi. org/10.1002/fft2.92

38. Sadrani, H., J. Dave, and Bharatkumar Rajiv Manuel Vyas. (2014). "Screening Of Potential Probiotic Lactobacillus Strains Isolated from Fermented Foods, Fruits and Of Human Origin". *Asian Journal of Pharmaceutical and Clinical Research*,Vol. 7, No. 7, Pp. 216-25.

39. Dunne C, O'Mahony L, Murphy L, Thornton G, Morrisey D, O'Halloran S et al. (2001). In vitro selection criteria for probiotic bacteria of human origin: Correlation with in vivo findings. *Am J Clin Nutrition*,73:386-392.

40. Mishra, V., & Prasad, D. (2005). Application of in vitro methods for selection of *Lactobacillus casei* strains as potential probiotics. *International Journal of Food Microbiology*,*103*(1), 109-115. https://doi. org/10.1016/j.ijfoodmicro.2004.10.04

41. Cinque B, La Torre C, Melchiorre E, et al. (2011). Use of probiotics for dermal applications in probiotics, *Probiotics, Eds., Berlin*: *Springer*, 221–241.

42. Ali SM, Yosipovitch G. (2013). Skin pH: From basic science to basic skin care. *Acta Dermato Venereologica*, 93: 261–267.

43. Liu Y, Wang L, Liu J, et al. (2013). A study of human skin and surface temperatures in stable and unstable thermal environments. *J Therm Biol*, 38: 440–448.

44. Gläser R, Harder J, Lange H, et al. (2005). Antimicrobial psoriasin (S100A7) protects human skin from Escherichia coli infection. *Nat Immunol*, 6: 57–64

45. Matthias J, Maul J, Noster R, et al. (2019). Sodium chloride is an ionic checkpoint for human TH2 cells and shapes the atopic skin microenvironment. *Sci Transl Med*, 11: 1–11.

46. Kivanc M, Yilmaz M, ̧ Cakir E. (2011). Isolation and identification of lactic acid bacteria from boza, and their microbial activity against several reporter strains. *Turkish J Biol*, 35 (3):313-324

47. Juntunen, M., Kirjavainen, P., Ouwehand, A., Salminen, S., Isolauri, E. (2001). Adherence of probiotic bacteria to human intestinal mucus in healthy infants and during rotavirus infection. *Clin. Diagn. Lab. Immunol,* 8, 293–296.

48. Ouwehand, A.C., Tuomola, E.M., Tölkkö, S., Salminen, S. (2001). Assessment of adhesion properties of novel probiotic strains to human intestinal mucus. *Int. J. Food Microbiol*, 64, 119–126.

49. Pithva SP, Shekh S, Dave JM, Vyas BRM. (2014). Probiotic attributes of autochthonous *Lactobacillus rhamnosus* strains of human origin. *Appl Biochem Biotechnol*, 173:259-277

50. Atanassova M, Choiset Y, Dalgalarrondo M, Chobert JM, Dousset X, Ivanova I, Haertle T. (2003). Isolation and partial biochemical characterization of a proteinaceous anti-bacteria and anti-yeast compound produced by *Lactobacillus paracasei* subsp. *paracasei* strain M3. *Int J Food Microbiol*, 87(1-2):63-73.

51. De Vuyst L, Leroy F. (2007). Bacteriocins from lactic acid bacteria: production, purification, and food applications. *J Mol Microbiol Biotechnol*, 13(4):194-199.

52. El-Naggar MYM. (2004). Comparative study of probiotic cultures to control the growth of *Escherichia coli* O157:H7 and *Salmonella typhimurium*. *Asian Network for Scientific Information Biotechnol*, 3:173-180.

53. FIGUEROA-GONZÁLEZ, Ivonne, Gabriela RODRÍGUEZ-SERRANO, Lorena GÓMEZ-RUIZ, Mariano GARCÍA-GARIBAYand Alma CRUZ-GUERRERO, (2019). "Prebiotic effect of commercial saccharides on probiotic bacteria isolated from commercial products", *Food Science and Technology*, 39 (3), 747–53.

Engineering Cefpodoxime Prodrug using Nanosuspension Approach to Modulate Solubility, Antimicrobial and Pharmacokinetic Profile

Prerana Bhosale[1], Priyanka Gawarkar-Patil[1], Atmaram Pawar[1], Vividha Dhapte-Pawar[1*]

[1] Department of Pharmaceutics, Poona College of Pharmacy, Bharati Vidyapeeth (Deemed to be University), Pune, Maharashtra 411038, India.

*Corresponding author: vv@bharatividyapeeth.edu

Abstract

Cefpodoxime proxetil (CP) is broad-spectrum antibiotic belongs to third-generation cephalosporin family. Its low solubility and bioavailability have been a challenge for drug delivery. Nanosuspension (NS) technology has been explored in drug delivery to address the issues of drugs with poor water solubility. The study focused on developing a CP nanosuspension (CP-NS) formulation using solvent-antisolvent precipitation technique. The CP-NS was synthesized by precipitation using 0.5 % w/v sodium lauryl sulphate and 1.5 % w/v poloxamer-188 under controlled ultrasonication. CP-NS was characterized for Fourier transform infrared (FTIR), Transmission electron microscopy (TEM), Differential scanning calorimetry (DSC), and X-ray diffraction (XRD). In vitro dissolution studies revealed that CP-NS exhibit increased dissolution rate 2-folds than pure drug and 1.3-folds higher than marketed formulation. In vivo pharmacokinetic studies revealed 4.3-fold improvement in oral bioavailability of CP-NS than pure drug and marketed formulation. In conclusion, the formulation of cefpodoxime proxetil nanosuspension showed promising results in terms of drug dissolution and antimicrobial activity for prodrug based active moieties.

Keywords: Cefpodoxime proxetil, Nanosuspension, Prodrug, Solubility enhancement, Oral bioavailability enhancement, Pharmacokinetic study.

Introduction

Antibiotics are crucial for prophylactic and therapeutic treatment of bacterial infections, and supporting complex medical procedures by effectively targeting and controlling bacteria. They have contributed to more than 70% reduction in fatalities from infectious disease (1). Cephalosporin are crucial antibiotics known for their broad-spectrum activity, making them efficient at combating diverse bacterial infections (2). They are widely used due to their efficacy, lower resistance rate and low toxicity compared to other antibiotic classes (3). Cefpodoxime proxetil (CP) belongs to third-generation cephalosporin family and a broad-spectrum antibiotic. They effectively target a wide range of gram-positive and gram-negative bacteria by inhibiting the synthesis of bacterial cell wall. They effectively treat urinary and respiratory tract infections. Cefpodoxime proxetil after oral administration absorbed through the GI tract. It undergoes hydrolysis to convert into active form cefpodoxime (4). Despite being formulated to enhance permeability and bioavailability, CP still has 50% oral bioavailability (5). It is due to poor solubility in an aqueous base, which results in CP with poor dissolution characteristic leads to lower bioavailability (6). CP shows pH-dependent solubility, showing typical gelation behavior in acidic conditions. To improve its solubility various conventional and novel drug delivery approaches were explored such as sol-

id dispersion (7), solid-lipid nanoparticles (SLN) (8), self-nanoemulsifying drug delivery system (SNEDDS) (9), nanoparticles (10), nano-emulsion (11), microparticles (12).

Nanosuspension (NS) technology has great potential in drug delivery to address solubility-related challenges of drugs with poor solubility (13). A reduction in drug particle size to the nanometer range enlarges surface area for dissolution, which improves bioavailability of drug (14). Nanosuspension are colloidal dispersion of drug particles at nano-scale in an aqueous base, stabilized by suitable stabilizers (surfactant, polymers, or mixture of both). Nanosuspension are unique owing to their simplicity and advantages over other formulation strategies (15). Nanosuspension are effective in controlled drug delivery systems, maintaining the drug in crystalline state with reduced particle size, that improves bioavailability. The nanosized particles enhance saturation solubility (16). Compared to liposome and other conventional colloidal drug carriers, nanosuspension are simple, cost-effective approach to produce a physically more stable product.

Two methods employed for manufacturing nanosuspension; Bottom-up process and top-down process (17). Solvent-antisolvent precipitation method has been employed to produce submicron sized particles for drugs with poor solubility. This is easy, scalable and cost-effective technique. The drug is dissolved in organic solvent and mix with miscible antisolvent (18). This creates a high concentration gradient, which enhances supersaturation by reducing the diffusional pathway around drug nanoparticles. The disruption of drug crystal into nanoparticles can generate high-energy surfaces, increasing saturation solubility, dissolution rate, and oral bioavailability (19). The increased surface area also increases saturation solubility for nanosized drug particles (5). To ensure a stable nanosuspension and prevent Ostwald ripening, a phenomenon where smaller particles dissolve and accumulate on larger ones, it is crucial to maintain uniform particle size. This uniformity avoids instability caused by large variations in particle size (20).

The present research focused on developing CP-NS to improve the solubility and bioavailability. The Box-Behnken design with three-level, three factor was employed to formulate CP-NS by solvent-antisolvent precipitation method using probe sonication technique. Further, CP-NS were analysed for particle size, zeta potential, polydispersity index (PDI), antimicrobial study, in vitro drug release, in vivo pharmacokinetic and stability study.

Materials and Methods

Chemicals

Cefpodoxime proxetil was received as gift sample from Indoco remedies, Mumbai India. Sodium lauryl sulphate (SLS), poloxamer-188 (P-188), polyvinylpyrrolidone (PVP) K30 were sourced through Loba (Mumbai, India). O-phosphoric acid (HPLC grade), acetonitrile (ACN), methanol (HPLC grade), potassium dihydrogen phosphate, sodium dihydrogen orthophosphate anhydrous, were purchased from Merck and Loba (Mumbai, India).

Preliminary studies

Selection of stabilizer - Stabilizer were screened among categories like: Anionic stabilizers (SLS), Non-ionic stabilizers (PVA, Tween 80, PEG, P-188), and Polymeric stabilizers (HPMC, PVP K30) (21). The CP is cationic in nature to provide better stabilization the anionic and non-ionic stabilizers were selected (22). The solubility of CP in the various stabilizer solutions was evaluated using incubator shaker. 1% w/v stabilizer solution (10 ml) prepared and excess amount of drug was added. These sample were shaken on an incubator shaker at the maximum speed of 20 rpm for 24 h to reach equilibrium (23). After 24 h, sample were filtered through Whatman filter paper. The aliquot was analysed by UV-spectrophotometer at 235 nm.

QbD approach for optimization of CP nano-suspension

Experimental design

The conventional approaches for drug formulation development often face challenges being time consuming, unpredictable and costly. To address these pitfalls Design of Experiment (DoE) was utilized. DoE provides systematic way to investigate the effect of variables on responses. It reduces costs and time while ensuring reliable, reproducible optimization and more accurate identification of optimal conditions (24). The Box-Behnken Design (BBD) provides several benefits over traditional methods, such as more efficient resources use and simpler experimentation (25). It requires fewer runs for accurate results, enabling precise modelling of interactions and quadratic effects. The BBD with three variables and three level were applied to optimize the CP-NS. In this design, the experimental space was considered as cube (26). As per BBD, 15 runs were conducted with three variables and three level. The mid-point was repeated three times. On the basis of preliminary analysis the experimental range of variables selected for design. The independent variables (X) are concentration of (stabilizer) P-188 (X_1), concentration of (surfactant) SLS (X_2), and ultrasonication time (X_3) with three levels (−1, 0, and +1). The dependent variables (Y) are particle size (Y_1) and percent entrapment efficiency (Y_2). These variables were chosen due to their significant effect on responses. Table 1 and 2 display the variable design and data of all 15 runs. The design and assessment of experiment were conducted using Design-Expert® software version 11.

Table 1. Variables and levels in Box-Behnken design

Factors	Levels		
Independent variables	Low	Medium	High
X□= Concentration of poloxamer-188 (mg)	10	30	50
X□= Concentration of SLS (mg)	5	10	15
X_3= Ultrasonication time (min)	5	10	15
Response variables			
R□: Particle size (nm)	Minimize		
R□: Entrapment efficiency (%)	Maximize		

Table 2. Box-Behnken design experimental runs.

Batch	X_1 (P-188: mg)	X_2 (SLS: mg)	X_3 (Time: min)
1	50	5	10
2	50	10	5
3	50	10	15
4	50	15	10
5	30	5	5
6	30	5	15
7	30	10	10
8	30	10	10
9	30	10	10
10	30	15	5
11	30	15	15
12	10	5	10
13	10	10	5
14	10	10	15
15	10	15	10

$$Yi = b0 + b1X_1 + b2X_2 + b3X_2 + b1X_1^2 + b2X_2^2 + b3X_3^2 \qquad .... (1) (26)$$

The response for each factor at particular level predicted by the regression equation expressed as coded variables. The relative impact of the variable can be determined by coded equation.

Preparation of nanosuspension

Cefpodoxime proxetil nanosuspension (CP-NS) was formulated by the solvent-antisolvent precipitation technique. Weighed quantity of CP was dissolved in ethanol. Simultaneously to prepare an aqueous solution the required quantity of P-188 as a stabilizer and SLS as surfactant was dispersed in distilled water. Ethanol-CP solution were dropwise added into aqueous base at 1200 rpm under magnetic stirring. This dispersion was further subjected to probe ultrasonication for 10 min with 30% amplitude as represented in Figure 1 (27).
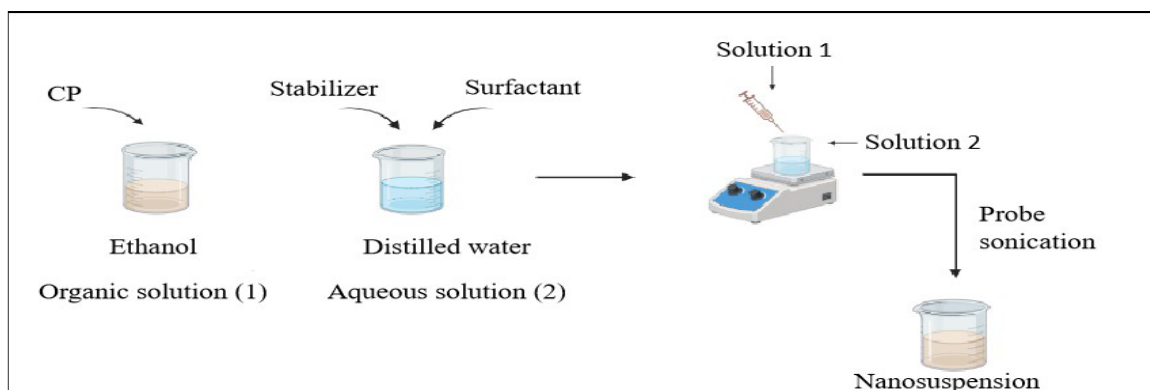

Figure 1. Preparation of cefpodoxime proxetil nanosuspension (CP-NS) by solvent-antisolvent precipitation method.

Analytical characterization of nanosuspension

Particle size and zeta potential

The particle size and zeta potential of CP-NS were analyzed by particle size analyzer (Nanopartica, HORIBA Scientific). All experiments were conducted in triplicates.

Entrapment efficiency

To determine entrapment efficiency (% EE), the free drug present in 1mL CP-NS dispersion was determined by centrifugation (Allegra 64R Benchtop Centrifuge, Beckman Coulter, USA) (28). 1mL of prepared formulation was centrifuged at 18,000 for 30 minutes. The supernatant is separated, filtered and analyzed by UV-spectrophotometer (JASCO V- 730, Japan) at 235 nm. The study was performed in triplicate. The entrapment efficiency was determined using the following equation:

$$\%EE = \frac{Total\ amount\ of\ drug\ added - amount\ of\ free\ drug}{Total\ amount\ of\ drug\ added} \times 100$$

Transmission electron microscopy

The morphological evaluation of CP-NS was analyzed by Transmission electron microscopy (TEM, Philips, CM 200). A thin layer of CP-NS placed on copper grid (#400) and negatively stained by phosphotungstic acid. The solution was applied to grid and allowed to sit for 60 seconds. At ambient temperature, the TEM images were captured (29).

FTIR analysis

FTIR spectra of CP, physical mixture (PM) and CP-NS were obtained with JASCO FTIR-4100 spectrometer (Japan). Potassium Bromide (KBr) was combined with sample (2-3mg) and filled in the cavity. The sample was scanned over the range of 4000 - 400 cm^{-1} wave numbers (30).

Saturation solubility

Solubility studies of CP and CP-NS formulation were evaluated by adding excess drug and lyophilized CP nanosuspension to the vial

containing water, hydrochloride buffer (0.1N HCL) and phosphate buffer (PBS). The vials were placed on shaker incubator for about 24h, then a specific volume of aliquots was taken and centrifuged at 15,000 rpm at 25ºC for 15 minutes (23).The supernatant was filtered and assayed using UV-visible spectrophotometer (JASCO V-730, Japan) at 235 nm. The results measured in triplicate.

Differential scanning calorimetry studies (DSC)

DSC was carried out using a thermal analysis system (DSC7020, HITACHI) of CP, P-188, SLS, PM, and CP-NS. The 1mg sample were heated at 1- 400°C at a constant rate of 10°C/min, in aluminium pan under a nitrogen atmosphere (31).

X-ray diffraction studies (XRD)

The XRD analysis of CP, PM and CP-NS were recorded on X-ray diffractometer (Miniflex 300/600, Rigaku Tokyo, Japan). The samples were kept in aluminium sample holder and scanning rate was about 1°/min and the scanning range of 2θ in the range of 2-80° (31).

In-Vitro dissolution profile

Dialysis bag technique was employed to determine the drug release profile of pure drug (CP dispersion), CP-NS formulation, and CP marketed formulation (suspension). The dialysis bag (molecular weight:12000 -14000 g/mol) was prepared by soaking it in dissolution media for 24 h before initiation of study. A pre-treated dialysis bag was filled with 2ml of CP-NS and sealed at both ends. The sac was placed in 40 ml of freshly prepared acidic medium (pH 1.2) for 4 h with stirring at 100 rpm on magnetic stirrer (REMI 1MLH). 1ml of sample were drawn at pre-determined time points (0.25, 0.5, 1, 1.5, 2, 2.5, 3, 4, and 5h) and same volume of fresh media added to maintain sink condition. The release study of CP dispersion and marketed formulation were conducted with same experimental conditions. The samples were filtered

and analyzed using UV-spectrophotometer at 235 nm. All experiment conducted in triplicate and data were analyzed using kinetic models (zero-order, first-order, korsemeyer-peppas, and Higuchi). The mechanism of drug release were determined by using the regression coefficient (r^2). Invitro release data of CP-NS was compared with pure drug and marketed formulations (32).

Antimicrobial efficacy study

The assessment of antimicrobial activity was done by agar well diffusion test. The medium used was Mueller Hinton agar for *E.coli* and *S.aureus*. Micro-organisms were inoculated into Mueller Hinton agar medium, and kept at 45ºC. A microbial suspension (100 µl) was spread uniformly on surface of Mueller Hinton agar for inoculation. Then, four perforation each of depth 5 mm were made in which the marketed formulation, CP, CP-NS and dimethyl sulfoxide (control) were placed. Petri-plates were incubated at 37ºC for 24 h. The size of inhibition zone (mm) around micro-organism was used to determine the results (33).

In-vivo pharmacokinetic study

Animal and dosing

Male wistar rats of 200-250 g were procured from Global Biosciences Pvt Ltd. The Institutional Ethics Animal Committee (IEAC) approved the investigation and experiment were conducted in compliance with CPCSEA guideline in India. Re. No. 1703/PO/Re/S/01/CPCSEA, dated 17/06/2016 Approval No. CPCSEA/PCP/2024-1-15. The rats were randomly assigned to three groups, each consisting six animals and housed under controlled conditions of 25±1ºC and humidity 55±5% with 12 h light/ dark condition. Before the initiation of experiment, the animals were fasted overnight but had free access to water. Oral administration of CP, CP-NS and CP marketed formulation at dose of 10 mg/kg were received by three groups of rats (12). After oral administration 0.5 ml blood was collected from the retro-orbital plexus at

predefined intervals of 0.5, 1, 2, 4, 6, 8, 12, and 24h. Plasma sample were collected and centrifuged at 6000 rpm for 15 min at 4 ºC and stored at -20 ºC (9,34).

Plasma sample preparation and analysis

CP was determined by HPLC (Jasco,PU-2080 plus, UV-2075plus, Japan) method. The mobile phase was composed of ammonium acetate buffer (pH 5) and acetonitrile 55:45 v/v and was eluted at flow rate of 1.0 ml/min with UV detection at 235 nm. Plasma samples were precipitated with methanol in 1:1 ratio. The sample centrifuged at 6000 rpm for 10 min and filtered by 0.45µm membrane filter. The supernatant (20µL) was introduced into the HPLC for analysis (35).

Pharmacokinetic and statistical analysis

Analysis of pharmacokinetic parameter was performed by PKSolver, Microsoft Excel add-in (version 2.0). The pharmacokinetic profiles of t_{max}, C_{max} and $AUC_{0 \to 24h}$ were determined.

Stability studies

The stability of CP-NS formulation were investigated under two distinct condition 4ºC and 30ºC/60% RH for 3 months. Particle size and PDI analysis of formulation were performed (36).

Results and Discussion

Selection of stabilizer

Preliminary selection of stabilizer was based on drugs solubility in selected stabilizer. CP showed maximum solubility in tween 80, which could be due to amphiphilic nature of CP. If drug is more soluble in stabilizer solution, leading to Ostwald ripening. It is phenomenon in which the particle size increases on storage leading to instability of nanosuspension. Hence tween 80 were not consider for further studies (9). P-188 shown lowest solubility as shown in Figure 2. Preparation of CP-NS with P-188 results in least particle size and PDI. On the other hand, the particle size of P-188 with SLS

remains unchanged compared to P-188 alone. Hence, to prevent the aggregation of nano-sized particle the combination of P-188 and SLS were preferred as steric stabilizer.
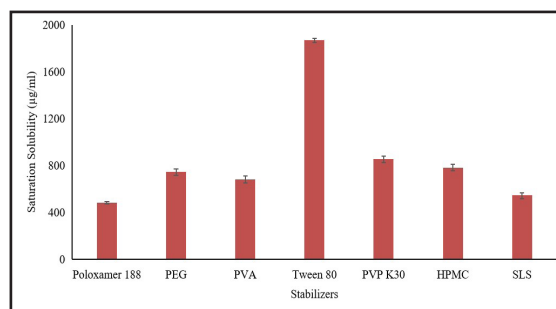
Figure 2. Saturation solubility of Cefpodoxime proxetil (CP) with different stabilizers.

Development of CP nanosuspension and experimental Design

The influence of the concentration of P-188 (X_1), concentration of SLS (X_2), and the ultrasonication time (X_3) on response particle size (Y_1) and entrapment efficiency (Y_2) were analyse by using Box-Behnken Design (BBD). Table 3 contain response information corresponding to each of 15 runs. The responses were analysed using various statistical parameters to select a quadratic model. The predicted R^2 and adjusted R^2 values ranges from 0.98 to 1, model with statistical significant p-value ($p < 0.05$) and p-value ($p > 0.10$) reflecting an insignificant lack of fit. The particle size (Y_1) and entrapment efficiency (Y_2) of the responses vary between 126±18 nm and 305±7 nm and 52.88±19.13% to 86.52±25.56%, respectively.

Table 3. BBD presenting the value of response obtained for CP nanosuspension

Run	X_1	X_2	X_3	Y_1	Y_2
	mg	Mg	min	nm	%
1	50	5	10	292 ± 4	64.47 ± 7.1
2	50	10	5	176 ± 12	52.88 ± 19.13
3	50	10	15	126 ± 18	83.26 ± 8.11
4	50	15	10	280 ± 14	68.32 ± 10.42
5	30	5	5	240 ± 18	59.65 ± 21.68
6	30	5	15	157±16	68.12 ± 9.78

Engineering cefpodoxime prodrug using nanosuspension approach to modulate solubility, antimicrobial and pharmacokinetic profile

7	30	10	10	152 ± 10	86.52 ± 25.56
8	30	10	10	143 ± 9	74.35 ± 13.25
9	30	10	10	148 ± 21	79.98 ± 6.47
10	30	15	5	209 ± 5	84.98 ± 12.5
11	30	15	15	176 ± 20	52.72 ± 19.44
12	10	5	10	305 ± 7	69.87 ± 16.34
13	10	10	5	230 ± 14	68.38 ± 2.15
14	10	10	15	126 ± 10	69.32 ± 8.74
15	10	15	10	298 ± 19	74.21 ± 17.14

[(X_1)-Concentration of Poloxamer-188, (X_2)-Concentration of SLS, (X_3)-Ultrasonication time, (Y_1)- Particle size and (Y_2)- Entrapment efficiency. Data are presented as mean ± SD (n = 3)]

Table 4 presents analysis of variance (ANOVA) for response variable of particle size (Y_1) and entrapment efficiency (Y_2). If p-value of model is ($p < 0.05$), ANOVA suggest response is significant. ANOVA determines the degree of influence, significance and correlation. Variance in adjusted R^2 and predicted R^2 was less than 0.3, indicating that the values of the response were precisely predicted by the model. Polynomial Eqs. (3), (4) are derived from regression analysis.

$$Y1 = 152 - 6A - 16.13B - 39.88C - 1.25AB + 42.75 AC + 24BC + 62.92A2 + 45.17B2 - 19.83C2 \quad .....(3)$$

$$Y2 = 85 - 2.23A + 0.84B - 2.61C - 0.29AB - 2.88AC - 7.10BC - 6.07A2 - 9.87B2 - 11.79C2 \quad ....(4)$$

In model, the negative coefficient indicates a contradictory effect, whereas a positive coefficient suggests a synergistic effect.

Table 4. Quadratic response surface model of the ANOVA for particle size and entrapment

| Source	Sum of square Particle size (nm)	Entrapment efficiency (%)	F-value Particle size (nm)	Entrapment efficiency (%)	P-value Particle size (nm)	Entrapment efficiency (%)
Model	54777.52	1222.89	8.33	27.47	0.0155	0.0010
X1	1352.00	39.92	1.85	8.07	0.2320	0.0362
X2	1176.13	5.76	1.61	1.17	0.2605	0.3297
X3	780.13	54.29	1.07	10.97	0.3490	0.0212
X1X2	6.25	0.3481	0.0085	0.0704	0.9299	0.8014
X1X3	4556.25	33.24	6.23	6.72	0.0547	0.0487
X2X3	3364.00	201.50	4.60	40.73	0.0848	0.0014
X1²	13255.41	135.97	18.13	27.49	0.0080	0.0033
X2²	17157.03	359.94	23.47	72.76	0.0047	0.0004
X3²	11101.64	512.88	15.19	103.68	0.0114	0.0002
Residual	3655.42	24.73	-	-	-	-
Lack of fit	710.75	17.62	0.1609	1.65	0.9143	0.3988
Pure error	2944.67	7.12	-	-	-	-
Cor Total	58432.93	1247.62	-	-	-	-
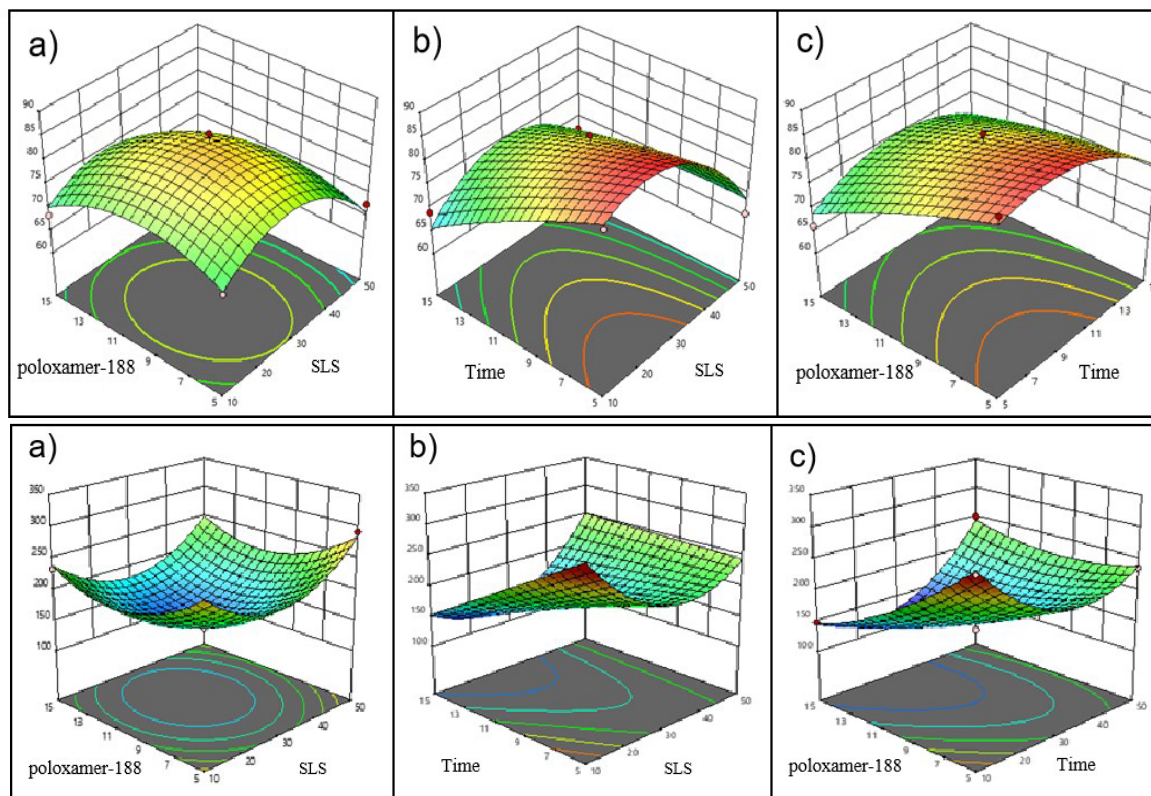
Figure 3. Response surface plot illustrating the effect of concentration of the Poloxamer-188, concentration of the Sodium lauryl sulphate (SLS) and Ultrasonication time upon 1) Particle size (nm) and 2) Entrapment efficiency (%).

Effect on particle size

Particle size is key parameter in improving the solubility of drugs with poor solubility. A decrease in particle size, increases surface area leading to improved saturation solubility. Figure 3-1. a) illustrates the impact of P-188 concentration on particle size. The optimal concentration of P-188 significantly reduces the particle size in the nanosuspension. However, both lower and higher concentrations of the stabilizer lead to increased particle size. At low stabilizer concentrations, resulting in larger particle sizes. The effect of concentration of SLS was similar to P-188. Furthermore, Figure 3-1.c) demonstrates that increasing ultrasonication time significantly reduces particle size in the nanosuspension. This reduction was attributed to the fragmentation of particles facilitated by ultrasonic waves (28).

Effect on entrapment efficiency

The concentration of P-188 significantly impacts entrapment efficiency, with both low and high concentrations. As P-188 concentration increases, flocculation and aggregate formation occur, resulting in lower entrapment efficiency (37). Conversely, increasing the concentration of SLS shows a slight improvement in entrapment efficiency, as depicted in Figure 3-2.b) Additionally, prolonged ultrasonication time gradually reduces entrapment efficiency, likely due to increased attrition and generation of mechanical energy. This extended sonication causes larger particles to break down into smaller ones, further affecting entrapment efficiency.

Establishment of design space and model validation

Design-Expert software (version 11) was used to assess design space in order to achieve optimized CP-NS. A numerical optimization approach was used to select optimized CP-NS, based on desirability value near to 1. The optimal formulation were determined by criteria of minimum particle size and maximum entrapment efficiency. The optimized nanosuspension (b7) was prepared with 0.5% w/v SLS, 1.5 % w/v P-188 under controlled sonication time. The observed R^2 and predicted R^2 values are 0.995- 0.988 shows a linear correlation (38). The results of validation trials showed robustness and feasibility of design.

TEM Analysis

The morphology of CP-NS was analysed by TEM. The resulting TEM micrograph of CP nanosuspension was presented in Figure 4. TEM analysis showed suspended nanoparticles was uniformly distributed and approximately spherical in shape. The size of the nanoparticles was found to be between 150-250 nm.
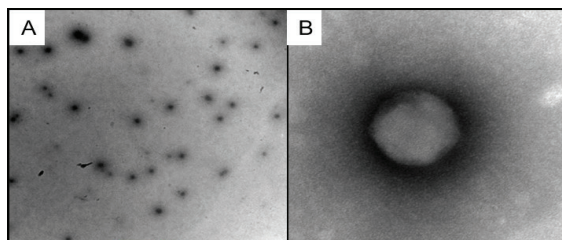

Figure 4. A. TEM image of Cefpodoxime proxetil (CP) nanosuspension on 500 nm scale and B. 100 nm scale.

FT-IR analysis

FTIR was used to evaluate any chemical modification between drug (CP) and stabilizer (P-188, SLS). The spectra of CP, P-188, SLS, PM and CP-NS were shown in Figure 5. CP displayed a characteristic amide C-N stretching vibration band at 1650 cm^{-1}, a C-O stretching band at 1074 cm^{-1} and carbonyl C-H band at

2950 cm^{-1} (39). The FTIR spectra of P-188 display aromatic C-H stretching peak at 2851 cm^{-1}, C-O-C poly (ethylene oxide) stretching at 1079 cm^{-1} and O-H stretching peak at 3404 cm^{-1}. For SLS C-O stretching at 1657 cm^{-1} and C-O stretching at 1657 cm^{-1} was observed. Consistent with the literature finding (40) Figure 5 presents the spectra for CP, P-188, and SLS. The interaction between the drug and stabilizer can be significantly influence these characteristic peaks, either by altering the intensity or causing a variation in wavenumber. The PM showed no spectral shift being simply overlay of CP, P-188, and SLS, suggesting the stabilizer and drug had no interaction.

Figure 5. FTIR spectra of A. Cefpodoxime proxetil (CP) B. Poloxamer-188 (P-188) C. Sodium lauryl sulphate (SLS) D. Physical mixture (PM) E. Cefpodoxime proxetil nanosuspension (CP-NS).

Differential scanning calorimetry

DSC analysis was conducted to confirm the physical state of CP in nanosuspension and compare it with CP, P-188, SLS and PM. As shown in Figure 6, CP exhibited single melting endothermic peak at 95.1ºC, with a fusion enthalpy of (ΔH) of 0.76 mW/min. The DSC profiles of P-188 and SLS exhibited sharp melting peaks at 49.53ºC and 198.47ºC respectively. The PM exhibited broadened endothermic peak of CP at 103ºC with an enthalpy change (ΔH) at 1.65 mW/min, indicating possible interaction between drug and excipients. The presence of distinct peak suggest the drug retain some of its crystalline properties in PM (41). The appearance of same peaks between PM and CP-NS

can be attributed to melting peaks of P-188 and SLS. In the CP-NS, melting peak of CP was absent, indicates reduction in crystallinity and conversion to amorphous state. The amorphization is attributed to nanosizing process and stabilization by excipient such as P-188 and SLS during the formation of nanosuspension (42). These finding suggest that during nanosuspension formation, CP nanoparticles transitioned from a crystalline state to amorphous

state which improve solubility and beneficial for enhancing the bioavailability of drug (43).
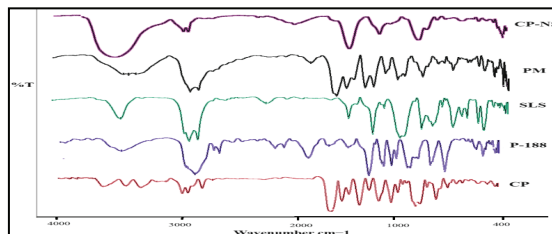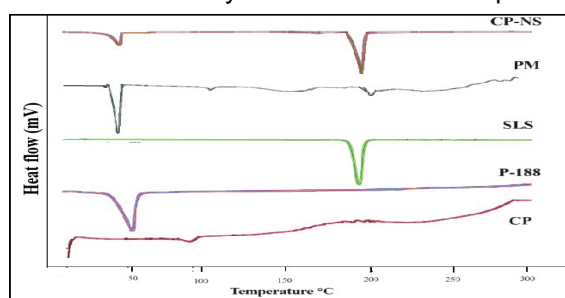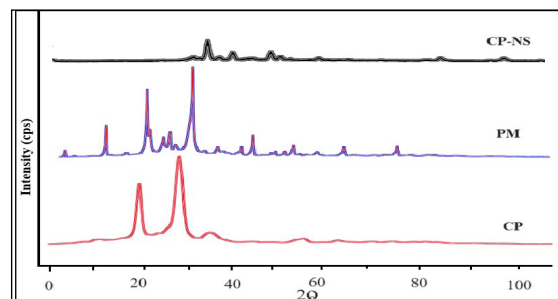
Figure 6. DSC patterns of A. Cefpodoxime proxetil (CP) B. Poloxamer-188 (P-188) C. Sodium lauryl sulphate (SLS) D. Physical mixture (PM) E. Cefpodoxime proxetil nanosuspension (CP-NS).

X-ray diffraction

XRD analysis were carried out for validation of crystalline form of CP and the amorphous state of CP nanosuspension. Figure 7 shows the XRD of CP, PM, and CP-NS. The diffraction pattern revealed that CP exhibited distinct high-energy diffraction peak at 19.88° and 23.35°, which demonstrated that CP was crystalline in nature. Due to crystalline structure, it often results in poor solubility. The diffraction pattern of the PM reveal the peak similar to CP which indicate CP in crystalline form. The CP-NS displayed peaks at 31.55° and 40.03°, with significant reduction in intensity of crystalline peaks and some of the characteristic peaks of CP was absent. This suggest that crystalline CP was transitioned to amorphous form in the nanosuspension (44). A drug in amorphous form possesses a higher-energy state, which pro-

vides the benefit of enhanced solubility. This results in a faster dissolution rate and consequently, improved oral bioavailability (45).

Figure 7. XRD spectrum of A. Cefpodoxime proxetil (CP) B. Physical mixture (PM) C. Cefpodoxime proxetil nanosuspension (CP-NS).

Stability studies

Physical stability study was carried out by storage of CP-NS at two different conditions at 4°C and 30°C/60% RH over a period of 3 months. The particle size and PDI was assessed after preparation and periodically over a 3 month under various conditions Table 5. The particle size of formulation stored at 30°C/60% RH increased significantly (p < 0.05) after 3 months. In contrast, the formulation stored at 4°C showed no significant change in particle size or PDI (38). The CP-NS formulation shown physical instability at 30°C/60% could be due to aggregation in nanosuspension, which was influenced by high temperature and humidity. These factors are known to adversely affect drug nucleation and accelerate the rate of crystallization.

Table 5. Comparison of the mean particle size and PDI of nanosuspension after 3 months of storage at 4°C and 30°C with initial values.

	Initial	1 month		3 month	
		4 °C	30 °C	4 °C	30 °C
Particle size (nm)	136 ± 5	140 ± 5	150 ± 8	145 ± 10	170 ± 10
PDI	0.22 ± 0.08	0.22 ± 0.3	0.23 ± 0.3	0.22 ± 0.4	0.24 ± 0.5

Saturation solubility

CP is crystalline in nature and exhibit poor solubility. The saturation solubility in water was 0.266 ± 0.004 mg/mL. However, upon formulation into nanosuspension (CP-NS) showed five-fold increase in saturation solubility in water. It is due to significant reduction of particle size in the nanosuspension. The reduced particle size leads to larger surface area, facilitating better interaction with dissolution media (46). The saturation solubility was carried out in different pH conditions (1.2, 6.8). As shown in Figure 8, the results of saturation solubility depicts CP exhibits pH-dependent solubility. CP has ionizable functional group that change with pH levels. In acidic pH drug remain protonated thus increasing its solubility. However, at alkaline pH, deprotonation can cause degradation of drug and decrease its solubility (47).
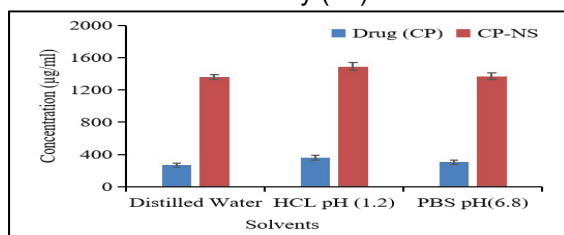
Figure 8. Saturation solubility of Cefpodoxime proxetil (CP) and Cefpodoxime proxetil nanosuspension (CP-NS) in distilled water, HCL pH (1.2) and PBS pH (6.8).

In-Vitro Dissolution Study

The dissolution profile for CP, CP-NS and CP marketed formulation were shown in Figure 9. The CP-NS exhibit better in-vitro drug release than CP and CP marketed formulation. The release of CP from the CP-NS was > 90% within 2 h, while those for pure drug was 40% and 65% for CP marketed formulation. The reason might be enhanced surface area by reducing particle size, decreases thickness of diffusional layer, and increases concentration gradient between particle surface and bulk solution, thereby improving bioavailability (46). Furthermore the dissolution rate significantly influence by state of drug in nanosuspension.

Previous studies, including XRD and DSC analysis, indicated the amorphization of CP in CP-NS formulation. The drug in amorphous form has increased molecular mobility and higher internal energy promoting solubility (48). CP-NS release followed the Korsmeyer–Peppas model (R=0.97, n=0.063) indicating exponential drug release over time.

Figure 9. Comparative in-vitro dissolution profile of the Cefpodoxime proxetil (CP), Cefpodoxime proxetil nanosuspension (CP-NS) and CP marketed formulation.

Antimicrobial Efficacy Study

The antimicrobial activity of CP were investigated by using *E. coli* and *S. aureus* micro-organism. For 24 h, the petri plates were incubated at 37ºC. The results were assessed by measuring diameter (mm) of the inhibition halo around microbial growth and the calculation of the area of inhibition (49). The antimicrobial activity of the CP-NS against the *E. coli* and *S. aureus* micro-organism can be depicted with the help of petri plate photograph. Figure 10 (1) and 10 (2) depicts the CP-NS showed 36.5 mm^2 and 32.6 mm^2 area of inhibition compared with CP marketed formulation, pure CP and DMSO against *E. coli* and *S. aureus* micro-organism, respectively.
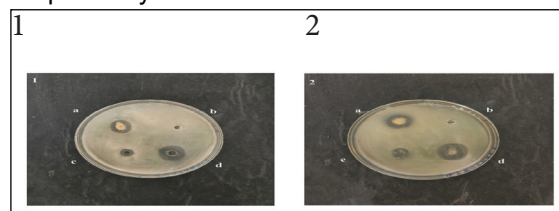
Figure 10. Average inhibition halo (mm) against 1. *Escherichia coli*, 2. *Staphylococcus aureus.*

In-vivo pharmacokinetic study

The plasma concentration of CP was measured by a HPLC method, which demonstrated linearity within the range of 1-1000 µg/mL and exhibited high accuracy and specificity.

The Table 6 present pharmacokinetic data for orally administered CP, CP marketed formulation and CP-NS. The plasma drug concentration-time profiles after oral administration at a dose of 10 mg/kg CP solution shown in Figure 11.

Table 6. Pharmacokinetic parameters of CP in wistar rats after oral administration of CP, CP marketed formulation, and CP-NS.

Parameters	CP	CP marketed formulation	CP-NS
C_{max} (µg/mL)	355±20	621±28	1624±214
T_{max} (h)	2	2	2
$AUC_{0\rightarrow24h}$ (µg/mL)	1542±34	2674±54	7117±320

*Data are presented as mean ± SD (n = 3).

Pharmacokinetic data reveals significant and remarkable insights. A significant difference was observed in the plasma concentration-time profile of CP, CP-NS, and CP marketed formulation (Figure 11). C_{max} and AUC are key parameters revealing insights about the rate and extent of absorption. The results shows 4.5-folds and 2.6-folds higher C_{max} of CP-NS when compared to C_{max} of CP and CP marketed formulation respectively. The relative bioavailability of CP-NS was 4.3-folds as compared to CP and CP marketed formulation. In-vivo results of current study were better than the literature which reports o/w submicron emulsion of CP with 2.1-folds enhanced AUC of optimized batch (50). The outcome of in-vivo study showed a remarkable enhancement in the absolute bioavailability of CP as nanosuspension. This was because the decrease in particle size leads to increase in rate of dissolution as explained by Noyes-Whitney equation.
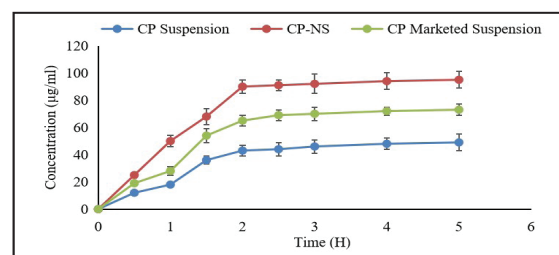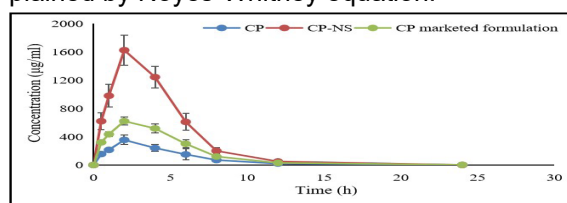

Figure 11. Plasma drug concentration time profile of the Cefpodoxime proxetil (CP), Cefpodoxime proxetil nanosuspension (CP-NS) and CP marketed formulation after oral administration (10 mg/kg).

Conclusion

Cefpodoxime proxetil nanosuspension using the solvent-antisolvent precipitation technique is successfully prepared to enhance solubility and antimicrobial activity. Optimization using the Box-Behnken Design resulted in batch (B7), which shows a low particle size and highest entrapment efficiency. The particle size of developed nanosuspension ranged from 126 ± 18 to 305 ± 7 nm. Physicochemical characterisation, such as DSC and XRD studies confirmed the formation of amorphous CP nanoparticles within the nanosuspension. The CP-NS showed a 5-fold enhanced solubility. In vitro dissolution studies revealed that CP-NS exhibit increased dissolution rate 2-fold than pure drug and 1.3-fold higher than marketed formulation. Stability studies indicated that nanosuspension was stable when stored at 4ºC. The storage conditions affected particle size and PDI. Antimicrobial efficacy studies demonstrated the effectiveness of CP-NS against *E.coli* and *S.aureus* micro-organism. Finally, in vivo pharmacokinetic data showed 4.3-fold improvement in bioavailability of CP-NS than pure drug and marketed formulation. Overall, CP-NS formulation showed promising results in terms of solubility enhancement and antimicrobial activity. Further studies, the pharmacodynamic study can be performed to confirm the safety and efficacy of the cefpodoxime proxetil nanosuspension. Studies on long-term stability will ensure the product's quality

and shelf life, which is necessary for a successful commercialization.

Acknowledgment

Author Contribution

Prerana Bhosale wrote original draft, methodology, validation, investigation. Dr. Vividha Dhapte-Pawar conceptualized, investigated, data curated. Priyanka Gawarkar-Patil reviewed and edited. Dr. Atmaram Pawar supervised and critiqued the manuscript.

Declaration of competing interest

The authors declare that they have no known competing financial interests or personal relationships that could have appeared to influence the work reported in this paper.

References

1. Aminov, R.I., 2010. A brief history of the antibiotic era: lessons learned and challenges for the future. *Frontiers in microbiology*, 1, p.134.

2. Mehta, D. and Sharma, A.K., 2016. Cephalosporins: A review on imperative class of antibiotics. *Inventi Rapid: Molecular Pharmacology*, 1(3), pp.1-6.

3. Christian, S.S. and Christian, J.S., 1997. The cephalosporin antibiotics. *Primary Care Update for OB/GYNS*, 4(5), pp.168-174.

4. Chappa, A.K., 2007. Case Study: Vantin: A Prodrug of Cefpodoxime. *Prodrugs: Challenges and Rewards Part* 1, pp.1387-1394.

5. Gao, Y., Qian, S. and Zhang, J., 2010. Physicochemical and pharmacokinetic characterization of a spray-dried cefpodoxime proxetil nanosuspension. *Chemical and Pharmaceutical Bulletin*, 58(7), pp.912-917.

6. Borin, M.T., 1991. A review of the pharmacokinetics of cefpodoxime proxetil. *Drugs*, 42(Suppl 3), pp.13-21.

7. Deepa, M., Trivedi, L.M., Kolay, A., Yadav, A.K., Nile, N.P., Tiwari, A.K., Bhyan, B., (2023). Development and evaluation of a mucoadhesive microsphere solid dispersion containing cefpodoxime. Journal of Cardiovascular Disease Research, 14(7), pp 106-129.

8. Nimbalkar, U.A., Dhoka, M.V. and Sonawane, P.A., 2011. Solid lipid nanoparticles for enhancement of oral bioavailability of cefpodoxime proxetil. *International Journal of Pharmaceutical Sciences and Research*, 2(11), p.2974.

9. Bajaj, A., Rao, M.R., Khole, I. and Munjapara, G., 2013. Self-nanoemulsifying drug delivery system of cefpodoxime proxetil containing tocopherol polyethylene glycol succinate. *Drug Development and Industrial Pharmacy*, 39(5), pp.635-645.

10. Özel, D. and Yurt, F., 2020. Investigation of radiolabelled chitosan nanoparticles bearing Cefpodoxime Proxetil, and in vitro antibacterial effect on Gram-positive Staphylococcus aureus and Gram-negative Escherichia coli. *Journal of Radioanalytical and Nuclear Chemistry*, 326, pp.1551-1558.

11. Xue, J. and Tian, J., 2023. Retrospective analysis of cefpodoxime proxetil dispersible tablets in the treatment of respiratory tract infection in children and study of the antibacterial effect of cefpodoxime proxetil nanoemulsion. *Materials Express*, 13(4), pp.717-723.

12. Khan, F., Katara, R. and Ramteke, S., 2010. Enhancement of bioavailability of cefpodoxime proxetil using different poly-

meric microparticles. *AAPS PharmSci-Tech*, 11, pp.1368-1375.

13. Yadollahi, R., Vasilev, K. and Simovic, S., 2015. Nanosuspension technologies for delivery of poorly soluble drugs. *Journal of Nanomaterials*, (1), p.216375.

14. Dizaj, S.M., Vazifehasl, Z., Salatin, S., Adibkia, K. and Javadzadeh, Y., 2015. Nanosizing of drugs: effect on dissolution rate. *Research in pharmaceutical sciences*, 10(2), pp.95-108.

15. Jindal, A. and Kumar, A., 2022. Physical characterization of clove oil based self Nano-emulsifying formulations of cefpodoxime proxetil: Assessment of dissolution rate, antioxidant & antibacterial activity. *OpenNano*, 8, p.100087.

16. Behera, A., Nayak, A.K., Mohapatra, R.K. and Rabaan, A.A. eds., 2024. Smart Micro-and Nanomaterials for Pharmaceutical Applications.

17. Park, J., Sun, B. and Yeo, Y., 2017. Albumin-coated nanocrystals for carrier-free delivery of paclitaxel. *Journal of Controlled Release*, 263, pp.90-101..

18. Chinthaginjala, H., Abdul, H., Reddy, A.P.G., Kodi, K., Manchikanti, S.P. and Pasam, D., 2020. Nanosuspension as Promising and Potential Drug Delivery: A Review. 2020. *Int J Life Sci. Pharm Res*, 11(1), pp.P59-66.

19. Aher, S.S., Malsane, S.T. and Saudagar, R.B., 2017. Nanosuspension: an overview. *Asian Journal of Research in Pharmaceutical Science*, 7(2), pp.81-86.

20. Ahmadi Tehrani, A., Omranpoor, M.M., Vatanara, A., Seyedabadi, M. and Ramezani, V., 2019. Formation of nanosuspensions in bottom-up approach: theories and optimization. *DARU Journal of Pharmaceutical Sciences*, 27, pp.451-473.

21. Dhapte, V. and Pokharkar, V., 2011. Polyelectrolyte stabilized antimalarial nanosuspension using factorial design approach. *Journal of Biomedical Nanotechnology*, 7(1), pp.139-141.

22. Dhapte, V., Kadam, V. and Pokharkar, V., 2013. Pyrimethamine nanosuspension with improved bioavailability: in vivo pharmacokinetic studies. *Drug delivery and translational research*, 3, pp.416-420.

23. Rao, M.R., Bajaj, A.N., Pardeshi, A.A. and Aghav, S.S., 2012. Investigation of nanoporous colloidal carrier for solubility enhancement of Cefpodoxime proxetil. *Journal of pharmacy research*, 5(5), pp.2496-2499.

24. Kaithwas, V., Dora, C.P., Kushwah, V. and Jain, S., 2017. Nanostructured lipid carriers of olmesartan medoxomil with enhanced oral bioavailability. *Colloids and Surfaces B: Biointerfaces*, 154, pp.10-20.

25. Fares, A.R., ElMeshad, A.N. and Kassem, M.A., 2018. Enhancement of dissolution and oral bioavailability of lacidipine via pluronic P123/F127 mixed polymeric micelles: formulation, optimization using central composite design and in vivo bioavailability study. *Drug delivery*, 25(1), pp.132-142.

26. Kuk, D.H., Ha, E.S., Ha, D.H., Sim, W.Y., Lee, S.K., Jeong, J.S., Kim, J.S., Baek, I.H., Park, H., Choi, D.H. and Yoo, J.W., 2019. Development of a resveratrol nanosuspension using the antisolvent precipitation method without solvent removal, based on a quality by design (QbD) approach. *Pharmaceutics*, 11(12), p.688.

27. Thorat, A.A. and Dalvi, S.V., 2012. Liquid antisolvent precipitation and stabilization of nanoparticles of poorly water soluble drugs in aqueous suspensions: Recent developments and future perspective. *Chemical Engineering Journal*, 181, pp.1-34.

28. Rangaraj, N., Pailla, S.R., Chowta, P. and

Sampathi, S., 2019. Fabrication of ibrutinib nanosuspension by quality by design approach: intended for enhanced oral bioavailability and diminished fast fed variability. *AAPS PharmSciTech*, 20, pp.1-18.

29. Patil, A.S., Hegde, R., Gadad, A.P., Dandagi, P.M., Masareddy, R. and Bolmal, U., 2021. Exploring the solvent-anti-solvent method of nanosuspension for enhanced oral bioavailability of lovastatin. Turkish Journal of Pharmaceutical Sciences, 18(5), p.541.

30. Li, S., Zhang, J., Fang, Y., Yi, J., Lu, Z., Chen, Y. and Guo, B., 2020. Enhancing betulinic acid dissolution rate and improving antitumor activity via nanosuspension constructed by anti-solvent technique. *Drug Design, Development and Therapy*, pp.243-256.

31. Shelar, D.B., Pawar, S.K. and Vavia, P.R., 2013. Fabrication of isradipine nanosuspension by anti-solvent microprecipitation–high-pressure homogenization method for enhancing dissolution rate and oral bioavailability. *Drug delivery and translational research, 3*, pp.384-391.

32. Md, S., Alhakamy, N.A., Akhter, S., Awan, Z.A., Aldawsari, H.M., Alharbi, W.S., Haque, A., Choudhury, H. and Sivakumar, P.M., 2020. Development of polymer and surfactant based naringenin nanosuspension for improvement of stability, antioxidant, and antitumour activity. *Journal of Chemistry*, 2020(1), p.3489393.

33. Mujtaba, A. and Kohli, K., 2016. In vitro/in vivo evaluation of HPMC/alginate based extended-release matrix tablets of cefpodoxime proxetil. *International journal of biological macromolecules*, 89, pp.434-441.

34. Pahwa, R.A.K.E.S.H., Rana, A.S., Dhiman, S.A.R.I.T., Negi, P.R.E.E.T.I. and Singh, I., 2015. Cefpodoxime proxetil: an update on analytical, clinical and pharmacological aspects. *J Curr Chem Pharm Sc*, 5(2), pp.56-66.

35. Patel, G. and Rajput, S., 2011. Stress degradation studies on cefpodoxime proxetil and development of a validated stability-indicating HPLC method. *Acta chromatographica*, 23(2), pp.215-234.

36. Jakubowska, E., Milanowski, B. and Lulek, J., 2021. A systematic approach to the development of cilostazol nanosuspension by liquid antisolvent precipitation (LASP) and its combination with ultrasound. *International Journal of Molecular Sciences*, 22(22), p.12406.

37. Jadhav, P.A. and Yadav, A.V., 2019. Design, development and characterization of ketorolac tromethamine polymeric nanosuspension. *Therapeutic Delivery*, 10(9), pp.585-597.

38. Shekhawat, P. and Pokharkar, V., 2019. Risk assessment and QbD based optimization of an Eprosartan mesylate nanosuspension: In-vitro characterization, PAMPA and in-vivo assessment. *International journal of pharmaceutics*, 567, p.118415..

39. Patil, P.S., Suryawanshi, S.J., Patil, S.S. and Pawar, A.P., 2024. HME-assisted formulation of taste-masked dispersible tablets of cefpodoxime proxetil and roxithromycin. *Journal of Taibah University Medical Sciences*, 19(2), pp.252-262.

40. Gundogdu, E., Koksal, C. and Karasulu, E., 2012. Comparison of cefpodoxime proxetil release and antimicrobial activity from tablet formulations: Complexation with hydroxypropyl-β-cyclodextrin in the presence of water soluble polymer. *Drug Development and Industrial Pharmacy*, 38(6), pp.689-696.

41. Niwa, T. and Danjo, K., 2013. Design of self-dispersible dry nanosuspension through wet milling and spray freeze-drying for poorly water-soluble drugs. *Euro-*

2267

pean *Journal of Pharmaceutical Sciences*, 50(3-4), pp.272-281.

42. Liu, D., Xu, H., Tian, B., Yuan, K., Pan, H., Ma, S., Yang, X. and Pan, W., 2012. Fabrication of carvedilol nanosuspensions through the anti-solvent precipitation–ultrasonication method for the improvement of dissolution rate and oral bioavailability. *Aaps Pharmscitech*, 13, pp.295-304.

43. Jiang, T., Han, N., Zhao, B., Xie, Y. and Wang, S., 2012. Enhanced dissolution rate and oral bioavailability of simvastatin nanocrystal prepared by sonoprecipitation. *Drug development and industrial pharmacy*, 38(10), pp.1230-1239.

44. Kakran, M., Sahoo, N.G. and Li, L., 2011. Dissolution enhancement of quercetin through nanofabrication, complexation, and solid dispersion. *Colloids and surfaces B: Biointerfaces*, 88(1), pp.121-130.

45. Yang, W., Johnston, K.P. and Williams III, R.O., 2010. Comparison of bioavailability of amorphous versus crystalline itraconazole nanoparticles via pulmonary administration in rats. *European journal of pharmaceutics and biopharmaceutics*, 75(1), pp.33-41.

46. Kathpalia, H., Juvekar, S. and Shidhaye, S., 2019. Design and in vitro evaluation of atovaquone nanosuspension prepared by pH based and anti-solvent based precipitation method. *Colloid and Interface Science Communications*, 29, pp.26-32..

47. Kakumanu, V.K., Arora, V. and Bansal, A.K., 2006. Investigation of factors responsible for low oral bioavailability of cefpodoxime proxetil. *International journal of pharmaceutics*, 317(2), pp.155-160.

48. Qiao, H., Chen, L., Rui, T., Wang, J., Chen, T., Fu, T., Li, J. and Di, L., 2017. Fabrication and in vitro/in vivo evaluation of amorphous andrographolide nanosuspensions stabilized by d-α-tocopheryl polyethylene glycol 1000 succinate/sodium lauryl sulfate. *International journal of nanomedicine*, pp.1033-1046.

49. Chavez-Esquivel, G., Cervantes-Cuevas, H., Ybieta-Olvera, L.F., Briones, M.C., Acosta, D. and Cabello, J., 2021. Antimicrobial activity of graphite oxide doped with silver against Bacillus subtilis, Candida albicans, Escherichia coli, and Staphylococcus aureus by agar well diffusion test: Synthesis and characterization. *Materials Science and Engineering: C*, 123, p.111934.

50. Nicolaos, G., Crauste-Manciet, S., Farinotti, R. and Brossard, D., 2003. Improvement of cefpodoxime proxetil oral absorption in rats by an oil-in-water submicron emulsion. *International journal of pharmaceutics*, 263(1-2), pp.165-171.

A Preliminary Bioinformatics Data Analysis of Single Nucleotide Polymorphisms of the PON1 Genes in Chronic Kidney Disease: In Silico Analysis

Supriya Pathi[1,2], Usha Sacchidanandha Adiga[2*]

[1] Department of Biochemistry, Saveetha Medical College and Hospital, Saveetha Institute of Medical and Technical Sciences, Thandalam, Chennai – 602 105, India.
Department of Biochemistry, Apollo Institute of Medical Sciences and Research Chittoor – 517 127, India
* Corresponding author: ushachidu@aimsrchittoor.edu.in

Abstract

Serum paraoxonase (PON1), a glycoprotein synthesized in the liver, protects against oxidative stress and lipid peroxidation, potentially reducing the risk of chronic kidney disease (CKD). A study using bioinformatics methods, such as PROVEAN (Protein Variation Effect Analyzer), SIFT (Sorting Intolerant from Tolerant), Polyphen 2, and I-Mutant 2.0 analyzed non-synonymous single nucleotide polymorphisms (SNPs) of the PON1 gene. The Kyoto Encyclopedia of Genes and Genomes (KEGG) pathway analysis and Gene Ontology (GO) enrichment were used to identify biological processes and pathways. SIFT analysis of the PON1 gene's SNPs showed that 55 and 33 were tolerable, and 22 were harmful alterations. According to PROVEAN analysis, 22 mutations were neutral, and 33 were harmful. Polyphen 2 revealed that 26 were damaging and 32 were benign. Thirty-four SNPs on I-Mutant analysis showed decreased thermodynamic stability, while twenty-one showed enhanced stability. The study found that the structure and function of the PON1 gene are impacted by mutations, with decreased stability predicted. These mutations may affect CKD's pathobiology and risk for cardiovascular disease. A wet lab investigation on PON1 pathways could help link CKD pathophysiology and progression.

Keywords: In silico, Single nucleotide polymorphisms, Serum paraoxonase (PON1), chronic kidney disease (CKD).

Introduction

Health issues associated with chronic kidney disease (CKD) are widespread and negatively impact people worldwide. According to the 2010 Global Disease Burden Report, chronic renal disease was the 27th leading cause of death worldwide in 1990. However, chronic renal disease moved up to the 18th spot on the list in 2010 (1). CKD is the term used to describe abnormalities in kidney structure or function that have affected health and have been present for at least three months. Despite the aetiology, CKD is indicated by kidney damage or an estimated glomerular filtration rate (eGFR) of less than 60 mL/min/1.73 m² that persists for three months or more. According to GFR, CKD is classified into six groups by the Kidney Disease Improving Global Outcomes (KDIGO) 2012 classification (G1 to G5, with G3 being further subdivided into 3a and 3b). It is also recommended that the cause of CKD be determined. The urinary albumin-creatinine ratio (ACR; mg/g or mg/mmol) in an early morning "spot" urine sample is used to categorize each stage of CKD. It also includes staging based on the three albuminuria levels (A1, A2, and A3) (2).

Primary care doctors must detect and treat CKD in its early stages since CKD is linked to serious health issues such as cardiovascular disease, end-stage renal disease (ESKD), and mortality (3). Patients with CKD have a range of cardiometabolic diseases, including diabetes, insulin resistance, hypertension, and dyslipoproteinaemia, in addition to other physical abnormalities that may contribute to oxidative stress (4).

Highly reactive atoms or molecules known as free radicals possess one or more unpaired electron(s) in their outer shell and can be generated t hrough the interaction of oxygen with specific compounds (5). These radicals can be generated within cells and act as oxidants or reductants by either gaining or losing a single electron (6). Reactive oxygen species (ROS) and reactive nitrogen species (RNS) refer to the reactive radical and non-radical derivatives of oxygen and nitrogen, respectively (7). Oxidative stress is defined by an imbalance in the production and elimination of reactive oxygen and nitrogen species (RONS), resulting from either their excessive generation or a diminished capacity to neutralize them and repair the resultant damage (8).

Free radicals and oxidative stress are recognized to be harmful to human health. Numerous studies demonstrate that free radicals do, contribute to the onset and progression of a variety of illnesses, including cardiovascular disease and cancer. The progression of CKD is primarily affected by oxidative stress, leading to glomerular damage, renal ischemia, and, in turn, contributing to inflammation, endothelial dysfunction, and arterial hypertension (9). Oxidative stress adversely affects the kidneys, which triggers the recruitment of inflammatory cells and the release of proinflammatory cytokines, culminating in an initial inflammatory phase.

Oxidative stress causes damaged cell components, including proteins, DNA, and lipids, to accumulate. Cells evolved several defense mechanisms, including detoxification, antioxidant enzymes, repair enzymes, and thiol-redox systems, to prevent the harmful effects of oxidative stress. The "antioxidant defense system" of the cells is generally understood to consist of cellular enzymatic and non-enzymatic antioxidant components that work together in a complex network to keep the generation and clearance of ROS/RNS in balance (10). Antioxidants are essential for shielding our bodies from the harm caused by free radicals. They cleanse excess free radicals and balance their production (11). The term "antioxidant enzymes" refers to the majority of the enzymatic elements of this antioxidant defense mechanism, such as glutathione peroxidase, superoxide dismutase, and catalase. Paraoxonase 1 (PON1) and other antioxidant enzymes are essential for combating oxidative stress and supporting HDL's antiatherogenic properties (12). The objective is to investigate whether PON1 plays a mechanistic role in the development of cardiovascular disease associated with chronic renal illness.

Investigations indicate that the activity and concentration of PON1 are influenced by two prevalent polymorphisms located in the coding region (at positions 55 and 192). Variations in PON1 serum concentrations and the incidence of cardiovascular disease have been linked to the leucine/methionine polymorphism at position 55 of the amino acid sequence (L55M) (13). The Q192 isoform has been shown to hydrolyze paraoxon and metabolize oxidized LDL more efficiently than the R192 isoform, indicating that the glutamine/arginine polymorphism at position 192 (Q192R) impacts the PON1 function (14). PON1 serves a crucial role in physiological processes, highlighted by the association between diminished PON1 activity and a heightened risk of cardiovascular disease.

Single-nucleotide polymorphisms, or SNPs, are the most prevalent genetic variation (15). As a result of the advancements, the dbSNP database of technologies for next-generation sequencing currently contains over 950 million SNPs in the human genome -(http://www.ncbi.nlm.nih.gov/SNP/) (16). SNPs are polymorphisms in a single nucleotide that affect

the DNA sequence (A, T, C, or G). SNPs are estimated to occur at a frequency of 1 in 1,000 bp across the genome. These minute variations might be transient or transversional. About 25% of SNPs cause silent mutations, which do not change translated amino acids; 25% cause missense mutations, sometimes known as coding SNPs or cSNPs, and 50% occur in noncoding regions. Known as synonymous SNPs, these quiet SNPs are probably not influenced by natural selection (17). Conversely, natural selection may affect nonsynonymous SNPs (nSNPs, change-encoded amino acids), which can result in pathology. Both synonymous and nonsynonymous SNPs affect pre-mRNA conformation (or stability) and promoter activity. They also modify a protein's subcellular location and capacity to bind its substrate or inhibitors (SNPs) (18). Thus, they might be responsible for genome evolution, drug deposition, and disease susceptibility.

Thanks to bioinformatics techniques for in silico gene analysis, screening a large number of people is no longer necessary to find a statistically significant association between genes and illnesses. Stated differently, these methods facilitate SNP pre-selection (19). Separating disease-associated SNPs from neutral SNPs would be highly beneficial before using wet lab-based techniques. In silico analysis can be helpful when independent future research cannot establish the links between the illnesses (20). Thus, it may be possible to distinguish between true and false positives using independent proof of SNP functioning discovered by applying prediction algorithms.

The study intends to perform an in silico analysis of PON1 and its receptor gene using bioinformatics tools such as sorting the intolerant from tolerant (SIFT), Protein Variation Effect Analyzer (PROVEAN), Polyphen 2, I-mutant software, and protein-protein interactions by STRING database to ascertain the likely detrimental effects of mutations and protein-protein interactions of these genes. The present study may indicate that experimental research is necessary to investigate the possible role of PON1 gene alterations in pathobiology,

progression, and risk of cardiovascular disease (CVD) in CKD.

This study aims to do a preliminary bioinformatics analysis of SNPs in the paraoxonase 1 (PON1) gene and investigate possible potential associations with CKD. The analysis was conducted using in silico techniques to identify functionally significant SNPs, predict the probable impact on PON1 gene expression or protein function, and explore their possible roles in the pathophysiology of CKD.

Materials and Methods

The analysis of the PON 1 gene using bioinformatic tools (SIFT, PROVEAN, Polyphen 2, and I-Mutant) is shown in Figure 1.
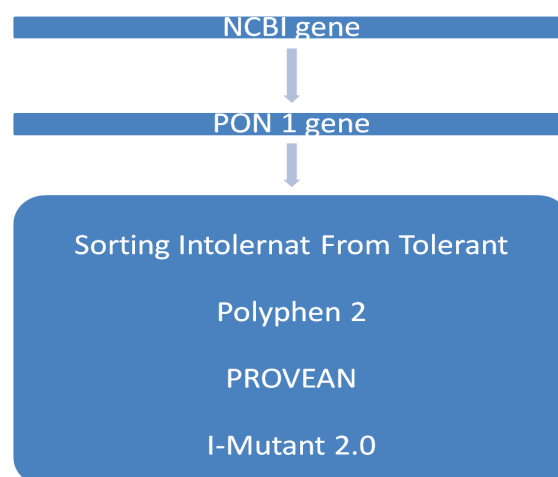
Figure 1: Illustrating the use of bioinformatics tools (SIFT, PROVEAN, Polyphen 2, and I-Mutant 2.0) for gene analysis.

Employing a bioinformatics program to analyze PON1 gene SNPs for stability, damage, and benignity. The main sources of information on the human PON1 gene were the National Center for Biological Information (http://www.ncbi.nlm.nih.gov/) (21). The polymorphism data on SNPs of the human PON1 gene and related metadata were obtained for the computational analysis from the publicly accessible online database dbSNP-NCBI (http://www.ncbi.nlm.nih.gov/SNP/) and protein sequence from FASTA(http://www.ncbi.nlm.nih.gov/SNP/).

Sorting intolerant from tolerant (sift) approach

The functional impact of damaging nsSNPs was evaluated by sorting intolerant from tolerant (SIFT), a sequence homology-based approach. To ascertain whether a change in an amino acid could affect protein function and, consequently, alter phenotype, SIFT (Sorting Intolerant From Tolerant) uses sequence homology (22). When used on human variation datasets, SIFT could differentiate between neutral polymorphisms and mutations implicated in disease. We applied SIFT to a database of missense substitutions linked to or involved in disease, assuming that amino acid alterations that cause disease are detrimental to protein function (23). SIFT calculates the normalized probability for each mutation in terms of the tolerance index (TI) score or SIFT score. SIFT scores can be classified as potentially intolerant (0.051-0.10), tolerant (0.201-1.00), borderline (0.101-0.20), or intolerant (0.00-0.05) (24). As the tolerance index rises, the probability that an amino acid substitution will have an effect falls.

Structural homology-based (PolyPhen) approach

The functional effects of coding nsSNPs were analysed using a structural homology-based approach (PolyPhen). A computational technique for identifying potentially useful nsSNPs is PolyPhen (25). By using fundamental physical and comparative concepts, this technique (Polymorphism Phenotyping 2) forecasts how modifications in amino acids may impact the structure and functionality of human proteins (26). Making use of PolyPhen 2 (http://genetics.bwh.harvard.edu/pph2). The possible effects of a change in an amino acid on the structure and functionality of the PON1 protein were examined. The protein sequence including the mutational site was submitted to the server along with two different amino acid variants. Predictions are based on a combination of structural, phylogenetic, and sequence annotation information that characterizes a substitution and where it occurs in the protein. The PolyPhen score assigns specificity and sensitivity values to nsSNPs and divides them into three primary categories: benign, perhaps harmful, and probably harmful.

Assess the functional impact of coding nsSNPs by PROVEAN

The function of the standalone PROVEAN software package distribution can be accessed online through the "PROVEAN Protein" interface. Its primary purpose is anticipating a protein sequence from any creature. The program generates PROVEAN scores after obtaining a protein sequence along with changes in amino acids. It then performs a BLAST search to identify homologous or supporting sequences (27). The Protein Variation Effect Analyzer or PROVEAN, predicts how each class of protein sequence variants—including insertions, deletions, and multiple substitutions in addition to single amino acid changes—will affect the alignment-based score (28). The score calculates how much a query sequence's sequence similarity to a protein sequence homolog changes when an amino acid variant of the query sequence is added or removed. If the protein variation's PROVEAN score is less than -2.5, it is predicted to have a "deleterious" effect; if it is larger than -2.5, it is predicted to have a "neutral" effect. The PROVEAN tool can be accessed at http://provean.jcvi.org (29).

Assessment of the functional impact of coding nsSNPs by I-Mutant 2.0

I-Mutant2.0 (http://folding.biofold.org/i-mutant/i-mutant 2.0.html), a support vector machine-based tool, is used to predict the impact of nonsynonymous mutations on protein stability. For the first time, I-Mutant2.0 can predict the extent to which a protein sequence mutation will or won't affect the folded protein's stability. Additionally, it can predict the changes in the stability of the altered protein structure (30). According to the technique, I-Mutant 2.0 scores larger than zero are assumed to indicate enhanced stability, whereas numbers less than zero will reflect lower stability.

STRING analysis

STRING refers to the Search Tool for the Retrieval of Interacting Genes (STRING). Finding knowledge about protein-protein interactions is a significant task in fundamental biological research and aids in the identification of new therapeutic targets for the treatment of a range of illnesses. Protein-protein interactions must be experimentally probed using time-consuming methods like affinity chromatography or co-immunoprecipitation. High-throughput testing methods include mass spectrometry and yeast two-hybrid screens. As a result of these developments, a variety of computer techniques have been created to forecast networks of protein-protein interactions by building databases like STRING (31). The STRING offers exceptionally thorough coverage and convenient access to information on both anticipated and experimental interactions. STRING assigns a confidence score to interactions within a stable and consistent identifier space, in addition to auxiliary information like as protein domains and three-dimensional structures. STRING version 9.0, accessible at http://string-db.org (32), covers over 1100 completely sequenced organisms. To find biological processes and pathways, KEGG pathway analysis and Gene Ontology (GO) enrichment were employed.

Results and Discussion

Identification of harmful and tolerant SNPs

Using the gene ID 5444, the dbSNP was used to get the SNPs in the human PON1 gene. Out of the 55 SNPs examined, 22 variants were determined to be harmful, and the remaining variants were to be tolerated when the SNPs were submitted to the SIFT tool to predict their impact on protein function. **Table 1** presents the comprehensive outcome.

Table 1: The number and percentage of SNPs damaging, tolerated, and decreased protein stability results of the PON1 gene.

Bioinformatic tools	PON1 gene (55 SNPs)	
SIFT	40% (22no's) Deleterious	60% (33no's) tolerated
Polyphen2	32% (18no's) damaged	37% (68no's) benign
PROVEAN	60% (33no's) (deleterious	40% (22no's) Neutral
I-Mutant 2.0	62% (34no's) decreased stability	48% (31 no's) increased stability

nsSNPs damaged by the PolyPhen 2 server

The PolyPhen 2 server received all 55 missense nsSNPs that were submitted to SIFT. Of the 55 SNPs, 26 were thought to be likely harmful. Table 2 shows that the results from the structurally based technique PolyPhen and the evolutionary-based approach SIFT showed a substantial correlation. Twenty -two of the SNPs identified by PolyPhen as likely harmful were also found to be harmful by SIFT, indicating that these nsSNPs may impair the structure and function of proteins.

Destructive nsSNPs discovered by I-Mutant 2.0

The stability of protein structural changes is predicted by using an online tool called I-Mutant 2.0. Table 2 displays the outcomes for each of the 55 missense SNPs' inputs. The free energy change upon mutation is anticipated to either increase or decrease. It was discovered that 34 of the 55 SNPs examined resulted in a drop in free energy.

Functional Characterization of PON1 by PROVEAN

PROVEAN predicts 33 out of 55 as deleterious and remaining as neutral mutations. Table 2 shows the outcomes for each of the 55 missense SNPs. The PROVEAN analysis yielded a greater number of harmful SNPs than the SIFT analysis did. This might be because, in addition to amino acid alterations, the PROVEAN tool can also evaluate insertions and deletions.

Table 2: PON1 gene SNP analysis using bioinformatic methods (SIFT, PROVEAN, Polyphen 2, and I-Mutant 2.0)

SNP	Amino acid change	SIFT score	SIFT median	SIFT prediction	POLYPHEN 2	Sensitivity	Specificity	PROVEAN score	Prediction (cut off = -2.5)	I-Mutant (2.0)
rs373190914	I48I	1	2.76	Tolerated				0.000	Neutral	0.19
rs372449149	T318I	0.052	2.75	Tolerated	0.993 (damaged)	0.70	0.97	-4.340	Deleterious	-2.13
rs372449149	T318I	0.058	2.63	Tolerated	0.993 (damaged)	0.70	0.97	-4.340	Deleterious	-213
rs371803280	V268M	0.005	2.75	Deleterious	0.452 (damaged)	0.89	0.90	-2.131	Neutral	-0.82
rs371803280	V268M	0.008	2.63	Deleterious	0.452 (damaged)	0.89	0.90	-2.131	Neutral	-0.82
rs371338407	P79R	0.004	2.79	Deleterious	0.705 (damaged)	0.86	0.92	-5.657	Deleterious	-1.21
rs371338407	P79R	0.004	2.83	Deleterious	0.705 (damaged)	0.86	0.92	-5.657	Deleterious	-1.21
rs370355032	P210S	0.187	2.75	Tolerated	0.761 (damaged)	0.85	0.92	-4.254	Deleterious	-1.67
rs370355032	P210S	0.292	2.63	Tolerated	0.761 (damaged)	0.85	0.92	-4.254	Deleterious	-1.67
rs369422555	W281C	0.001	2.63	Deleterious	1.000 (damaged)	0.00	1.00	-9.675	Deleterious	0.64
rs369422555	W281C	0.001	2.75	Deleterious	1.000 (damaged)	0.00	1.00	-9.675	Deleterious	0.64
rs368620674	F120S	0.001	2.76	Deleterious	1.000 (damaged)	0.00	1.00	-6.235	Deleterious	-0.60
rs368620674	F120S	0.007	2.67	Deleterious	1.000 (damaged)	0.00	1.00	-6.235	Deleterious	-0.60
rs368248410	I271V	0.22	2.63	Tolerated	0.081	0.93	0.85	-0.728	Neutral	-0.32
rs368248410	I271V	0.226	2.75	Tolerated	0.081	0.93	0.85	-0.728	Neutral	-0.32
rs368206333	G344C	0	2.63	Deleterious	1.000 (damaged)	0.00	1.00	-8.352	Deleterious	2.00
rs368206333	G344C	0	2.74	Deleterious	1.00 (damaged)	0.00	1.00	-8.352	Deleterious	2.00
rs367566813	M88T	0.008	2.76	Deleterious	0.594 (damaged)	0.87	0.91	-4.007	Deleterious	0.02
rs367566813	M88T	0.009	2.71	Deleterious	0.594 (damaged)	0.87	0.91	-4.007	Deleterious	0.02
rs202062288	M127I	0.341	2.75	Tolerated	0.000	1.00	0.00	1.652	Neutral	0.65
rs202062288	M127I	0.405	2.66	Tolerated	0.000	1.00	0.00	1.652	Neutral	0.65
rs201783178	R18G	0.434	3.02	Tolerated	0.000	1.00	0.00	2.879	Neutral	-1.10
rs199693212	F292S	0.167	2.75	Tolerated	0.828 (damaged)	0.84	0.93	-2.833	Deleterious	-1.11
rs199693212	F292S	0.178	2.63	Tolerated	0.828 (damaged)	0.84	0.93	-2.833	Deleterious	-1.11
rs199616322	P59S	0.412	2.76	Tolerated	0.023	0.95	0.81	-3.959	Deleterious	0.66

A preliminary bioinformatics data analysis of single nucleotide polymorphisms of the PON1 genes in chronic kidney disease: In silico analysis

rs199616322	P59S	0.416	2.75	Tolerated	0.023	0.95	0.81	-3.959	Deleterious	0.66
rs189946844	E123V	0.129	2.67	Tolerated	0.036	0.94	0.82	-3.315	Deleterious	-0.71
rs189946844	E123V	0.129	2.76	Tolerated	0.036	0.94	0.82	-3.315	Deleterious	-0.71
rs185623242	S302L	0.001	2.63	Deleterious	1.000 (damaged)	0.00	1.00	-5.268	Deleterious	-1.28
rs185623242	S302L	0.001	2.75	Deleterious	1.000 (damaged)	0.00	1.00	-5.268	Deleterious	-1.28
rs150657027	A6V	0.858	2.96	Tolerated	0.000	1.00	0.00	-0.552	Neutral	0.01
rs149100710	E49K	0.021	2.71	Deleterious	0.995 (damaged)	0.68	0.97	-3.303	Deleterious	-0.11
rs148911901	M289K	0.174	2.79	Tolerated	0.000	1.00	0.00	-2.897	Deleterious	-0.90
rs148911901	M289K	0.323	2.71	Tolerated	0.000	1.00	0.00	-2.897	Deleterious	-0.90
rs148785172	A126T	1	2.66	Tolerated	0.000	1.00	0.00	2.009	Neutral	1.50
rs148785172	A126T	1	2.75	Tolerated	0.000	1.00	0.00	2.009	Neutral	1.50
rs147867887	T121I	0.506	2.67	Tolerated	0.000	1.00	0.00	0.938	Neutral	-1.14
rs147867887	T121I	0.525	2.76	Tolerated	0.000	1.00	0.00	0.938	Neutral	-1.14
rs146211440	S23A	1	2.94	Tolerated	0.000	1.00	0.00	0.621	Neutral	-0.70
rs145997673	G330S	0.009	2.63	Deleterious	0.982 (damaged)	0.75	0.96	-4.544	Deleterious	-0.29
rs145997673	G330S	0.009	2.75	Deleterious	0.982 (damaged)	0.75	0.96	-4.544	Deleterious	-0.29
rs144612002	I48V	0.517	2.76	Tolerated	0.001	0.99	0.15	-0.467	Neutral	0.19
rs144390653	M127R	0.001	2.66	Deleterious	0.005	0.97	0.74	-2.799	Deleterious	0.65
rs144390653	M127R	0.001	2.75	Deleterious	0.005	0.97	0.74	-2.799	Deleterious	0.65
rs141948033	N19D	0.514	3.02	Tolerated	0.000	1.00	0.00	0.008	Neutral	0.84
rs141665531	P40L	0.115	2.92	Tolerated	0.003	0.98	0.44	-5.480	Deleterious	0.03
rs141598837	K340R	0.234	2.75	Tolerated	0.036	0.94	0.82	-1.626	Neutral	-0.74
rs141598837	K340R	0.279	2.63	Tolerated	0.036	0.94	0.82	-1.626	Neutral	-0.74
rs138512790	C42R	0	2.78	Deleterious	1.000	0.00	1.00	-10.594	Deleterious	-0.47
rs112078575	K151R	0.804	2.79	Tolerated	0.000	1.00	0.00	0.285	Neutral	-2.35
rs112078575	K151R	0.833	2.69	Tolerated	0.000	1.00	0.00	0.285	Neutral	-2.35
rs80019660	A201V	0.202	2.75	Tolerated	0.771 (damaged)	0.85	0.92	-1.627	Neutral	1.72
rs80019660	A201V	0.475	2.62	Tolerated	0.771 (damaged)	0.85	0.92	-1.627	Neutral	1.72
rs72552788	L90P	0.001	2.71	Deleterious	1.000 (damaged)	0.00	1.00	-5.744	Deleterious	-1.69
rs72552788	L90P	0.001	2.76	Deleterious	1.000 (damaged)	0.00	1.00	-5.744	Deleterious	-1.69

Table 3 shows the accepted range of damaging and Tolerant SNPs using SIFT, Ployphen, and PROVEAN bioinformatic tools and the accepted range of their stability through I-Mutant 2.0.

Figure 2 Shows the Percentage of deleterious and Tolerant SNPs by using Bioinformatic tools (SIFT, PROVEAN, Polyphen 2, and I-Mutant 2.0).

Table 3: Bioinformatic tools (SIFT, PROVEAN, Polyphen 2, and I-Mutant 2.0) showing damaging and tolerated ranges of the PON1 gene.

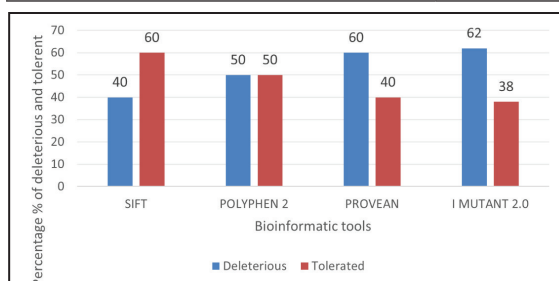| BIOINFORMATIC TOOL	Damaged/Deleterious	Tolerated
SIFT	0.0 – 0.05	0.05 – 1
POLYPHEN 2	0.5 – 1	0.00 – 0.5
PROVEAN	<-2.5	>-2.5
I-Mutant 2.0	<0 (decreased stability)	>0 (increased stability)

Figure 2: Comparison of deleterious and tolerated PON1 gene by bioinformatic tools (SIFT, PROVEAN, Polyphen 2, and I-Mutant 2.0).

Using STRING analysis, Figure 3 depicts the PON1 protein-protein interaction (PPI) network. The network has 50 edges and 11 nodes (proteins), with a clustering coefficient of 0.949 and a high average node degree of 9.09. The proteins are at least somewhat physiologically related to one another, according to the PPI enrichment p-value of 1.11e-16. The network's nodes are proteins. The edges represent the proposed functional links. Eight different colored lines representing the presence of the eight different categories of evidence that were taken into consideration while predicting the linkages were drawn on an edge in evidence mode (Fig. 3).

Bluish-green lines are derived from carefully selected databases; pink lines are experimentally determined; green lines indicate gene neighborhoods; violet lines indicate gene co-occurrences; reddish-green lines indicate text mining; black lines indicate co-expression; and blue lines indicate protein homology. Table 4 shows the predictions of the functional partner genes with the PON1 gene through the STRING Analysis. This table also explains the Co-expression and Experimental interaction of various genes and their combined score with the PON1 gene.
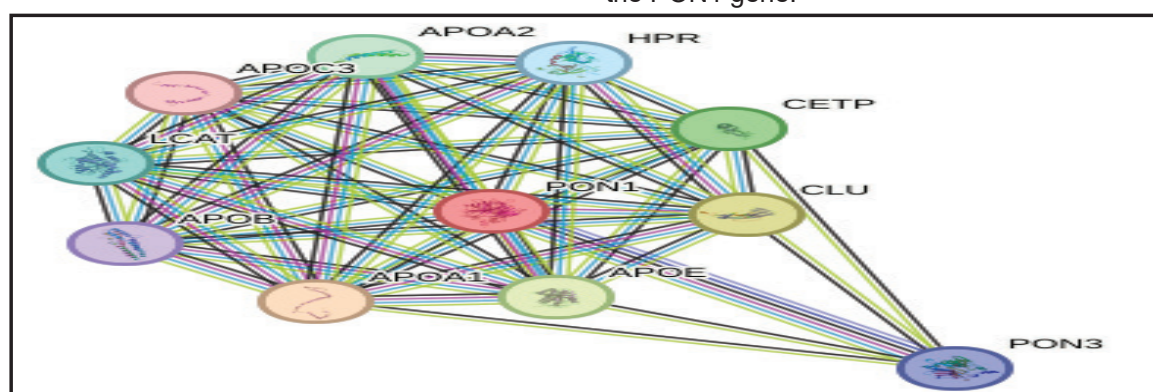

Figure 3: STRING analysis showing PON1 interacting with other proteins

A preliminary bioinformatics data analysis of single nucleotide polymorphisms of the PON1 genes in chronic kidney disease: In silico analysis

Table 4: Predicted functional partner genes with PON1 gene

Nodes	Neighbour hood on chromosome	Gene fusion	Co-occurrence	Co-expression	Experimental interaction	Databases annotated	Automated text mining	Homology	Combined score
APA1	0	0	0	0.81	0	0.720	0.996	0	0.998
CLU	0	0	0	0	0.292	0.720	0.983	0	0.996
APOE	0	0	0	0.683	0	0.720	0.918	0	0.977
CETP	0	0	0	0.090	0.	0.720	0.890	0	0.968
APOA2	0	0	0	0.920	0	0.720	0.845	0	0.967
LCAT	0	0	0	0.138	0	0.720	0.874	0	0.965
HPR	0	0	0	0.784	0	0.720	0.833	0	0.962
PON3	0	0	0.068	0	0.817	0.700	0.090	0.964	0.957
APOB	0	0	0	0.378	0	0.720	0.818	0	0.952
APOC3	0	0	0	0	0	0.720	0.732	0	0.933

Figure 4 shows the k-means clustering of proteins involved in PON1 and associated metabolic pathways. The proteins have been grouped into clusters based on their biological roles. Cluster 1 (red) highlights high-density lipoprotein synthesis with nine genes, including LCAT and APOA1, which play a multifaceted role in triglyceride homeostasis and prevent stress-induced aggregation of blood plasma proteins. Cluster 2 (green) includes CETP synthesis, with one gene involved in the regulation of reverse cholesterol transport. Cluster 3 (blue) highlights PON 3 synthesis, which works similarly to hydrolyzing aromatic lactones and lactones with aliphatic substituents in rings of five or six, but not simple lactones or lactones with polar substituents.
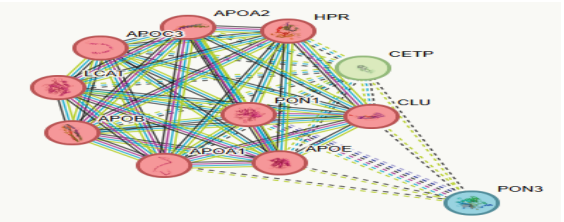

Figure 4: Showing K-means cluster analysis of PON1 with other proteins

Figure 5 shows the MCL clustering of proteins involved in PON1 and associated metabolic pathways. The proteins have been grouped into clusters based on their biological roles: MCL clustering shows only one cluster (red) highlighting high-density lipoprotein synthesis, eleven genes, including CETP, LCAT, APOA1, etc. (Fig. 5), which inhibits the aggregation of blood plasma proteins brought on by stress and has a variety of functions in maintaining triglyceride homeostasis.
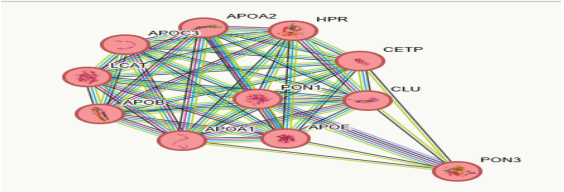

Figure 5: Showing MCL cluster analysis of PON1 with other proteins

Figure 6 shows the DBSCAN clustering of proteins involved in PON1 and associated metabolic pathways. The proteins have been grouped into clusters based on their biological roles: DBSCAN clustering shows only one cluster (Red) highlighting high-density lipoprotein synthesis, ten genes, including CETP, LCAT, APOA1, etc. (Fig. 6), which inhibits the aggregation of blood plasma proteins brought on by stress and has a variety of functions in maintaining triglyceride homeostasis.
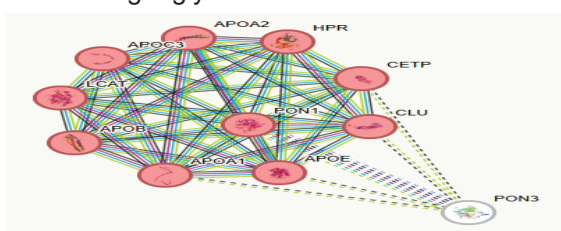

Figure 6: Showing DBSCAN cluster analysis of PON1 with other proteins

Figure 7 highlights the biological processes associated with PON1 and its interacting proteins. Notable terms include: Lipoprotein metabolism is involved in reverse cholesterol transport, plasma lipoprotein particle remodeling, high-density lipoprotein remodeling, and triglyceride-rich lipoprotein particle remodeling. Cholesterol transport and cholesterol efflux play a significant role in cholesterol homeostasis. The enrichment of these terms supports the theory that disruptions in PON1 or its network can impact lipid metabolic pathways, and its decreased levels may potentially lead to cardiovascular risk in CKD Patients. The KEGG pathway analysis identifies significant metabolic pathways involving PON1 gene.

Cholesterol metabolism is directly involved in absorbing, synthesizing, and transporting cholesterol in the body; the PPAR signaling pathway controls the expression of genes related to the intake, storage, oxidation, and metabolism of fatty acids. Participates in the process of vitamin absorption and digestion. These enriched pathways demonstrate PON1's centrality in maintaining cholesterol homeostasis, and the network can impact lipid metabolic pathways; its decreased potentiality leads to cardiovascular risk in CKD patients.
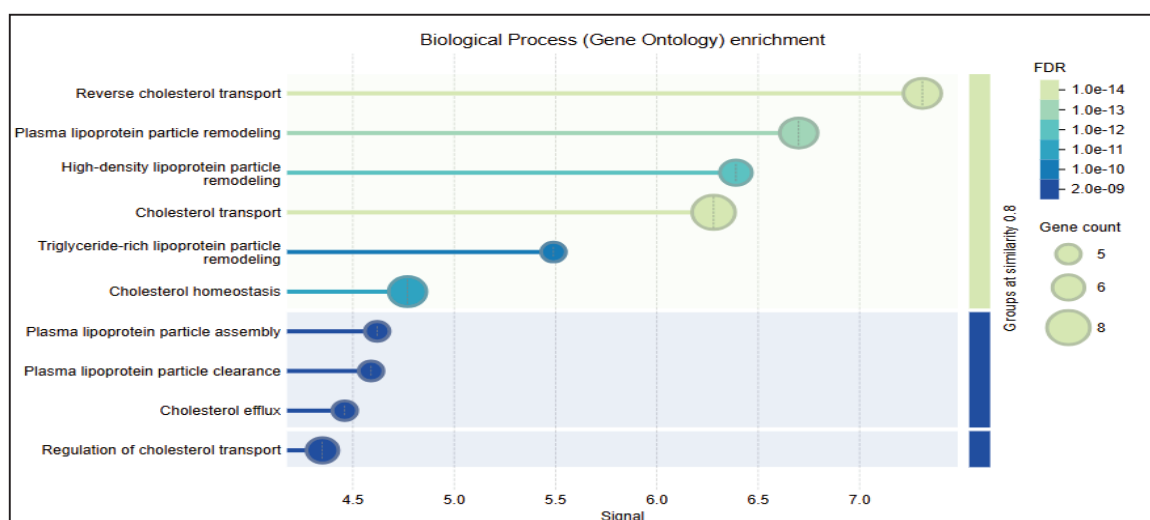
Figure 7: Gene Ontology (GO) biological processes enrichment of PON1 gene by STRING Analysis

The results across figures and tables collectively depict PON1 as a central enzyme in lipid metabolism. Its interactions with other proteins like apoproteins and lipoproteins and their biosynthesis pathways, as well as its relevance to various biological processes, highlight its significance. These findings provide a strong foundation for the decreased PON1

gene potentiality, which leads to cardiovascular risk in CKD Patients.

Discussion

The susceptibility of these patients to CVD often makes care more challenging, even with advancements in CKD management approaches. A possible key factor in the disproportionate morbidity and mortality from cardiovascular disease is the defective High-Density Lipoprotein (HDL). The PON-1 enzyme, which is produced by the liver, binds to High-Density lipoprotein (HDL) cholesterol and circulates. Reduced PON-1 activity has also been connected to adverse outcomes and a higher risk of CVD (33). The HDL-associated protein PON1 can hydrolyze oxidized LDL cholesterol, perhaps protecting against atherosclerosis. Additionally, PON1 can break phospholipid peroxidation adducts, which may have cytoprotective effects (34). The degree of coronary lesion was predicted by the decline in PON1 activity in serum, which was demonstrated to have a significant protective function in the development of atherosclerosis (35). Many inflammatory conditions, including systemic lupus erythematosus, rheumatoid arthritis, diabetes mellitus, and several hepatic and renal conditions, such as renal failure, psoriasis, and macular degeneration, are linked to low serum PON1. These disorders are likewise characterized by elevated rates of CHD and malfunctioning HDL, which is thought to be (though not confirmed) brought on by decreased PON1 activity (36). Multiple polymorphisms in the coding and promoter areas affect PON1 function and gene expression levels. The most prevalent polymorphisms in the area that codes for PON1 are Q192R, which contains a leucine (L) to methionine (M) substitution at codon 55 and a glutamine (Q) to arginine (R) change at codon 192 (35).

The PON1 gene was analyzed in silico using SIFT, PolyPhen-2, PROVEAN, and I-Mutant, which yielded important information about the structural and functional effects of its genetic variants. The outcomes of these instruments show how particular single nucleotide polymorphisms (SNPs) may affect PON1's stability and enzymatic activity, which are essential for its physiological function in detoxification and antioxidation. SIFT, PolyPhen-2, PROVEAN, and I-Mutant results indicate lower protein stability and higher harmful and detrimental scores. This may have important ramifications for oxidative stress-related diseases like cardiovascular and neurological problems.

The protein-protein interaction (PPI) network, biochemical pathways, and metabolic processes linked to PON1 are all thoroughly examined in the STRING ANALYSIS research. Every figure and table produced by this study emphasizes a distinct aspect of the biological network of PON1 and its relevance to human health and illness.

A comprehensive understanding of PON1's function in metabolism is offered by the combination of STRING analysis, clustering techniques, GO enrichment, and KEGG pathway mapping. The study confirms PON1's pivotal role in cholesterol metabolism and its subsequent impact on the risk of cardiovascular disease.

Conclusion

According to this preliminary bioinformatics research, single nucleotide polymorphisms (SNPs) in the PON1 gene may play a part in the aetiology of CKD. SIFT, PROVEAN, PolyPhen-2, I-Mutant, and STRING were used to determine the potential impacts of genetic variations on the structure, function, and interactions of the PON1 protein. Utilizing in silico tools, we identified key SNPs that may influence PON1 function, particularly in oxidative stress and lipid metabolism pathways, which are critical in developing CVD risk in CKD progression. Future research should concentrate on bridging computational predictions with functional studies to investigate the molecular significance of PON1 variations in CKD and evaluate their

potential as diagnostic or therapeutic targets.

Conflicts of Interest

The authors declared that they have no conflicts of interest.

Acknowledgements

References

1. Ogunmoyole, T., Apanisile, Y., Makun, O., et al.; Vernonia amygdalina Leaf Extract Protects Against carbon tetrachloride-induced hepatotoxicity and Nephrotoxicity: Possible Potential in the Management of Liver and Kidney Diseases. Curr. Trends Biotechnol. Pharm. 2022:16(4), 540–552.

2. Inker LA, Astor BC, Fox CH, Isakova T, Lash JP, Peralta CA, et al.; Kurella Tamura M, Feldman HI. KDOQI US commentary on the 2012 KDIGO clinical practice guideline for the evaluation and management of CKD. Am J Kidney Dis. 2014;63(5):713-35.

3. Van der Velde M, Matsushita K, Coresh J, et al.; Chronic Kidney Disease Prognosis Consortium. Lower estimated glomerular filtration rate and higher albuminuria are associated with all-cause and cardiovascular mortality: a collaborative meta-analysis of high-risk population cohorts. Kidney Int. 2011;79(12):1341-1352.

4. Matsushita K, Ballew SH, Wang AY-M, Kalyesubula R. Epidemiology and risk of cardiovascular disease in populations with chronic kidney disease. Nat Rev Nephrol. 2022;18(10):696-707.

5. Chandrasekaran A, Idelchik MDPS, Melendez JA. Redox control of senescence and age-related disease. Redox Biol. 2017;11:91-102.

6. Lobo V, Patil A, Phatak A, Chandra N. Free radicals, antioxidants, and functional foods: impact on human health. Pharmacogn Rev. 2010;4(8):118-126.

7. Powers SK, Ji LL, Kavazis AN, Jackson MJ. Reactive oxygen species: impact on skeletal muscle. Compr Physiol. 2011;1(2):941-969.

8. Salisbury D, Bronas U. Reactive oxygen and nitrogen species: impact on endothelial dysfunction. Nurs Res. 2015;64(1):53-66.

9. Balasubramanian S. Progression of chronic kidney disease: mechanisms and interventions in retardation. Apollo Med. 2013;10(1):19-28.

10. Halliwell B, Gutteridge J. Antioxidant defenses: endogenous and diet-derived. In: Halliwell B, Gutteridge J, editors. Free Radicals in Biology and Medicine. New York: Oxford University Press; 2007.

11. Lalthansangi, C., RK Lalremtluangi, Lalhmingliani, E, et al.; Evaluation of the Free Radical Scavenging Activities and Antibacterial Activities of the Extracts of Lindernia ruellioides (Colsmann) Pennell. Curr. Trends Biotechnol. Pharm. 2024:18(4), 2036–2047.

12. James R, Deakin S. The importance of high-density lipoproteins for paraoxonase-1 secretion, stability, and activity. Free Radic Biol Med. 2004;37(12):1986-1994.

13. Blatter Garin MC, James RW, Dussoix P, et al. Paraoxonase polymorphism Met-Leu54 is associated with modified serum concentrations of the enzyme. A possible link between the paraoxonase gene and increased risk of cardiovascular disease in diabetes. J Clin Invest. 1997;99(1):62-66.

14. Costa LG, Cole TB, Vitalone A, Furlong CE. Measurement of paraoxonase

(PON1) status as a potential biomarker of susceptibility to organophosphate toxicity. Clin Chim Acta. 2005;352(1-2):37-47.

15. Chanock S. Candidate genes and single nucleotide polymorphisms (SNPs) in the study of human disease. Dis Markers. 2001;17(2):89-98.

16. Sherry ST, Ward MH, Kholodov M, Baker J, Phan L, Smigielski EM. The NCBI database of genetic variation. Nucleic Acids Res. 2001;29(1):308-311.

17. Halushka MK, Fan JB, Bentley K, Hsie L, Shen NP, Weder A, Cooper R, Lipshutz R, Chakravarti A. Patterns of single nucleotide polymorphisms in candidate genes for blood pressure homeostasis. Nat Genet. 1999;22(3):239-247.

18. Kimchi-Sarfaty C, Oh JM, Kim I-W, Sauna ZE, Calcagno AM, et al. A silent polymorphism in the MDR1 gene changes substrate specificity. Science. 2007;315(5811):525-528.

19. Ramensky V, Bork P, Sunyaev S. Human non-synonymous SNPs: server and survey. Nucleic Acids Res. 2002;30(17):3894-3900.

20. Emahazion T, Feuk L, Jobs M, Sawyer SL, Fredman D, St Clair D, et al. SNP association studies in Alzheimer's disease highlight problems for complex disease analysis. Trends Genet. 2001;17(7):407-413.

21. Sherry ST, Ward MH, Kholodov M, Baker J, Phan L, Smigielski EM, et al. dbSNP: The NCBI Database of Genetic Variation. Nucleic Acids Res. 2001;29(1):308-311.

22. Ng PC, Henikoff S. Accounting for human polymorphisms predicted to affect protein function. Genome Res. 2002;12(3):436-446.

23. Bairoch A, Apweiler R. The SWISS-PROT protein sequence database and its supplement TrEMBL in 2000. Nucleic Acids Res. 2000;28(1):45-48.

24. Xi T, Jones IM, Mohrenweiser HW. Many amino acid substitution variants identified in DNA repair genes during human population screenings are predicted to impact protein function. Genomics. 2004;83(6):970-979.

25. Ramensky V, Bork P, Sunyaev S. Human non-synonymous SNPs: server and survey. Nucleic Acids Res. 2002;30(17):3894-3900.

26. Adzhubei IA, Schmidt S, Peshkin L, Ramensky VE, Gerasimova A, Bork P, et al. A method and server for predicting damaging missense mutations. Nat Methods. 2010;7(4):248-249.

27. Choi Y, Chan AP. ROVEAN web server: a tool to predict the functional effect of amino acid substitutions and indels. Bioinformatics. 2015;31(16):2745-2747.

28. Choi Y, Sims GE, Murphy S, Miller JR, Chan AP. Predicting the functional effect of amino acid substitutions and indels. PLoS One. 2012;7(10):e46688.

29. Narayana Swamy A, Valasala H, Kamma S. In silico evaluation of nonsynonymous single nucleotide polymorphisms in the ADIPOQ gene associated with diabetes, obesity, and inflammation. Avicenna J Med Biotechnol. 2015;7(3):xx-xx.

30. Capriotti E, Fariselli P, Casadio R. Mutant2.0: predicting stability changes upon mutation from the protein sequence or structure. Nucleic Acids Res. 2005;33(Web Server issue):W306-W310.

31. Pedamallu CS, Posfai J. Open source tool for prediction of genome-wide protein-protein interaction network based on ortholog information. Source Code Biol Med. 2010;5:8.

32. Szklarczyk D, Franceschini A, Kuhn M,

Simonovic M, Roth A, Minguez P, et al. The STRING database in 2011: functional interaction networks of proteins, globally integrated and scored. Nucleic Acids Res. 2011;39(Database issue):D561-D568.

33. Dube P, Khalaf FK, DeRiso A, Mohammed CJ, Connolly JA, Battepati D, et al. A Cardioprotective role for paraoxonase-1 in chronic kidney disease. Biomedicines. 2022;10(2301):xx-xx.

34. Shunmoogam N, Naidoo P, Chilton R. Paraoxonase (PON)-1: a brief overview on genetics, structure, polymorphisms, and clinical relevance. Vasc Health Risk Manag. 2018;14:137-143.

35. Samouilidou EC, Liaouri A, Kostopoulos V, Nikas D, Grapsa E. The importance of paraoxonase 1 activity in chronic kidney disease. Ren Fail. 2024;46(2):2376930.

36. Mackness M, Mackness B. Human paraoxonase-1 (PON1): gene structure and expression, promiscuous activities and multiple physiological roles. Gene. 2015;567(1):12-21.

Chronomodulated Therapy for the Treatment of Type II Diabetics by Using α-Glucosidasel Inhibitor

M. Sreelatha*[1], P.V. Swamy[2], P. Shailaja[3]

[1]Dept. of Pharmaceutics, Vagdevi College of Pharmacy, Gurazala, Andhra Pradesh.
[2]Dept. of Pharmaceutics, Shri Vishnu College of Pharmacy, Bhimavaram, Andhra Pradesh.
[3]Dept. of Pharmaceutics, A.U College of Pharmaceutical Sciences, Andhra University, Visakhapatnam, Andhra Pradesh.

* Corresponding author: msreelatha9@gmail.com

Abstract

Miglitol is an Anti-diabetic having a place with the class of α-glucosidase inhibitors, it has ability to bring down the postprandial glucose level in type-II diabetic patients. The present work was aimed to prepare miglitol pulsincaps to reduce the dose frequency and increase the patient compliance. Arrangement of pulsicapsules is associated with the four distinct stages: First stage involved preparation of immediate release granules and optimization of immediate release granules which were prepared by using crospovidone as superdisintegtrant in different conc. (MCM1-MCM6) by wet granulation method and granules were evaluated for the flow properties, drug content and in-vitro dissolution. Based on the results MCM5 was optimized to prepare the pulsincaps. In the second stage insoluble bodies of the capsules was prepared by treating with the formaldehyde solution. Third step was preparation of hydrogel plugs with 6 hr. lag time and the final stage was assembling of pulsincaps with three pulses of immediate release granules (MCM5) which were separated by two hydrogel plugs. The prearranged pulsincaps were assessed for in vitro drug release in three distinctive dissolution media. From the results CDC8 was optimized based on the predetermined lag time and drug release. Stability studies led at 40±2˚C/75±5% RH showed no note worthy changes inferring that an effective pulsatile drug delivery system of Miglitol was designed.

Keywords: Miglitol, α-glucosidase inhibitor, Pulsincaps, Crospovidone, Accelerated stability Studies.

Introduction

Most convenient route of drug administration is oral route due to its large surface area. Conventional drug delivery approaches are afflict by issues pertaining to the systemic toxicity and repeated dosing (1).

The classical drug delivery system has many limitations such as (2); (i) An improper time of drug release, (ii) Ultimate side effects on the body.

To avoid the all above snags and to meet the following requirements like: (i) Improve the site-specific targeted drug delivery, (ii) Correlation of the drug release process with the patient circadian rhythm, (iii) A careful control delivery of the highly toxic drugs, (iv) Use of more drugs in one system like pulsatile and controlled release drug delivery systems.

In the instances mentioned above, it is

better to optimize the drug release from a dosage form that will supply the necessary drug concentration at a certain time only (3).

Nonetheless, in the field of present day's drug treatment, developing considerations have been centered around pulsatile delivery of the drug for which ordinary controlled drug release framework with a ceaseless delivery are not great but rather a requirement for a beat of remedial focus in the intermittent way goes about as a push for the improvement of "Pulsatile Drug Delivery System". In these systems a predetermined amount of the drug was released rapidly and transiently within short time period following a predetermined lag time (3).

Diabetes mellitus (DM) is one of the most serious health crises of the 21st century, and the majority of ministries and public health authorities are focusing on the disease's contemporary impact and consequences. Only in 2012, it was reported that at least 1.5 million people died as a results of diabetes. Diabetic patients are estimated to number around 642 billion by 2040 (4).

Diabetes mellitus necessitates long term therapy with medications such as sulfonylureas, which may harm the pancreas quickly with the immediate release dosage form. Finally, medicines that cause tolerance should not be given at a constant rate because the drug's effect dimishes at a constant dose level. Furthermore, when a drug level is kept constant, drug toxicity may grow with the time. In some instances, it is advisable to use a dosage form that will deliver the desired medication concentration at a certain time point only (5).

Miglitol (6) is a newer class of α- glucosidase inhibitor which is derived from 1- deoxy-nijirimycin structurally related to glucose. It is completely absorbed from GI tract with fewer side effects when compared to the acarbose.

MGL competitively inhibits the glycosidase at the small intestine brush borders, which is responsible for the breakdown of the complex polysaccharides in to simple glucose. This results in decrease in the postprandial glycaemia. Due to its short biological half-life (2-3 h), there is a need to develop pulsatile drug delivery system which can overcome its multi-dosing per a day and to increase the patient compliance, and reduce drug toxicity.

Materials and Methods

Material

MGL was obtained as gift sample from Mylan laboratories limited, Kazipally, Hyderabad, India. Crospovidone and Aerosil from Otto Chemical biochemika reagents. Mumbai. Metalose was a gift from Signet Chemical Corporation Pvt. Ltd, Mumbai. Sodium Carboxy Methyl Cellulose was obtained from Excel Fine Chemical, A.P., Magnesium Stearate was obtained from S.D Fine Chem Ltd, Mumbai, Methanol and other reagents used were standard analytical grade.

Methods

Formulation and evaluation of miglitol immediate release granules:

Miglitol immediate release immediate release granules were prepared by wet granulation process, by using various proportions of crospovidone as superdisintegrant were added to MGL and MCC along (3% w/v 50% methanol) to get the wet mass. The coherent mass was passed through the sieve no.22 (IP Standard) and the granules were dried at 60˚C for one hour using hot air oven. Then the dried granules were packed in a poly-bag for further use. Formulation of MGL immediate release core granules was given in the Table-1.

Table -1: Different formulations of Miglitol immediate release granules

Ingredientsiforigranulesiinimg	Formulation code					
	MCM1	MCM2	MCM3	MCM4	MCM5	MCM6
Miglitol	25	25	25	25	25	25
Crospovidone	0	2	4	6	8	10
Micro crystalline cellulose ((MCC)	42	40	38	36	34	32
PVPiK30	5	5	5	5	5	5
Methanol	Qs	Qs	Qs	Qs	Qs	Qs

Flow properties of granules

Bulk density (7)

It is mathematically expressed as:

$$\text{Bulk density} = \frac{\text{Weight of thr granules (w)}}{\text{Bulk volume of the granules (V}_0)}$$

Procedure

Accurately weighed powder was transferred in to measuring cylinder and noted down the volume occupied by the powder in ml.

Hausner's ratio (8)

The hausner's ratio <1.25 show free flowing of granules and > 1.25 indicates poor flow properties of granules.

$$\text{Hausner's ratio} = \frac{\text{Tapped bulk density}}{\text{Bulk density}}$$

Carr's compressibility index (8)

It indicated the compressibility of powder or granules. Powder or granules which have smaller the Carr's index value it has good compressibility.

Consolidation Index (%)	Flow
5-15	Excellent
12-16	Good
18-21	Fair to passable
23-35	Poor
33-38	Very poor
>40	Very very poor

Angle of repose (9)

Angle of repose was used to measure the flow properties. Angle of repose was measured by fixed funnel method of Banker and Anderson.

$$\tan \theta = \frac{h}{r}$$

Where
θ = Angle of repose
h = height of pile
r = Radius of the base of the pile

Drug content (9)

Drug content was measured by dissolving the 10 mg of granules in 10 ml methanol and the solution was filtered and 1 ml filtrate was diluted with suitable dissolution medium. The diluted sample absorbance was measured at 210 nm using UV-Visible spectrophotometer. The results were given in the Table-3.

In-vitro Dissolution studies of immediate release granules (9)

Immediate release granules dissolution studies were carried out by using USP II dissolution apparatus (Dissolution model: 8 VDA). The test was carried out by taking granules equivalent 25 mg drug and performed in three different dissolution media like 0.1 N HCl, pH 7.4 phosphate buffer and pH 6.8 phosphate buffer. Test was conducted by taking 900 ml of dissolution medium at a temp. 37± 0.5°C for 2 h and paddles were rotated at a speed of 75

rpm. A sample of 5 ml dissolution medium was withdrawn at predetermined time interval (5, 10, 15, 30, 45, 60, 90 and 120 min). Samples were suitably diluted and analyzed UV-Visible spectrophotometer at 210 nm. Three trails were done and mean % drug release was calculated.

Preparation of Pulsincaps

Solubility modification of hard gelatin capsules (10)

About 200 capsules of '0' size were taken. Bodies and caps were separated. The separated bodies were kept on the wire mesh placed in the desiccator which contained 25 ml of 37% v/v formaldehyde. To this a pinch of potassium permanganate was added and the desiccator was tightly closed. The bodies were exposed to formaldehyde vapours until proper solubility was achieved. Then the bodies were dried at room temp for 24 h to remove the excess formaldehyde. After drying the treated bodies were joined with untreated caps and kept in the poly bags for future use.

Evaluation of treated bodies (11)

Qualitative Analysis for formaldehyde content

Preparation of formaldehyde standard solution

Suitable volume of formaldehyde was diluted with water to get 20 μg/mL concentration.

Preparation of test sample

Twenty five treated bodies were taken and cut into small pieces and dissolved in 40 ml of distilled water by stirring with magnetic stirrer for 1 h to get excess amount of formaldehyde. Then the solution was filtered and volume made up to 50 ml with distilled water.

Procedure for testing the concentration of Formaldehyde

One ml of test solution was taken, to this 4 ml of distilled water and 5 ml of 99.5% v/v acetyl acetone were added. Then this solution was heated for 40 min at 40˚C. At the same time 1 ml of standard formaldehyde was treated in the same manner taken as reference. Then the two solutions, i.e., test and reference samples were compared for color intensity. The color of the test sample was not more intensive than the reference sample.

Preparation of hydrogel plugs (12)

Two polymers like Metalose 90SH 4000, Sodium Carboxy Methyl Cellulose were initially selected for the preparation of hydrogel plugs which were swellable polymers. The polymers were taken in two different Drug: Polymer ratios, i.e., 1:2 and 1:3 and these polymers were mixed with two diluents MCC and DCP. To this magnesium stearate and Aerosil were added to increase the flow properties of powder and it was directly compressed with 6 mm flat round punches in punching machine. Different formulations of hydrogel plugs were given in the Table 2.

Table 2: Different formulations of Hydrogel plugs

Ingredients mg/ Plug	Metalose 90 SH 4000	Sodium CMC	MCC	DCP	Aerosil	Magnesium stearate	Total Wt Ofi plug mg
MMC1	50	….	48	….	1	1	100
MDC2	50	….	….	48	1	1	100
MMC3	75	….	23	….	1	1	100
MDC4	75	….	….	23	1	1	100
CMC5	….	50	48	….	1	1	100
CDC6	….	50	….	48	1	1	100
CMC7	….	75	23	….	1	1	100
CDC8	….	75	….	23	1	1	100

Physicochemical characterization of Hydrogel plugs (13)

Weight variation

Twenty hydrogel plugs were taken and test was conducted according to IP standard procedure.

Thickness

Hydrogel plugs thickness was measured by using vernier calipers.

Hardness test

Monsanto's hardness tester was used to measure the hardness of plugs. It was expressed in kg/cm^2.

Preparation of pulsicapsules (14)

Treated bodies and untreated caps of the '0' size capsules were taken for filling. Immediate release core granules formula MCM5 was optimized for the preparation of Miglitol pulsicapsules. Then the pulsicapsules were assembled inside the treated bodies with three doses of optimized core granules and each dose was separated by hydrogel plug then closed with untreated caps. The assembled pulsicapsules contained three doses of Miglitol granules and two hydrogel plugs.

In-vitro dissolution studies of pulsicapsules (15)

Dissolution studies were carried out by using USP II apparatus. Here three dissolution media were used to simulate the pH changes along the GI tract.

Acid stage

Stomach has acidic pH this was maintained by using 0.1N HCl (900 ml) for first 2 h because it is average gastric emptying time. Then the acid was removed and refilled with phosphate buffer.

Buffer stage

After gastric emptying the contents were goes into intestine which having the basic pH. Then pH 7.4 phosphate buffer (900 ml) was used for next 3 h transit time of small intestine. After 3 h 7.4 buffer was replaced with pH 6.8 phosphate buffer to maintain the colonic pH for remaining 13 h. Paddles were rotated at 75 rpm and temperature was maintained at 37±0.5°C. 5 ml of sample was withdrawn from the dissolution basket and replaced with the same volume with respective dissolution medium to maintain the sink conditions. Samples were analyzed at 210 nm by using UV-Visible spectrophotometer.

Stability studies (16)

Stability studies were conducted to predict the shelf life of a product. The optimized formula was exposed to different conditions in stability chamber and analyzed for appearance, drug content and in-vitro dissolution drug release. The obtained results were compared with initial month results.

Results and Discussion

Flow properties of immediate release granules:

All prepared granules were uniform in size and flow properties of core granules of six formulations indicated that the granules were free flowing and drug content in the range of 99.26 ± 0.82 to 99.85 ± 0.11 and results were given in the Table 3.

In-vitro Dissolution studies of immediate release granules:

Three different dissolution media was used in these studies. Different concentrations of crospovidone results in significant increase in drug release profile. The formulation MCM1 without crospovidone showed less % drug release and MCM2-MCM4 formulation released the less % of drug than MCM5 and MCM6 because it contains low amount of superdisintegrant. The formulation MCM6 drug release was completed within one hour due to high amount of superdisintegrant. Hence MCM5 was optimized based on the flow properties, drug content and drug release profile. The results were given in the Tables 4, 5 & 6 and Figures 1, 2 &3.

Sreelatha *et al*

Table 3: Flow properties of immediate release core granules:

Formulation Code	Bulk density (g/cm³)	Tapped density (g/ml)	Compressibility Index (%)	Hauser's ratio	Angle ofi repose (˚)	Drug Content (%)
MSM1	0.623±0.05	0.698±0.02	10.32±0.06	1.11±0.05	24.39±0.11	99.81±0.34
MSM2	0.634±0.03	0.704±0.05	10.78±0.05	1.12±0.07	24.17±0.81	99.32±0.17
MSM3	0.627±0.02	0.715±0.06	10.67±0.01	1.10±0.04	25.19±0.05	99.26±0.82
MSM4	0.642±0.04	0.745±0.03	10.45±0.04	1.12±0.03	27.03±0.11	99.88±0.21
MSM5	0.639±0.01	0.759±0.02	9.78±0.04	1.10±0.05	24.08±0.45	99.95±0.11
MSM6	0.645±0.06	0.773±0.08	10.05±0.07	1.09±0.02	24.11±0.87	99.83±0.56

All values were expressed mean±s.d., n=5

Table 4: The *in vitro* drug release profile for immediate release granules in 0.1N HCl

Time (min)	Cumulative% Drug Release*					
	MCM1	MCM2	MCM3	MCM4	MCM5	MCM6
0	0	0	0	0	0	0
15	17.46±0.87	23.42±0.93	27.97±0.23	35.44±0.56	38.87±0.51	46.03±0.73
30	36.98±0.56	46.98±0.47	45.76±0.96	58.09±0.71	57.96±0.37	79.83±0.27
45	52.44±0.43	56.65±0.63	78.41±0.57	73.87±0.23	72.98±0.34	86.78±0.41
60	74.83±0.87	78.64±0.43	81.23±0.47	85.34±0.63	83.88±0.75	98.98±0.67
90	82.34±0.56	84.86±0.95	88.75±0.68	92.87±0.61	95.37±0.56	
120	88.67±0.34	91.66±0.95	93.77±0.98	95.98±0.23	99.73±0.17	

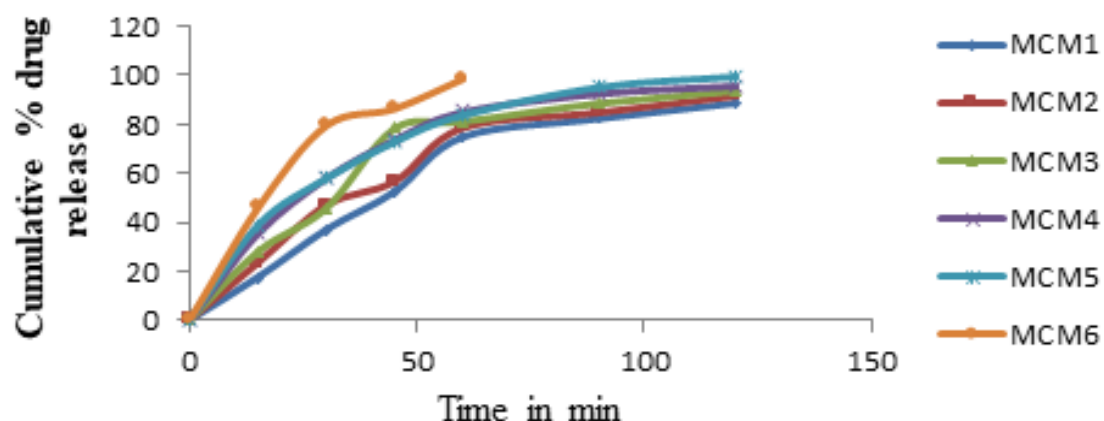All values were expressed as mean±s.d., n=3

Fig.1: Comparative %drug release profile for immediate release granules of MCM1-MCM6 in 0.1N HCl

Chronomodulated therapy for the treatment of type ii diabetics by using α-glucosidasel inhibitor

Table 5: The *in-vitro* drug release profile for immediate release granules in pH 7.4iPhosphateiBuffer

Time (Min)	Cumulative % Drug Release*					
	MCM1	MCM2	MCM3	MCM4	MCM5	MCM6
0	0	0	0	0	0	0
15	17.06±0.98	25.45±0.86	29.78±0.12	33.64±0.76	37.56±0.45	45.68±0.98
30	38.98±0.56	48.07±0.37	51.87±0.34	54.79±0.47	68.97±0.65	76.95±0.56
45	49.98±0.47	73.67±0.61	74.67±0.76	78.05±0.36	82.45±0.72	85.03±0.52
60	67.57±0.34	80.01±0.65	83.75±0.58	86.98±0.86	89.92±0.73	97.98±0.41
90	84.23±0.68	86.96±0.55	89.45±0.43	91.09±0.62	93.45±0.45	
120	86.76±0.23	91.97±0.78	95.78±0.94	96.98±0.89	99.67±0.91	

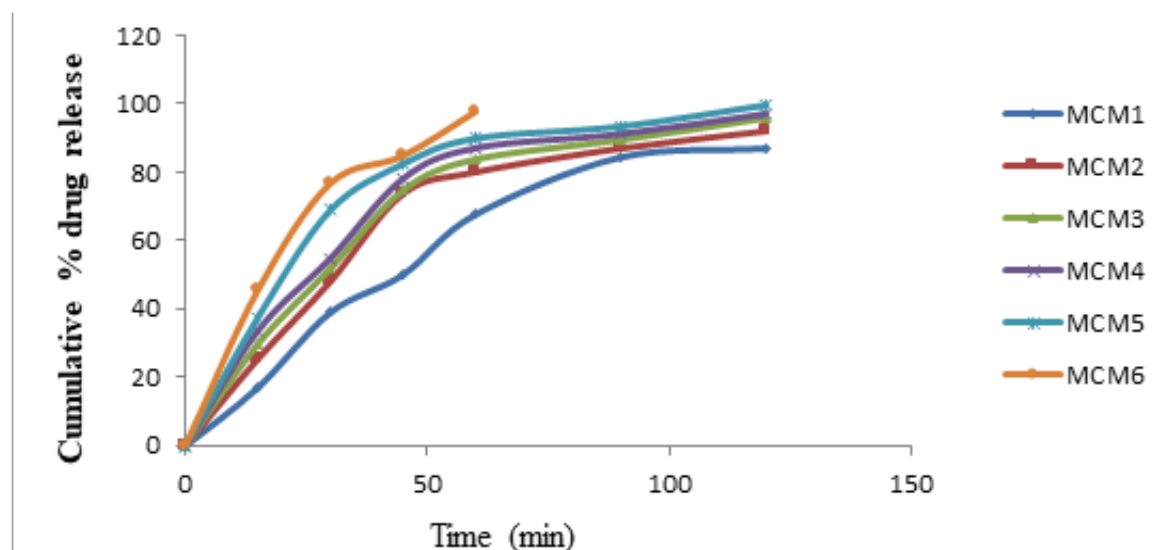All values were expressed as mean±s.d., n=3

Fig.2: Comparative % drug release profile for immediate release granules of MCM1-MCM6 in pH 7.4iPhosphateiBuffer

Table 6: The *in-vitro* drug release profile for immediate release granules in pH 6.8 Phosphate Buffer

Time (min)	Cumulative % Drug Release*					
	MCM1	MCM2	MCM3	MCM4	MCM5	MCM6
0	0	0	0	0	0	0
15	15.34±0.97	23.45±0.65	23.32±0.56	37.43±0.42	39.35±0.73	46.45±0.13
30	35.57±0.56	46.63±0.74	48.65±0.53	55.01±0.35	60.67±0.21	69.98±0.25
45	57.43±0.34	69.23±0.38	70.12±0.68	78.09±0.64	81.45±0.16	87.75±0.34
60	72.98±0.57	75.98±0.55	79.65±0.24	85.54±0.24	87.23±0.27	98.95±0.15
90	85.67±0.97	81.12±0.69	85.89±0.67	90.45±0.81	93.45±0.76	
120	87.12±0.97	93.02±0.85	94.56±0.62	95.32±0.36	99.87±0.13	

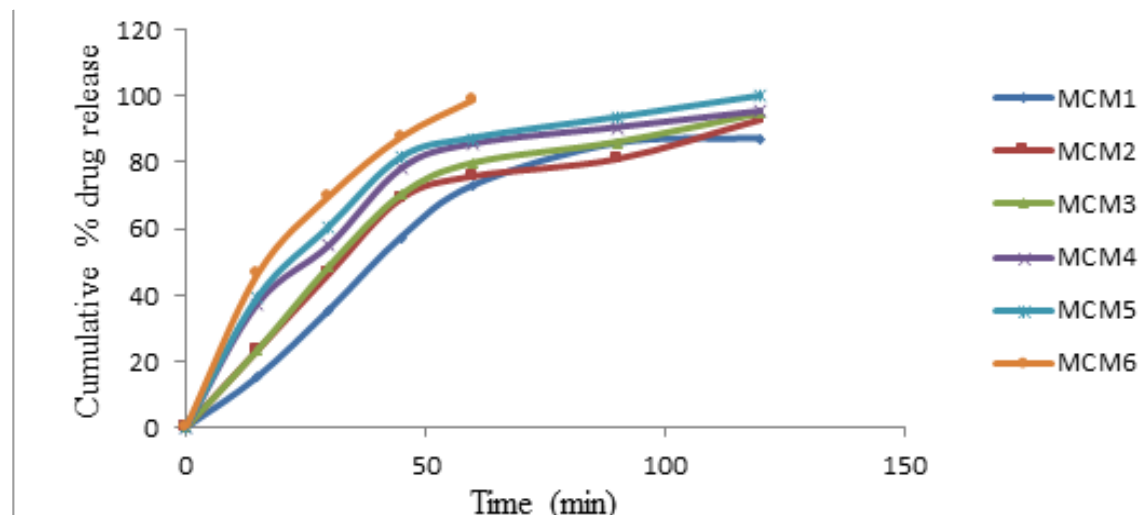All values were expressed mean±s.d., n=3

Sreelatha *et al*

Fig.3: Comparative %drug release profile for immediate release granules of MCM1-MCM6 in pH 6.8iPhosphateiBuffer

Post compression characterization of hydrogel plugs:

Hydrogel plugs were evaluated for post compression parameters like weight variation, thickness and hardness. This ranges from 98.89 ±1.15 to 101.1±0.02, 3.41±0.45 to 3.45±0.78 and 4.1±0.05 to 4.7±0.01 respectively. The results were given in the Table 7.

Table 7: Evaluation ofihydrogeliplugs

Hydrogel plug code	Weight variation (mg)	Thickness (mm)	Hardness (kg/cm^2)	Lag time* (h)
MMC1	100±0.75	3.45±0.08	4.5±0.02	2.30
MDC2	99±0.98	3.42±0.78	4.3±0.01	2.45
MMC3	100±0.23	3.44±0.45	4.2±0.02	3.45
MDC4	98.89 ±1.15	3.45±0.78	4.7±0.01	4.15
CMC5	101.1±0.02	3.42±0.78	4.1±0.05	4.45
CDC6	100±0.23	3.41±0.91	4.3±0.98	5.15
CMC7	100±0.54	3.41±0.45	4.5±0.01	5.45
CDC8	99.5±0.65	3.42±0.91	4.7±0.01	6.00

All values were expressed as mean±s.d., n=6

*All values were expressed as mean±s.d., n=3

Pulsincaps In-vitro dissolution studies:

Dissolution studies revealed that there is no effect of dissolution media on drug release.

All these 8 pulsincaps were prepared with two different polymers in two ratios 1:2, 1:3 and two diluents were used i.e., MCC which is a hydrophilic in nature, and another one is DCP which is hydrophobic in nature.

All prepared pulsicapsules shown the desired drug release in 0.1N HCl for first 2 h, nearly 100% release which was first pulse.

Chronomodulated therapy for the treatment of type ii diabetics by using α-glucosidasel inhibitor

The formulations MMC1, MDC2, MMC3, MDC4 pulsicapsules prepared with Metalose 90 SH 4000 as hydrogel plug shows minimum lag time of 2 h 30 min and maximum lag time of 4 h 15 min. In these formulations the second pulse starts 6 h 30 min which is not desirable.

Formulations CMC5, CDC6, CMC7, and CDC8 prepared with sodium carboxy methyl cellulose as hydrogel plug shown maximum lag time of 6 h, which was a predetermined lag time. CDC8 formulation was optimized because of its predetermined lag time of 6 h. CDC8 formulation contains 1:3 ratio of drug: polymer and DCP as diluents. Its maximum drug release of 99.79% in first pulse which was rapid,   the second pulse release was started at 8th h (98.97%)

and third pulse release was started at 16th h (99.87%). Hence the formulation CDC8 was selected for stability studies.

During the *in-vitro* studies it was observed that the cap was dissolved within 5 min and first dose was released initially and rapidly then hydrogel plug was exposed to dissolution medium and absorbs the surrounding medium to get wetted and converted into soft mass, ejected from the capsule body and release the second pulse and same procedure was observed for release of third pulse. The formation of soft mass of hydrogel depends on its nature and amount of polymer and nature of diluents used. The results were given in the Tables 8, 9 and 7 & Figures 4 and 5.

Table 8: The *in vitro* drug release profiles of pulsincaps formulations Metalose 90 SH 4000.

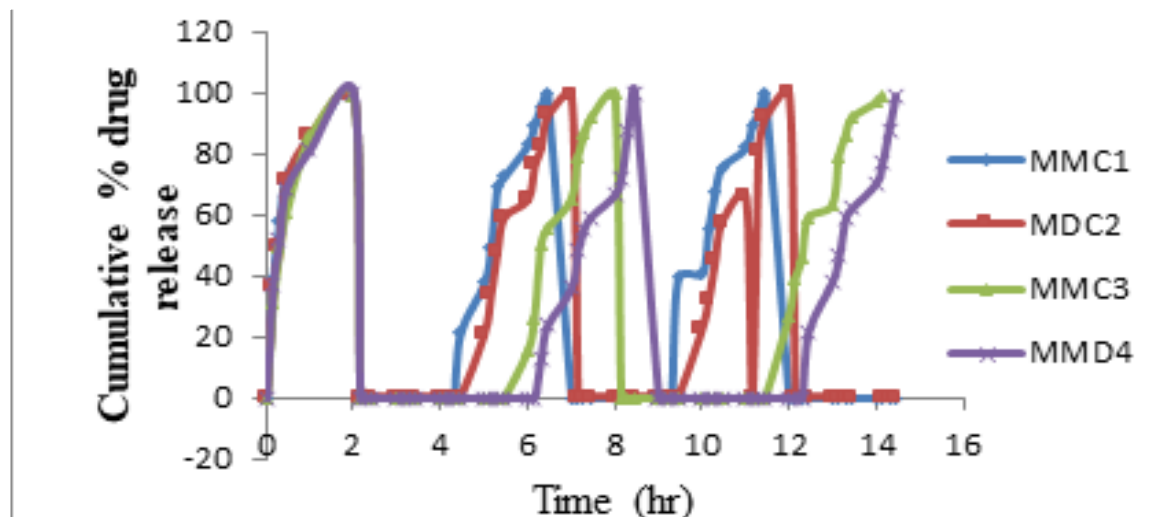| Buffer	Time(h)	Cumulative % drug release*			
	Formulation code				
	MMC1	MDC2	MMC3	MMD4	
0.1 N HCl 0.15 0.30 0.45 1 2	0	0	0	0	0
	38.87±0.27	35.98±0.24	31.09±0.45	36.76±0.57	
	57.96±0.98	49.34±0.46	48.87±0.65	51.97±0.34	
	72.98±0.67	71.29±0.89	60.88±0.45	68.34±0.75	
	83.88±0.56	85.93±0.32	85.83±0.56	81.08±0.72	
	99.37±0.43	99.23±0.78	99.23±0.82	99.45±0.21	
pH 7.4 phosphate buffer 4 5	3	0	0	0	0
	0	0	0	0	
	37.56±0.89	20.78±0.98	0	0	
pH 6.8 phosphate buffer 7 8 9 10 11 12 13	6	82.92±0.45	64.96±1.22	15.47±2.42	0
	0	99.01±0.98	65.24±2.34	35.76±2.34	
	0	0	99.45±0.43	66.35±0.76	
	0	0	0	0	
	40.67±2.45	22.34±1.09	0	0	
	81.89±0.34	65.92±0.56	0	0	
	….	99.57±0.53.	26.45±1.56	0	
	….	….	63.45±1.09	37.97±1.45	
	14	….		78.9±0.21	69.99±0.21
	14.15	….	….	98.97±0.98	76.98±0.56
	14.30	….	….		87.90±0.78
	14.45	….	….		98.68±0.96

Allivaluesiwereiexpressedias mean±s.d., n=3

Fig.4: Cumulative % drug release profile of Miglitol pulsicapsules formulations MMC1, MDC2, MMC3, MDC4.

Table 9: The *in-vitro* drug release profile of pulsicapsule of formulations sodium carboxy methylcellulose

Buffer	Time (h)	Cumulative % drug release*			
		Formulation code			
		CMC5	CDC6	CMC7	CDC8
0.1 N HCl	0.00	0	0	0	0
	0.15	21.34±0.78	19.99±1.22	23.45±0.89	22.98±0.55
	0.30	43.57±0.57	35.78±0.76	36.78±0.23	46.56±0.45
	0.45	67.89±0.97	57.89±3.67	57.90±0.76	59.86±0,23
	1.00	76.86±0.45	83.55±0.89	85.78±0.64	87.09±0.87
	2.00	97.98±1.57	98.68±0.65	96.89±3.46	97.90±1.75
pH 7.4 phosphate buffer	3.00	0	0	0	0
	4.00	0	0	0	0
	5.00	0	0	0	0
pH 6.8 phosphate buffer	6.00	0	0	0	0
	7.00	20.98±1.55	0	0	0
	8.00	71.90±0.33	56.09±0.21	21.98±0.41	0
	9.00	98.59±0.67	86.75±2.45	67.93±0.96	57.67±0.72
	10 .00	0	0	97.01±2.67	97.87±0.92
	11.00	0	0	0	0
	12.00	0	0	0	0
	13.00	0	0	0	0
	14.00	0	0	0	0
	15.00	59.80±0.44	21.98±0.67	0	0
	16.00	85.86±0.24	66.68±0.21	22.09±0.67	0
	17.00	….	99.01±0.05	65.67±0.98	65.89±0.56
	18.00	….	….		99.87±0.23

*All values are expressed as Mean ± SD, n=3

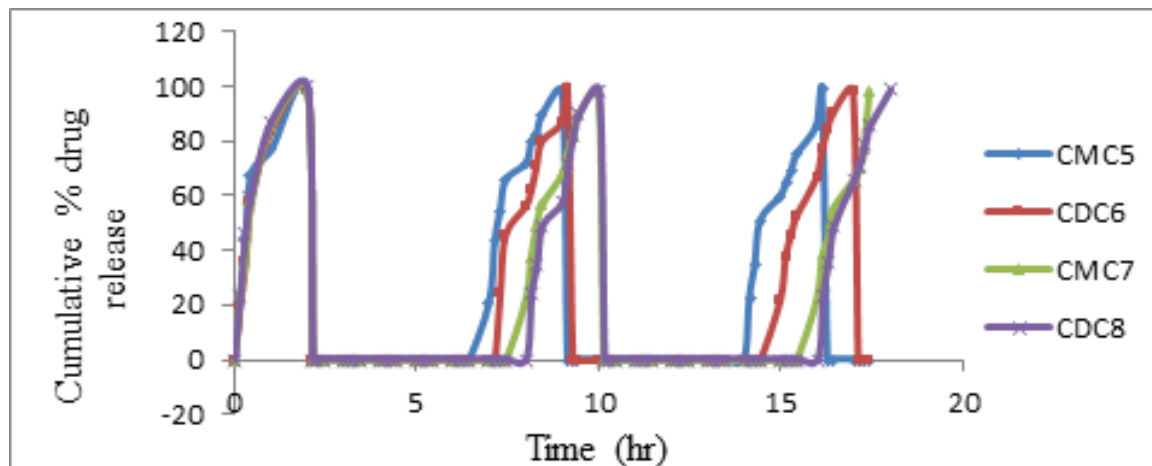Chronomodulated therapy for the treatment of type ii diabetics by using α-glucosidasel inhibitor

Fig.5: Cumulative % drug release profiles of miglitol pulsicapsules CMC5, CDC6, CMC7, and CDC8.

Stability studies:

The optimized formulation CDC8 was subjected to accelerated stability studies at 25±2º C/60±5% RH, 40±2º C/74±5% RH for 6 months and monitored the appearance, drug content and *in-vitro* drug release profile. The stored formulation tested after 3 months and 6 months for appearance, drug content and *in-vitro* profile. There were no note-worthy changes in appearance. Based on the statistical data analysis the t-test value was found to be -2.49 which indicate there was no significant changes in drug content and *in-vitro* profile up to six months. The results were given in the Table 10 and Fig.6

Table 10: Stability studies data for optimized formulation CDC8 before and after storage

Test	Initial	Storage conditions			
		25±2ºC/60±5% RH		40±2ºC/74±5%RH	
		3 months	6 months	3 months	6 months
Description	Complies	Complies	Complies	Complies	Complies
Drug content (%)	99.98±0.2	100.03±0.3	99.42±4.13	99.28±2.25	99.11±1.23

All values were expressed as mean±s.d., n=6.
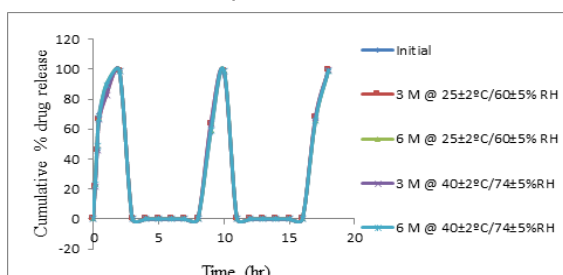
Fig.6: Comparative dissolution profiles of optimized formulationCDC8 before

And after storage at 25±2ºC/60±5% RH, 40±2ºC/74±5%RH

Conclusion:

From the present studies it can be concluded that the prepared Miglitol pulsicapsules has displayed promising *in vitro* characteristics. This will provide an ideal dosage regimen to reduce the dose frequency and drug toxicity with more patient compliance. The CDC8 (optimized formulation) has the good release profile up to 18 h with predetermined lag time of 6 h. Thus, the Optimized formulation can be considered as one of the promising preparations to control the postprandial glucose level in type-II diabetes.

Sreelatha *et al*

References:

1. Nokhodchi A, Raja S, Patel P, Asare-Addo K. The role of oral controlled release matrix tablets in drug delivery systems. BioImpacts: BI. 2012;2(4):175-87. doi: 10.5681/bi.2012.027.

2. Li J, Mooney DJ. Designing hydrogels for controlled drug delivery. Nature Reviews Materials. 2016;1(12):1-7. doi: 10.1038/natrevmats.2016.71.

3. Survase S, Kumar N. Pulsatile drug delivery: Current scenario. CRIPS. 2007; 8(2):27-33

4. Mehmet EO, Ioannis DK, Panoraia IS. Diabetes Mellitus: A Review on Path physiology, Current Status of Oral Medications and Future Perspectives. Acta Pharm. Sci. 2017, 55(1),61-82. DOI: 10.23893/1307-2080.APS.0555

5. Pozzi F, Furlani P, Gazzaniga A, Davis SS, Wilding IR. The time clock system: a new oral dosage form for fast and complete release of drug after a predetermined lag time. Journal of controlled release. 1994; 31(1):99-108. doi.org/10.1016/0168-3659(94)90255-0.

6. Reddy, V. S., Sahay, R. K., Bhadada, S. K., Agrawal, J. K., &Agrawal, N. K. Newer oral anti-diabetic agents. Journal, Indian Academy of Clinical Medicine. 2000;1(3);245-251. doi: 10.1007/s11739-011-0677-5.https://www.scribd.com/document/522301984/02.

7. Indian Pharmacopoeia New Delhi, Ministry of Health and Family Welfare, Govt. of India, Controller of publications, vol.-II, 1996; Page No. 734-736.

8. Banker GS, Anderson NR. Tablets. In: Lachman L, Liberman HA, Kanig JL. eds. The Theory and Practice of Industrial Pharmacy. Mumbai, India Varghese Publishing House; 1987:293–345.

9. 9. United States Pharmacopoeia 29-NF 24.The Official Compendia of Standards. Asian ed. Rockville, MD: United States Pharmacopoeia Convention Inc. (2006), 2679-2681.

10. Krögel I, Bodmeier R. Pulsatile drug release from an insoluble capsule body controlled by an erodible plug. Pharmaceutical research. 1998;15(3):474-81. doi: 10.1023/a:1011940718534.

11. Sandeep M, Kishore VS, Sudheer B, Ershad S, Adithya K. Design and development of chronopharmaceutical drug delivery of lansoprazole. Asian Journal of Pharmaceutical Research and Development.2013 Sep 1:63-70.

12. Shamima Nasrin Ashima Aziz, Mohiuddin Ahmed Bhuiyan. Design, formulation and in vitro evaluation of sustained release pulsatile capsule of metoprolol tartrate, IJPSR 2015; 6(7): 2755-2761.doi:10.13040/IJPSR.0975-8232.6(7).2755-61. https://www.researchgate.net/publication/279479968

13. Ashwini, M., & Ahmed, M. G. Design and evaluation of Pulsatile drug delivery of Losartan Potassium. Dhaka University Journal of Pharmaceutical Sciences 2014; 12(2): 119–123. https://doi.org/10.3329/dujps.v12i2.17610.

14. Ross AC, Macrae RJ, Walther M, Stevens HN. Chronopharmaceutical drug delivery from a pulsatile capsule device based on programmable erosion.Journal of pharmacy and pharmacology. 2000; 52(8):903-9. doi: 10.1211/0022357001774787.

15. 15..Sai Krishna MV, Saikishore V, Sravani SL, Rudrama Devi G. Design and characterization of pulsatile drug delivery of metaprolol tartrate. Indo Am J P Sci, 2017. 2017; 04(05):1052-1059. DOI:10.13040/IJPSR.0975-8232.11(1).358-64

16. ICH Harmonized Tripartite guidelines on "Stability Testing of New Drug Substances and Products Q1A(R2)",6 February, 2003.

Formulation Development and Characterization of Ritonavir Loaded Controlled Release Matrix Tablet

Sujit Shinde[1], Gita Chaurasia[2*]

[1, 2] Department of Pharmaceutics, Siddhant College of Pharmacy, Sudumbare, Pune, Maharashtra-412109, India

*Corresponding Author: gitagc19@gmail.com

Abstract

The aim of this study was to design Ritonavir loaded controlled-release matrix tablet (CRMT) for the treatment against Human immunodeficiency virus, with an emphasis on the drug's pharmacokinetic and physicochemical characteristics for enhanced therapeutic efficacy and decreased gastrointestinal side effects. The tablet was prepared by using rate-controlling polymers like Hydroxy-propyl methyl cellulose (HPMC) K4M and xanthan gum by direct compression method. Formulation batches F1-F9 were developed, optimized using 3^2 full factorial design and evaluated for pre and post compressional studies. Drug-excipients studies were performed by IR spectra and DSC thermogram. All batches of powder blends were evaluated for particle size, angle of repose, bulk density, tapped density, % Compressibility index and Hausner's ratio. The prepared tablets were characterized for Weight variation, Hardness, Thickness, Friability, % Drug content, % Swelling index and *In-vitro* cumulative drug release study up to 12h. Analysis of variance was used to handle acquired data for statistical analysis. In conclusion, maximum drug release 96.29% and swelling index 81.29±0.09%, was observed in F9, after 12 h of studies and found stable under short term stability study as per ICH guideline. The article developed a potential scope in reducing the dose-dependent gastrointestinal toxicity of ritonavir with fewer side effect and a hope in future.

Keywords: Ritonavir, Matrix tablet, Hydroxy-propyl methyl cellulose, Controlled release tablet, Human immunodeficiency virus protease

Introduction

Tablet is the preferred way to provide medications orally, which have advantages including precise dosing, ease of use, patient compliance, cost effective, and extended shelf life (1). Present work aimed development of controlled release tablet to reduce dose-dependent adverse effects and optimize therapeutic benefits. In comparison to traditional delivery systems, matrix-controlled release has shown benefits include longer drug half-lives and enhanced effectiveness, lower toxicity, and better patient comfort. Drug release from a porous monolithic matrix involves the simultaneous penetration of surrounding liquid, dissolution of drug and leaching out of the drug through tortuous interstitial channels and pores (2). Ritonavir, is a Protease inhibitor, inhibits cytochrome P450-3A4 and used to treat HIV/AIDS was selected as suitable candidate for the present work due to suitable biological half- life of ~3-5 h. Literature revealed that the high inter-individual variability in pharmacokinetics was reported with greater than six-fold variability in through concentrations among patients given 600 mg ritonavir every 12 h (3). An approach of developing CRMT of ritonavir to reduce its daily dose frequency and gastrointestinal side effects in

higher dose. For this 300 mg tablet was aimed to develop by direct compression method. The release rate of drug was controlled by using optimized concentration of natural polymers HPMC K4M and xanthan gum by diffusion or dissolution method. Hydrophilic polymer matrix system is widely used for designing oral controlled release delivery systems for long duration towards site of action, because of their flexibility to provide a desirable drug release profile, cost effectiveness, and a broad regulatory acceptance (4,5).

Materials and Methods

Ritonavir was received as a gift sample from Cipla Pt. Ltd. Goa. Xanthan gum, Avicel PH 101, Talc, Magnesium stearate, HPMC K4M were obtained as gift samples by blue cross laboratory, Nashik. The analytical grade chemicals and all other reagents used for the assessment were provided by Research-Lab Fine Chem Mumbai. Freshly prepared distilled water is used throughout the work.

Preformulation study

Physical characteristics

The drug ritonavir was studied visually for organoleptic characteristics such as colour, Odor and appearance. Melting point of drug was determined by glass capillary method whose one end was sealed and kept in melting point apparatus.

Determination of solubility

Accurately weight 5 mg ritonavir was added to 10 ml of different solvents like Distilled water, Methanol, Ethanol, Dimethyl formamide, Di methyl-sulfoxide, Phosphate buffer (PB) (pH 6.8, 7.4 and 7.8) solution in the 10 ml volumetric flask and kept aside for 24 h. After 24 h solutions were diluted suitably and filtered through Whatman filter paper. The drug content was analysed by UV spectrophotometric method in triplicate using equation as follows-

Solubility (mg/ml) = Initial - Final concentration of drug

Loss on drying (LOD)

Weighed 1gm of the drug in weighing bottle and kept in the hot air oven at 105^0 C for 2 h and after allowed it to cool. Weighed the contents and the bottle and %LOD was calculated (n=3) as follows-

$$\% \text{ LOD} = \frac{\text{Initial weight} - \text{final weight}}{\text{Initial weight}} X\ 100$$

Identification of drug

The drug was identified by IR spectra and Differential scanning calorimetry (DSC) methods. Potassium bromide pellet technique was used in the Shimadzu instrument at frequency range of 500-4000 cm^{-1} with scanning speed of 4.0 cm-1 and the graph was recorded. For DSC (STAR*SW 12.10 instrument), a weighted sample was placed in a crucible and thermogram was recorded at scanning rate of 10ºC per min and at 40-150°C.

Quantitative estimation of drug

The UV was used for estimation of the drug by UV-2400 PC series, Shimadzu, Japan, in the present study. The drug concentration was estimated (n=3), in the range 10-50µg/ml in PB pH 7.4 and ethanol mixture (10:1) [PBE mixture]. All aliquots were scanned from 200-400 nm to obtain the value of maximum wavelength and calibration curve was prepared (6).

Drug–excipients compatibility study

Physical mixture of drug and polymers (HPMC K4M and Xanthan gum) was prepared by kneading method in 1:1 molar ratio. All sample was stored and analysed by FTIR and DSC method.

Formulation and development of CRMT

Optimization of polymer concentration by 3^2 full factorial Design

For the present work 3^2 full factorial design selected over 2 factors were evaluated at three possible level (-1, 0, 1) using release retardant polymers HPMC K4M (X_1) in concentration 20, 30, 40 mg and Xanthan gum (X_2) in concentration 30, 40, 50 mg as independent

variable, in 9 batches and % Swelling index (Y) was studied for each as dependant variable up to 12 h (7).

Precompression studies

All batches of polymer were mixed with another excipient to develop CR matrix powder blend and analyzed for different parameters.

Mean Particle size determination

Mean vesicle size of prepared formulations F1-F9 was observed by a calibrated electron optical microscope Olympus, India (8). Dilute suspension of all formulation was prepared separately and one drop from each sample was spread on slide; a cover slip was placed over it and observed. The arithmetic mean was determined by following equations. Where, n is the total number of particles counted and d is projected diameter.

$$Arithmetic\ mean = \sum nd/ \sum n$$

Bulk and Tapped density

All formulation F1-F9 was evaluated for Bulk density by placing the powder blend in a measuring cylinder of bulk density apparatus and Tapped density was calculated by three tap method and calculated by using the formula (n=3) and reported.

Bulk density = (Total weight of powder/granules) / (total volume of powder/granules)

Tapped density = (Total weight of powder/granules) / (Tapped volume of powder/granules)

Compressibility index (CI) and Hausner's ratio

CI was determined by placing the powder formulation F1-F9 each in a measuring cylinder and the volume (V_0) was noted before tapping. After compression again volume (V) was noticed and calculated by follows below equations. Hausner's is the ratio of tapped density to bulk density.

$$CI = \frac{(1-V)}{V0} \times 100$$

Hausner's ratio = (Tapped density) / (Bulk density)

Angle of repose (θ)

Powder of each formulation F1-F9 was placed in the funnel separately and allowed to flow freely. With the help of vernier callipers the height and radius of the heap were measured and noted in triplicate reading and calculated by formula as follows-

tan θ = h /r, Where h = height of heap, r = radius of heap

Method of preparation of CRMT

All the ingredients of F1-F9 were weighed accurately and passed through sieve no. 120 and blended thoroughly to obtain uniform mixing and tablets were prepared by direct compression method (9). The machine was adjusted to produce an approximate weight of 300 mg tablet and stored for further study in Table 1.

Evaluation of Prepared CRMT

weight variation

Twenty tablets were taken from each formulation and weighed individually. Average weight was calculated as per I.P. (n=3).

Thickness test

Prepared tablets were evaluated for their thickness using a Bernier calliper in millimetre. Average of three readings were taken and the results were tabulated (n = 3).

Hardness test

All formulations CR tablets were evaluated for their hardness using Pfizer hardness tester as per I.P. Average of three reading were taken and tabulated (n = 3).

Friability test

Twenty tablets of each batch were weighed initially (W1) and put it into friability test apparatus by keeping rotation speed of 25 rpm for 4 minutes. Then weighed again after 4 minutes (W2) and % friability has been calculated in triplicate as follows (10)-

% friability = (W1-W2) / W1 × 100

Drug content

From each formulation three random-

ly selected tablets were weighed accurately and powdered equivalent to 10 mg of drug. Dissolved by shaking and diluted suitably using PBE mixture into 10 ml volumetric flask. Then, filtered and analysed by UV method against PBE as blank. Averages of triplicate readings were taken and calculated (11).

Percentage swelling index

Three tablets from each formulation were weighed individually (W_1) and immersed in a Petri dish containing PB pH 7.4 for pre-determined times (15min, 30min,1h, 2h, up to 12h). After immersion tablets were wiped off the excess surface water and weighed after hydration (W_2). The % swelling index was calculated in triplicate (12).

$$\% \text{ Swelling Index} = \frac{(W2-W1)}{W2} \times 100$$

In-vitro % cumulative drug release study

The drug release profile was studied for each formulation using USP dissolution testing apparatus II using a paddle at 50 rpm with 900 ml PB pH 7.4 at 37±0.5°C. Aliquots of 10 ml were withdrawn at 15 min, 30 min, 1h, 2h, up to 12h respectively and the same volume was replaced with PB pH 7.4. The drug content was analysed by spectrophotometrically. The % cumulative drug release was calculated using calibration curve at 239nm (n=3). The data were studies for different kinetic models (13, 14, 15).

Physical stability study

A protocol of stability study was carried out on optimized formulation for short term stability study conditions at refrigeration temperature (4±2)ºC, room temperature (25±2)ºC and 40ºC, 75% RH as per ICH guidelines for a period of 3 months. After every month time interval physical appearance and residual drug content was determined and reported in triplicate (16).

Results and Discussion

Preformulation studies showed that ritonavir is the off whitish amorphous, odourless, bitter metallic taste powder and has average melting point of 127°C. The drug is found sol-

uble in ethanol, Dimethyl formamide, Di methyl-sulfoxide, insoluble in distilled water and sparingly soluble in buffer solutions. The observed % Loss on drying for drug was 0.02 % w/w within the I.P. limit. Drug showed maximum absorbance at 239nm in PBE mixture in concentration range of 10-50µg/ml, r^2 =0.9998 and Slope y = 0.0162x, that followed Beer-Lambert's law shown in Figure 1.
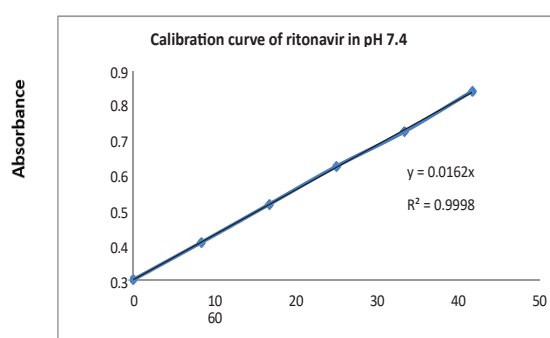

Figure 1: Calibration curve of Ritonavir

Identification and drug–excipients compatibility study (1:1Molar) was carried out by IR and DSC methods. As a result, drug was found no significant interactions with natural polymers used under study. The IR study showed absorption frequencies (cm^{-1}) of common peaks includes; N-H stretching of amines at 3357.3, O-H stretching of aliphatic primary amines at 3330.91, C-H stretching of alkene (3098.88), C-H stretching of alkane (2964.47), C=O stretching of unsaturated ester (1714.67), C=C stretching of conjugated alkane (1620), N-O stretching of nitro compound (1523.57), C-O stretching of alkyl aryl ester (1235.59), C=C bending of alkene (703.20) (17). The DSC thermogram of drug and its physical mixture with selected polymers exhibited little or no change in enthalpy value and found compatible with excipients. For preparing powder blends of selected polymers optimization of different concentration was done by 3^2 full factorial design in nine batches and % swelling index were calculated and reported (n=3) as shown in Table 1.

Table 1: Optimization by 3^2 full factorial design

Batch	HPMC K4 M (X1)	Xanthan Gum (X2)	% Swelling index (Y) (mean±SD)
1	20 (-1)	30 (-1)	48.31±0.37
2	20 (-1)	40 (0)	56.82±0.91
3	20 (-1)	50 (1)	71.54±0.10
4	30 (0)	30 (-1)	51.74±0.22
5	30 (0)	40 (0)	63.28±0.54
6	30 (0)	50 (1)	77.65±0.77
7	40 (1)	30 (-1)	54.36±0.36
8	40 (1)	40 (0)	68.34±0.06
9	40 (1)	50 (1)	81.29±0.09

All 9 batches were evaluated and as a result second order polynomial equation was derived from equation $y = b_o + b_1 + x_1 + b_2 x_2 + b_3 x_1^2 + b_4 x_2^2 + b_5 \, x_1 x^2$, where y is the response (% Swelling index at 2 h). The average results of changing one variable at a time from its low to high value showed by main effect (x_1, x_2) and interaction ($x_1 x_2$) showed the response changes with combined effect of variables. The coefficients corresponding to linear effects (b_1, b_2), interaction (b_5) and quadrate effect (b_3, b_4) were determined from the results of the study. The fitted equation for response was: Y = [6.1–5.98 x 10^{-2} x_1 –2.03 x_2 x 10^{-1} + 1.83x_1^2 + 3.45 x 10^{-2} x_2^2 – 1.67 $x_1 x_2$] x 10^{-2}, where values of b_o, b_1, b_2, b_3, b_4, and b_5 were 0.05214, -0.00065, -0.00429, 0.00176, 0.00951and -0.01287 respectively. Before compression powder bed of all formulations were studied for various rheological characteristics like Particle size, bulk density, tapped density, compressibility index, Hausner's ratio and angle of repose shown in Table 2. The results of the studies indicated that the powder bed is easily compressible, and hence can be compressed into a compact mass of tablet.

Table 2: Pre-compressional studies

Formulation code	Mean Particle size (µm, Mean±SD)	Angle of repose(θ) (Mean± SD)	Bulk density (gm/cm³) (Mean± SD)	Tapped density (gm/cm,³ Mean± SD)	Compressibility index (%) (Mean± SD)	Hausner's ratio (Mean± SD)
F1	98.3±0.12	24.23±0.61	0.31±0.27	0.46±0.42	15.62±0.50	1.20±0.04
F2	102.1±0.36	31.52±0.32	0.38±0.04	0.42±0.65	15.90±0.42	1.35±0.46
F3	108.2±0.53	27.17±0.27	0.34±0.90	0.44±0.12	18.62±0.97	1.71±0.95
F4	96.4±0.31	28.76±0.38	0.37±0.12	0.43±0.08	13.83±0.32	1.15±0.74
F5	106.7±0.22	27.72±0.97	0.34±0.95	0.49±0.32	15.48±0.70	1.26±0.61
F6	104.8±0.13	28.56±0.41	0.40±0.71	0.47±0.09	13.79±0.93	1.39±0.81
F7	94.5±0.64	28.39±0.93	0.39±0.73	0.46±0.18	14.65±0.58	1.20±0.08
F8	103.9±0.54	27.41±0.96	0.35±0.15	0.41±0.34	19.45±0.22	1.23±0.41
F9	97.6±0.09	28.57±0.88	0.37±0.43	0.44±0.94	15.12±0.73	1.14±0.46

Evaluated powder blend of each formulation were directly compressed on 10 station rotary pilot press punching machine to obtained maintenance dose of 300mg as per

the composition shown in Table 3. The formulated CRMT F1-F9 were evaluated for different parameters. The observed values for weight variation (297±0.29 to 303±0.52 mg), Thickness (4.27±0.92 to 4.39±0.55mm), hardness (3.64±0.18 to 4.69±0.23 kg/cm^2), % Friability (0.27±0.68 to 0.35±0.46), and % Drug content (85.42±0.81 to 95.18±0.52) was found. The % swelling index is the water uptake nature of

the polymer properties that affect the onset of swelling. Study was carried out for all formulations F1-F9 tablet for a period for 12 h. It was observed that swelling has been increases with increase in amount of HPMC K4M and xanthan gum. Maximum swelling was attained at 12 h. The following order of swelling was ascertained F9 >F6 >F3 >F8 >F5 >F2 >F7 >F4 >F1 resulted in Table 4.

Table 3: Composition of formulation

Ingredients (mg)	F1	F2	F3	F4	F5	F6	F7	F8	F9
Ritonavir	100	100	100	100	100	100	100	100	100
HPMC K4M	20	20	20	30	30	30	40	40	40
Xanthan Gum	30	40	50	30	40	50	30	40	50
Avicel PH 101	144	131	124	137	124	114	124	114	104
Magnesium stearate	3	3	3	3	3	3	3	3	3
Talc	3	3	3	3	3	3	3	3	3
Total	300	300	300	300	300	300	300	300	300

Table 4: Evaluation of prepared Tablets

Formulation code	Hardness (kg/cm^2) (Mean± SD)	Thickness (mm) (Mean± SD)	Friability % (Mean± SD)	Weight variation (mg) (Mean± SD)	%Drug content (Mean± SD)	% Swelling Index up to 12 h (Mean± SD)
F1	4.42±0.55	4.32±0.23	0.32±0.12	302±0.62	89.29±0.47	48.31±0.37
F2	4.69±0.23	4.28±0.76	0.29±0.52	298±0.14	93.61±0.56	56.82±0.91
F3	4.79±0.09	4.36±0.14	0.35±0.46	302±0.55	88.52±0.19	71.54±0.10
F4	3.94±0.43	4.39±0.55	0.31±0.38	302±0.67	90.06±0.36	51.74±0.22
F5	4.10±0.92	4.27±0.92	0.29±0.47	297±0.29	91.65±0.72	63.28±0.54
F6	3.78±0.87	4.36±0.09	0.28±0.11	298±0.81	87.22±0.41	77.65±0.77
F7	4.38±0.45	4.33±0.18	0.31±0.09	298±0.49	92.19±0.93	54.36±0.36
F8	4.41±0.29	4.29±0.79	0.29±0.17	303±0.52	85.42±0.81	68.34±0.06
F9	3.64±0.18	4.31±0.98	0.27±0.68	301±0.78	95.18±0.52	81.29±0.09

In vitro % cumulative drug release was studied in F1-F9 using USP dissolution apparatus II (using paddle) under suitable maintained conditions for a period of 12 h. Content of drug was analysed at 239nm by UV method. The obtained data were computed graphically (Graph A). The different kinetic models were studied and observed that data were fitted to linearity

in zero order (r^2 = ≥ 0.995), first order (r^2 = ≥ 0.867) and Higuchi model (r^2 = ≥ 0.674) showed in graph B, C and D. Graph E represents Korsemeyer's Peppas released curves (r^2 = ≥ 0.90) for all formulations and n value was found to be ≥ 0.5 which indicate that indicates anomalous or non-fickian diffusion shown in Figure 2. The drug release occurs probably by diffusion, ero-

sion and dissolution methods through polymers. On the basis of all studied evaluation parameters F9 was selected as optimized formulation due to maximum drug release in controlled manner up to 12h, high swelling index. Stability study was carried out on chosen formulation F9.

It was observed that no interaction and physical change reported and no significant decrease in residual drug content for a period of 3 months under short term stability study shown in Figure 3.
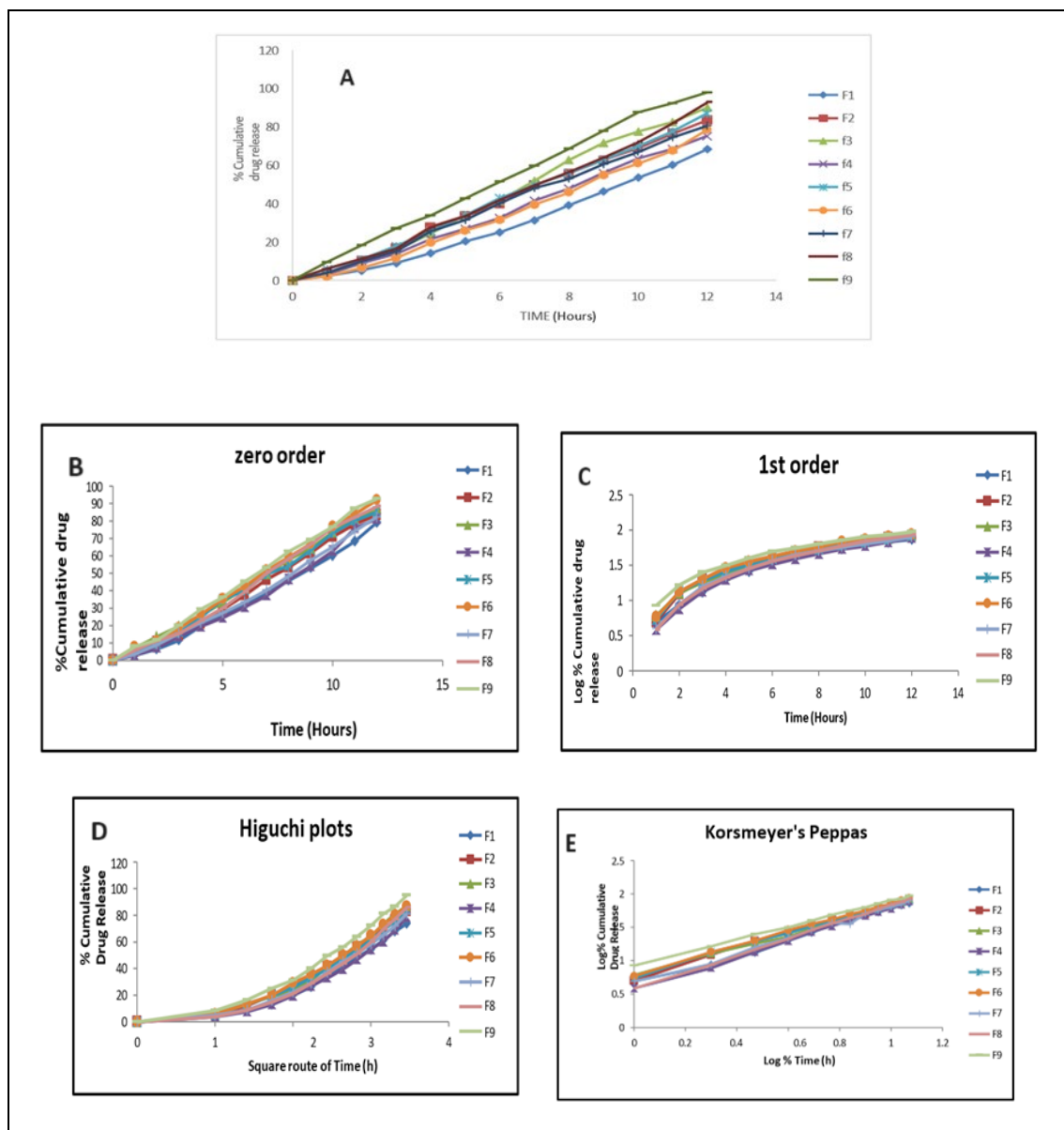

Figure 2: *In Vitro* % cumulative drug release (A) and Kinetic studies of cumulative drug release (B, C, D, E) from F1-F9
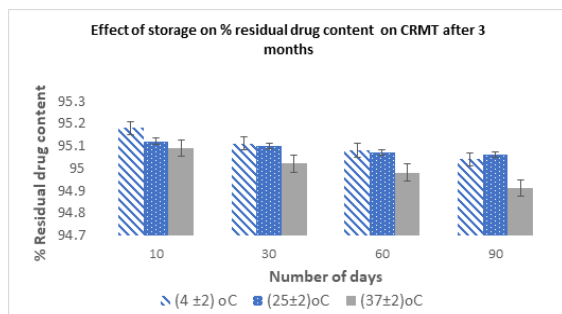
Figure 3: Effect of storage on residual drug content on CRMT after 3 months (Mean± SD)

Conclusion

In conclusion, CRMT of ritonavir was success-fully developed to release drug for prolonged duration. The release of 15-20% of drug within first hour could help in the maintaining of mini-mum effective concentration quickly and avoid the use of loading dose in the formulation. Hence, the developed CRMT of ritonavir can be potentially useful in clinical treatment of HIV.

Conflict of interest

Nil

Acknowledgement

Authors are thankful to Principal, Siddhant college of Pharmacy, Pune for guidance. Also thankful to search engine and library to provide data and support.

References

1. Prajapati, G.B and Patel, R.K. (2010). Design and in vitro evaluation of novel nicorandil sustained release matrix tablets based on combination of hydrophilic and hydrophobic matrix systems. *International Journal of Pharmaceutical Sciences review and research,* 1:33-35.

2. Raghavendra, R.N.G., Prasanna, K.R. and Sanjeev, N.B. (2013). Review on matrix tablets as sustained release. *International Journal of Pharmaceutical Research and Allied Sciences*, 2(3):1-17.

3. British Pharmacopeia, vol 1, London: London stationary office; 2003:495.

4. Ch. Sudha, V.P.L., Narendra, K.R., and Hema, V. (2017). Formulation and evaluation of Zolmitriptan controlled release matrix tablet. *Indian Journal of Research in Pharmacy and Biotechnology,* 5(2): 124-128.

5. Nokhodchi, A., Raja, S., Patel, P. and Asare-Addo, K. (2012). The role of oral controlled release matrix tablets in drug delivery systems. *Bioimpacts*, 2(4):175-87.

6. Mohammad, Y.P., Shakeel, M., Kiran, B. and Irfan, A.A. (2019). Development and validation of UV-Visible spectrophotometric method for estimation of ritonavir in bulk and formulation. *The Pharma Innovation Journal*, 8(4): 30-34.

7. Prajapati, B.G., Patel, G.N. and Solanki, H. (2010). Formulation and statistical optimization of time controlled pulsatile release propranolol hydrochloride compressed coated tablet. *e -Journal of Science and Technology,* 5: 9-19.

8. Martin, A., Swarbrick, J. and Cammarata, A. (1991). Physical Pharmacy, Verghese publishing house, Bombay, Third edition, pp. 492-506.

9. Shambhavi, P., Vasudha, B. and Rajendra, K.J. (2019). Formulation Development and In Vitro Characterization of Zolmitriptan Controlled Release Drug Delivery Systems. *INNOSC Theranostics and Pharmacological Sciences*, 2(1):8-13.

10. Lachman, L., Leiberman, H.A. and Kanig, J.L. (1990). The Theory and Practice of Industrial Pharmacy. Varghese publishing house, Bombay. 3rd Edition. pp.296.

11. Indian Pharmacopoeia, Government of In-dia, Ministry of Health and Family Welfare, Vol. II, 1996, published by Controller of Publications, Delhi, A-147,736.

2302

12. Arora, G., Malik, K., Singh, I., Arora, S. and Rana, V. (2011). Formulation and evaluation of controlled release matrix mucoadhesive tablets of domperidone using Salvia plebeian gum. *Journal of Advance Pharmaceutical Technology & Research,* 2(3):163-169.

13. Higuchi, T. (1961). Rate of release of medicament from ointment bases containing drugs in suspension. *Journal of Pharmaceutical Sciences,* 50:874–5.

14. Korsmeyer, R.W., Gurny, R., Doelker, E., Buri, P. and Peppas, N.A. (1983). Mechanisms of solute release from porous hydrophilic polymers. *International Journal of Pharm*aceutics,15:25–35.

15. Peppas, N.A. (1985). Analysis of Fickian and non-fickian drug release from polymers. *Pharmaceutica Acta Helvetiae*, 60:110–111.

16. Bajaj, S., Singla, D. and Sakhuja, N. (2012). Stability testing of pharmaceutical products. *Journal of Applied Pharmaceutical Science,* 2(3):129-138.

17. Bonthagarala, B., Dasari, V. and Kotra, V. (2019). Enhancement of solubility and dissolution rate of BCS class II drug ritonavir using liquisolid technique. *International Journal of Pharmaceutical Sciences and research,* 10(5): 2430-2438.

In vitro Acetylcholinesterase Inhibitory Activity of Selected Sri Lankan Medicinal Plants

Waradana Sadin de Silva[1], Champika Dilrukshi Wijayarathna[1] and Hondamuni Ireshika De Silva[1*]

[1] Department of Chemistry, Faculty of Science, University of Colombo, Sri Lanka.

*Corresponding Author: hicdesilva@chem.cmb.ac.lk

Abstract

Acetylcholinesterase (AChE) inhibition is a well-accepted therapeutic strategy for Alzheimer's disease and many categories of dementia. Medicinal plants are promising sources of useful AChE inhibitors and have been used to treat Alzheimer's disease by people around the world. This investigation was carried out to assess the AChE inhibitory activities of the crude organic extracts of nine Sri Lankan medicinal plants. Air dried, powdered samples of different plant parts were sequentially extracted with 3 organic solvents to yield a total extract of the individual plant part. These extracts were tested for AChE inhibitory activity using Ellman's assay in 96-well microplates. Galantamine (IC_{50} 1.57 ±0.01 µg/ml) was used as the standard acetylcholinesterase inhibitor and all the tests were done in triplicates. Potent AChE inhibitory activities were shown by the leaf extracts of *Wrightia antidysenterica* and *Flueggea leucopyrus* with IC_{50} values of 64±0.5 µg/ml and 107±0.1 µg/ml, respectively. Furthermore, *Zingiber cylindricum* rhizome extract and *Areca concinna* seed extract also exhibited considerable AChE inhibitory activities with IC_{50} values of 189±1.4 µg/ml and 217±1.2 µg/ml, respectively. Hence, it can be concluded that *W. antidysenterica* and *F. leucopyrus* possess potent anti-cholinesterase activity and can be used to isolate drug leads with anti-acetylcholinesterase activity.

Introduction

Alzheimer's disease is the most prevailing neurodegenerative disease and is becoming one of the major human mental health concerns today. Neuronal death and great synaptic loss in the brain regions accountable for cognitive functions, especially the hippocampus, the entorhinal cortex, cerebral cortex and the ventral striatum are the main characteristics of Alzheimer's disease (1). Previous research works have revealed that the malfunction of the cholinergic system can cause memory deficiency (2). Brains of the affected patients with Alzheimer's disease had shown deterioration of acetyl-cholinergic neurons. Enzyme acetylcholinesterase (AChE) cause activities of cholinergic neurons to be lessened in cerebral cortex and modification of acetylcholinesterase activity in the parietal and frontal cortex has a relationship with dementia (3). Pharmacological treatment for this disease has not yet at a satisfactory level for controlling neurodegeneration or any other alternative.

Medicinal plants have been used to treat neurodegenerative diseases including Alzheimer's disease and memory related disorders for many years in different parts of the world (4). Converse to synthetic drugs, it

is reported that drugs of plant origin are not coupled with many side effects and have a vast therapeutic potential to cure various diseases (5). Several scientific investigations have revealed the importance of medicinal plants in the enhancement of nervous system function (6). Therefore, numerous compounds having potential anticholinesterase activity have been isolated from plant families such as Arecaceae, Apocynaceae, Zingiberaceae and Lycopodiaceae (6,7).

Huperzine A, a natural compound isolated from the medicinal plant *Huperzia serrata*, is a selective inhibitor of AChE. Subsequently, Huperzine A was subjected to extensive studies as a lead compound for the expansion of novel effective anti-acetylcholinesterase medications for the treatment of Alzheimer's disease comparative to those approved synthetic drugs by the Food and Drug Association in USA, such as galanthamine, rivastigmine and donepezil (7).

In Sri Lanka traditional physicians prepare various medications utilizing endemic and native medicinal plants to treat several neurological diseases (8,9). However, only a few research studies had been carried out in Sri Lanka on identification of potential drugs for Alzheimer's disease and no reported compounds have been isolated as potential drug leads for Alzheimer's disease from plants in Sri Lanka (10,11). In the current study, Sri Lankan medicinal plants from seven different families, Balsaminaceae, Arecaceae, Apocynaceae, Zingiberaceae, Dilleniaceae, Phyllanthaceae, and Rubiaceae were investigated for their AChE inhibitory activity.

Materials and Methods

Sample collection

Fresh plant parts of *Wrightia antidysenterica, Impatiens repens, Zingiber cylindricum, Dillenia retusa, Curcuma albiflora, Phoenix pusilla, Areca concinna, Flueggea leucopyrus* and *Knoxia zeylanica* (leaves, stem bark, roots and fruit) were collected from different locations of Sri Lanka. All the plants were authenticated by the Bandaranaike Memorial Research Institute Herbarium, Nawinna, Sri Lanka. The collected plant samples were washed under running tap water, chopped and air dried in shade for about 72 hours and then ground into fine powders using a grinder. These powders were stored in sealed bottles at 4 °C until used.

Preparation of plant extracts

All the solvents used for extraction purposes were analytical grade solvents (Sigma Aldrich, Germany). Powdered plant parts were extracted first with 250 ml of methanol and the extraction was repeated with the same volume of methanol. These extracts were filtered with Whatman No1 filter paper. Then the residual powder was extracted using 250 ml of Methanol:CH_2Cl_2 1:1 mixture and the extraction was repeated with 250 ml of the same. Next, the residual powder was extracted twice with 250 ml of dichloromethane. Finally, the filtrates were combined to obtain the total extract of each plant part. The organic solvent was evaporated to dryness under reduced pressure at room temperature using a rotary evaporator (BUCHI-R-200). The obtained crude extracts were further dried using N_2 gas. All the samples were stored in sealed bottles at 4 °C until further use.

Determining percentage yield

The masses of the powdered plant specimen and the resulting dry crude extract were used to calculate the percentage yield, using the following equation (12),

$$\text{Percentage Yield(\%)} = \frac{W_2 - W_1 \times 100}{W_0}$$

Where W_2 is the mass of the dry plant extract and the glass bottle, W_1 is the mass of the glass bottle and W_0 is the mass of the dried powder of the plant specimen.

Waradana *et al*

Reagents for ellman's assay

5,5′-Dithio-bis(2-nitrobenzoic acid) (DTNB), acetylthiocholine iodide (ATCI), acetylcholinesterase type VI-S, Galantamine were purchased from Sigma-Aldrich, Germany. All the solvents and reagents used were analytical grade. For the screening of acetylcholinesterase inhibitory activity of plant parts, plant extracts were dissolved in methanol, to be used in modified Ellman's assay (13, 14).

Ellman's assay

Acetylcholinesterase was dissolved in 0.1 M phosphate buffer (pH 8.0) to prepare an 18 U/mL stock solution and it was stored at 4 °C. The stock acetylcholinesterase was diluted to 0.3 U/mL before use. Acetylthiocholine iodide of 6.2 mM and 5,5′-dithio-bis(2-nitrobenzoic acid) (DTNB) of 7.6 mM solutions were prepared. Freshly prepared reagents were used for each acetylcholinesterase inhibition assay. Ellman's assay was adjusted to final volume of 240 µl in 96 well microplates. 0.3 U/mL acetylcholinesterase (50 µl) (0.015 AChE Units), 0.1 M pH 8.0 potassium phosphate buffer (125 µl), 7.6 mM DTNB (25 µl) and crude extract/sample dissolved in methanol (10 µl) were used in the modified Ellman reaction mixture. Reaction mixture was incubated for 30 min at 30 °C, and the enzymatic reaction was initiated by adding 30 µl of 6.2 mM acetylthiocholine iodide (ATCI). Absorbance was measured at 412 nm in every 11 seconds for a duration of 220 seconds (SPECTROstar Nano Plate Reader). Enzyme inhibition was calculated as a percentage compared to an assay with 10 µl of methanol instead of the sample extract (SB). All the experiments were done in triplicate. pH 8.0 potassium phosphate buffer was used as the blank instead of acetylcholinesterase enzyme. Galantamine was used as the positive control.

Percentage AChE inhibition was calculated by using equation -1 (13, 14),

Percentage AChE inhibition = [(SB - S) / SB] × 100 ---------- 1

SB = variation in the absorption of the blank sample (0 s – 220 s)

S = variation in the absorption of the test sample extract (0 s – 220 s)

Statistical analysis

Data were analyzed using GraphPad Prism 9 software. All the assays were carried out in triplicates. Values were expressed as means ± standard deviations. IC_{50} (Concentration providing 50% inhibition) values were estimated from the plot of AChE inhibition percentage against extract concentration.

Results and Discussion

It is well-documented that the deterioration in mental and cognitive functions associated with Alzheimer's disease is due to the depletion of cortical acetyl-cholinergic neurotransmission. Acetylcholinesterase inhibitory compounds inhibit or stop AChE enzymes from cleaving acetylcholine.

Therefore, AChE inhibitors can suppress the degradation of acetylcholine and improve concentrations of acetylcholine, which leads to improved communication between nerve cells. Consequently, this stabilises or reduces the symptoms of Alzheimer's disease (15). AChE inhibitor drugs, including physostigmine and donepezil show some increase in the cognitive functions of Alzheimer's patients. However, due to the less selectivity of acetylcholinesterase inhibitory drugs in the market, patients experience numerous side effects (16,17). Of the 18 plant extracts investigated the highest percentage yield (16.07 %) was obtained for the organic extract of fruit of *D. retusa* and the lowest percentage yield (5.91 %) was given by *W. antidysenterica bark* extract (Table 1). These changes in the percentage yield can be due to the differences in chemical composition, the solubility of the solvent, and the bioactive compound density.

In vitro Acetylcholinesterase inhibitory activity of selected sri lankan medicinal plants

Table 1. Percentage yields of plant extracts

Plant species	Family	Plant part	Sample Code	Percentage Yield (w/w %)
I. repens	Balsaminaceae	Whole plant	IR-P	9.44
P. pusilla	Arecaceae	Leaves	PZ-L	10.31
		Bark	PZ-B	7.21
W. antidysenterica	Apocynaceae	Leaves	WA-L	11.45
		Bark	WA-B	5.91
		Seeds	WA-S	9.39
Z. cylindricum	Zingiberaceae	Leaves	ZC-L	6.15
		Rhizome	ZC-R	7.45
C. albifora	Zingiberaceae	Rhizome	CA-R	8.99
		Leaves	CA-L	8.36
A. concinna	Arecaceae	Seeds	AC-S	14.22
D. retusa	Dilleniaceae	Leaves	DR-L	11.28
		Bark	DR-B	8.33
		Fruit	DR-F	16.07
F. leucopyrus	Phyllanthaceae	Leaves	FL-L	11.38
		Bark	FL-B	6.94
K. zeylanica	Rubiaceae	Roots and stem	KZ-RS	7.52
		Leaves	KZ-L	11.23

The standard AChE inhibitor Galantamine displayed notable activity even at 1 µg/ml concentration (41.1% ±0.1 µg/mL). IC_{50} value of Galantamine was 1.57 ±0.01 µg/mL and achieved maximum 68% AChE inhibition at 8 µg/ml concentration (Table 2).

Table 2. AChE inhibition of Galantamine

Galantamine (µg/ml)	AChE inhibition (%)	Galantamine IC_{50} (µg/ml)
0.1	8.0±0.0	
0.2	13.2±0.2	
0.4	22.3±0.3	
1	41.1±0.1	1.57 ±0.01
2	54.1±0.2	
4	60±0.0	
8	68.2±0.1	

Data are given as the mean of at least three independent experiments ± S.D.

The analyzed 8 plant extracts displayed considerable anti-AChE activity and achieved 50% AChE inhibition before reaching the highest concentration (400 µg/ml) used in the study (Table 3). Only W. antidysenterica (Leaf), D. retusa (Fruit and leaf), A. concinna (Seeds) and F. leucopyrus (Leaf) extracts were active at 40 µg/ml concentration. The highest percentage inhibition was achieved by the W. antidysenterica with a value of 85±0.6% at 400 µg/mL concentration. Phoenix pusilla and D. retusa bark extracts did not show any inhibition

Waradana et al

of AChE enzyme even at 400 µg/mL. Crude organic extracts obtained from barks of the tested plants did not show 50% inhibition. In the Zingiberaceae family, both *Z. cylindricum* and *C. albiflora* showed moderate activity toward AChE (below 25%) at 80 µg/ml concentration. However, both rhizome samples of *Z. cylindricum* and *C. albiflora* achieved 50% AChE inhibition below 250 µg/ml concentration. Out of these two plants in the Zingiberaceae family, *C. albiflora* rhizome was more active having an IC_{50} value of 189±1.4 µg/ml. *Phoenix pusilla* plant parts did not show any AChE inhibition even at 200 µg/ml. However, *P. pusilla* leaves extract showed low inhibition of the AChE enzyme (7.7±1.6%.) at 400 µg/ml.

Table 3. Anti-acetylcholinesterase activities of crude extracts

Plant species	Family	Plant part	Sample Code	AChE inhibition (%)				
				40 (µg/ml)	80 (µg/ml)	100 (µg/ml)	200 (µg/ml)	400 (µg/ml)
I. repens	*Balsaminaceae*	Whole plant	IR-P	-	-	-	8.4±0.1	15.1±0.2
P. pusilla	*Arecaceae*	Leaves	PZ-L	-	-	-	-	7.7±1.6
		Bark	PZ-B	-	-	-	-	-
W. antidysenterica	*Apocynaceae*	Leaves	WA-L	32.6±0.5	58±1.1	72±0.6	81±0.9	85±0.6
		Bark	WA-B	-	-	-	13±1.9	27.26±0.7
		Seeds	WA-S	-	8.9±0.1	18±0.1	31±0.1	50±0.0
Z. cylindricum	*Zingiberaceae*	Leaves	ZC-L	-	-	-	-	5.7±0.6
		Rhizome	ZC-R	-	18.7±0.6	24.3±0.3	42.7±1.2	57.6±0.4
C. albifora	*Zingiberaceae*	Rhizome	CA-R	-	24.3±0.6	30.4±0.6	49.1±0.2	62.3±0.2
		Leaves	CA-L	-	-	-	9.3±0.6	15.3±0.1
A. concinna	*Arecaceae*	Seeds	AC-S	10±0.1	23.3±1.1	33.0±0.1	46.1±0.1	58.1±0.2
D. retusa	*Dilleniaceae*	Leaves	DR-L	12.3±0.1	18.0±0.0	22.2±0.2	38.9±0.1	51.0±0.1
		Bark	DR-B	-	-	-	-	-
		Fruit	DR-F	3.2±0.3	16.0±1.0	21.7±0.6	36.3±0.3	52.1±0.1
F. leucopyrus	*Phyllanthaceae*	Leaves	FL-L	22.2±0.3	46.4±0.1	54.7±0.3	60.2±0.2	69.5±0.1
		Bark	FL-B		-	3.7±0.6	9.0±0.0	10.0±0.1
K. zeylanica	*Rubiaceae*	Roots and stem	KZ-RS		-	-	-	6.3±0.6
		Leaves	KZ-L	-	10.5±0.5	16.6±0.5	32.7±1.5	33.0±0.0

* Galantamine was used as positive control (IC_{50} 1.57 ±0.01 µg/mL). Data are given as the mean of at least three independent experiments ± S.D.

It is notable that leaf extracts of *W. antidysenterica* and *F. leucopyrus* showed potent acetylcholinesterase inhibitory activity at lower concentrations. These two extracts showed AChE inhibition even at 20 µg/ml concentration with a percentage inhibition value of 4±0.0% and 13±0.0%, respectively (Figure 1). Both achieved over 50% AChE inhibition when the concentrations were increased to 100 µg/ml. At this concentration, *W. antidysenterica* displayed potent inhibition with a percentage inhibition value of 72±0.6%.
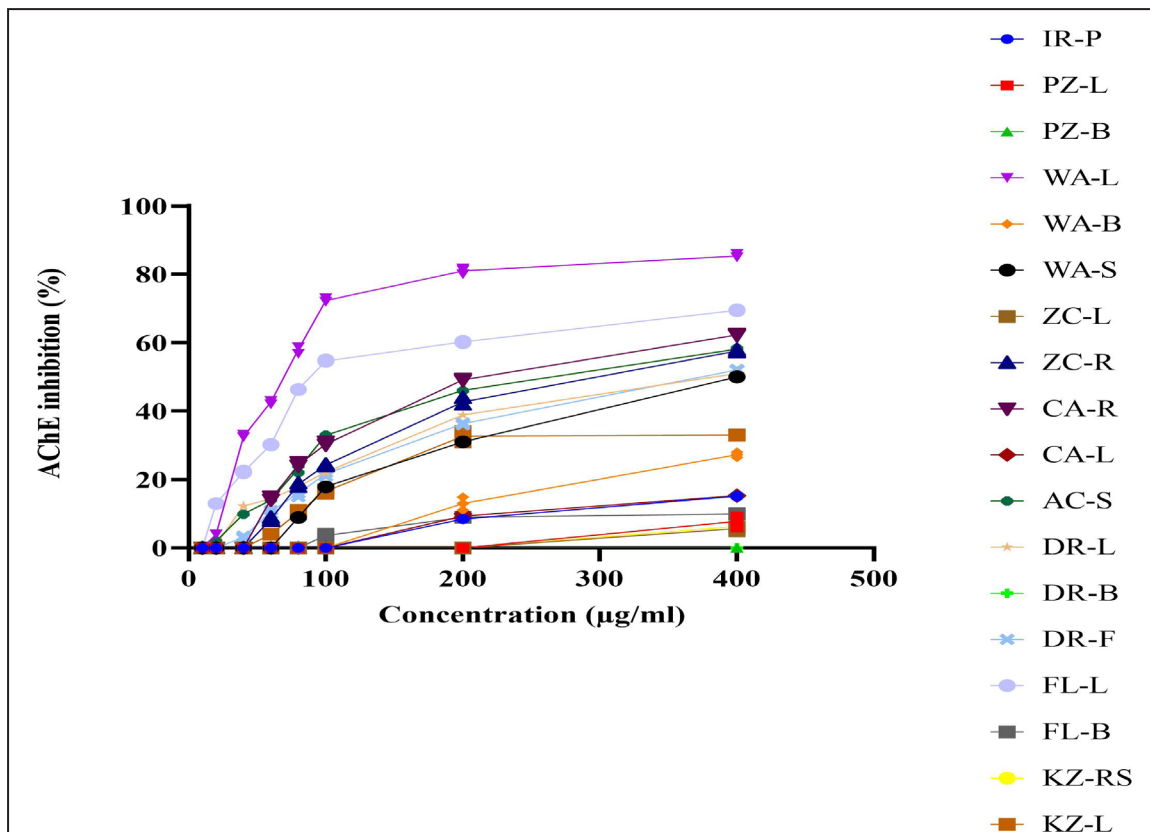
Further purification of *W. antidysenterica* and *F. leucopyrus* organic plant extracts would be useful in isolating compounds with higher AChE inhibitory activities due to their potent activities at low concentrations. From the tested organic extracts of plant parts, the highest AChE inhibitory activity with an IC_{50} value of 64 ±0.5 µg/mL was reported from the leaf extract of *W. antidysenterica* (Table 4).

Table 4. The IC_{50} value of percentage AChE inhibition of plant extracts

Plant species	Family	Plant part	Sample code	IC_{50}/ (µg/ml)
W. antidysenterica	*Apocynaceae*	Leaves	WA-L	64±0.5
		Seeds	WA-S	400±0.2
Z. cylindricum Family	*Zingiberaceae*	Rhizome	ZC-R	249±1.3
C. albiflora	*Zingiberaceae*	Rhizome	CA-R	189±1.4
A. concinna	*Arecaceae*	Seeds	AC-S	217±1.2
D. retusa	*Dilleniaceae*	Leaves	DR-L	373±0.6
		Fruit	DR-F	359±1.1
F. leucopyrus	*Phyllanthaceae*	Leaves	FL-L	107±0.1

Data are given as the mean of at least three independent experiments ± S.D.

Furthermore, leaf extract of *Flueggea leucopyrus* showed good AChE inhibitory activity with an IC_{50} value of 107 ±0. µg/mL. *Curcuma albifora* rhizome extract and *Areca concinna* seed extract exhibited AChE inhibiting activities with IC_{50} values of 189±1.4 µg/mL and 217±1.2 µg/mL, respectively. The results of this study suggest that these Sri Lankan plants may have potential as therapeutic agents for the treatment of Alzheimer's disease. The next step will be to isolate the active drug leads of the crude organic extracts. Subsequently, IC_{50} values can then be compared with known AChE inhibitors. This can lead to an evaluation of whether these medicinal plants could be a novel source of potential drugs for Alzheimer's disease.

Conclusion

Of the nine plants investigated *W. antidysenterica, Z. cylindricum, D. retusa, C. albiflora, A. concinna* and *F. leucopyrus* showed promising anti-cholinesterase activity and achieved 50% AChE inhibition at 400 µg/ml. The crude extract of *W. antidysenterica* leaf exhibited the most potent AChE inhibition activity with an IC_{50} value of 64 ±0.5 µg/ml. Leaf extracts of *F. leucopyrus* and *W. antidysenterica* exhibited more than 20% AChE inhibition even at 40 µg/ml concentration. Thus, this initial screening provides valuable information for further studies to isolate anti-cholinesterase active compounds from Sri Lankan medicinal plants.

Declaration of interest

The authors declare that there is no conflict of interest. The authors alone are responsible for the content of the paper.

References

1. Selkoe, D.J. (2001). Alzheimer's disease: genes, proteins, and therapy. Physiol Rev, 81(2): 353-356.

2. Cummings, J.L., Morstorf, T., Zhong, K. (2014). Alzheimer's disease drug-development pipeline: Few candidates, frequent failures. Alzheimer Res Ther, 6(4): 37-43.

3. Auld, D.S., Kornecook, T.J., Bastianetto, S., Quirion, R. (2002). Alzheimer's disease and the basal forebrain cholinergic system: relations to beta-amyloid peptides, cognition and treatment strategies. Prog Neurobiol, 68(8): 209-245.

4. Uniyal, S.K., Singh, K.N., Jamwal, P., Lal, B. (2006). Traditional use of medicinal plants among the tribal communities of Chhota Bhangal. Wes Him J Ethnobiol Ethnomedicine, 2(14): 1-14.

5. Maelicke, A. and Albuquerque, E.X. (2000). Allosteric modulation of nicotinic acetylcholine receptors as a treatment strategy for Alzheimer's disease. Eur J Pharmacol, 393(1): 165-170.

6. Ahmed, F., Ghalib, R.M., Sasikala, P., Ahmed, K.K.M. (2013). Cholinesterase inhibitors from botanicals. Pharmacogn Rev, 7(14): 121-130.

7. Keller, C., Kadir, A., Forsberg, A., Porras, O., Nordberg, A. (2011). Long-term effects of galantamine treatment on brain functional activities as measured by PET in Alzheimer's disease patients. J Alzheimers Dis, 24(1): 109-123.

8. Singh, A.K., Naithani, V., Bangar, O.P. (2012). Medicinal plants with a potential to treat Alzheimer and associated symptoms. Int J Nutr Pharmacol Neurol Dis, 2: 84-91.

9. Samad, S.A. and de Silva, W.S. (2021). Phytochemical analysis and antibacterial efficacy of extracts of *Dipterocarpus zeylanicus*. Life: Int. J. Health Life Sci, 6(3): 35–53.

10. Abeysekara, W.P.K.M., Premakumara, G.A.S., Ratnasooriya, W.D. (2015). Anti-cholinesterase Activity of Bark and Leaf Extracts of Ceylon Cinnamon (*Cinnamomum zeylanicum*) in Vitro.

Proceedings of the 71st Annual Sessions Sri Lanka Association for the Advancement of Science. Colombo, Sri Lanka.

11. Samaradivakara, S.P., Samarasekera, R., Handunnetti, S.M., Weerasena, O.V.D.S. (2016). Cholinesterase, protease inhibitory and antioxidant capacities of Sri Lankan medicinal plants, Ind Crops Prod, 83: 227-234.

12. Anokwuru, C.P., Anyasor, G.N., Ajibaye, O., Fakoya, O., Okebugwu, P. (2011). Effect of Extraction Solvents on Phenolic, Flavonoid and Antioxidant activities of Three Nigerian Medicinal Plants. Nat, 9(7): 53–61.

13. Ellman, G.L., Courtney, K.D., Andres, V., Featherstone, R.M. (1961). A new and rapid colorimetric determination of acetylcholinesterase activity. Biochem Pharmacol, 7: 88-95.

14. Zelík, P., Lukesova, A.., Voloshko, L.N., Stys, D., Kopecky, J. (2009). Screening for acetylcholinesterase inhibitory activity in cyanobacteria of the genus Nostoc. J Enzyme Inhib Med Chem, 24(2):531-6.

15. Grossberg, G.T. (2003). Cholinesterase inhibitors for the treatment of Alzheimer's disease: getting on and staying on. Curr Ther Res, 64(4): 216-35.

16. Almeida, O.P. (1998). Treatment of Alzheimer's disease, critical evaluation of the use of anticholinesterases. Arch Neuropsychiatry, 56(38): 688-696.

17. Su, Y., Wang, Q., Wang, C., Chan, K., Sun, Y., Kuang, H. (2014). The treatment of Alzheimer's disease using Chinese Medicinal Plants: From disease models to potential clinical applications. J. Ethnopharmacol, 152(3): 403 - 423.

Optimizing Formulation and Economic Evaluation of Phosphate Solubilizing Bacteria for Enhanced Cauliflower Growth and Yield

Parmeshwar Singh[1] [3], Laiq ur Rahman[3], Rajeev Kumar2, Anju Meshram*[1], Ravi Kant Singh*[2]

[1]Amity Institute of Biotechnology, Amity University Chhattisgarh, Raipur-493225, Chhattisgarh, India
[2]Amity Institute of Biotechnology, Amity University Uttar Pradesh, Noida -201313, Uttar Pradesh, India
[3]Plant Tissue Culture Lab, Biotechnology Division, CSIR-Central Institute of Medicinal Plants Research, Lucknow, Uttar Pradesh -226015 India

*Corresponding Author:rksingh1@amity.edu

Abstract

A shortage of phosphorus (P), a necessary mineral ingredient for agriculture, may result in lower grain quality, productivity, and growth in cereal crops. Much of the phosphorus that is sprayed in agricultural contexts is immobilized in the soil, which limits the amount of phosphorus that is available to plants. This study focused on investigating the microbial communities in the rhizosphere of cauliflower crops from Kanpur, Unnao, and Lucknow districts in India, known for their fertile soils and favorable agricultural conditions. Soil samples were collected and screened for phosphate-solubilizing bacteria (PSB) and nitrogen-fixing bacteria. PSB was isolated using Pikovskaya's agar medium, and nitrogen-fixing bacteria were identified through nitrogen-free media supplemented with a bromothymol blue indicator. Morphological, biochemical, and molecular techniques were employed for characterization. The isolated strains were then tested for their impact on cauliflower growth and yield parameters under controlled conditions. Results showed significant enhancements in plant growth and yield parameters, suggesting potential applications in agricultural practices.

Keywords: Agricultural, Cauliflower Growth, Nitrogen-Fixing Bacteria, Phosphate-Solubilizing Bacteria, Rhizosphere.

Introduction

Phosphorus is not only a vital nutrient for plant growth and metabolism but also a limited natural resource, presenting a challenge to the sustainable development of the global economy. The readily accessible amount of phosphorus is insufficient to meet the growth demands of plants, particularly in the soils of subtropical forests, where severe phosphorus deficiency significantly hampers plant development and productivity (1,2). The phosphorus fertilizer recovery rate in soil is relatively low, ranging from 15 to 20%, with the rest becoming fixed in the soil. Globally, around 52.4 billion tons of phosphorus fertilizer are used annually to maintain soil fertility. Therefore, improving crops' capacity to efficiently absorb and utilize phosphorus is crucial from ecological and economic perspectives alike (3,4).

Recent studies have demonstrated that "phosphate-solubilizing bacteria" (PSB) play a beneficial role in enhancing plant growth. These microorganisms solubilize insoluble phosphate

in the soil, which is essential for plant development, in addition to fixing nitrogen and releasing auxins. Research indicates that incorporating PSB into seeds or soil can enhance the solubilization of fixed soil phosphorus or applied phosphates, thereby promoting plant growth. For example, Hansen *et al.* demonstrated that inoculating *Bacillus simplex* significantly improved winter wheat plants, leading to increased phosphorus concentrations in root biomass and elevated levels of magnesium, manganese, and sulfur in shoot biomass (5,6). The efficiency of phosphorus-solubilizing microorganisms in soil may be affected by native microorganisms and soil conditions, which might make it difficult for them to establish sustained colonization. On the other hand, endophytes are essential to the plant's micro-ecosystem. They support overall plant development, improve plant tolerance to stresses, pests, and diseases, and aid in the fixation of nitrogen (7,8). Cauliflower (*Brassica oleracea* var. *botrytis*) is a prominent crop species in southern India, cultivated extensively for its economic importance. Despite its importance, the productivity of fir forests has declined in recent years due to intensive management practices and shorter rotation periods (9,10). Additionally, the soil in southern regions, characterized by high iron and aluminum content along with strong leaching, leads to phosphorus fixation and inactivation. This results in very low phosphorus utilization rates in the soil. This severely limits the sustainable development of *Brassica oleracea* var. *plantations*. Figure 1 shows the selection process of PSB and their growth-promoting mechanisms in potted *Brassica oleracea* var. *plants*. The figure highlights the steps involved in isolating and identifying effective PSB strains that enhance plant growth. It also details the various mechanisms through which these bacteria promote growth, such as nutrient solubilization and hormone production. Additionally, the figure demonstrates the significant impact of PSB application in wheat fields, showcasing improved growth and yield. This visual representation emphasizes the potential of PSB as a sustainable agricultural practice.
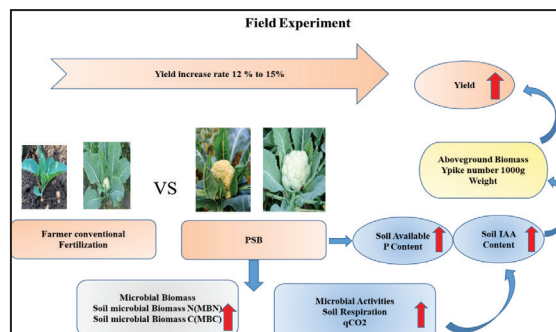
Figure 1: Detailed Selection and Impact Analysis of Phosphate-Solubilizing Bacteria (PSB) on *Brassica oleracea var*. and Wheat Cultivation.

Therefore, investigating the impact of PSB on the growth of *Brassica oleracea var.* is crucial for potential applications of PSB in forestry. Bioinoculant of rhizobia can effectively improve agricultural yield and productivity which indicates that Rhizobium is an effective Plant growth promoting microbe (11,12). In this study, PSB was isolated and screened from the stems, roots, as well as leaves of "*Brassica oleracea var*". The focus of the investigation was on traits that promote development, including siderophore generation, "indole-3-acetic acid" (IAA) synthesis, nitrogenase activity, and "1-Aminocyclopropane 1-Carboxylate" (ACC) deaminase activity (13,14). The study investigated the effects of PSB inoculation on plant growth, nitrogen absorption, and soil enzyme activity using "*Brassica oleracea var.*" as a model. These results are essential for producing useful understandings for creating and using PSB as biological fertilizer in forest applications.

Phosphorus is vital for plant growth, but its limited availability in soils poses a significant challenge for agriculture. Sustainable solutions, such as the use of phosphate-solubilizing bacteria (PSB), have shown promise in enhancing phosphorus availability. Research has demonstrated that various strains of PSB can significantly improve plant growth, soil health, and nutrient uptake. These beneficial microorganisms increase the bioavailability of phosphorus, promote root and shoot development, and reduce

the need for chemical fertilizers, thereby supporting sustainable agricultural practices and improving crop yields.

Z. Iqbal *et al.* (15) explored the phosphorus (P) is necessary for agriculture, its fixation in soils restricts plant accessibility, which affects grain output and growth. To increase P availability, this research looks at sustainable methods that use phosphate-solubilizing bacteria. *Bacillus subtilis* ZE15, *Bacillus megaterium* ZE32, *Bacillus megaterium* ZR3, and *Bacillus sp.* ZR19 were the four bacterial strains tested in Pikovskaya's broth, both with and without insoluble phosphorus (P). While organic acids were generated by all cultures, strain ZE15 showed the greatest capacity to solubilize phosphorus, reaching up to 130.00 µg mL−1. According to these results, Bacillus species may improve the solubilization or mineralization of the rhizosphere, which would increase phosphorus intake and facilitate future agricultural uses.

Z. Wang *et al.* (16) experimented to improve plant development and solubilizing phosphorus (P), PSB also helps to mitigate the negative effects of excessive agricultural fertilizers on soil health. This study identified *Pseudomonas moraviensis*, *Bacillus safensis*, as well as *Falsibacillus pallidus* as three effective PSB that can produce "indole-3-acetic acid" (IAA) and solubilize phosphate in sandy fluvo-aquic soils. Furthermore, the labile phosphorus percentage in the soil was dramatically enhanced by PSB by 122.05% (P<0.05), whereas the stable phosphorus fraction was significantly decreased by 46.80% (P<0.05). Moreover, PSB increased soil microorganism biomass and activity, indicating their potential to aid in the development of sustainable agriculture. These results highlight PSB as long-term sustainable resources that may improve soil health and agricultural output.

J. Chen *et al.* (17)7 endophytic phosphate solubilizing bacteria were screened out from Chinese fir, and were characterized for plant growth-promoting traits. Based on morphological and 16S rRNA sequence analysis, the endophytes were distributed into 5 genera of which belong to Pseudomonas, Burkholderia, Paraburkholderia, Novosphingobium, and Ochrobactrum. HRP2, SSP2 and JRP22 were selected based on their plant growth-promoting traits for evaluation of Chinese fir growth enhancement. The growth parameters of Chinese fir seedlings after inoculation were significantly greater than those of the uninoculated control group. The results showed that PSBs HRP2, SSP2 and JRP22 increased plant height (up to 1.26 times analyzed the Chinese fir trees that were used to extract PSB, which were then tested for their capacity to stimulate plant development. In comparison to controls, three strains (SSP2, HRP2, and JRP22) considerably improved Chinese fir seedling growth characteristics including biomass, plant height, and stem diameter. Indicators of soil fertility, such as total nitrogen, potassium, phosphorus, and accessible nutrients, were also enhanced by these PSBs. According to the research, PSBs are useful biological agents for sustainable agroforestry that improve agricultural yields and environmental health without using chemical fertilizers as much.

S. Batool and A. Iqbal (18) discussed the PSB were isolated from rhizospheres of different plants to improve the nutrition and development of Triticum aestivum. Ten PSB strains were chosen from a group of thirty isolates based on their strong "phosphate solubilization" and PGP. Under ideal circumstances, these strains showed efficient phosphate solubilization and generated useful substances like hydrogen cyanide, ammonia, siderophores, and indole acetic acid. PSB injection dramatically increased root/shoot development (10% to 90%) and seed germination (50% to 80%) in laboratory testing. Improved seed germination (40%–80%) as well as increases in shoot length (5% to 34.8%) and seed weight (5% to 96%) were seen in field testing. According to the research, these PSB strains have promise as bio fertilizers that might eventually replace chemical fertilizers in sustainable *Triticum aestivum L.* production.

A. Nosheen *et al.* (19) investigated the use of biofertilizers on the Thori cultivar of Kasumbha has a positive impact, enhancing the quality of feedstock for biodiesel production. Biofertilizers improve soil fertility and nutrient availability, leading to healthier plant growth and higher yields. This, in turn, results in better-quality seeds with higher oil content, making them more suitable for efficient biodiesel production. The number of plant leaves, leaf area, and number of seeds per capitulum were all greatly enhanced by the administration of biofertilizer both alone and in conjunction with chemical fertilizer. Agronomic traits like plant height, branch number, and capitulum count were notably improved with biofertilizer alone compared to control. Seed yield and oil content, including beneficial seed phenolics, were enhanced by biofertilizer and chemical fertilizer treatments. Biofertilizer treatment alone yielded the highest biodiesel production, with optimal oleic acid content, while maintaining lower acid values and free fatty acids. This study supports biofertilizers as effective alternatives to chemical fertilizers, promoting sustainable and environmentally friendly agricultural practices.

S. B. Sharma *et al.* (20)in both organic and inorganic forms, its availability is restricted as it occurs mostly in insoluble forms. The P content in average soil is about 0.05 % (w/w developed that Phosphorus (P) is vital for plant growth but often limited in availability due to soil fixation and insolubility. Chemical P fertilizers are energy-intensive and environmentally harmful, prompting interest in phosphate-solubilizing microorganisms (PSM) as eco-friendly alternatives. PSM, including bacteria and fungi, enhances P availability through biological processes. However, their performance in field conditions varies, necessitating improvements like genetic modifications or co-inoculation techniques. This review discusses PSM diversity, solubilization mechanisms, phosphatase roles, influencing factors, and future applications for sustainable agriculture.

N. Kishore *et al.* (21)phosphorus (P discussed the essential elements required for plant growth include phosphorus (P), nitrogen (N), and potassium (K). Phosphorus is the most limiting nutrient after nitrogen. Even though there are several forms of P in soil, it is seldom available in a form that plants can use, which often calls for the use of expensive or harmful chemical fertilizers. When used in the rhizosphere, "phosphate solubilizing microorganisms" (PSMs) provide a sustainable substitute by increasing P availability in a variety of ways. Certain PSMs also function as biocontrol agents and PGPR, enhancing soil health and shielding plants from diseases. Thanks to technological developments, PSMs may be altered to improve their advantageous characteristics. Nonetheless, there are still problems and knowledge gaps, which are examined in this thorough analysis of PSMs.

Prior studies and findings show that phosphate-solubilizing bacteria (PSB) offer a sustainable and effective solution to the challenge of phosphorus availability in agriculture. By enhancing phosphorus solubilization, promoting plant growth, and improving soil health, PSB reduce reliance on chemical fertilizers and contribute to more environmentally friendly farming practices. Continued research and application of PSB can play a crucial role in achieving higher agricultural productivity and sustainability.

Material And Methods

Research design

Soil samples were carefully collected from the rhizosphere regions of cauliflower crops grown in the districts of Kanpur, Unnao, and Lucknow, India. These regions are renowned for their fertile lands and conducive agricultural conditions, making them prime areas for cauliflower production in the country. The favorable climatic conditions and nutrient-rich soil composition in these districts greatly enhance the robust growth and high yield of cauliflower

crops. The study aimed to comprehensively investigate the microbial populations in the rhizosphere of cauliflower crops by systematically collecting soil samples from these specific regions. By focusing on Kanpur, Unnao, and Lucknow, the study aimed to leverage the agricultural potential of these areas to explore the diversity and functionality of phosphate-solubilizing or nitrogen-fixing bacteria in cauliflower rhizospheres.

Sample

Using a nitrogen-free medium enhanced with a bromothymol blue indicator, soil samples taken from the cauliflower rhizosphere were examined for the presence of nitrogen-fixing bacteria. Nitrogen-fixing bacteria possess the enzymatic machinery to convert atmospheric nitrogen into ammonia, thereby contributing to soil fertility and plant nutrition. Colonies exhibiting a characteristic blue color change in the medium, indicative of nitrogen fixation activity, were selected for further identification and characterization. Identification methods similar to those described for PSB were employed for the nitrogen-fixing microbes isolated from the soil samples. Morphological, biochemical, and molecular techniques were utilized to characterize and classify the nitrogen-fixing bacterial strains at the genus and species levels. These methods yielded valuable insights into the taxonomic diversity and functional potential of the nitrogen-fixing microbial community associated with the cauliflower rhizosphere.

The isolation of PSB began with the serial dilution technique, a standard method for isolating microorganisms from environmental samples. One gram of soil from the cauliflower rhizosphere was weighed and suspended in 9 milliliters of sterile saline solution (0.85% NaCl) for thorough homogenization. Serial dilutions of the soil suspension were prepared, ranging from undiluted (10^{-1}) to 10^{-5}, with each step involving the transfer of an aliquot into a new saline solution volume. This process reduced microbial population density, enhancing the isolation of individual bacterial colonies. On Pikovskaya's agar medium, which is specific for PSB and uses "tricalcium phosphate" (TCP) as the phosphorus source, aliquots from these dilutions were spread out. The plates were incubated at 28°C for five to seven days to allow bacterial colonies to proliferate. Following incubation, the plates were inspected for morphologically distinct colonies exhibiting clear zones indicative of phosphate solubilization. These colonies were selected for further purification and characterization by subculturing onto fresh Pikovskaya's agar plates to ensure purity. This process of successive subculturing eliminated potential contaminants, resulting in pure cultures suitable for subsequent analyses and characterization.

Data collection

A soil auger, a specialized tool designed for efficient soil sampling, was employed to collect representative soil samples from the designated cauliflower rhizosphere regions. Sampling was conducted at a depth ranging from 0 to 20 centimeters beneath the soil surface, ensuring the inclusion of the rhizosphere zone where the majority of plant-microbe interactions occur. Careful attention was paid to avoid contamination and to maintain the integrity of the collected samples. For each experimental technique, three runs were conducted to guarantee the accuracy and consistency of the findings. To demonstrate the diversity within the dataset, the study's results were presented as mean values ± standard deviation. Statistical analyses were conducted using dedicated software packages like SPSS or R, following standard methodologies. Graphical representations, elucidating the trends and patterns observed in the data, were meticulously prepared using software tools like Graph Pad Prism or Microsoft Excel, facilitating a clear and concise presentation of the findings. An organized description of the steps required in isolating, characterizing, and characterizing PSB, particularly for cauliflower development is shown in Table 1, along with numerical results.

Table 1: Quantitative Analysis of Isolation, Identification, and Characterization Processes of PSB for Enhancing Cauliflower Growth.

S.No.	Step	Numeric Value
1.	Soil Sample Collection	20 soil samples collected
2.	Sampling Depth	0-20 cm depth
3.	Preparation of Soil Suspension	1 gram of soil sample suspended in 9 ml of saline solution
4.	Serial Dilution	Dilutions prepared from 10^{-1} to 10^{-5}
5.	Spread Plating	Aliquots plated onto Pikovskaya's agar medium
6.	Incubation Period	5-7 days at 28°C
7.	Colony Selection	Morphologically distinct colonies with clear zones selected
8.	Purification of Selected Colonies	Subcultured onto fresh Pikovskaya's agar plates
9.	Morphological Characterization	Colony morphology observed
10.	Gram Staining	Gram staining performed for classification
11.	Biochemical Tests	Catalase, oxidase, and sugar fermentation tests conducted
12.	Molecular Identification	16S rRNA gene sequencing performed for precise identification
13.	Phosphate Solubilization Efficiency Assessment	NBRIP broth method used
14.	Organic Acid Production	High-performance liquid chromatography (HPLC) or colorimetric assays performed
14.	Plant Growth-Promoting Substances" Assessment	Indole acetic acid" (IAA) and siderophore production assessed

Data analysis

Pure cultures of the isolated PSB underwent a thorough morphological examination to identify key characteristics indicative of bacterial taxonomy and classification. Colony morphology, including features such as size, shape, color, elevation, and texture, was carefully observed and documented. Additionally, cellular morphology, including cell shape, arrangement, and motility, was assessed through microscopic examination of bacterial smears prepared from pure cultures. Gram staining, a crucial differential staining technique, was used to classify bacterial isolates as either Gram-positive or Gram-negative based on the makeup of their cell walls. Subsequently, comprehensive biochemical tests were carried out to enhance the biochemical characteristics of the separated PSB strains. A variety of metabolic activities and enzymatic reactions characteristic of bacterial physiology were covered in these experiments. In particular, the enzyme catalase, which catalyzes the breakdown of hydrogen peroxide into oxygen along with water, was found using the catalase test. The oxidase test was used to measure cytochrome c oxidase activity, which helped distinguish various bacterial species according to their capacity for respiration. To evaluate the bacterial isolates' capacity to metabolize different sugars as carbon sources and get insight into their metabolic flexibility and substrate usage patterns, experiments on sugar fermentation were also conducted.

In parallel with morphological and biochemical characterization, molecular identification techniques were employed to achieve a comprehensive and precise taxonomic classification of the isolated PSB strains. Table 2, shows the biochemical and microbial activity in soil samples from varied locations and depths

across Kanpur, Unnao, and Lucknow. The highly conserved 16S ribosomal RNA (rRNA) gene, a ubiquitous molecular marker prevalent across bacterial taxa, was targeted for amplification and sequencing. The "Polymerase Chain Reaction" (PCR) was used to amplify the 16S rRNA gene with universal primers, followed by sequencing of the resulting DNA fragments. Phylogenetic analysis followed by comparison of these sequences with reference databases enabled precise taxonomic identification and classification of the isolated PSB strains at both the genus and species levels (22). In addition to offering a reliable method of species identification, this molecular technique also gave insightful information on the genetic diversity and evolutionary relationships within the isolated bacterial community. The National Botanical Research Institute's Phosphate (NBRIP) broth technique was one of the standard tests used to quantitatively evaluate the isolated PSB strains' phosphate solubilization efficiency. This study assessed PSB's capacity to solubilize phosphate in its insoluble forms, including tricalcium phosphate (TCP). Under ideal circumstances, the PSB isolates were inoculated into NBRIP broth that had been supplemented with insoluble phosphate sources. Using established techniques, the broth's soluble phosphate content and pH variations were recorded regularly throughout the incubation period. The degree of phosphate solubilization shown by every strain was measured by measuring the gradual rise in soluble phosphate concentration and the corresponding decrease in pH. The comparison between the control group and the plants infected with PSB Isolates 1, 2, and 3 is shown in Table 3, which also includes the shoot length (cm), root length (cm), fresh weight (g), as well as dry weight (g). In comparison to the control group, Table 4 displays the quantity of curds, curd weight (g), and curd diameter (cm) of cauliflower plants infected with PSB Isolates 1, 2, and 3.

Table 2: Biochemical and Microbial Activity of Soil Samples from Different Locations and Depths in Kanpur, Unnao, and Lucknow.

Sample ID	Location	Soil Depth (cm)	Nitrogenase Activity	ACC Deaminase Activity	IAA Production	Siderophore Production	PSB Isolation (CFU/g)
1	Kanpur	0-20	3.5 U/mg	1.2 U/mg	15 µg/mL	+	1.5×10^6
2	Unnao	0-20	3.7 U/mg	1.1 U/mg	13 µg/mL	++	1.7×10^6
3	Lucknow	0-20	3.2 U/mg	1.3 U/mg	14 µg/mL	+	1.6×10^6

CFU/g: "Colony-Forming Units" per gram of soil.

- U/mg: Enzyme activity units per milligram of protein.
- +: Presence of activity.
- ++: Higher presence of activity.

Table 3: Growth Parameters of Plants Inoculated with PSB Isolates and Control.

Growth Parameter	PSB Isolate 1	PSB Isolate 2	PSB Isolate 3	Control
Shoot Length (cm)	30.2	31.5	29.8	25.4
Root Length (cm)	15.1	15.8	14.9	12.3
Fresh Weight (g)	350	360	340	280
Dry Weight (g)	50	52	48	40

Table 4: Yield Parameters of Cauliflower Plants Inoculated with Phosphate-Solubilizing Bacteria (PSB) Isolates and Control

Yield Parameter	PSB Isolate 1	PSB Isolate 2	PSB Isolate 3	Control
Number of Cards	12	13	11	8
Curd Weight (g)	600	620	590	500
Curd Diameter (cm)	20	21	19	16

Result and Discussion

Selected strains of Phosphate-Solubilizing Bacteria (PSB) and nitrogen-fixing microbes, either isolated individually or in combination, underwent comprehensive growth assays to assess their synergistic impacts on cauliflower growth and yield. Surface-sterilized cauliflower seeds were inoculated with these selected bacterial strains to establish microbial associations prior to planting. Sterilized soil, mimicking natural rhizosphere conditions, was filled in pots, and the inoculated seeds were sown under controlled environmental conditions.

Growth parameter measurements

Plant growth parameters, such as fresh weight, shoot length, root length, and dry weight, were carefully measured at designated intervals throughout the growth period. Additionally, yield parameters such as the number of curds, curd weight, and curd diameter were recorded at harvest to assess the impact of microbial inoculation on cauliflower productivity. To clarify any noteworthy variations between treatment groups and to speculate about possible synergistic effects of PSB as well as nitrogen-fixing microorganisms on cauliflower growth and yield, statistical studies were carried out. Figure 2 illustrates the impact of various PSB isolates on plant development metrics, including shoot length, root length, fresh weight, and dry weight. The most significant improvement in plant development is shown in PSB Isolate 2, which reached the maximum shoot length of 31.5 cm, root length of 15.8 cm, fresh weight of 360 grams, and dry weight of 52 grams. With shoot lengths of 30.2 cm or 29.8 cm, root lengths of 15.1 cm as well as 14.9 cm, fresh weights of 350 grams and 340 grams, as well as dry weights of 50 grams and 48 grams, respectively, PSB Isolates 1 and 3 also exhibit notable advantages over the control group. The control group, on the other hand, had the lowest values for all parameters shoot length of 25.4 cm, fresh weight of 280 grams, root length of 12.3 cm, and dry weight of 40 grams because they did not get PSB therapy. This information demonstrates how well PSB isolates work to encourage plant development, with PSB Isolate 2 being especially helpful.
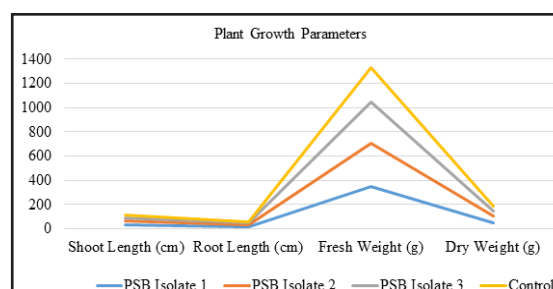
Figure 2: The Graph Shows the Plant Growth Parameter.

To establish a baseline for comparison, control pots devoid of bacterial inoculation were meticulously maintained under identical environmental conditions throughout the experiment. These control pots were used as reference points to evaluate the effects of microbial inoculation on cauliflower growth and yield parameters. By eliminating the confounding influence of microbial treatments, the control group facilitated the accurate evaluation of the specific effects attributable to the introduced bacterial strains.

Evaluation of yield parameters

At harvest, yield parameters crucial for assessing cauliflower productivity were systematically recorded. These parameters included the number of curds, curd weight, and curd diameter, which collectively reflect the quality and quantity of cauliflower produced. The harvest data offered valuable insights into the efficacy of microbial inoculation in enhancing cauliflower yield and marketable quality compared to the control group. Figure 3 compares the growth metrics of cauliflower treated with different phosphate-solubilizing bacteria (PSB) isolates against a control group. The metrics assessed include the number of curds, curd weight, and curd diameter. PSB Isolate 1 resulted in 12 curds with an average weight of 600 grams and a diameter of 20 cm. PSB Isolate 2 showed the best performance, producing 13 curds with an average weight of 620 grams and a diameter of 21 cm. PSB Isolate 3 resulted in 11 curds, each averaging 590 grams and 19 cm in diameter. In contrast, the control group, which did not receive PSB treatment, had the lowest values, with only 8 curds averaging 500 grams in weight and 16 cm in diameter. These results indicate that PSB isolates significantly enhance cauliflower growth, evidenced by increased curd number, weight, and diameter compared to the control.
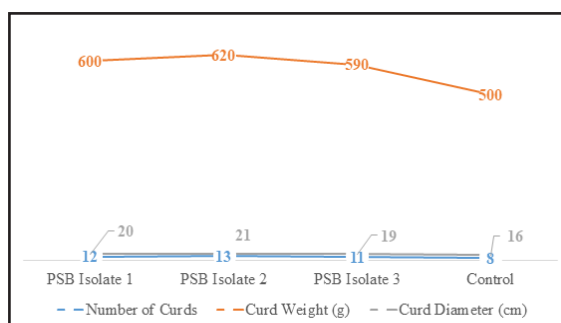
Figure 3: The graph shows the Yield Parameters.

To identify meaningful distinctions between the treatment groups and the control, rig-orous statistical analyses were conducted using established methods such as "Analysis of Variance" (ANOVA), followed by post hoc tests like Tukey's "honestly significant difference" (HSD) test. These analytical approaches allowed for a comprehensive assessment of treatment effects on diverse growth and yield parameters, ensuring robust interpretation of the results with a high level of confidence. Statistical significance was defined at $p < 0.05$ to uphold the reliability and validity of the findings.

Conclusion

This research showed that phosphate-solubilizing or nitrogen-fixing bacteria were present and active in the rhizosphere of cauliflower crops grown in the districts of Kanpur, Unnao, and Lucknow. The isolated bacterial strains exhibited promising effects on cauliflower growth and yield, underscoring their potential as biofertilizers in sustainable agriculture. Further research could explore optimizing bacterial inoculants for broader agricultural applications, enhancing crop productivity and soil health management strategies. These findings highlight the promise of PSB as sustainable alternatives to chemical fertilizers, offering potential benefits for agricultural practices aiming at improved crop productivity and soil health. Future research directions could explore optimizing PSB inoculation strategies and their broader applications across different agricultural contexts.

Acknowledgement

Conflict of interest

The authors declare that they have no conflict of interest.

References

1. Amri, M., Rjeibi, M.R., Gatrouni, M., Mateus, D.M.R., Asses, N., Pinho, H.J.O. and Abbes, C. (2023). Isolation, Identification, and Characterization of Phosphate-Solubilizing Bacteria from Tunisian Soils. *Microorganisms* 11:783.

2. Chen, Y.P., Rekha, P.D., Arun, A.B., Shen, F.T., Lai, W.A. and Young, C.C. (2006). Phosphate solubilizing bacteria from subtropical soil and their tricalcium phosphate solubilizing abilities. *Applied Soil Ecology* 34(1):33-41.

3. Alam F, Khan A, Fahad S, Nawaz S, Ahmed N, et al. (2022). Phosphate solubilizing bacteria optimize wheat yield in mineral phosphorus applied alkaline soil. *Journal of the Saudi Society of Agricultural Sciences* 21(5):339-348.

4. Zhou, Y., Zhao, X., Jiang, Y., Ding, C., Liu, J. and Zhu, C. (2023). Synergistic remediation of lead pollution by biochar combined with phosphate solubilizing bacteria. *Science of the Total Environment* 861:160649.

5. Sharma, S., Company, S., Ballhausen, M.B., Ruppel, S. and Franken, P. (2020). Interaction between Rhizoglomus irregulare and hyphae attached phosphate solubilizing bacteria increases plant biomass of Solanum lycopersicum. *Microbiological Research* 240: 126556.

6. Munir, I., Bano, A. and Faisal, M. (2019). Impact of phosphate solubilizing bacteria on wheat *(Triticum aestivum)* in the presence of pesticides. *Brazilian Journal of Biology* 79(1):29-37.

7. Ahemad, M. (2015). Phosphate-solubilizing bacteria-assisted phytoremediation of metalliferous soils: a review. *3 Biotech* 5(2):111-121.

8. Cheng, Y., Narayanan, M., Shi, X., Chen, X., Li, Z. and Ma, Y. (2023). Phosphate-solubilizing bacteria: Their agroecological function and optimistic application for enhancing agro-productivity. *Science of the Total Environment* 901:166468.

9. Ibáñez, A., Diez-Galán, A., Cobos, R., Calvo-Peña, C., Barreiro, C., Medina-Turienzo, J., Sánchez-García, M. and Coque, J.J.R. (2021). Using rhizosphere phosphate solubilizing bacteria to improve barley (*Hordeum vulgare*) plant productivity. *Microorganisms* 9(8):1619.

10. Damo JLC, Ramirez MDA, Agake SI, Pedro M, Brown M, Sekimoto, H., Yokoyama, T., Sugihara, S., Okazaki, S. and Ohkama-Ohstu, N. (2022). Isolation and Characterization of Phosphate Solubilizing Bacteria from Paddy Field Soils in Japan. *Microbes and Environments* 37(2):ME21085.

11. Datta, A., Singh, R.K. and Tabassum, S. (2015). Isolation Characterization and Growth of Rhizobium strains under optimum conditions for effective biofertilizer production. *International Journal of Pharmaceutical Sciences Review and Research* 32(1):199−208.

12. Datta, A., Singh, R.K., Kumar, S. and Kumar, S. (2015). An Effective and Beneficial Plant Growth Promoting Soil Bacterium Rhizobium. A Review. *Annals of Plant Sciences* 4(1):933-942.

13. Wu, F., Li, J., Chen, Y., Zhang, L., Zhang, Y., Wang, S., Shi, X., Li, L. and Liang, J. (2019). Effects of phosphate solubilizing bacteria on the growth, photosynthesis, and nutrient uptake of *Camellia oleifera* abel. *Forests* 10:348.

14. Rahayu, Y.S., Yuliani, and Trimulyono, G. (2019). Isolation and identification of hydrocarbon degradation bacteria and phosphate solubilizing bacteria in oil-contaminated soil in Bojonegoro, East Java, Indonesia. *Indonesian Journal of Science*

and Technology 4(1):134-147.

15. Iqbal, Z., Ahmad, M., Raza, M.A., Hilger, T. and Rasche, F. (2024). Phosphate-Solubilizing Bacillus sp. Modulate Soil Exoenzyme Activities and Improve Wheat Growth. *Microbial Ecology* 87(1):31.

16. Wang, Z., Zhang, H., Liu, L, Li, S., Xie, J., Hue, X. and Jiang, Y. (2022). Screening of phosphate-solubilizing bacteria and their abilities of phosphorus solubilization and wheat growth promotion. *BMC Microbiology* 22:296.

17. Chen, J., Zhao, G., Wei, Y., Dong, Y,, Hou, L. and Jiao, R. (2021). Isolation and screening of multifunctional phosphate solubilizing bacteria and its growth-promoting effect on Chinese fir seedlings. *Scientific Reports* 11:9081.

18. Batool, S. and Iqbal, A. (2019). Phosphate solubilizing rhizobacteria as alternative of chemical fertilizer for growth and yield of *Triticum aestivum* (Var. Galaxy 2013). *Saudi Journal of Biological Sciences* 26:1400−1410.

19. Nosheen, A., Yasmin, H., Naz, R., Keyani, R., Mumtaz, S., et al. (2022). Phosphate solubilizing bacteria enhanced growth, oil yield, antioxidant properties and biodiesel quality of Kasumbha. *Saudi Journal of Biological Sciences* 29:43−52.

20. Sharma, S.B., Sayyed, R.Z., Trivedi, M.H. and Gobi, T.A. (2013). Phosphate solubilizing microbes: Sustainable approach for managing phosphorus deficiency in agricultural soils. *Springer Plus* 2:587.

21. Kishore, N., Pindi, P.K. and Reddy, S.R. (2015). Phosphate-solubilizing microorganisms: A critical review. In Plant Biology and Biotechnology: Plant Diversity, Organization, Function and Improvement. pp 307−333.

22. Boroumand, N., Behbahani, M. and Dini, G. (2020). Combined Effects of Phosphate Solubilizing Bacteria and Nanosilica on the Growth of Land Cress Plant. *Journal of Soil Science and Plant Nutrition* 20:232−243.

Screening and Purification of L-asparaginase Production by *Aspergillus quadrilineatus* Using Agro Wastes and Vegetable Peels

Rupa Acharya[1] , Tapaswini Kanungo[1] , Nibha Gupta[1]

[1]Regional Plant Resource Centre, Bhubaneswar, 751015 Odisha, India.
*Corresponding Author: nguc2003@yahoo.co.in

Abstract

Enzymes are the name for the biocatalysts that are created by living cells. These are intricate protein molecules that start chemical reactions essential to life. They are colloidal, thermolabile, and have a particular action. L-asparaginase (also called L-asparagine amido hydrolase, E.C.3.5.1.1) is an extracellular enzyme that has attracted a lot of attention since it is used as an anticancer drug. To assess the growth capacity of the selected fungus *Aspergillus quadrilineatus*, a preliminary experiment was carried out using vegetable peels and agricultural waste as substrate. The by-products that were utilized included wheat bran, cornmeal, gram flour, wheat flour, rice flour, rice husk, and peels from green peas, onions, carrots, and papayas. On the other hand, papaya peel medium worked well as a source of media for improving growth in *Aspergillus species*. This work focuses on the purification, mass-scale production, screening, and characterization of the Fusarium proliferative-derived L-asparaginase enzyme. The crude enzyme was removed, followed by precipitation with ammonium sulphate, filtration over a Sephadex column, and ion exchange chromatography to further purify the L-Asparaginase. The reaction of the enzyme to different temperatures, pH values, substrate concentrations, and incubation times was evaluated in order to define it. Because it can catalyze the conversion of l-asparagine to l-aspartic acid and ammonia, l-asparaginase is one such crucial enzyme that has found commercial usage in the food and pharmaceutical industries. Although l-asparaginase may be produced by a variety of bacterial and fungal sources, researchers are particularly interested in how these organisms might generate the enzyme commercially utilizing less expensive substrates.

Keywords: Fungi, Vegetables, L-asparaginase, *Aspergillus quadrilineatus*, papaya peels.

Introduction

India, a global leader in agriculture with the greatest irrigated crop area, is a resource hub for producing agricultural wastes; according to reports, the country produces 1500 lakh tons of agricultural trash annually (1) (shakambari *et al*.,2017). These agricultural wastes typically consist of bagasse, straw, fruit and vegetable peels, husks, and other agricultural materials produced during processing that have been shown to be used in the creation of numerous value-added goods. By using fermentation technology to transform these nutrient-rich byproducts into valuable bioproducts, the method can reduce environmental pollution risks while simultaneously minimizing production costs(2) (Pallem *et al*., 2018). A portion of the organic wastes have been utilized to make garbage enzyme, which is used to treat household, municipal, and industrial wastes as well as create antibacterial agents. Various wastes, including those from

the sugar industry, municipal solid wastes, and even agricultural wastes, have been employed as an alternate substrate to increase the synthesis of several of these crucial enzymes. L-asparaginase is one such significant enzyme that is used in the food and pharmaceutical industries due to its ability to catalyze the conversion of L-asparagine to L-aspartic acid and ammonia. For their growth, acute lymphoblastic leukemia (ALL) and tumor-suspected cells depend on the circulating asparagine that is produced by normal cells. Asparagine is a non-essential amino acid. The leukemic cells are deprived of circulating asparagine, which results in cell death, due to asparaginase's catalysis of the conversion of L-asparagine to aspartic acid and ammonia. According to Hosamani and Kaliwal *et al*., (2011)(3), L-aspartate functions as a precursor molecule for ornithine in the urea cycle and creates oxaloacetate in the transamination reaction in the gluconeogenic pathway, which leads to the synthesis of glucose in humans. L-asparaginase activity was originally reported by Lang in 1904 (4); and Clementi in 1922 (6). Kidd reported in 1953(7) that guinea pig serum may produce transplanted lymphomas in vivo in mouse and rat cells. This was eventually linked to the serum's L-asparaginase activity (Dolowy *et al*., 1966)(8). However, it was challenging to produce and purify this enzyme on a large scale from guinea pigs for therapeutic use, which prompted researchers to look for other sources with comparable anti-leukemic properties. Microorganisms, animals, and plants all naturally contain asparaginase. In order to address these financial concerns, we must discover a different source for microbe cultivation. The solution to replace synthetic culture medium is to use massive amounts of agricultural waste products for the cultivation of microorganisms, especially fungus. In order to maximize enzyme production during submerged fermentation, the current work was designed to use vegetable peels and agricultural waste products such as wheat bran, rice husk, corn flour, gram flour, rice flour, onion peels, garlic peels, carrot peels, papaya peels, green pea peels, and corn peels as substrate.

For this investigation, papaya peels with the highest level of enzyme activity were selected. There are several reports on *Aspergillus quadrilineatus* producing L-asparaginase, but there are none on the full purification and characterisation of the free and immobilized enzyme. Thus, we report on the purification of fermentation conditions for *Aspergillus quadrilineatus* L-asparaginase synthesis in this study.

Materials and Methods

Screening of different basal media for L-asparaginase production

Twelve numbers of basal media (Wheat bran, Corn flour, Gram flour, Wheat flour, Rice flour, Rice Husk, Corn peels, Onion peels, Carrot peels, Papaya peels and Green peas peels, garlic peels) were used for present study. All the vegetable peels were collected, air dried and then oven dried at 50°C for 48 hours. For studying the effect of L-asparagine, 250 ml of each basal medium were prepared. The organism *Aspergillus quadrilineatus* was inoculated by punching out 0.6 mm of the agar-plate culture and transferred broth medium. Cultures were incubated at 30°C, for 6 days of incubation period. The culture filtrate produced in each treatment was tested for L-asparaginase enzyme production.

Estimation method

The ammonia measurement procedure was carried out by conducting an enzyme assay using Nesslerization method as described by Imada(8). To make the enzyme test mixture, 0.5ml of 0.04M L-asparagine was mixed with 0.5ml of Tris HCl buffer (pH 8.6). Then 0.5ml of enzyme and 0.5ml of distilled water were added. Subsequently, the combination was subjected to incubation for 30 minutes at a temperature of 37°C degrees Celsius. Following the incubation period, the reaction was halted by introducing 0.5ml of 30% TCA. To estimate the enzyme activity, 7ml of distilled water was combined with 0.5ml of enzyme mixture followed by the addition of 1ml of Nesseler's Reagent. Next, the op-

tical density was measured at a wavelength of 480nm using a spectrophotometer to estimate the enzyme activity. The quantity of ammonia emitted by the test sample was evaluated by comparing it to the reference graph. The measurement of the enzymatic activity of L-asparaginase was conducted using International Units (IU). An International Unit (IU) of L-asparaginase activity is the amount of enzyme required to produce one micromole of ammonia per milliliter per minute at a temperature of 37°C and a pH of 8.6.

Purification studies

Mass production, extraction and purification

The organism was introduced into the selected broth media using carrot peels and kept in a stationary environment at a temperature of 30ºC for 6 days. The samples were collected following the appropriate incubation period. The samples then subjected to treatment with a 0.05 M Tris-HCL buffer at a pH of 8.5. The sample was centrifuged at a speed of 600 rpm for 20 minutes at a temperature of 4^0C which led to the formation of a liquid. The statement described above was considered to be the basic composition of the enzyme. The enzyme activity and protein content were quantified and thereafter, the sample underwent the initial purification phase using ammonium sulfate precipitation.

Ammonium sulphate precipitation

The initial solution underwent precipitation by adding finely powdered ammonium sulfate until it reached a saturation level of 80%. The temperature was kept constant at 4ºC. The material underwent centrifugation at a speed of 6000 rpm for 10 minutes, continuing overnight. Afterward, the pellet that was retrieved was dissolved in a Tris-HCl buffer solution with a pH of 8.5, which had a concentration of 0.05 M (Suchita *et al*.,2010) (9).

Sephadex G-100 gel filtration

The samples that underwent precipitation with ammonium sulfate were assessed for their enzymatic activity and protein concentration. Afterward, they were subjected to gel filtration using Sephadex G-100 (Patro and Gupta,2012) (10).

Gel-column preparation and sample application

A glass tubing chromatography column measuring 60 cm in height and 2.2 cm in diameter was utilized. The eluent was 0.05 M Tris-HCL buffer with a pH of 8.5. To inhibit the formation of bubbles within the gel bed. Then the eluent was transferred from securely sealed brown bottles into containers containing the same temperature. The gel slurry was prepared by dissolving 5 grams of Sephadex in 200 ml of 0.05 M Tris-HCL buffer and allowing it to swell at room temperature for twenty-four hours. The column was secured and closed using Sephadex. Ammonium sulphate was used to precipitate the samples which were then continuously poured onto the column. The resulting fractions were collected in containers with a volume of 5ml. A random assortment of the gathered fractions underwent protein and enzyme activity analysis, and the fractions demonstrating exceptional enzyme activity were combined.

Ion exchange chromatography

The column was constructed by dissolving the necessary quantity of DEAE-cellulose in Tris-HCl buffer overnight. After the packaging procedure, the column was rinsed with 5M KCl to produce the desired weak ion exchange material. This was followed by rinsing with 5M NaOH to remove ionic charges from the ion exchanger. Afterward, the material was washed with distilled water and a 0.05 M Tris-HCl buffer solution at a pH of 8.5. Following the utilization of Sephadex for fractionating the peak fractions, they were next transferred to the ion exchange column where 5 ml of the fractions were gathered. After assessing the protein and enzyme activity of the samples and the fractions comprising the most active enzymes were consolidated and stored in a deep freezer.

Enzyme characterization based on partial purification

Substrate Specificity

The assay mixture was enriched with several substrates, such as L-arginine, L-phenylalanine, L-histidine, L-glutamine, and L-aspartic acid, to evaluate the enzyme's inclination towards a range of substrates. The substrates were present at a concentration of 0.04M, with L-asparagine serving as a control.

PH optima

The pH of the Tris-HCl buffer in the reaction mixture was methodically varied between 3 and 10 to identify the most favorable pH for enzyme activity. The enzymatic activity was measured at different pH values.

Temperature tolerance

The enzyme was maintained at temperatures ranging from 30 to 50ºCbefore its addition to the reaction mixer for the assay.

Incubation period

The enzyme was incubated at varying temperatures of 30, 37, and 50ºCbefore its addition to the reaction mixer for the assay.

Results and Discussion

Screening of substrates

The selection of a suitable substrate for submerged state fermentation is an important factor because it determines the production cost of the entire process. In this work, carrot peels have been selected for the production of asparaginase based on its nutritional composition, cost and availability. The results in (Table 1 and Fig.1) demonstrate that the highest level of L-asparaginase synthesis was observed i.e.3.0 IU/ml when carrot peels was used as the substrate followed by other substrates used as basal media. However, Varalakshmi and Raju,(2013) (11) reported that maximum L-asparaginase activity was achieved in a medium containing

Bajra seed flour as the substrate whereas corn cob showed the lowest activity from *Aspergillus terrus.* whereas Abha Mishra *et al*., (2006) (12) reported production of L-asparaginase from *Aspergillus Niger* using agricultural substrates like bran of Cajanus Cajan, Phaseolus mungo and Glycine max.

Table 1. Screening of different substrates for L-asparaginase production by *Aspergillus quadrilineatus*

Samples	Enzyme activity (U ml^{-1})
Carrot peels	0.25±0.008
Papaya peels	2.99±0.011
Green pea peels	0.21±0.017
Corn peels	0.07±0.00
Onion peels	0.095±0.006
Garlic peels	0.11±0.00
Rice Husk	0.08±0.00
Rice flour	0.035±0.007
Gram flour	0.055±0.003
Corn flour	0.06±0.00
Wheat flour	0.022±0.003
Wheat bran	No Growth
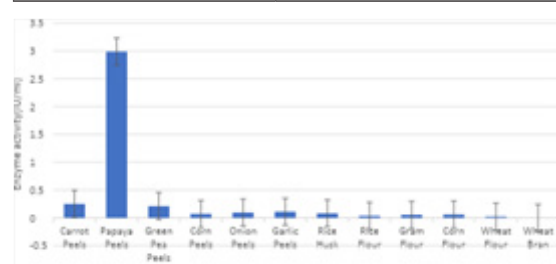
Fig-1: Screening of different substrates for L-asparaginase production by *Aspergillus quadrilineatus*

Purification studies

The enzyme L-asparaginase was purified from the culture filtrate of *Aspergillus quadrilineatus* using ammonium sulphate precipitation, ion exchange chromatography followed by gel filtration. The purification procedure summarized in (Table-2). The first step

of purification by ammonium sulphate precipitation achieved 0.99fold purification with 106% enzyme recovery. The second purification step was performed by gel filtration using Sephadex G-100 column. This step showed 1.04-fold increase in enzyme activity with 126.66% enzyme recovery. The final step of purification was done by ion exchange chromatography using DEAE cellulose The fractions showing L-asparaginase activity in this step were collected and pooled. The final step of purification resulted in 1.05-fold increase in enzyme activity with yield of 136.60% enzyme recovery.

Table 2. Purification profile of L-asparaginase from *Aspergillus quadrilineatus.*

Steps	Collected volume(ml)	Total activity (IU)	Total protein(mg)	Specific activity (IU/mg)	purification fold	Yield (%)
culture filtrate	3200	300	125	2.4	0	100
Ammonium sulfate precipitation	150	320	134	2.38	0.99	106.66
Gel filtration	120	380	151	2.51	1.04	126.66
Ion exchange chromatography	100	410	162	2.53	1.05	136.60

L-asparaginase from various vegetable peels and agro waste substrates have been purified and characterized and reported earlier. Similar findings were made by Aparna & Raju (2015) (13), who discovered that the ratios of these substrates showed a synergistic relationship and that corn ear and cauliflower stem greatly enhanced l-asparaginase synthesis by *A. terreus* MTCC 1782. According to Dias *et al*., (2015) (14), *A. niger* LBA02 produced a maximum L-asparaginase production of 89.22U/g when a ternary mixture containing equal amounts of soybean meal, cottonseed meal, and wheat bran was used. After 96 hours of fermentation, yields increased by 13.53, 13.53, and 71.5-fold, respectively, in comparison to the individual feedstocks. Furthermore, employing Passion fruit peel flour as a substrate, *A. niger* LBA02 l-asparaginase activity reached 2380.11U/gds (de Cunha *et al.,* 2018) (15). Maximum l-asparaginase yield for *A. niger* was supported using the bran of Glycine max (39.9±3.92U/gds), *Phaseolus mungo* (30.7±3.69U/gds) and *Cajanus cajan* (26.14±3.67U/gds) (Mishra, 2006) (16). L-asparaginase production by *Pseudomonas plecoglossicida* RS1 was increased twofold by onion peel extract and garlic peel extract supplemented with (0.3% w/w) L-asparagine. Several studies examined the asparagine content of wastes used as substrates. Further, pomegranate peel powder contains asparate in a ratio of 0.3g/100g (Rowayshed *et al*., 2013) (17).
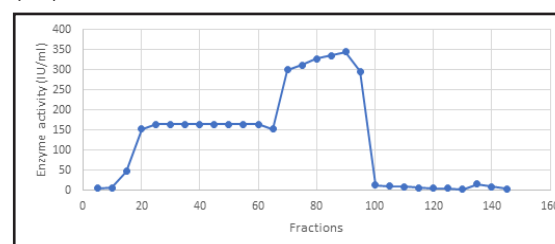
Fig-2: purification of L-asparaginase from the *Aspergillus quadrilineatus* gel filtration column chromatography (Sephadex G-100) of the fractions collected from ammonium sulphate precipitation fractions.
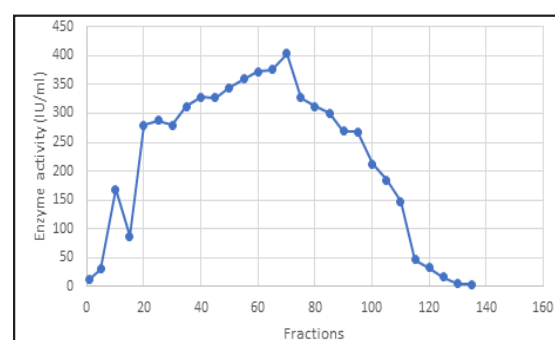
Fig-3: Purification of L-asparaginase from *Aspergillus quadrilineatus* ion exchange column chromatography fractions.

Characterization of partially purified enzyme

Another crucial element that needs to be adjusted and regulated is temperature. It is unclear how temperature affects the synthesis of enzymes (Chaloupka, 1985) (18). The current investigation examined the impact of incubation temperature on A. terreus's ability to produce L-asparaginase. As a result, the synthesis of L-asparaginase was shown to be highest at 37°C (4.11 IU/ml) and minimal at 50°C (1.60 IU/ml). According to Sarqius *et al*., (2004) (19), 30°C is ideal for submerged fermentation employing *A. tamarii* and *A. terreus* to produce L-asparaginase. According to Manna et al. (1995) (20), 37°C is the ideal temperature for *Pseudomonas stutzeri* to be at its most active. For the synthesis of L-asparaginase to be successful, the substrate's initial pH level is crucial. According to earlier research (Sivaramakrishnan *et al*., 2006) (21), pH plays a significant role in controlling development, metabolism, and the synthesis of enzymes. Since each creature has a unique pH optimal range, any changes to these ranges may cause an organism's enzyme function to decline (Adinarayana and Ellaiah, 2002) (22). The current investigation found that this fungus produced the most enzyme at pH 8 (4.28 IU/ml), and that pH values over 10 caused the fungus to produce less L-asparaginase. At pH 10, the least amount of enzyme was produced (0.43IU/ml). Similar findings indicating that pH 7.0 is ideal for L-asparaginase synthesis during submerged fermentation have been reported by De Angeli *et al*., (1970) (23). Koshy *et al*., (1997) (24) discovered that *Streptomyces plicatus* produces the most L-asparaginase at a pH of 8.0. The analysis of substrate specificity demonstrated that the enzyme acts as a catalyst, particularly using L-asparagine as its substrate. When enzyme production was examined under various reaction times, a significant amount of variance was seen, with the highest output being detected at 10 minutes.

Table 3. Effect of pH, Temperature, and substrate on partially purified L-asparaginase.

Parameters	Enzyme activity (U ml^{-1})
Temperature Effect	
30	3.57
37	4.11
50	1.6
Incubation Period Effect	
10 min	4.22
20 min	3.85
30 min	3.02
40 min	2.2
Effect of PH	
3	3.09
4	3.11
5	3.25
6	3.69
7	3.75
8	4.28
9	1.2
10	0.43
Effect of Substrate Specificity	
L-arginine	2.52
L-phenylalanine	2.24
L-Histidine	2.06
L-Glutamine	2.33
L-aspartic	3.10
L-asparagine	4.54

Conclusion

The observations obtained in this study found that *Fusarium proliferative* has the capability to produce substantial amount of L-asparaginase enzyme. For the submerged state fermentation process, carrot peel is found to be the best substrate and it clearly enhances the

practicality of this work by the way of economically feasible for the large-scale production of L-asparaginase. The L-Asparaginase was further purified using gel filtration chromatography with a Sephadex G-100 column. The final overall yield recovery was 121.21%, and the purification resulted in a fold increase of 0.95. Research on the physical factors affecting the effectiveness of pure L-Asparaginase has shown that it remains functional throughout a wide pH range of 8 and at a temperature of 37ºC. The enzyme demonstrates a high level of selectivity towards its natural substrate, L-asparagine and demonstrates a high level of stability at a pH of 8.

Acknowledgments

References

1. Shakambari, G., Kumar, R.S., Ashokkumar, B.,Varalakshmi, P. Agro wastes utilization for cost-effective production of L-asparaginase by Pseudomonas plecoglossicida RS1 with anticancer and acrylamide mitigation potential. *Acs Omega*.,2017;2,8108-8117. Doi.10.1021/ascomega.7b01429.

2. Pallem, C., Solid-state fermentation of corn husk for the synthesis of Asparaginase by Fusarium oxysporum. *Asian J Pharm Pharmacol*.,2019; 5(4),2007678-681.

3. Hosamani, R. and Kaliwal, B.B.,L-asparaginase an anti-tumor agent production by Fusarium equiseti using solid state fermentation. *Int J Drug Discov*.,2011; 3(2),88-99.

4. Lang, S., Über desamidierung im Tierkörper. *Beitr chem Physiol Pathol*.,1904; 5,321-345.

5. Clementi, A.,La désamidation enzymatique de l'asparagine chez les différentes espéces animales et la signification physio logique de sa presence dans l'organisme. *Archives Internationales de Physiologie*., 1922;19(4), pp.369-398.

6. Kidd, J.G.,.Regression of transplanted lymphomas induced in vivo by means of normal guinea pig serum: I. course of transplanted cancers of various kinds in mice and rats given guinea pig serum, horse serum, or rabbit serum. *The Journal of experimental medicine*.,1953; 98(6), 565-582.

7. Dolowy, W.C., Henson, D., Cornet, J. and Sellin, H., Toxic and antineoplastic effects of l-asparaginase: Study of mice with lymphoma and normal monkeys and report on a child with leukemia. *Cancer*,1966; 19(12),1813-1819.

8. Imada A, Igarasi S, Nakahama K, Isono M. Asparaginase and glutaminase activities of microorganisms. *J. Gen. Microbial*.,1973; 76(1): 85- 99.

9. Suchita C, Warangkar and Chadrahas N Khobragade. Purification, characterization, and effect of Thiol compounds on Activity of the Erwinia carotovora L-asparaginase. *Enzyme research*,2010.

10. Patro, K.R., Basak, U.C., Mohapatra, A.K. and Gupta, N.,Development of new medium composition for en d production of L-asparaginase by Aspergillus f. *Journal of environmental biology*.,2012; 35, 295-300.

11. Varalakshmi, V. and Raju, K.J., Optimization of l-asparaginase production by Aspergillus terreus mtcc 1782 using bajra seed flour under solid state fermentation. *Int J Res Eng Technol*.,2013;121-129.

12. Aparna, C., Raju Jaya, K.Optimization of process parameters for L-asparaginase

production by Aspergillus terreus MTCC 1782 under solid state fermentation using mixed substrate. *International Journal of Research in Engineering and Technology*.,2015; 4(5), 354-360.

13. Dias, F.F.G., de Castro, R.J.S., Ohara, A., Nishide,T.G., Bagagli, M.P., Sato, H.H.Simplex centroid mixture design to improve L-asparaginase production in solid-state fermentation using agroindustrial wastess. *Biocatalysis and Agricultural Biotechnology*., 2015;4(4), 528-534.

14. da Cunha, M.C., Silva, L.C., Sato, H.H., de Castro, R.J.S. Using response surface methodology to improve the L-asparaginase production by Aspergillus niger under solid-state fermentation. *Biocatalysis and Agricultural Biotechnology*.,2018; 16,31–36.

15. Mishra, A., Production of L-asparaginase, an anticancer agent, from Aspergillus niger using agricultural waste in solid state fermentation. *Applied biochemistry and biotechnology*.,2007;*135*,33-42.

16. Rowayshed, G., Salama, A., Abul-Fadl, M., AkilaHamza, S., Mohamed, E. A. Nutritional and chemical evaluation for pomegranate (Punica granatum L.) fruit peel and seeds powders by products. *Middle East Journal of Applied Sciences.,2013;*3, 169–179.

17. Chaloupka, J.,Regulation of the synthesis of extracellular proteinases in bacilli. In *Environmental Regulation of Microbial Metabolism.,1985;* 287-293.

18. Manna, S., Sinha A., Sadhukan R., Chakrabarty SL. Purification, characterization and antitumor activity of L-asparaginase isolated from Pseudomonas stutzeri MB-405. *Curr Microb*.,1995; 30: 291-298.

19. Sivaramakrishnan S, Gangadharan D, Nampoothiri KM, Soccol CR, Pandey A. αamylases from microbial sources-an overview on recent developments. *Food Tech Biotech*., 2006; 44: 173-184.

20. Adinarayana, K., Ellaiah P. Response surface optimization of the critical medium components for the production of the alkaline protease by a newly isolated Bacillus sp. *J Pharm Pharmaceu Sci*., 2002; 5: 272–278.

21. De-Angeli C., Pocciari F., Russi S., Tonolo A., Zurita VE., Ciaranf E., Perin A. Effect of L-asparaginase from Aspergillus terreus on ascites sarcoma in the rat. Nature, 1970; 225: 549-550.

22. Koshy, A., Dhevendaran, K., Georgekutty, M. I., & Natarajan, P. L-asparaginase in Streptomyces plicatus isolated from the alimentary canal of the fish, Gerres filamentosus (Cuvier). *Journal of Marine Biotechnology*,1997; *5*(2-3), 0181-0185.

Advancing Cleanroom Contamination Control Strategies with Automation and AI: Current Status and Future perspectives in the Manufacturing of Parenterals

Tata Santosh[1,2], Prafulla Kumar Sahu*[1], SR Parthasarathy*[2]

[1]School of Pharmacy, Centurion University of Technology and Management, Odisha, India
[2]M/s GMP Pharma Consultants, Hyderabad, India

*Corresponding Author: prafulla.sahu@cutm.ac.in

Abstract

Contamination in parenterals affects products' critical quality attributes and patient safety. lapses are frequently noticed, leading to product recalls. The most recent Annex-1 guidance expects manufacturers of parenteral products to evolve with a holistic contamination control strategy covering unit operations, processes and activities. The operation segments in cGMP environment are described wholly under 6M's (Men, material, machines, Methods/processes, Mother nature/environment and Measurement/controls) and their respective subfunctions. We discussed the role of critical controls to validate the process The need for automated equipment compliant with GAMP 5, the focus areas requiring technological advancement using artificial intelligence (AI) are discussed. Novel automation controls that can be installed in existing manufacturing units and the corresponding outcome for an improved CCS is summarized.

Keywords: Contamination Control Strategy, GAMP 5, ICH, GMP, Aseptic Process Simulation, Automation

Introduction

The most recently released Annex-1 draft guidance on the manufacture of sterile products (1) discussed the need for development of a comprehensive CCS. It emphasized the need for a top-down approach to understand the critical control points (CCPs) that affect product quality. The knowledge of process analytical technologies (PAT) (7) coupled with the principles of ICH Q10 (2) helps us to lay down the necessary controls. Regardless of the degree of controls laid down, we carry a residual risk. Among the various risk assessment techniques (2), the Hazard Analysis Critical Control Point (HACCP) is versatile and ideally summarizes the CCPs. In order to prepare a holistic contamination control strategy (CCS) document and apply the principles of HACCP in its entirety, we opted for the 6M approach (3-5). We graded the overall compliance requirements under the 6M tree. Based on the data of lapses reported for one or more of the CCS elements in various regulatory notices and/or warning letters, we summarized the vulnerable areas where redundancy of controls is required. Corrective and preventive actions (CAPAs) for lapses are usually tedious; however, modern automation tools can aid to effectively map the vulnerable areas on a real time basis and further correlate the root cause with existing data libraries thus helping to evolve with a more robust CAPA. Very often, product quality risk is eliminated by reducing manual intervention and improved automation. GAMP5 guidelines are designed to ensure that automated systems comply with the cGMP standards. (6). The advantages of automation and AI for achieving an improved CCS is presented.

6m classification & identification of CCPS in an aseptic environment

The 6M Technique aids in identifying process inefficiencies and helps to drive continuous improvement in the manufacturing environment (5-7). The scope of 6M for general aseptic operations is indicated in figure 1. CCPs for general aseptic operation are discussed. In instances demanding distinct attention to testing and controls, such as large-volume parenteral (LVPs) and powder injectables, we have dedicated sections within this review to address these specific areas.

Facility
Clean room controls

All intersection points through which materials, men and waste move are areas of concern. The guidance on the facility requirements for aseptic operations is widely available (8, 9). Facilities are qualified before their intended use. Equipment qualifications, simulation studies and validations are often conducted to identify the CCPs. Notably, the design must ensure the absence of uncleanable recesses (10, 11). Process areas are designed such that sink or drain provisions are absent in the Grade A/B areas. All other drains are microbially monitored for flora. Modern building designs ensured dedicated corridors for waste movement and separate passages for RM / FG movements to prevent contamination. A positive pressure variance with the surrounding is a vital CCP. Hence, a pressure differential of no less than 15 pascals between two distinct classified zones (regulation mandates NLT 12 pascals) and a pressure differential of at least 6 pascals (regulation mandates NLT 4 pascals) between two rooms with identical classification (regulation mandates NLT 4 pascals) is routinely upheld. Calibrated magnehelic gauges capable of recording and generating alarms are often placed to enhance monitoring capabilities. All the Cleanrooms are qualified and classified based on applications. Grade A (Filling area, sterile laundry receipt, LAFs area, Mobile LAFs, sampling area for pre-sterilized components), Grade B (filtration area, Receipt area for filtered liquid, blending area of sterile APIs, receipt area of filtered liquid, blending area for sterile APIs, peripheral area of filling), Grade C (laundry washing, Compounding area, equipment washing area, secondary change rooms, unloading pre-sterilized components, handling pre-sterilized components) and Grade D (Primary change room, equipment washing area, vial washing area, plug washing area) areas are equipped with terminal HEPA (H14) (12-21). CNC areas (Vial inspection, Packaging and labelling, RM stores, Microbiology waste disposal area, Quality unit, Finished Goods store) are equipped with 5μ filtered air. Lux level in the vial inspection area is a CCP and shall range from 2000 – 3750 lux depending on operation.

Men
Training, gowning qualification, health & hygiene

Human activity in the cleanrooms is the primary reason for particulate and microbial contamination (24). CCPs such as routine self-inspection, materials for apparels, garment sterilization, maintenance and the overall gowning processes are critical. Standards for cleanroom garments are described (22) and their quality can be assessed using various procedures (23). The Helmke Drum test (28) that verifies the particle shedding, especially when a garment is washed multiple times, is critical. The number of wash cycles for garments is hence validated. Sterilized garments shall have a definite validity period and the sterility assurance level shall be NLT 10^{-6} after sterilization

Gowning qualification tests the operator's proficiency to don and doff the garments correctly and conduct EM in Grade B areas. Re-qualification criteria, other than during annual frequency, is also required. No specified swab sampling locations were described in literature (1); hence, companies develop a risk-based approach to identify the locations for sampling (25).
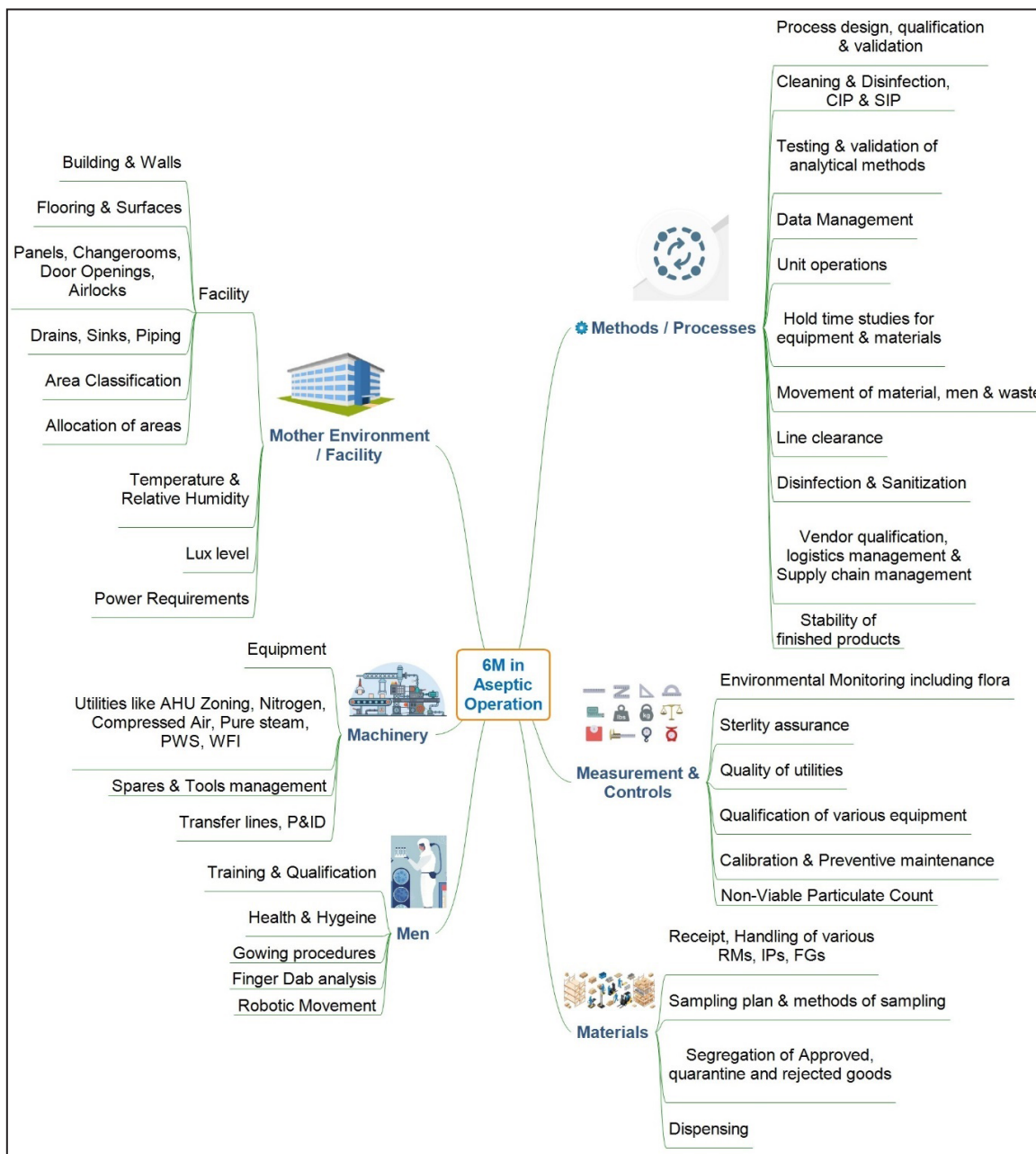
Figure 1: CCPs in an aseptic environment based on 6M classification.

Personnel suffering from communicable diseases such as tuberculosis, influenza, etc., including bruises and skin infections such as psoriasis and contact dermatitis, shall be prohibited (26). The health of the operators is monitored. Companies implemented thermal screening methods during the COVID-19 pandemic. Any undue absenteeism during the pan-

demic mandated the management to re-confirm that the personnel attended to the company in a clean environment.

Machinery (equipment, utilities & tools)

Control on the usage and maintenance of process equipment, utilities and spares is utmost critical as they are located in the Grade A area. A line clearance procedure enlisting the various CCPs is undertaken before the start of the activity. The handling of machinery, utilities and tools is video recorded for traceability during the operation.

Process equipment & utilities

Automation reduced human intervention and improved data integrity. All qualified process equipment is enabled with the highest degree of automation to prevent contamination (13, 28-30). Machinery equipped with data loggers and PLCs that are capable of real time recording and generating alarms, shall comply with 21 CFR Part 11 and GAMP5 recommendations (27). Filter membranes shall comply with ISO 16610-21 (31). Qualified utilities mostly undergo contact with the product solutions and hence filtered through 0.2µ porosity filters. A list of CCPs for various critical utilities is enlisted (see table-1). Purified water forms the input material for WFI generation and its quality is monitored continuously. The most recent water purification systems employed the use of variable frequency drive to meet flow velocity requirements (NLT 1.3 mt/sec). The most recent equipment are designed to give SMS alerts to the personnel concerned when the operating limits are deviated. Also, hooter alarms are equipped to alert the engineering personnel if there is a deviation in the set point conditions.

Tools & spares management

All tools introduced into core areas are sterilized and remain within, prohibiting their exit to maintain sterility. If a sterile equipment or tool accidentally drops to the floor, refrain from retrieving and using it. Instead, ensure that the room is equipped with extra sterile supplies. Additionally, all gloves and tools are designated for single use and subsequently discarded, upholding stringent cleanliness standards within the environment. Glove ports are sterilized and employed for contamination-free operations. Latex gloves, pre-sterilized through Ethylene oxide or Gamma sterilization, are tested for sterility in batches, ensuring their suitability for use. These gloves are also powder-free to prevent particulate contamination. Silicone tubes, integral for transferring gases and liquids, undergo autoclave sterilization and testing for leachates, compliant with USP <1663 & 1664> (32).

Materials and Methods

Receipt of raw materials (RM)

RMs shall be received from approved vendors only. Pre-shipment samples for sterile APIs, rubber stoppers and other gamma-sterilized materials, including sterile personnel protective equipment (PPEs), are received and tested for sterility. Upon confirmation of the sterility, the order quantity is requested for release from the supplier's site, and after receipt, it is verified against an inward checklist. Thermo-sensitive materials shall be adequately packed along with a temperature datalogger, and upon receipt, shall be stored in designated storage conditions.

Sampling & dispensing

Non-sterile APIs are subjected to 100% sampling while the excipients are sampled based on (Square root of N + 1) (9). For bulk receipts, AQL sampling methods can be followed (33). Sampling for sterile APIs shall not be done, and results of the pre-shipment sample are taken as final for approving the lot. For buffers, anti-oxidants and preservatives that are intended as powders for reconstitution separate procedural controls are required *(*see discussion under *CCPs for Powder injectables)*. Sampling shall be done only after satisfactory visual inspection using dedicated and compatible tools. Clean and unclean equipment hold-time

studies shall also apply to the sampling tools. Reverse LAF systems complying with ISO 5 or Grade A/B requirements are used for dispensing. Line clearance is verified before carrying out the activity.

Controls for In-process materials

In-process materials shall only be prepared in the Grade B area until complete manufacturing. Hold time studies for solutions are done to study the effect of any unforeseen interventions during the process. The quality parameters at the end of the hold time shall be comparable with that of the finished product.

Storage & despatch of finished goods

Finished Goods (FGs) shall be stored in controlled environmental conditions with adequate protection from heat and light. The quantity reconciliation must be readily available, and despatch procedures shall follow the first-expiry-first-out methodology. Retention samples of each of the batches shall be stored at designated locations with physical lock and key to enable the investigation of complaints/queries that may arise after despatch. The retention period for finished goods batch samples is 1 year more than the designated shelf life. For RMs, the designated shelf life is up to 6 months from the date of receipt. The storage and despatch of intact sealed containers contribute very little to the overall contamination control strategy.

Methods (Processes & simulations)

Process qualification & routine unit operations

The process qualification shall involve the identification of CPPs with a challenge to consistently achieving the CQAs throughout the product life cycle. Ideally, procedural controls are established. The CCPs in the process are identified and documented. For filter membranes, the compatibility, integrity, adsorbent properties and filtration time often limit the batch size for viscous solutions. The overall process flow is described in figure 2.

Aseptic process simulation (APS)

Unlike in terminal sterilization, where parametric release of materials is permitted (47, 48)], the products manufactured by aseptic filling are exposed to a high degree of risk. Media fill studies (APS) are applicable for aseptically filled products only. Media fill studies are processes by which the product is not manufactured, but instead, media is prepared and filled into containers as though the product is made. The process undergoes all the steps that are there for a given product. All the unit operations involved in manufacturing the product must be carried out as part of media fill studies. These must be conducted under stress conditions to ensure the product can withstand any inadvertent contamination. The entire activity has to be carried out as though it is a routine process and not staged to have additional precautions than customarily practised. This may give a false negative result. Guidance on the number of containers to be taken for the media fill study was provided by the Parenteral Drug Association (34). The industry does not allow any failures in the APS. Any failure calls for thorough investigation and identification of the organism, at least to its genus level, its source and remediation to prevent recurrence. Three consecutive APS runs are usually done for the initial simulation. Based on the production load, the quality team can decide the number of runs for periodic confirmation.

Media fill studies are performed under various circumstances, including facility qualification, significant changes to the water system, facility, or air handling unit (AHU), the introduction of a new product, batch failures, or when environmental counts exceed alert limits. These studies are routinely conducted every six months to ensure aseptic processing integrity. In cases where the same product is filled in different volumes or weights, bracketing can be applied to streamline testing. Additionally, simulations are conducted for different dosage forms to validate sterility assurance across various manufacturing conditions.

Filling of containers

The volume of product to be filled need not be the volume that is filled in a container. The reason is that, during incubation, the vials are kept so that the entire product contact surface area is covered, including the closure if applicable. (Up-right, Inverted, horizontal positions during the incubation period).

To simulate dry powder (lyophilized), sterile mannitol is filled into containers and sterile media is subsequently added and sealed as a part of unit operation. The mannitol dissolves immediately and does not alter the characteristics of the media.

For aqueous gels, the media is added into the gel without the active ingredient and the preservatives and filled.

Table -1: Controls for various utilities in parenterals, compendial requirements and best practices in the industry

	CCPs for various utilities	Compliance requirements	Routine Practice
Compressed Air	Oil content < 0.5 mg/m³ Dew point -40°F NVP matter ≤ 90000 for 0.5μ and ≤ 1000 for 5.0μ Bio load = Nil Max discharge air pressure < 7 kg/cm²	ISO 8573	For the service lines, a filter integrity test is done once every six months (± one month) during non-production days. The service line filter is replaced once in 2 years (± one month)
Nitrogen	Purity > 99.5% Oxygen < 0.5ppm CO / CO₂ < 1ppm Water < 3ppm Oil content < 0.5 mg/m³ Dew point -40°F NVP matter ≤ 90000 for 0.5μ and ≤ 1000 for 5.0 μ Bio load = Nil	ISO 8573	Purity > 99.999% Oxygen < 2 ppm CO / CO₂ < 1ppm Total Impurities < 4 ppm Water < 3ppm The nitrogen line is built with a hydrophobic service line filter of 0.2μ porosity that is replaced once every 2 years. Filter integrity tests in service lines are also done once every 6 months.
Pure Steam	pH = 5.0 to 7.0 of condensate Conductivity < 1.1 μs/cm at 20°C of condensate Temperature, Pressure: Correlates with dry saturated steam Non-condensable gases < 40ml/kg Moisture < 5% Superheat < 50°C at atmospheric pressure Bacterial Endotoxins <0.25 EU/ml of condensate		pH = 5.0 to 7.0 of condensate Conductivity < 1.1 μs/cm at 20°C of condensate Temperature, Pressure: Correlates with dry saturated steam. Non-condensable gases < 4.0% Moisture < 5% Superheat < 25°C at atmospheric pressure Bacterial Endotoxins <0.25 EU/ml of condensate **Other practices** Controlling the % of make-up water < 15% to maintain steam quality. Pipeline velocity below 25 m/sec that allows effective removal of entrained moisture using steam traps Use of strainers to protect control valves and steam traps. Steam condensate should meet the current monograph of WFI.

Contamination control strategies in aseptic operations

Water Purification System	TOC (ppb) NMT 500	Pharm. Eur, USP JP	Reverse osmosis and ozonization coupled with Ultrafiltration are currently being used.
	Conductivity (µS/cm) @ 20°C NMT 1.0		
	Nitrates (ppm) should be absent		
	Heavy Metals (ppm) should be absent		
	Aerobic Bacteria (cfu/ml) <100 / ml		
	Pathogens: absent per ml		
WFI	Same as Purified water additionally,	Pharm. Eur, USP, JP	Reverse osmosis, ozonization, ultrafiltration, and electrodeionization (EDI) are currently used. Multi-column distillation
	Endotoxins (IU/ml) <0.25 EU/ ml		
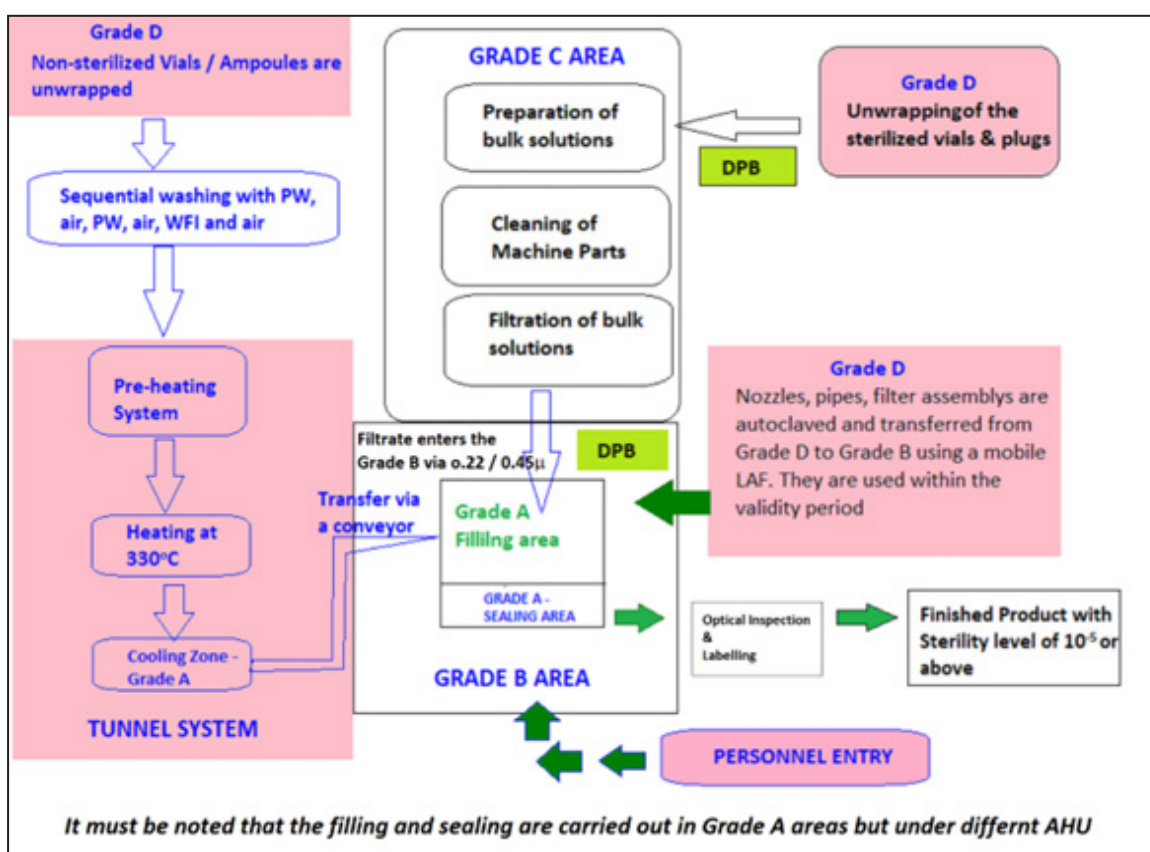
Figure-2: Processes in the aseptic area

Figure legend: the red background indicates zones of high risk. DPB – dynamic pass boxes are routinely equipped with 0.22 µ filters (H14 grade)

Media qualification

Soybean casein digest broth is the medium of choice for this activity. The media is qualified to ensure that the media can identify any single cell in the entire operation. The organisms used are prescribed in USP The lots used for media preparation shall be pre-qualified. The number of environmental isolates to be used may be more than one. All these organisms should have shown copious growth on incubation prior to the commencement of the study.

Cleaning, sanitization & disinfection

The primary methods for cleaning industrial equipment involve Clean-In-Place (CIP) and Steam-In-Place (SIP), which utilize chemical or heat treatments. Before this, it is essential to attempt the removal of process residues and particles using high-pressure water cleaning or steam. Alkali-based disinfectants and detergents are commonly employed in CIP systems, with sodium hydroxide being one of the most widely used options. It is crucial to validate the cleaning process for equipment to ensure its effectiveness.

Regular hand sanitization with an effective hand sanitizer is necessary for personnel engaged in Grade A/B areas. In Europe, established standards (EN 149913 and EN 150025A) describe the validation approach for hand sanitizers [35-38].

CIP & SIP

CIP and SIP are automated processes utilizing water, chemicals, and heat to sanitize equipment effectively. One CIP cycle will usually take between 60 and 90 minutes and generally operate at 100°C. SIP enhances the sterilization achieved through the CIP process by employing steam at temperatures ranging from 120°C to 135°C for 30 minutes. An important factor affecting the SIP is the quality of steam (See table-1).

Factors that influence the CIP & SIP are the operating temperature and pressure, the concentration of the chemical, the heating duration, and the viscous nature of the material to be cleaned. Several chemicals used in the CIP process have been found incompatible with elastomeric seals. In most CIP and SIP applications, VMQ silicones and hydrogenated acrylonitrile butadiene rubber (HNBR) are unsuitable due to their limited compatibility. Fluoroelastomer (FKM) materials also exhibit weaknesses when exposed to alkaline and acidic substances. Ethylene propylene diene monomer (EPDM) is generally suitable for sealing aseptic technology but falls short when confronted with more rigorous CIP procedures. In contrast, Perfluoroelastomer is resistant to chemical media and high temperatures, making it the universally preferred material for CIP and SIP processes.

Hold time studies for equipment and materials

According to the WHO Technical Report Series No. 992, 2015, Annex 4, hold-time studies determine the permissible duration for holding materials at various production stages to ensure product quality remains within acceptable limits. The study design must accurately represent the holding times at each stage, as they directly impact the final product's overall quality, making hold time a critical control point (CCP) in the industry. Various routine and unforeseen interventions can extend hold times, including filter assembly blockages, volume or fill weight corrections, crew changes during shift transitions, intermittent sampling, component adjustments, operational delays, periodic replenishment of materials, sensor replacements, conveyor or guide rail modifications, spillage, container replacements, temporary increases in personnel, and simulations of failures such

as UPS or AHU malfunctions. Additionally, exceeding the allowed frequency for opening entry doors in Grade B areas and non-robotic human movement for short durations can also influence hold time. These events are commonly simulated during process validation to assess their impact on production and ensure compliance with quality standards. During the interventions, batch production time can be extended to a few hours, during which bio-load can increase. Hence, material hold-time studies are done during process validation.

The clean equipment hold time involves verification of microbial load on the contact surfaces, while the unclean equipment holds time verifies both chemical and microbial load. Swab samples are collected from designated locations, and the residue per unit area is calculated. The unclean equipment hold time is of pivotal importance. Formulation residues left over on the surface of the equipment can undergo degradation due to one or more factors, such as temperature, humidity, oxidation, or hydrolysis. It is important to note that, during the selection of a cleaning aid, operators rely on the solubility of the active ingredient. In principle, no data is available on the solubility of impurities or degradation products likely to be formed during exposure. Hence, deviating from the established unclean hold time can cause the carryover of the chemical residues into subsequent batches. A checkpoint here is to verify the TOC of the swab sample and ensure that it is comparable to WFI limits. On several occasions, the regulatory agency requested that unknown peaks due to extended hold time be identified. Analysts relied on advanced HPLC-based techniques for identifying and quantifying such impurities or referred to the stability-indicating methods to see if such peaks occurred during product development or due to the stress conditions during product storage (40,41).

Cleaning validation

An efficient cleaning procedure allows the contaminants to be effectively removed below acceptable levels. Residue levels not exceeding 10 ppm are considered reasonable, and a safety factor of 0.001 is recommended in the current PDA guidelines; however, the industry follows the least of the two (42, 43)., In routine practice, detergents are prohibited as their composition and surface compatibility is unknown. A suitable sodium lauryl sulphate (SLS) concentration either alone or in combination with suitable ICH class 3 solvents (44) with a fixed number of rinse cycles shall be done with final WFI recirculation at 80°C. The residue of SLS can be quantified. The TOC of the final rinse samples should not exceed 500 ppb. The residual carryover can be more prominent with sterile powders, wherein insoluble residues may stick to the inner surfaces of long pipes and bends. Solubility information is paramount in such cases.

Measurement (*routine controls and monitoring*)

Sterility assurance

Sterility assurance is the degree of certainty that a given product or unit, which is claimed to be sterile, indeed meets the criteria of sterility. The test is destructive, and several controls over practices, utilities and the environment. Besides controls over the elements described in the 6M environment, additional aspects such as reducing or eliminating the number of interventions, implementing a closed, restricted access barrier system (RABS), and adequate process simulations that include preventive testing and periodic vendor qualifications contribute to sterility assurance.

Environmental monitoring (EM)

The readiness of the environment shall include compliance verification over Viable and non-viable particulate matter (14, 15). The air quality correlates with the product quality. Periodic performance verification for air quality are given in Table 2.

Table -2: Performance verification tests for AHU/HVAC

Utilities	Performance verification tests and Frequency
AHU / HVAC	Airflow velocity, volume and Air changes test Filter integrity test Differential pressure test (Real Time basis) Airflow pattern test Airborne non-viable count (Particle count) Particle Recovery test Temperature control and humidity test Airborne viable count (Microbial quality of air)

Environmental flora

Why should these isolates be included in GPTs? The rationale is that if organisms are indeed present in the product, the utilized media should be able to detect their presence. Environmental isolates may be sporadic or predominant and vary with seasons. The predominant isolates must be identified up to the species level by available software – VITEK 2. These organisms need to be maintained as a part of the library with its details of morphology and photographs. Once the organisms are identified, it has to be ascertained that the media used – Reasoner's 2A (R2A) agar (if the isolate is waterborne), Soyabean casein digest agar (if it is from environment or people), and Fluid thioglycolate (if water, environment and people) will be able to identify its presence. So, these organisms form a part of Growth promotion tests (GPTs). GPT should encompass one organism from each family in the isolates.

Non-viable particulate count

In a study conducted by the NIH (45), the Continuous monitoring of non-viable airborne particles shows a correlation with airborne colonies and serves as an acceptable proxy for the daily evaluation of cleanroom performance.

However, the USP still mandates using agar contact plates for particle counting in ISO 7 areas. Continuous monitoring of the non-viable particles can help monitor the trend, and such equipment will work as an early warning system. **Specific CCPs for Powder injectables**

Apart from the active pharmaceutical ingredient, the powder injectables have buffers, antioxidants and preservatives. In order to test the microbial load, the inhibition properties of buffers, anti-oxidants and preservatives are neutralized such that the microbial recovery is maximum (46). Powder injectables are either blended and filled or filled as such. The vials are sterilized in a tunnel system validated for non-viable particulates (NVP) and BET, ensuring contamination is avoided. The entire quantity of the API or the excipients are consumed in once instance and left overs are discarded.

Routine quality control testing of the finished product involves reconstitution of the contents using filtered WFI under LAF. The vials are inspected to ensure that particles of definite micron sizes are within limits. The particulate matter shall comply with the limits prescribed under USP <788>. The powder injectable product process is simulated by filling pre-sterilized mannitol powder. As powder injectables are generally moisture sensitive, the temperature in the classified area is maintained below 20˚C and RH below 35 %. Controlling moisture is essential for controlling microbial burden.

Specific CCPs for large-volume parenteral

Any volume of more than 100 ml is known as LVP and are terminally sterilized. As the product does not have preservatives, the bio-burden has to be least. Polypropylene (PP) granules made under ISO 8 conditions are used for LVPs and glass is prohibited.

Gamma sterilized granules are blown into heating and blowing with filtered and qualified compressed air. Other required parts of the bottle are also made of PP and are pre-sterilized. The solutions are prepared under ISO 7

tions, personnel control, contamination prevention, and overall compliance with quality standards.

Achieving enhanced efficiency through automation

Automation and robotics, combined with single-use systems, are transforming aseptic processing by streamlining operations, minimizing human intervention, and reducing the risk of contamination or errors. Advances in analytical testing, such as rapid sterility testing can yield results in under seven days, a significant improvement over the traditional 14-day incubation period required by compendial sterility standards. However, regulatory guidelines for viable particulate monitoring are based on CFUs, which do not easily correlate with results from fluorescent particle counting. Manufacturers need to validate new methods against existing standards to prove their equivalence or superiority.

Rapid microbial methods, using biofluorescent particle counters instead of settle plates, offer real-time microbial data during aseptic processing, enabling immediate responses to EM failures and reducing the risk of batch losses. Further innovations in EM systems now allow for real-time differentiation between viable and non-viable particles, capturing viable particles on a growth medium as they are detected. This advancement shortens the timeframe for identifying EM excursions, crucial for preventing delays and shortages in parenteral supplies.

Automation and robotics are also revolutionizing visual inspection in drug manufacturing. Automated visual inspection (AVI) combined with AI for image analysis [66] enhances defect and particle detection, reduces false reject rates, and improves process efficiency. The use of standardized, ready-to-use components, such as pre-sterilized vial nests, has also streamlined production by eliminating steps like vial washing and sterilization, reducing glass vial damage, and enabling more efficient filling processes.

Despite these advancements, robotics still face challenges, particularly in handling unexpected events. Future innovations may involve integrating vision systems and AI to enable robots to respond to unplanned interventions, further reducing human involvement and enhancing operational flexibility. To fully leverage these technologies, manufacturers must adopt flexible implementation strategies that maximize the benefits of automation and robotics. Some automation tools that can enhance cleanroom performance metrics are listed in table-3.

Table 3: Some automation controls that need to be implemented in the Grade A / B areas

Automation control	Intended purpose	Expected improvement in CCS
Implementation of differential pyro-electric Infrared sensor [51] and a camera at entry points of Grade A/B Area	To capture real-time data about the number of operators inside the critical area (Grade A/B).	This process can limit the number of operators inside the Grade A/B area and thus help reduce contamination. Linking this device with the interlocking doors can provide restricted access into the Grade A/B areas.
Implementing wearable Performance metrics monitoring devices [52, 53]	To monitor the working personnel's real-time health status, stress levels, fitness, etc.	Failure to meet the fitness and hygiene norms will prevent operators from entering the sterile environment.
Implementation of Real-time attention monitoring and behaviour recognition systems [54, 55]	To enable monitoring and recording of behaviour in the clean rooms.	Any deviation in the operator's behaviour can alert the quality personnel immediately. Improving the awareness of the pupil working in the Grade A areas can be easy with the help of recorded videos.

Implementation of screeners to verify the training [56]	Only qualified and trained operators are allowed inside the cleanroom	While this is already in place, monitoring the real-time readiness of the personnel and enabling access to qualified personnel has to be implemented.
Installation of capacitance proximity sensors for the detection of waste [57]	To detect and remove any leftover material in the dispensing, labelling and packaging areas	In the dispensing area, it provides electronic evidence of thorough line clearance. Currently, this is done manually.
		Implementing this system in the labelling and packaging areas will prevent mix-ups and mislabelling of products.
Quick response coding systems on the labels [58]	To verify the accuracy of labelled contents	This practice is already being followed in India by manufacturers of APIs. Implementation by formulation manufacturers is pending.
Real-time Temperature data logging and transmission system [59]	To ensure that the goods are transferred to the destination under controlled conditions.	This will support generating data for transportation validation and provide trend data on logistics and supply chain control.

Ai for an efficient CCS

AI tools can extract the key drivers that facilitate the identification of CCPs and work as enablers for knowledge management (50). Developing process performance dashboards that act as enablers for statistical decision making is possible. Ideally AI can enhance the throughput during real time monitoring and predictive analytics, automated surface decontamination, defect detection during packaging, process optimization, automated EM, training simulation and smart CAPA implementation. This is a herculean task. By integrating the real-time and historical data points and personnel behaviour trends, the next challenge is to build a robust CCS strategy. A straightforward framework involves mapping all vulnerable unit operations, areas, and controls that could lead to non-compliance while providing real-time trend data for monitoring. Establishing performance metrics for each operator in core areas is required. Performance metrics coupled with analysing historical events aids in identifying root causes and assessing the effectiveness of corrective and preventive actions (CAPAs). Integrating data sets to compare actual practices with established procedures through real-time audio and video monitoring enhances oversight. Operators' movements and health status within Grade A/B facilities can be monitored using thermographic cameras, while infrared or optical sensing devices help regulate the number of personnel in critical areas. Environmental monitoring (EM) locations should be strategically determined based on room design, personnel movement, and airflow direction. Additionally, continuous improvements in isolator and equipment design can further enhance compliance and operational efficiency.

AI-powered algorithms must be designed to gather data within the 6M framework of the manufacturing processes and integrate data from disparate sources and formats, including sensor data, laboratory results, hypothesis testing and historical records. AI algorithms can then be used to build predictive manufacturing process models. As optimization progresses, AI algorithms learn from past iterations and refine their strategies to converge on optimal solutions more efficiently. Once optimized process parameters are identified, AI systems can continuously monitor manufacturing operations in real time to ensure that the process remains within specified limits. Sensor data and feedback from monitoring systems are fed back into the AI algorithms, allowing them to adjust to maintain optimal conditions and respond to changes or disturbances in the process environment. These algorithms use techniques

Contamination control strategies in aseptic operations

such as gradient descent, genetic algorithms, or reinforcement learning to search for the best set of parameters within the vast space of possible combinations. By leveraging AI-powered optimization algorithms, pharmaceutical companies can significantly improve manufacturing efficiency, leading to higher productivity, lower production costs, and better-quality products.

Future scope

The recent advancements in automation that reduced the process and product risks are discussed. Applications of novel automation devices for trending the behaviour, real time health and fatigue status of personnel in the core areas are presented. The role of AI in process optimization, continuous process improvement and implementing an effective CCS to minimize the risk of rework and/or recall is discussed.

A granular understanding of each of the processes is a pre-requisite for AI to percolate. Integration of the existing data libraries and refinement of the critical data is quite challenging. Yet, with technological upgrades, it must be possible to compound products without interventions in much smaller cleanrooms where the risk of contamination is considerably lower. Automation should be coupled with artificial intelligence (AI) to recognize and decontaminate vulnerable equipment surfaces. Such systems may take the support of real-time monitoring devices. Also, fully automated gloveless isolators can mitigate the risk of contamination.

Technological advancement aimed at reducing manual intervention, building accurate and rapid analytical methods, automatic alert systems, faster or automated screening of defects in primary packaging materials, filter membranes etc is due.

Current rapid test methods such as VITEK-2 systems are helpful in EM (61-65). This process is only indicative but needs to be more conclusive. Rapid detection and instant characterization of infected surfaces, such as finger dab tests, can be developed, but environmental flora challenges persist. The flora, along with mutant variants, may keep changing with seasons. Hence, detection is only probabilistic and not confirmed because data on such mutant strains may need to be updated. If the database is updated, the performance qualification needs to be redone. Such challenges prevail even with the support of AI.

Conclusion

A novel method of identifying the CCPs using the 6M framework is presented. Quality lapses in the CCPs leading to product recalls and/or warning letters are presented. Novel and emerging automation devices that find applications in reducing process / product risk are presented. Key areas where the support of AI and automation needs technological advancement are discussed. A guidance for integrating AI with existing processes is presented. This can very much help industry for building a robust CCS compliant with regulatory requirements.

Declarations of Interest

None

Declaration of Generative AI and AI assisted technologies in the writing process

None.

Contributors

All authors have contributed equally during the preparation of this manuscript.

Funding

Abbreviations used:

Active Pharmaceutical Ingredients: API

Air changes per hour: ACPH

Air handling unit: AHU

Annual product quality review: APQR

Artificial intelligence: AI

Aseptic process simulation: APS

Bacterial Endotoxin Test: BET

Bill of materials: BOM

Clean but not classified: CNC

Clean-In-Place: CIP

Colony forming units: cfu

Contamination control strategy: CCS

Corrective action & preventive action: CAPA

Critical control points: CCPs

Critical material attributes: CMAs

Critical process parameters: CPPs

Critical quality attributes: CQAs

Environmental Monitoring: EM

Finished Goods (FG)

Growth promotion tests: GPTs

Hazard Analysis Critical Control Point: HACCP

High density polyurethane: HDPE

High efficiency particulate air: HEPA

Human-machine interface: HMI

Institute of Environmental Sciences and Technology: IEST

Key performance indicators: KPIs

Laboratory information management system: LIMS

Laminar Air Flow: LAF

Large volume parenteral: LVP

Non-viable particulates: NVP

Not less than: NLT

Out of specification: OOS

Out of trend: OOT

Polypropylene: PP

Polyurethane Foam (PUF)

Process Analytical Technology: PAT

Programmable logical controls: PLCs

Quality management system: QMS

Quality by Design : QbD

Raw materials: RM

Restricted access barrier system: RABS

Relative Humidity: RH

Steam-In-Place: SIP

Uninterruptible Power Supply: UPS

User Requirement Specifications: URS

Water for Injection: WFI

References

1. Annex-1, Manufacture of Sterile Products, European Medicines Agency, Available at: https://health.ec.europa.eu/system/files/2022-08/20220825_gmp-an1_en_0.pdf.

2. ICH Q10, 2008, Pharmaceutical Quality System, Available at: https://database.ich.org/sites/default/files/Q10%20Guideline.pdf.

3. American Society for Quality, Fishbone Diagram, Available at: http://www.org/learn-about-quality/causeanalysis-tools/overview/fishbone.html.

4. Ishikawa, K., & Loftus, J. H. (1990). Introduction to Quality Control. Tokyo, Japan: 3A Corporation.

5. Liliana, L. (2016). A new model of Ishikawa diagram for quality assessment. In *Proceedings of the 20th Innovative Manufacturing Engineering and Energy Conference (IMANEE 2016)*, Kallithea, Greece, *IOP Conf. Ser. Mater Sci Eng, 161*, 012099.

6. ISPE GAMP 5. (2022). A Risk-Based Approach to Compliant GxP Computerized Systems (Second Edition). ISPE.

2344

7. ICH Q8, 2005–2008. Pharmaceutical Development, Available at: https://database.ich.org/sites/default/files/Q8%28R2%29%20Guideline.pdf.

8. WHO Technical Report Series No. 961, 2011, Annex 6. WHO Good Manufacturing Practices for Sterile Pharmaceutical Products. Available at: https://www.who.int/docs/default-source/medicines/norms-and-standards/guidelines/production/trs961-annex6-gmp-sterile-pharmaceutical-products.pdf.

9. WHO Technical Report Series No. 1044, 2022, Annex 2. WHO Good Manufacturing Practices for Sterile Pharmaceutical Products. Available at: https://www.who.int/publications/m/item/trs1044-annex2.

10. 21 CFR Part 210, 2005. Available at: http://www.accessdata.fda.gov/scripts/cdrh/cfdocs/cfcfr/CFRSearch.cfm?CFRPart=210.

11. 21 CFR Part 211, 2005. Available at: http://www.accessdata.fda.gov/scripts/cdrh/cfdocs/cfcfr/CFRSearch.cfm?CFRPart=211.

12. Eaton, T. (2019). Pharmaceutical Cleanroom Classification Using ISO 14644-1 and the EU GGMP Annex 1 Part 2: Practical Application. *Eur J Parenter Pharm Sci, 24*, 4. doi:10.37521/ejpps.24402.

13. International Standardization Organization. (2015). ISO 14644-1-2015: Cleanrooms and Associated Controlled Environments—Part 1: Classification of Air Cleanliness by Particle Concentration.

14. International Standardization Organization. (2015). ISO 14644-2-2015: Cleanrooms and Associated Controlled Environments—Part 2: Monitoring to Provide Evidence of Cleanroom Performance Related to Air Cleanliness by Particle Concentration.

15. International Standardization Organization. (2019). ISO 14644-3-2019: Cleanrooms and Associated Controlled Environments—Part 3: Test Methods.

16. International Standardization Organization. (2022). ISO 14644-4-2022: Cleanrooms and Associated Controlled Environments—Part 4: Design, Construction and Start-Up.

17. International Standardization Organization. (2004). ISO 14644-5-2004: Cleanrooms and Associated Controlled Environments—Part 5: Operations.

18. US Food and Drug Administration. (2004). Guidance for Industry: Sterile Drug Products Produced by Aseptic Processing—Current Good Manufacturing Practice. Available at: https://www.fda.gov/media/71026/download.

19. International Society for Pharmaceutical Engineering. (2018). ISPE Baseline Guide, Vol. 3, Sterile Product Manufacturing Facilities (3rd ed.). North Bethesda, MD: International Society for Pharmaceutical Engineering.

20. Sodec, F., & Halupczok, J. (1996). Qualitative Comparison of Clean Rooms with Different Air Distribution Systems. Report presented at the International Confederation of Contamination Control Societies Congress.

21. Bartz, H. (1990). Local Laminar Airflow Units with Temperature Gradients. Report presented at the International Confederation of Contamination Control Societies Congress.

22. Institute of Environmental Sciences and Technology. (2011). IEST-RP-CC003.4, "Garment System Considerations for Cleanrooms and Other Controlled Environments."

23. Jan Eudy. Fabric and Garment Testing for Cleanrooms, Flame Resistance, and Sterilization Compatibility. Available at: https://

www.agomat.com.ar/downloads/Fabric_and_Garment_Testing_for_Cleanrooms.pdf.

24. Ruchir, P. (2023). Aseptic Processing: Behaviours, Processes and Controls. Available at: https://www.ivi.int/wp-content/uploads/2023/02/Pansuriya-Ruchir_Aseptic-processing-behaviors-processes-and-controls.pdf.

25. USP <1116> Microbiological Control and Monitoring of Aseptic Processing Environments.

26. The Drugs and Cosmetics Act & Rules, Government of India, 2001. Available at: https://rajswasthya.nic.in/Drug%20Website%2021.01.11/Revised%20Schedule%20%20M%204.pdf.

27. 21 CFR Part 11, 2005. Available at: https://www.ecfr.gov/current/title-21/chapter-I/subchapter-A/part-11.

28. International Standardization Organization. (2002). ISO 1302:2002: Geometrical Product Specifications (GPS)—Indication of Surface Texture in Technical Product Documentation.

29. International Standardization Organization. (1996). ISO 3274:1996: Geometrical Product Specifications (GPS)—Surface Texture: Profile Method—Nominal Characteristics of Contact (Stylus) Instruments.

30. International Standardization Organization. (1997). ISO 4287:1997, Geometrical Product Specifications (GPS)—Surface Texture: Profile Method—Terms, Definitions and Surface Texture Parameters.

31. International Standardization Organization. (2011). ISO 4287:1997, ISO 16610-21:2011, Geometrical Product Specifications (GPS)—Filtration—Part 21: Linear Profile Filters: Gaussian Filters.

32. United States Pharmacopeia (USP) <1663 & 1664> Validation of Microbial Recovery from Pharmacopeial Articles.

33. International Standardization Organization. (1999). ISO 2859-1:1999, Sampling Procedures for Inspection by Attributes—Part 1: Sampling Schemes Indexed by Acceptance Quality Limit (AQL) for Lot-by-Lot Inspection.

34. PDA Technical Report No. 22 – Process Simulation for Aseptically Filled Products. (2011).

35. EN 1499. (2015). Chemical Disinfectants and Antiseptics. Hygienic Handwash. Test Method and Requirements (Phase 2/Step 2).

36. EN 1500. (2015). Chemical Disinfectants—Quantitative Carrier Test to Evaluate the Bactericidal Activity of a Hygienic Handrub Solution (Phase 2/Step 2).

37. Best, M., & Kennedy, M. E. (1992). Effectiveness of Handwashing Agents in Eliminating *Staphylococcus aureus* from Gloved Hands. *J Appl Bacteriol*, 73, 63–66.

38. Larson, E., Mayur, K., & Laughon, B. (1989). Influence of Two Handwashing Frequencies on Reduction in Colonizing Flora with Three Handwashing Products Used by Health Care Personnel. *Am J Infect Control*, 17, 83–88.

39. WHO Technical Report Series No. 992, 2015, Annex 4. TRS 992, Annex 4: General Guidance on Hold Time Studies. Available at: https://www.who.int/publications/m-item/trs992-annex4.

40. Sahu, P. K., Ramisetti, N. R., Cecchi, T., Swain, S., Patro, C. S., & Panda, J. (2018). An Overview of Experimental Designs in HPLC Method Development and Validation. *J Pharm Biomed Anal*, 147, 590-611. doi:10.1016/j.jpba.2017.05.006.

41. Galla, V. K., Jinka, R., & Sahu, P. K. (2020). Separate Quantification of Anastrozole and Letrozole by a Novel Stability-Indicat-

ing Ultra-Fast LC Method. *Sep Sci Plus*, 3, 294–305. doi:10.1002/sscp.202000018.

42. Parenteral Drug Association, PDA Technical Report 29: Points to Consider for Cleaning Validation, 2012. Available at: https://www.pda.org/bookstore/product-detail/1901-tr-29-revised-2012-cleaning-validation.

43. Lamei, R. S., & Asgharian, R. (2020). Evaluation of Swab and Rinse Sampling Procedures and Recovery Rate Determination in Cleaning Validation Considering Various Surfaces, Amount, and Nature of the Residues and Contaminants. *Iran J Pharm Res*, 19, 383-390. doi: 10.22037/ijpr.2020.1101173.

44. ICH Q3C(R6) on Impurities: Guideline for Residual Solvent, 2019. Available at: https://www.ema.europa.eu/en/documents/scientific-guideline/international-conference-harmonisation-technical-requirements-registration-pharmaceuticals-human-use_en-33.pdf.

45. Raval, J. S., Koch, E., & Donnenberg, A. D. (2012). Real-Time Monitoring of Non-Viable Airborne Particles Correlates with Airborne Colonies and Represents an Acceptable Surrogate for Daily Assessment of Cell-Processing Cleanroom Performance. *Cytotherapy*, 14, 1144-1150. doi: 10.3109/14653249.2012.698728.

46. United States Pharmacopeia (USP) <1227> Validation of Microbial Recovery from Pharmacopeial Articles.

47. Pharmaceutical Inspection Convention Scheme. Guidance on Parametric Release, 2007. Available at: https://picscheme.org/docview/3448.

48. United States Pharmacopeia (USP) <1222> Terminally Sterilized Pharmaceutical Products – Parametric Release.

49. Ohle, L. M., Ellenberger, D., Flachenecker, P., et al. (2021). Chances and Challenges of a Long-Term Data Repository in Multiple Sclerosis: 20th Birthday of the German MS Registry. *Sci Rep*, 11, 13340. doi:10.1038/s41598-021-92722-x.

50. Walid, E. A., & Shady, E. A. (2023). Advanced Data Analysis as an Enabler to Near Real-Time Contamination Control Strategy Evaluation. *GMP J*, 37, 14-23.

51. Fatih, E., Ali, Z. A., & Ahmet, E. C. (2015). A Robust System for Counting People Using an Infrared Sensor and a Camera. *Infrared Phys Technol*, 72, 127-134. doi:10.1016/j.infrared.2015.07.019.

52. Seshadri, D. R., Li, R. T., Voos, J. E., et al. (2019). Wearable Sensors for Monitoring the Physiological and Biochemical Profile of the Athlete. *npj Digit Med*, 2, 72. doi:10.1038/s41746-019-0150-9.

53. Drummond, C. K., Lewandowski, B., & Massaroni, C. (2022). Wearable Technology for Human Performance. *Front Physiol*, 13, 871159. doi:10.3389/fphys.2022.871159.

54. Trabelsi, Z., Alnajjar, F., Parambil, M. M. A., Gochoo, M., & Ali, L. (2023). Real-Time Attention Monitoring System for Classroom: A Deep Learning Approach for Student's Behavior Recognition. *Big Data Cogn Comput*, 7, 48. doi:10.3390/bdcc7010048.

55. Shijie, B., Chen, L., Yongwei, F., Yutian, R., Tongzi, W., Guann, P. L., & Bingbing, L. (2021). Machine Learning-Based Real-Time Monitoring System for Smart Connected Worker to Improve Energy Efficiency. *J Manuf Syst*, 61, 66-76. doi:10.1016/j.jmsy.2021.08.009.

56. Ocheja, P., Flanagan, B., Ueda, H., et al. (2019). Managing Lifelong Learning Records through Blockchain. *RPTEL*, 14, 4. doi:10.1186/s41039-019-0097-0.

57. Vishnu, S., Ramson, S. R. J., Rukmini,

M. S. S., & Abu, M. A. M. (2022). Sensor-Based Solid Waste Handling Systems: A Survey. *Sensors*, 22, 2340. doi:10.3390/s22062340.

58. Final GSR 823(E), Amendment in Rule 96 for Mandating Bar or QR Code on the Label of Top 300 Brands in Drugs Rules, Government of India. Available at: https://cdsco.gov.in/opencms/opencms/system/modules/CDSCO.WEB/elements/download_file_division.jsp?num_id=OTIwMg==.

59. Peng, L., Qingbin, L., & Pinyu, J. (2014). A Real-Time Temperature Data Transmission Approach for Intelligent Cooling Control of Mass Concrete. *Math Probl Eng*, 514606. doi:10.1155/2014/514606.

60. Medicines & Healthcare products Regulatory Agency (MHRA). (2018). 'GXP' Data Integrity Guidance and Definitions. Available at: https://assets.publishing.service.gov.uk/government/uploads/system/uploads/attachment_data/file/687246/MHRA_GxP_data_integrity_guide_March_edited_Final.pdf.

61. Ling, T. K., Liu, Z. K., & Cheng, A. F. (2003). Evaluation of the VITEK 2 System for Rapid Direct Identification and Susceptibility Testing of Gram-Negative Bacilli from Positive Blood Cultures. *J Clin Microbiol*, 41, 4705-4707. doi:10.1128/JCM.41.10.4705-4707.2003.

62. Funke G, Monnet D, deBernardis C, von Graevenitz A, Freney J. Evaluation of the VITEK 2 system for rapid identification of medically relevant gram-negative rods. J Clin Microbiol 1998;36:1948-52. doi: 10.1128/JCM.36.7.1948-1952.

63. Gavin PJ, Warren JR, Obias AA, Collins SM, Peterson LR. Evaluation of the Vitek 2 system for rapid identification of clinical isolates of gram-negative bacilli and members of the family Streptococcaceae. Eur J Clin Microbiol Infect Dis 2002;21:869-74. doi: 10.1007/s10096-002-0826-x

64. Hansen DS, Jensen AG, Nørskov-Lauritsen N, Skov R, Bruun B. Direct identification and susceptibility testing of enteric bacilli from positive blood cultures using VITEK (GNI+/GNS-GA). Clin Microbiol Infect 2002;8:38-44. doi: 10.1046/j.1469-0691.2002.00372.x.

65. Jossart MF, Courcol RJ. Evaluation of an automated system for identification of Enterobacteriaceae and nonfermenting bacilli. Eur J Clin Microbiol Infect Dis 1999;18:902-7. doi: 10.1007/s100960050429.

66. Farkas D, Madarász L, Nagy ZK, Antal I, Kállai-Szabó N. Image Analysis: A Versatile Tool in the Manufacturing and Quality Control of Pharmaceutical Dosage Forms. Pharmaceutics. 2021 May 10;13(5):685. doi: 10.3390/pharmaceutics13050685. PMID: 34068724; PMCID: PMC8151645.

Hydroxyapatite Doped with *Alpinia galanga* (L.) Willd. Rhizome Extract Exhibits Potential Antioxidant and Antibacterial Features

Seethalakshmi Subramaniam[1], Anusuya Nagaraj [1], Suja Samiappan[1,*]

[1] Department of Biochemistry, Bharathiar University, Coimbatore – 641 046, Tamil Nadu
*Corresponding Author: suja.s@buc.edu.in

Abstract

The study focused on doping of hydroxyapatite (HAp) with *Alpinia galanga* (L.) Willd. rhizome extract (Agr) to impart antioxidant and antimicrobial features to HAp by a green approach. The HAp was synthesized by sol-gel method using ortho-phosphoric acid and calcium nitrate tetrahydrate as precursors. The HAp was doped with Agr by the wet-precipitation method. The X-ray diffraction (XRD) showed that HAp and HAp-Agr biocomposite were crystalline. The FTIR study validated the successful impartation of Agr into HAp by confirming the presence of functional groups as alcoholic, phosphate, and carbonate groups in HAp-Agr biocomposite. The field emission scanning electron microscope analysis showed that HAp and HAp-Agr biocomposite were irregular and agglomerated. Moreover, energy dispersive X-ray (EDX) analysis showed the entrapment of phytomolecules of Agr into HAp-Agr biocomposite. The Zeta potential analysis revealed that HAp and HAp-Agr biocomposite were stable with −24.6 and -10.7 mV, respectively. The hydrodynamic size distribution of HAp and HAp-Agr biocomposite were 191.5 and 280.7 d. nm, respectively. The HAp-Agr biocomposite exhibited potential antioxidant activity, and its IC_{50} value (concentration required to scavenge 50% of free radicals) was 133.92 ± 4.08 and 141.24 ± 6.79 µg/mL in DPPH and ABTS assays, respectively. The HAp-Agr biocomposite exhibited a broad range of antibacterial activity against Gram-ve and Gram+ve bacteria by broth-dilution technique. This work highlighted that the as-synthesized HAp-Agr biocomposite had notable antioxidant and antibacterial characteristics and highly apt for biomedical application.

Keywords: Hydroxyapatite, *Alpinia galanga* (L.) Willd., antioxidant, antibacterial.

Introduction

The swift advancement of modern nanotechnology is broad and utilized in scientific fields, encompassing medical, health, environment, nanoelectronics, national security, etc. Nanotechnology enables the formulation and use of biological, physical, and chemical properties at the molecular or atomic level, particularly within nanoscale dimensions. The rapid progression of nanotechnology in medicine utilizes nanomaterials to monitor, treat, manage, diagnose, and prevent cellular damage induced by infections. Nanomedicine encompasses several biomedical applications, such as dental implants, wound healing, drug delivery, tissue engineering, and medical equipment. The principal aim of nanomedicine is to deliver therapy to the human body at atomic and molecular scales while safeguarding the integrity of healthy cells and tissues (1, 2, 3).

The chemical formula for hydroxyapatite (HAp) is $Ca_{10}(PO_4)_6(OH)_2$, presenting a calcium-to-phosphorus ratio of 1.67. HAp features a hexagonal crystalline structure. The purest form of the powder is white; nevertheless, naturally occurring varieties exhibit brown, yellow, or green types. Nano-hydroxyapatite is the most stable calcium phosphate compound across diverse temperatures, pH levels, and fluid compositions. HAp exhibits biocompatibility, osteoconductivity, bioactivity, non-toxicity, and a non-inflammatory nature. HAp is predominantly utilized in bone and dental enamel applications. HAp can be produced using various techniques, including dry, wet, high-temperature, combination, and biogenic synthesis. These synthesis methods may employ either chemical or naturally occurring precursors. HAp is synthesized from chemical compounds or derived from natural sources, such as animals, marine organisms, shells, plants, and algae. Synthesized HAp using chemical techniques exhibited a substantial surface area, increased porosity, and reduced crystallinity. Surface modification of HAp enhances its characteristics and optimizes its applications. Chemically produced HAp exhibits limited stability and durability, hence constraining its use in the biomedical field. The constraints of synthetically generated HAp prompted the utilization of natural precursors and biopolymers for its manufacture. HAp elicits no adverse reactions in humans, as it is a naturally occurring compound in the body. HAp has several applications, including bone tissue engineering, antimicrobial uses, anticancer therapies, dental implants, bioimaging, and water purification. In bone tissue engineering, HAp is utilized to synthesize new bone tissue and repair bone. The use of HAp in cancer treatment can eradicate neoplastic cells. The doped HAp compositions showed enhanced efficacy in eliminating cancer cells. The production of HAp from chemical or natural sources, including mammalian bones, shells, minerals, and metal ion-doped variants (such as iron, zinc, copper, silver, gold, cerium, and magnesium), demonstrates an inhibitory effect against bacteria (4, 5).

The HAp in dental enamel serves to prevent and reverse cavities, diminish sensitivity, whiten teeth, and ensure non-toxicity and biocompatibility. In several sectors, HAp is extensively utilized in cosmetic applications to enhance skin firmness. It is now used as a hair care product to improve strength and nourish the hair. HAp is used in sunscreen to mitigate UV damage and photoaging. Consequently, HAp is seen as a safer and environmentally beneficial option. Biosynthesized HAp is a potent component with many uses and significant advantages in skeletal, hair, cosmetic, dental, water treatment, and pharmaceutical delivery contexts (6).

Recently, significant attention has been focused on doping HAp with plant extracts. Plants are rich in bioactive substances such as polyphenols, flavonoids, terpenoids, and alkaloids. These substances could exhibit properties such as antibacterial, anti-inflammatory, antioxidant, and potentially osteogenic effects (7, 8). The composite formed by incorporating plant bioactive chemicals into HA may exhibit properties such as antibacterial effects, anti-inflammatory responses, and the promotion of osteoblastogenesis (9, 10).

The present study is focused on the preparation of a composite of HAp with *A. galanga* (L.) Willd. rhizome extract and examine their antioxidant and antibacterial properties. The *Zingiberaceae* family, encompasses *A. galanga* (L.) Willd., also commonly known as galangal or greater galangal, is classified as a perennial plant. This spice is prominently utilized in Indonesian and other Southeast Asian cuisines. This plant is highly significant and is widely employed in traditional medicine in several countries, especially within India's Ayurvedic medicinal system. In Asia, these rhizomes have historically been employed as spices and flavoring agents because of their strong, fragrant fragrances and piquant flavor. A renowned traditional Chinese medication, they have been widely utilized to address gastrointestinal ailments such as indigestion,

Hydroxyapatite doped with *Alpinia galanga* (L.) Willd. rhizome extract exhibits potential antioxidant and antibacterial features

gastro-cold vomiting, and abdominal pain. *A. galanga* (L.) Willd. rhizome extract rich with pharmacologically active compounds like β-turmerone, α-turmerone, and cymene (11).

In this study, HAp was prepared by sol-gel method and followed by incorporated with *A. galanga* (L.) Willd. rhizome extract by wet-precipitation method. The HAp and HAp-*A. galanga* (L.) Willd. rhizome extract (HAp-Agr) biocomposite was characterized by nanotechnology approaches. Following, the antioxidant and antibacterial potential of the HAp-Agr biocomposite was demonstrated.

Materials and Methods
Chemicals and reagents

Muller-Hinton agar (MHA), tetracycline, DPPH, ethanol, ABTS, ortho-phosphoric acid (O-PA), ammonia, potassium persulfate, Muller-Hinton broth (MHB), ascorbic acid, methanol, tryptic soy broth, saline, nutrient broth, sodium hydroxide, and calcium nitrate tetrahydrate (CNT) were received from HiMedia, Mumbai, India. The other chemicals and reagents in the study were analytical grade and obtained from Merck, Bengaluru, India. The plasticware was obtained from Tarsons Products, Kolkata, India.

Collection and preparation of plant extract

The fresh rhizomes of *A. galanga* (L.) Willd. were collected from the agriculture market in Coimbatore, India. The rhizomes of *A. galanga* (L.) Willd. were dried for three weeks at room temperature under dark. The dried rhizomes of *A. galanga* (L.) Willd. were ground into powder using the blender. Fifty grams of fine powder were immersed in 250 mL of hydroethanolic at ambient temperature and agitated in a shaker for three days, adopting the cold maceration technique (12). Following this, the hydroethanolic solution was filtered through the Whatman no. 1 filter paper, and the filter was collected. Then, the obtained filtrate was lyophilized at -39°C and concentrated the filtrate. The collected *A. galanga* (L.) Willd. rhizome extract (Agr) was stored at 4°C for further analysis.

Synthesis of HAp and HAp-Agr biocomposite

The *HAp* was prepared using the sol-gel technique (10). The precursor compounds for calcium and phosphate are calcium nitrate tetrahydrate and orthophosphoric acid, respectively. Double distilled water was utilised to make 1 M calcium nitrate tetrahydrate and 0.6 M orthophosphoric acid, each agitated separately for 30 minutes. The orthophosphoric acid solution was added dropwise to the calcium nitrate tetrahydrate solution. The precipitated solution was agitated vigorously for one hour following its introduction. A pH of 10 was maintained, and the solution was kept for 24 hours aging. The precipitate was dried below 200°C in the oven for 6 hours. The obtained product was subjected to furnace treatment for 3 hours at temperatures varying from 300°C to 900°C.

The hydroxyapatite and rhizomes of *A. galanga* (L.) Willd. rhizome extract (HAp-Agr) biocomposite was prepared by the wet-precipitation process (10). In the first step, the equal ratio of HAp and Agr was stirred overnight at 80 rpm in 50 mL of ethanol solution, which confirms an equal mixing of the materials. After that, the precipitated solution was obtained and dried for 24 hours at 35°C in an oven. Finally, the dried sample was ground into a fine powder and sieved.

Characterization of HAp and HAp-Agr biocomposite

To comprehend the crystallinity and phase analysis of the prepared materials, electron-based X-ray diffractometry (XRD) was typically employed. The prepared materials (HAp and HAp-Agr biocomposite) were scanned in the 2theta ranges from 10° to 80° using steps of 0.06° and 10 s of counting time utilizing the diffractometry analysis. The data were then recorded using a Bruker Eco D8 XRD diffractometer (Berlin, Germany) that used Cu-Kα radiation and operated at 40 kV and 25 mA.

The peak locations and intensities are compared with the support of JCPDS (09-432) reference patterns to figure out particle crystallinity (9, 10).

Fourier transform infrared (FTIR) spectroscopy (Shimadzu, Tokyo, Japan) was used to identify the capping and reducing agents as well as the available functional groups in the produced HAp, Agr, and HAp-Agr biocomposite. To acquire the spectrum spanning the 400–4000 cm^{-1} wavelength range, the prepared samples were compressed for two minutes onto a 2-mm disk after being mixed 1:100 with potassium bromide (9, 10).

A field emission scanning electron microscopy (FESEM) with the model name of FEI Quanta 250 FEG-SEM (Thermo Fisher Scientific, USA) was used to investigate the particles' (HAp and HAp-Agr biocomposite) morphological shape and size with the maximum accelerating and operating voltage of 30 kV. The samples were coated with gold sputter coating before image capture. The samples' chemical composition was also recorded in energy dispersive X-rays (EDX) analysis combined with the same microscopy (9, 10).

Similar surface electric charges cause electrostatic repulsion, which makes the dispersion more stable, where the particles are less prone to agglomerate. A measurement of the electric charge at the particle's surface, called zeta potential, is frequently used to evaluate its stability. To determine the average zeta potentials, the prepared samples (HAp and HAp-Agr biocomposite) were dispersed and taken to the Zetasizer with a 60-second analysis period. Further, the samples' hydrodynamic diameter range and polydispersity index (PdI) were measured using dynamic light scattering (DLS) at 25°C with a scattering angle of 90° (Malvern Instruments Ltd, Malvern, United Kingdom) (9, 10).

Antioxidant activity of HAp-Agr biocomposite
DPPH assay

As-synthesized HAp-Agr biocomposite was collected at different concentrations (up to 300 μg/mL), and the volume was standardised to 100 μL using methanol. Approximately 3 mL of a 0.1 mM methanolic solution of DPPH was introduced to the aliquots of HAp-Agr biocomposite and thoroughly vortexed. Ascorbic acid was utilized as the standard. A negative control was established by incorporating 100 μL of methanol into 1 mL of a 0.1 mM methanolic DPPH solution. The tubes were let to remain in the dark for 15 minutes at ambient temperature. The sample's absorbance was measured at 517 nm relative to the blank. The radical scavenging activity of the samples was quantified as IC$_{50}$, representing the concentration necessary to block 50% of DPPH free radicals concentration (Gunti (13).

ABTS assay

The overall antioxidant activity of the HAp-Agr biocomposite was assessed using the ABTS radical cation decolorisation test. ABTS^{*+} was generated by incubating a 7 mM aqueous solution of ABTS with 2.4 mM potassium persulfate in the dark for 12 to 16 hours at ambient temperature. Before the experiment, this solution was diluted in ethanol (about 1:89, v/v) and equilibrated at 30°C, resulting in an absorbance of 0.700 ± 0.02 at 734 nm. Following the addition of 1 mL of diluted ABTS^{*+} solution to 100 μL of different concentrations of HAp-Agr biocomposite (up to 300 μg/mL). Following, test samples were thoroughly vortexed and incubated in darkness for 30 minutes at room temperature. The standard was ascorbic acid. The absorbance was recorded against the blank at 734 nm (14).

Antibacterial activity of HAp-Agr biocomposite
Minimum inhibitory concentration (MIC)

The antibacterial activity of HAp-Agr biocomposite was tested against Gram-ve bacteria (*Pseudomonas aeruginosa* – MTCC 741, *Escherichia coli* – MTCC 1302, and *Salmonella typhimurium* – MTCC 1254) and Gram+ve bacteria (*Staphylococcus aureus* –

MTCC 740, *Streptococcus pyogenes* – MTCC 0442, and *Bacillus subtilis* – MTCC 1133). To determine the antibacterial effectiveness of HAp-Agr biocomposite, the standard broth dilution method (CLSI M07-A8) was utilized, and it supports the assessment of the visible growth of microbes in the broth (15). Briefly, after the various pure Gram-positive and Gram-negative bacterial cultures had grown overnight distinctly in nutrient broth. The growth density was adjusted to the 1×10^8 CFU/mL concentration using the 0.5 McFarland standard.

First, the microplate wells were filled with 100 µL of Muller Hinton broth (MHB), and then the same volume with different concentrations of HAp-Agr biocomposite (up to 600 µg/mL) was added. Negative control wells without HAp-Agr biocomposite. The positive control is tetracycline. Next, all the wells aside from the negative control well were filled with distinctly 5 µL of bacterial cultures. At OD_{600}, the initial and final spectrum values were obtained before and after incubation (24 hrs). The Synergy H1 plate reader (BioTek, USA) was used to record bacterial growth. The MIC value was predicted by the lowest concentration of HAp-Agr biocomposite, at which no bacterial growth was noticeably present (16).

Minimum bactericidal concentration (MBC)

The Muller Hinton agar (MHA) plates were utilized to assess the MBC of HAp-Agr biocomposite. About 50 µL aliquots were collected from the MIC value (no evident bacterial growth) wells and placed on MH agar plates. They were then incubated for 24 hours at 37°C. Based on visual inspection, the MBC endpoint was identified by the HAp-Agr biocomposite concentration that minimized or killed the bacterial population at ≥ 99.9%. The pre- and post-incubated MHA plates were used to make this observation on the presence or absence of bacteria (17).

Statistical analysis

Three separate runs of the experiment

were conducted for antioxidant and antibacterial studies, and the mean ± standard deviation was used to represent the results. One-way ANOVA was used to process the data, and $p < 0.05$ was considered significant.

Results and Discussion

Synthesis and characterization of HAp and HAp-Agr biocomposite

The sol-gel method was used in this study to successfully synthesize HAp using CNT and PA as precursors. After thoroughly washing the synthesized HAp with distilled water to remove NH_4 and NO_3, it was successfully calcined at 900°C. Following this, HAp was doped with Agr using the wet-precipitation method. The resulting combination was dried at 35°C and used for characterization.

XRD analysis

Powder X-ray diffraction (XRD) is a reliable method for determining the compounds' natural phase. With the support of XRD analysis, the sol-gel synthesized HAp and precipitated HAp-Agr biocomposite intense diffractogram patterns as a function of 2θ value are shown in Figure 1. Also, Table 1 presents the respected *hkl* plane numbers of HAp and HAp-Agr biocomposite.

The HAp patterns are initially characterized by distinct and emphasized peaks. The acquired diffracted reflection planes are subjected to HAp, and their hexagonal structure both were proved following the International Centre for Diffraction Data (ICDD) card number [09-0432]. HAp displays a narrow, high, or intense peak, indicating a high degree of crystallinity, and it was found in the distinctive peak at 2theta of 31.28 °C. The study by Niziołek et al. likewise showed a similar pattern of results (18).

In HAp-Agr biocomposite, the recorded characteristic peaks were narrow and intense, and they were recognized to have a similar 2theta range to HAp. Additionally, there were no extra

peaks, and the results from both samples (HAp and HAp-Agr biocomposite) showed that only the crystalline phase was present. However, there was a slight shifting in the diffraction patterns with reduced intensity (low crystalline); it might be due to the phytometabolites' occupation within the HAp pattern, which does not affect its stability (9). Similarly, the green biosynthesized hydroxyapatite-silver nanocomposite mediated by aqueous Indian curry leaf (*Murraya koengii*) extract was characterized by Bee et al. (19). They observed the changes in the slight degree of silver substitution in the apatite lattice during the bio-reduction process that lowers the crystallinity of HAp. Additionally, they showed that the destabilization of HAp was unaffected by the absence of any new peak calcium phosphate phase in the XRD pattern of nanocomposite samples produced by the curry leaf-mediated bio-reduction method.
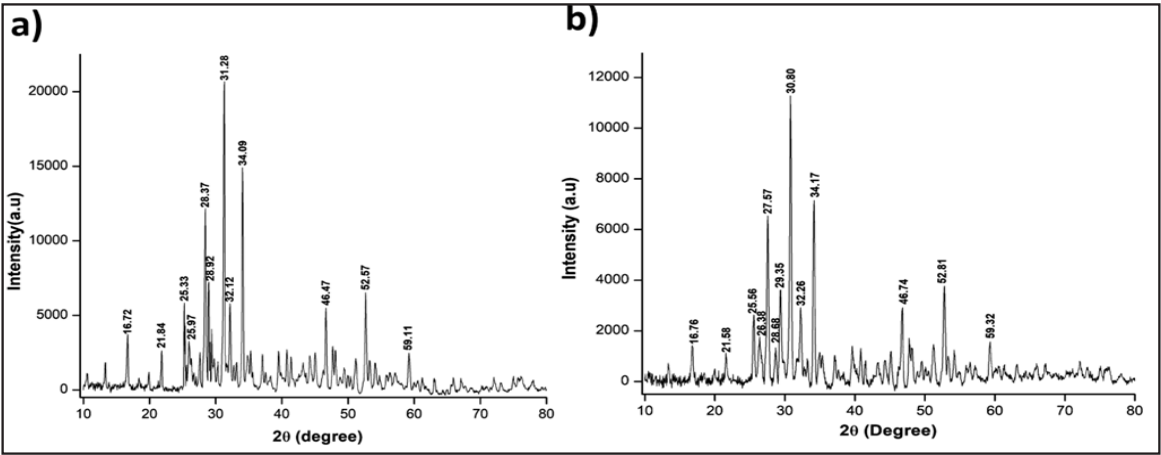
Figure 1: XRD pattern of (a) HAp and (b) HAp-Agr biocomposite.

Table 1: X-ray diffractometric 2theta angle with *hkl* plane numbers for HAp and HAp-Agr biocomposite.

hkl plane number	2theta angle	
	HAp	HAp-Agr biocomposite
101	16.72	16.76
200	21.84	21.58
201	25.33	25.56
002	25.97	26.38
102	28.37	26.68
210	28.92	29.35
211	31.28	30.8
112	32.12	32.26
202	34.09	34.17
222	46.47	46.47
402	52.57	52.81
420	59.11	59.32

FTIR analysis

The characteristic group of frequencies found in a sample provides insight into the nature and purity of the substance. FTIR analysis is an effective and ideal analytical technique used to determine the functional groups and chemical structures of inorganic and organic phases.

According to Figure 2a, the distinctive peaks of HAp are responsible for all of the peaks observed in the FTIR spectra. The peaks are indicative of the symmetric stretching of the O-H group in HAp and can be caused by the presence of absorbed moisture. They appear in the wavenumbers 3438.56, 2922.85 cm^{-1}, and 2084.71 cm^{-1}. The symmetric stretch 1643.59 cm^{-1} may result from carbon dioxide absorption from the atmosphere. Furthermore, PO_4 groups were detected in the synthetic HAp at the distinctive peak 1038.05 cm^{-1} (stretching

of P–O bond), which is very much alike to those seen in naturally occurring hydroxyapatite. The O-P-O group's asymmetric bending modes were shown by the absorption spectral band in the 584.89 cm^{-1} wavenumber. The majority of the PO$_4^{3-}$ group was located in the 400–600 cm^{-1} range of overlapping spectral bands. Thus, it was verified that the manufactured material is HAp based on this functional group observation; additionally, it was remarkably comparable to the results of the previously published studies (20, 21).

The active functional groups from a *Zingiberaceae* family of *A. galanga* (L.) Willd. Rhizome extract's (Agr) phytometabolites were determined using FTIR spectroscopy and are displayed in Figure 2b. The characteristic stretching spectrum length beyond 3000 cm^{-1} is responsible for free hydroxyl groups, which are characteristics of phenolic compounds. The sharp asymmetric absorption band at 2979.07 cm^{-1} indicates the presence of triterpenoids and saponin compounds with C–H stretching of the aliphatic functional group. While the spectral peak at 2895.32 cm^{-1} showed asymmetric and symmetric stretches of alkenes. The vibrational C≡N stretching was found in the 2590.63 cm^{-1} spectral length of the nitrile group of compounds. Absorption at 2333.81 and 1674.99 cm^{-1} represents the vibrational stretching of the C=C group in the aromatic compounds, and at 1404.60 cm^{-1} shows the vibrational bending S=O (sulphate ester) group. The carbonyl group of compounds was found to form a C-O bond at a wavenumber of 1134.22 cm^{-1}. The fingerprint regions of 939.60 cm^{-1} (O-H), 808 cm^{-1} (=CH), and overlapping peaks (579.09 and 503.31 cm^{-1}) of the C=C group of compounds were identified as carboxylic, aromatic, and alkynes, respectively. The ether functional group was visible in the strong absorption bending spectra at 1036.91 cm^{-1}. It was significantly supported by comparing the active functional groups of Agr using the study results of Imchen et al. and Ahmad et al. (22, 23).

In the case of HAp-Agr biocomposite

(Fig. 2c), the stretching and bending modes of absorption peaks were identified at 3718.46, 3426.75, 2970.04, 2692.41, 2347.53, 1696.08, 1520.90, 1030.56, and 646.57 cm^{-1}. Also, the IR spectra were obtained using the combined group of HAp and Agr compounds with decreased intensity. Additionally, a shift in the HAp-Agr biocomposite absorption peaks was found, which may be the result of a structural change brought by the functional groups of Agr's active secondary metabolite on the HAp surface. The Agr may also serve as a reducing, stabilizing, and capping agent during the formation of HAp-Agr biocomposite. These encouraging results made it abundantly evident that HAp and Agr had a positive interaction during the composite synthesis process. The findings were highly comparable to those of the Wei et al. study (24). Another work by Das and colleagues reported that, in comparison to synthetic HAp alone, the IR spectrum of simple green synthesized HAp nanoparticles showed altered absorption peaks, indicating a significant interaction between HAp and polydomaine (20).
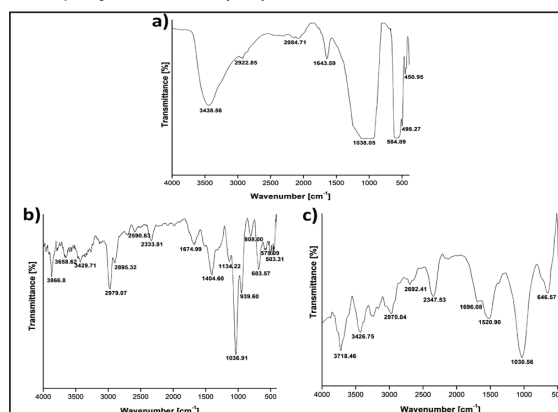
Figure 2: FTIR spectra of (a) HAp, (b), Agr, and (c) HAp-Agr biocomposite.

FESEM analysis

The HAp and HAp-Agr biocomposite morphological shapes are shown in Figure 3. The majority of the HAp particles exhibited irregular faceted shapes with joined boundaries of one crystal to another crystal, according to

the results. The distribution and shape of HAp particles in the composite were made with Agr through the action of adsorption. Still, this covering (adsorption) property of Agr did not affect the morphologies of the HAp particles. Rather, the HAp-Agr biocomposite exhibited an agglomerated cluster-like morphological structure, indicating that only the particles' aggregation and distribution into the HAp are altered.

In addition to morphological observation, Image J software was used to analyze the homogeneity and uniformity of particle dispersion in the studied samples. By counting several approximation particles (50-70), the average size distribution of the manufactured materials was determined to be 227.21 nm (HAp) and 397.99 nm (HAp-Agr biocomposite), respectively, as shown by the histogram (Fig. 4). Because of the particles' propensity to aggregate, the average size of HAp-Agr biocomposite is larger than that of HAp. A similar finding was made by Namasivayam et al., which shows that the average size of free hydroxyapatite nanoparticles is less than that of the triphala-loaded hydroxyapatite nanocomposite, and they postulated that this could be because of the appearance of floccular aggregated particles (25).

EDX analysis

The atomic weight and chemical makeup of virgin HAp, Agr, and HAp-Agr biocomposite were ascertained via energy-dispersive spectrum analyses (Fig. 5 and Table 2). The primary presence of calcium, phosphorous, and oxygen in HAp is shown in Figure 5a. The EDX spectral graph of Agr showed with carbon and oxygen peaks are depicted in Figure 5b. Moreover, the available concentration of carbon in the HAp-Agr biocomposite, together with calcium, phosphorous, and oxygen, was seen in Figure 5c. Thus, as can be seen from the graph, the blended phytomolecules of Agr have been encapsulated with HAp. As a result, FESEM and EDS spectra suggest that HAp and Agr are co-deposited in HAp-Agr biocomposite. According to a study by Vinayagam et al. the HAp formation was shown in the EDX results, where the peaks for calcium, phosphorous, and oxygen were visible. The elemental composition also showed the presence of carbon, which is likely due to the phytochemicals used in the synthesis of *Muntingia calabura*-hydroxyapatite nanoparticles (26).

Figure 5: EDX spectra of (a) HAp, (b) Agr, and (c) HAp-Agr biocomposite.

Figure 3: SEM image of (a) HAp and (b) HAp-Agr biocomposite.
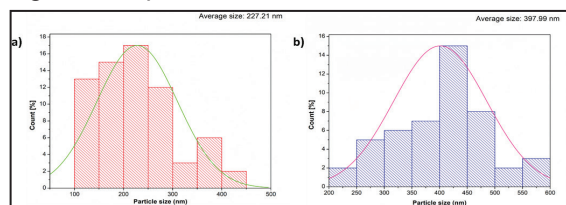
Figure 4: SEM size distribution of (a) HAp and (b) HAp-Agr biocomposite.

Table 2: Chemical composition of HAp, Agr, and HAp-Agr biocomposite by EXD analysis

Elements	HAp	Agr	HAp-Agr biocomposite
Ca (%)	38.01	—	11.91
P (%)	13.16	—	10.57
O (%)	47.62	27.14	35.02
C (%)	—	70.95	40.57
Total (%)	98.79	98.09	98.07

Zeta potential analysis

Zeta potential can indicate the potential physical stability of the materials prepared under different conditions. The HAp and HAp-Agr biocomposite surface charge and stability features were investigated by measuring their zeta potential values, which are shown in Figure 6. The zeta potential values for HAp and HAp-Agr biocomposite were found to be −24.6 and -10.7 mV, respectively. This value serves as a crucial parameter in assessing the dispersion status and surface charge of the particles because the particles have their electrostatic repulsion, which denotes they are sufficiently strong to maintain their stability. Comparing a coherent result with the Zeta potential of the produced amorphous calcium phosphate family using *Aloe vera* extract, the measurement was −28.7 mV, which is like our study findings (27).
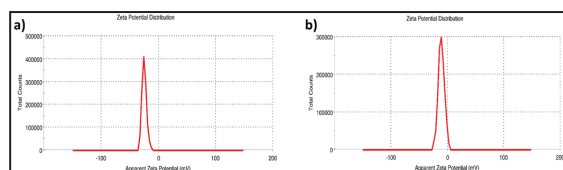
Figure 6: Zeta potential of (a) HAp and (b) HAp-Agr biocomposite.

DLS analysis

The DLS method was used to investigate the particle size distribution of HAp and HAp-Agr biocomposite. The hydrodynamic mean size of HAp and HAp-Agr biocomposite was found to be 191.5 and 280.7 d. nm, respectively (Fig. 7), and this is related to the findings of the FESEM study. Since PDI values below 0.5 are suggestive of monodispersity particles, the polydispersity index (PDI) values of 0.186 (HAp) and 0.719 (HAp-Agr biocomposite) indicated the material's polydisperse nature (28). The supporting study by Abdelmigid and colleagues found that HAp nanoparticles made from *Punica granatum L.* peel, along with the coffee ground extract, had a higher zeta potential negativity of −9.37 mV and -16.9 mV, and the smallest size with 229.6 nm and 167.5 nm, respectively (29).

As a result, the produced materials (HAp and HAp-Agr biocomposite) might offer a superior solution in orthopedics. Even Sathiyavimal et al. recently stated that HAp's clinical trial has validated its potential for use as a coating material over orthopedic implants, and research is currently concentrating on HAp in the development of composites for increased strength and efficiency (30).
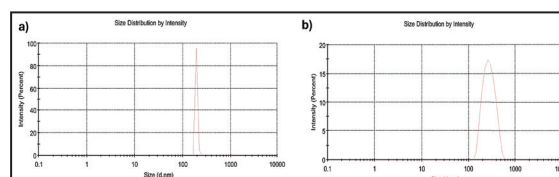
Figure 7: DLS spectra of (a) HAp and (b) HAp-Agr biocomposite

Antioxidant activity of HAp-agr biocomposite

For biomedical applications, improved HAp's capacity to fend off oxidative stress is essential. Osteointegration can be enhanced, and inflammation can be avoided by lowering ROS at the implant-tissue interface. Despite being biocompatible, hydroxyapatite has little intrinsic antioxidant capacity. According to the findings, doping HAp with elements like as cobalt, selenium, silver, zinc, copper, and plant extracts can help overcome these drawbacks by boosting antioxidant activity, enhancing biocompatibility, and possibly supporting medicinal uses (9, 10, 31).

In our study, as-synthesized HAp was doped with *A. galanga* (L.) Willd. rhizome extract by wet-precipitation method and prepared HAp-Agr biocomposite. The antioxidant activity of as-synthesized HAp-Agr biocomposite was assessed by DPPH and ABTS assays. The HAp-Agr biocomposite showed dose-dependent free radical scavenging potential in both DPPH and ABTS free radical scavenging assays (Fig. 8). The IC_{50} value of The HAp-Agr biocomposite was determined as 133.92 ± 4.08 and 141.24 ± 6.79 μg/mL in DPPH and ABTS free radical scavenging assays, respectively.
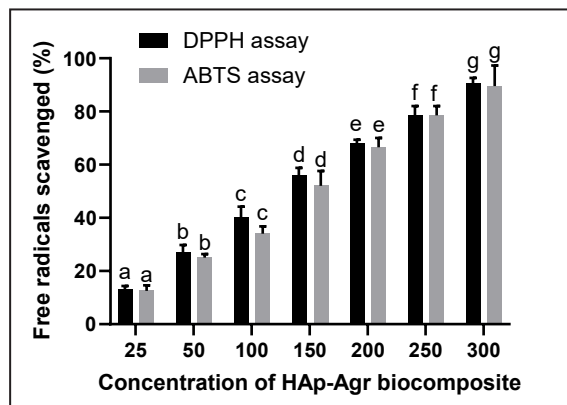
Figure 8: Dose-dependent antioxidant potential of HAp-Agr biocomposite by DPPH and ABTS assay. HAp-Agr biocomposite's dose-dependent antioxidant capability using the DPPH and ABTS assays. Three separate runs of the experiment were conducted, and the mean ± standard deviation was used to represent the results. One-way ANOVA was used to process the data, and $p < 0.05$ was considered significant. The specific study (DPPH or ABTS free radical assay) uses different alphabetical letters to indicate the statistical significance between the various test concentrations of the HAp-Agr biocomposite by Tukey's test.

The HAp doped with metals such as cobalt, copper, zinc, and selenium, as well as plant extracts, introduces redox-active sites that can scavenge free radicals and reduce oxidative stress. This process improves electron transport to counteract free radicals and shield cells from harm caused by ROS (32). The performance of implants and tissue regeneration may be improved by combining the antioxidant HAp with other bioactive substances, such as growth factors. Thus, doping of HAp with plant extracts is quite useful as an oxidative stress reliever in the biomedical field (9, 10, 31).

Antimicrobial activity of HAp-Agr biocomposite

Pure HAp has no antimicrobial activity, which is problematic for implants because bacterial infections (such as biofilm formation) can cause implants to fail. The antimicrobial effectiveness of HAp can be increased by doping it with metal ions and plant extracts (33).

However, from the standpoint of biocompatibility, doping HAp with metals is not ideal because it has drawbacks and causes organ toxic effects. Doping HAp with plant extracts, which frequently include natural antimicrobial components, is therefore very ideal and is a recent method to improve its antimicrobial activities while preserving biocompatibility (9, 10).

In our study, as-synthesized HAp-Agr biocomposite through a green chemistry approach has shown potential antimicrobial activity against bacterial pathogens by micro-well dilution technique (Table 3). HAp-Agr biocomposite showed potential antibacterial activity on Gram-ve and Gram+ve bacteria. However, HAp-Agr displayed potentially more significant antimicrobial activity on Gram-ve related to Gram+ve bacteria. Because of their distinct cell wall structure, HAp-Agr biocomposite demonstrated greater antimicrobial action against Gram-negative bacteria. Gram-negative bacteria are particularly vulnerable to damage from HAp-Agr biocomposite because of their thin peptidoglycan layer and lipopolysaccharide outer membrane. The superior antibacterial activity of HAp-Agr biocomposite was observed against Gram-ve bacteria *Pseudomonas aeruginosa* – MTCC 741 with MIC and MBC values of 340.68 ± 12.06 and 428.94 ± 10.71 µg/mL, respectively. The lower antibacterial activity of HAp-Agr biocomposite was observed against Gram+ve bacteria *Bacillus subtilis* – MTCC 1133 with MIC and MBC values of 496.27 ± 18.57 and 620.55 ± 17.24 µg/mL, respectively.

Table 3: The antibacterial potential of HAp-Agr biocomposite by broth-dilution technique.

Bacteria	MIC (µg/mL)	MBC (µg/mL)
Gram-negative bacteria		
Pseudomonas aeruginosa – MTCC 741	340.68 ± 12.06	428.94 ± 10.71
Escherichia coli – MTCC 1302	372.22 ± 11.84	434.09 ± 14.33
Salmonella typhimurium – MTCC 1254	381.81 ± 12.02	468.26 ± 18.07

Gram-positive bacteria		
Staphylococcus aureus –MTCC 740	470.66 ± 13.68	568.89 ± 21.41
Streptococcus pyogenes – MTCC 0442	483.23 ± 14.71	610.35 ± 18.90
Bacillus subtilis – MTCC 1133	496.27 ± 18.57	620.55 ± 17.24

According to the researchers, bioactive substances such as polyphenols, flavonoids, and terpenoids found in plant extracts have antimicrobial qualities through rupturing bacterial cell membranes, preventing enzyme activity, or obstructing bacterial DNA replication (34, 35, 36). As a result, adding plant extracts to HAp may provide antimicrobial properties. Additionally, doping HAp with plant extracts provides a sustainable and environmentally acceptable substitute for metal doping (9, 10). According to our research, HAp-Agr produced using a green chemistry method is appropriate for orthodontic applications where bacterial infections may cause issues.

Conclusion

The HAp was successfully prepared using the sol-gel approach. The phytomolecules of Agr were imparted into the HAp by wet-precipitation method and fruitfully synthesized HAp-Agr biocomposite. The nanotechnological analysis showed that the as-synthesized HAp-Agr biocomposite was stable, had nano size, crystalline nature, had an irregular shape, and was agglomerated. As-synthesized HAp-Agr biocomposite exhibited potential antioxidant activity under *in-vitro*. Moreover, HAp-Agr biocomposite exhibited a broad range of antibacterial activity against Gram-ve and Gram+ve bacteria. Thus, the study concluded that antioxidant and antibacterial properties were successfully imparted into the HAp from Agr. As-synthesized HAp-Agr biocomposite could be highly applicable as an antioxidant and antimicrobial agent in the orthopaedic field.

Conflict of interest

Authors declare no conflict of interest

References

1. Salamanca-Buentello, F., and Daar, A. S. (2021). Nanotechnology, equity and global health. *Nature Nanotechnology*, 16(4), 358-361.

2. Rosaiah, G., Mangamuri, U. K., Sikharam, A. S., Devaraj, K., Kalagatur, N. K., Kadirvelu, K., and Vardhan, S. V. M. (2022). Biosynthesis of selenium nanoparticles from *Annona muricata* fruit aqueous extract and investigation of their antioxidant and antimicrobial potentials. *Current Trends in Biotechnology and Pharmacy*, 16(1), 101-107.

3. Lakshmeesha, T. R., Murali, M., Ansari, M. A., Udayashankar, A. C., Alzohairy, M. A., Almatroudi, A., Alomary, M. N., Asiri, S. M. M., Ashwini, B. S., Kalagatur, N. K., Nayak, C. S., and Niranjana, S. R. (2020). Biofabrication of zinc oxide nanoparticles from Melia azedarach and its potential in controlling soybean seed-borne phytopathogenic fungi. *Saudi Journal of Biological Sciences*, 27(8), 1923-1930.

4. Noori, A., Hoseinpour, M., Kolivand, S., Lotfibakhshaiesh, N., Ebrahimi☐Barough, S., Ai, J., and Azami, M. (2024). Exploring the various effects of Cu doping in hydroxyapatite nanoparticle. *Scientific Reports*, 14(1), 3421.

5. Liu, Y., Wang, Z., Liu, X., Chen, H., Huang, Y., Li, A., Pu, Y., and Guo, L. (2025). Study on Mechanical Properties, Optical Properties, Cytotoxicity of TiO_2-HAP Nanoparticles-Modified PMMA and Photodynamically Assisted Antibacterial Activity Against *Candida Albicans* in Vitro. *International Journal of Nanomedicine*, 2695-2709.

6. Carella, F., Degli Esposti, L., Adamiano, A., and Iafisco, M. (2021). The use of calcium phosphates in cosmetics, state of the art and future perspectives. *Materials*, 14(21), 6398.

7. Kondabolu, U. L., Babitha, B., Kalagatur, N. K., Nagaraj, A., and Velumani, S. (2023). Phytochemical Analysis in *Pithecellobium dulce* Fruit Peel Extract. *Current Trends in Biotechnology and Pharmacy*, 17(3), 1052-1059.

8. Sathelly, K., Kumar Kalagatur, N., Kiranmayi Mangamuri, U., Obul Reddy Puli, C., and Poda, S. (2022). Anticancer potential of *Solanum lycopersicum* L. extract in human lung epithelial cancer cells A549. *Indian Journal of Biochemistry and Biophysics (IJBB)*, 60(1), 76-85.

9. Nagaraj, A., Kalagatur, N. K., Kadirvelu, K., Shankar, S., Mangamuri, U. K., Sudhakar, P., and Samiappan, S. (2022). Biomimetic of hydroxyapatite with Tridax procumbens leaf extract and investigation of antibiofilm potential in *Staphylococcus aureus* and *Escherichia coli*.

10. Nagaraj, A., and Samiappan, S. (2019). Presentation of antibacterial and therapeutic anti-inflammatory potentials to hydroxyapatite via biomimetic with Azadirachta indica: An in vitro anti-inflammatory assessment in contradiction of LPS-induced stress in RAW 264.7 Cells. *Frontiers in Microbiology*, 10, 1757.

11. Aziz, I. M., Alfuraydi, A. A., Almarfadi, O. M., Aboul-Soud, M. A., Alshememry, A. K., Alsaleh, A. N., and Almajhdi, F. N. (2024). Phytochemical analysis, antioxidant, anticancer, and antibacterial potential of *Alpinia galanga* (L.) rhizome. *Heliyon*, 10(17).

12. George, E., Kasipandi, M., Vekataramana, M., Kumar, K. N., Allen, J. A., Parimelazhagan, T., and Gopalan, N. (2016). In vitro anti-oxidant and cytotoxic analysis of *Pogostemon mollis* Benth. *Bangladesh Journal of Pharmacology*, 11(1), 148-158.

13. Gunti, L., Dass, R. S., and Kalagatur, N. K. (2019). Phytofabrication of selenium nanoparticles from *Emblica officinalis* fruit extract and exploring its biopotential applications: antioxidant, antimicrobial, and biocompatibility. *Frontiers in microbiology*, 10, 931.

14. Vundela, S. R., Kalagatur, N. K., Nagaraj, A., Kadirvelu, K., Chandranayaka, S., Kondapalli, K., Hashem, A., Abd_Allah, E. F., and Poda, S. (2022). Multi-biofunctional properties of phytofabricated selenium nanoparticles from Carica papaya fruit extract: Antioxidant, antimicrobial, antimycotoxin, anticancer, and biocompatibility. *Frontiers in microbiology*, 12, 769891.

15. Nagaraj, A., Ghosh, O. S. N., Ghneim, H. K., AlSheikh, Y. A., Mohammed, K., Poda, S., and Kalagatur, N. K. (2025). Fe_2O_3-type iron oxide nanoparticles from *Aerva lanata* leaf extract exhibit antibiofilm, discriminatory toxicity in cancer cells, and theranostic against oxidative stress in zebrafish. *Chemical Physics Impact*, 100849.

16. Ameh, T., Zarzosa, K., Dickinson, J., Braswell, W. E., and Sayes, C. M. (2023). Nanoparticle surface stabilizing agents influence antibacterial action. *Frontiers in Microbiology*, 14, 1119550.

17. Kakian, F., Mirzaei, E., Moattari, A., Takallu, S., and Bazargani, A. (2024). Determining the cytotoxicity of the Minimum Inhibitory Concentration (MIC) of silver and zinc oxide nanoparticles in ESBL and carbapenemase producing Proteus mirabilis isolated from clinical samples in Shiraz, Southwest Iran. *BMC Research Notes*, 17(1), 40.

18. Niziołek, K., Słota, D., Sadlik, J., Łachut, E., Florkiewicz, W., and Sobczak-Kupiec, A. (2023). Influence of Drying Technique on Physicochemical Properties of Synthetic Hydroxyapatite and Its Potential Use as a Drug Carrier. *Materials*, 16(19), 6431.

19. Bee, S. L., Bustami, Y., Ul-Hamid, A., and

Hamid, Z. A. (2022). Green biosynthesis of hydroxyapatite-silver nanoparticle nanocomposite using aqueous Indian curry leaf (*Murraya koengii*) extract and its biological properties. *Materials Chemistry and Physics*, 277, 125455.

20. Das, T. K., Ganguly, S., Bhawal, P., Mondal, S., and Das, N. C. (2018). A facile green synthesis of silver nanoparticle-decorated hydroxyapatite for efficient catalytic activity towards 4-nitrophenol reduction. *Research on Chemical Intermediates*, 44, 1189-1208.

21. Pai, S., Kini, M. S., Mythili, R., and Selvaraj, R. (2022). Adsorptive removal of AB113 dye using green synthesized hydroxyapatite/ magnetite nanocomposite. *Environmental research*, 210, 112951.

22. Imchen, P., Ziekhrü, M., Zhimomi, B. K., and Phucho, T. (2022). Biosynthesis of silver nanoparticles using the extract of *Alpinia galanga* rhizome and *Rhus semialata* fruit and their antibacterial activity. *Inorganic Chemistry Communications*, 142, 109599.

23. Ahmad, E., Athar, A., Nimisha, Zia, Q., Sharma, A. K., Sajid, M., Bharadwaj, M., Ansari, M. A., and Saluja, S. S. (2024). Harnessing nature's potential: *Alpinia galanga* methanolic extract mediated green synthesis of silver nanoparticle, characterization and evaluation of anti-neoplastic activity. *Bioprocess and Biosystems Engineering*, 47(8), 1183-1196.

24. Wei, W., Li, J., Han, X., Yao, Y., Zhao, W., Han, R., Li. R., Zhang, Y., and Zheng, C. (2021). Insights into the adsorption mechanism of tannic acid by a green synthesized nano-hydroxyapatite and its effect on aqueous Cu (II) removal. *Science of The Total Environment*, 778, 146189.

25. Namasivayam, S. K. R., Venkatachalam, G., and Bharani, R. A. (2021). Noteworthy enhancement of wound-healing activity of triphala biomass metabolite-loaded hydroxyapatite nanocomposite. *Applied Nanoscience*, 11, 1511-1530.

26. Vinayagam, R., Kandati, S., Murugesan, G., Goveas, L. C., Baliga, A., Pai, S., Varadavenkatesan, T., Kaviyarasu, K., and Selvaraj, R. (2023). Bioinspiration synthesis of hydroxyapatite nanoparticles using eggshells as a calcium source: Evaluation of Congo red dye adsorption potential. *Journal of Materials Research and Technology*, 22, 169-180.

27. Beigoli, S., Hekmat, A., Farzanegan, F., and Darroudi, M. (2021). Green synthesis of amorphous calcium phosphate nanopowders using *Aloe Vera* plant extract and assessment of their cytotoxicity and antimicrobial activities. *Journal of Sol-Gel Science and Technology*, 98, 508-516.

28. Bhatnagar, S., Kobori, T., Ganesh, D., Ogawa, K., and Aoyagi, H. (2019). Biosynthesis of silver nanoparticles mediated by extracellular pigment from *Talaromyces purpurogenus* and their biomedical applications. *Nanomaterials*, 9(7), 1042.

29. Abdelmigid, H. M., Morsi, M. M., Hussien, N. A., Alyamani, A. A., Alhuthal, N. A., and Albukhaty, S. (2022). Green synthesis of phosphorous-containing hydroxyapatite nanoparticles (nHAP) as a novel nano-fertilizer: preliminary assessment on pomegranate (*Punica granatum* L.). *Nanomaterials*, 12(9), 1527.

30. Sathiyavimal, S., Vasantharaj, S., LewisOscar, F., Pugazhendhi, A., and Subashkumar, R. (2019). Biosynthesis and characterization of hydroxyapatite and its composite (hydroxyapatite-gelatin-chitosan-fibrin-bone ash) for bone tissue engineering applications. *International journal of biological macromolecules*, 129, 844-852.

31. Kumar, R., Shikha, D., Sinha, S. K., Guerra-López, J. R., and Aboudzadeh, N. (2024). Assessment of antioxidant activity, thrombogenicity and MTT assay of bioceramic phosphate as a biomaterial. *Journal of the Australian Ceramic Society*, 1-11.

32. Kalagatur, N. K., Abd_Allah, E. F., Poda, S., Kadirvelu, K., Hashem, A., Mudili, V., and Siddaiah, C. (2021). Quercetin mitigates the deoxynivalenol mycotoxin induced apoptosis in SH-SY5Y cells by modulating the oxidative stress mediators. *Saudi journal of biological sciences*, 28(1), 465-477.

33. Hassanain, M., Abdel-Ghafar, H. M., Hamouda, H. I., El-Hosiny, F. I., and Ewais, E. M. (2024). Enhanced antimicrobial efficacy of hydroxyapatite-based composites for healthcare applications. *Scientific Reports*, 14(1), 26426.

34. Dixit, N.M., Kalagatur, N.K., Poda, S., Kadirvelu, K., Behara, M. and Mangamuri, U.K. (2022). Application of *Syzygium aromaticum*, *Ocimum sanctum*, and *Cananga odorata* essential oils for management of Ochratoxin A content by *Aspergillus ochraceus* and *Penicillium verrucosum*: An in vitro assessment in maize grains. *Indian Journal of Biochemistry and Biophysics*, 59, 172-182.

35. Efenberger-Szmechtyk, M., Nowak, A., Czyżowska, A., Śniadowska, M., Otlewska, A., and Żyżelewicz, D. (2021). Antibacterial mechanisms of Aronia melanocarpa (Michx.), Chaenomeles superba Lindl. and Cornus mas L. leaf extracts. *Food Chemistry*, 350, 129218.

36. Kalagatur, N. K., Nirmal Ghosh, O. S., Sundararaj, N., and Mudili, V. (2018). Antifungal activity of chitosan nanoparticles encapsulated with *Cymbopogon martinii* essential oil on plant pathogenic fungi *Fusarium graminearum. Frontiers in pharmacology*, 9, 610.

In Vitro Effects of Homoeopathic *Streptococcus pneumoniae* Nosode on a *Streptococcus pneumoniae* Culture

Nokwanda Dudu Zulu[1], Sindile Fortunate Majola[2], Khine Swe Swe Han[3], Yesholata Mahabeer[4], Suresh Babu Naidu Krishna[5]

[1]Department of Homoeopathy, Durban University of Technology, Durban-4000, South Africa
[2]Department of Homoeopathy, Durban University of Technology, Durban-4000, South Africa
[3]Department of Medical Microbiology, Inkosi Albert Luthuli Central Hospital, NHLS, Durban-4000, South Africa
[4]Department of Medical Microbiology, University of KwaZulu-Natal, NHLS, Durban-4000, South Africa
*Corresponding Author: sureshk@dut.ac.za

Abstract

Globally, antimicrobial resistance is a huge healthcare concern and is projected to cause 10 million deaths worldwide by 2050 if the current trend of irrational utilization of antibiotics continues. The search for new antimicrobials continues to be a pressing need in humanity's battle against bacterial infections. Several in vitro studies have yielded positive results on homoeopathic nosodes and other homoeopathic remedies. However, none of the in vitro or in vivo studies has been conducted on S. pneumoniae nosode. To test this paradigm, we assessed the in vitro effects of homoeopathic S. pneumoniae nosode on an S. pneumoniae culture. S. pneumoniae ATCC49619 was obtained from the National Health Laboratory Service, University of KwaZulu-Natal. The homeopathic remedies tested were S. pneumoniae nosode 6CH, 9CH, 30CH, and 200CH. Antimicrobial susceptibility testing was performed using disc diffusion and minimum inhibitory concentration (MIC). The positive control used was ceftriaxone, and the negative control was 20%ethanol. No significant inhibitory effect of any of the tested homoeopathic remedies, S. pneumoniae nosode 6CH, 9CH, 30CH, and 200CH including 20%ethanol on S. pneumoniae could be found. S. pneumoniae demonstrated susceptibility to ceftriaxone. The MIC of ceftriaxone was 2µg/ml. In conclusion, the study revealed that the tested nosode, S. pneumoniae nosode 6CH, 9CH, 30CH, and 200CH exhibited no antibacterial potential against S. pneumoniae. These findings are in concordance with the hypothesis that homoeopathic remedies are based on host effects: such as activation of the immune system, rather than direct impact on pathogens.

Keywords: Antimicrobial resistance, Streptococcus pneumoniae, Homoeopathic nosodes, in vitro Microbiology test

Introduction

Antimicrobial resistance (AMR) is an escalating global challenge, resulting in limited treatment options, and remains a significant concern in healthcare(1, 2). According to the World Health Organization (WHO), 10 million people including 4.1 million people in Africa, are expected to die from AMR organisms by 2050. Bacteria can develop resistance to antibiotics through mutation or acquisition of resistant genes from other bacteria(3, 4). One of the causes of antibacterial resistance is the misuse of antibiotics in agriculture, animal populations, and human medicine, which creates selection

pressure that enables the development of resistant bacterial strains (5, 6).

The situation is aggravated by the increased incidence of infections with multi-drug-resistant bacterial strains, underscoring the need for new treatment options that can eliminate pathogens and prevent drug resistance. Consequently, alternative approaches, such as homoeopathy should be considered (7, 8).

Homoeopathy is an alternative medicinal therapeutic approach based on the Law of Similars. Despite being around for over 200 years, remains one of the most controversial traditional medicine treatments due to a lack of in vitro and in vivo studies(9, 10). Homoeopathic medications are prepared from biological materials, such as live and inactivated organisms, or diseased materials. Nosodes are homoeopathic remedies prepared from inactivated microorganisms such as bacteria, disease products (fluids or tissue), or viruses(11). Using the minimum inhibitory concentration method, C. albicans K. pneumoniae, E. coli and Salmonella typhi polyvalent nosodes exhibited antibacterial effects not only against their respective microorganism but also against other selected organisms (12).

The lack of data and the limited in vitro studies conducted on nosodes revealed a gap that needs to be addressed in the homoeopathy field. Generally, it is accepted that homoeopathic medication works in vivo by stimulating the immune system, thereby enhancing its effectiveness. The study aims to assess the effect of isopathic nosode (S.pneumoniae) on the S. pneumoniae strain, which has become a serious health problem.

Materials and Methods

Research design

This panel observational study was conducted at the National Health Laboratory Service, Department of Medical Microbiology, Inkosi Albert Luthuli Hospital for 2 weeks in June 2024. Ethical clearance was obtained from the Institutional Research Ethics Committee (IREC). *Streptococcus pneumoniae* ATCC 49619 was utilized.

Preparation of the homoeopathic nosode

For the in vitro testing, a homoeopathic nosode was utilized in low potencies (6CH and 9CH), medium (30CH), and high potencies (200CH). *S. pneumoniae* nosode 6CH (20% ethanol) was purchased from Comed Health in Pretoria (Waltloo), South Africa. The nosode was prepared according to the German Homoeopathic Pharmacopoeia method 44(13, 14). The *S. pneumoniae* nosode 6CH was diluted and agitated in 20% ethanol to potencies 9CH,30CH, and 200CH(14)

Potencies were stored at the Department of Homoeopathy Laboratory, Durban University of Technology (DUT) at temperatures between 4C and 6C, ensuring they did not freeze. The bio-safety measures were followed during the preparation process. The transfer of 1 drop of the previous potency for preparation of subsequent potency was conducted in the controlled, aseptic environment (in a laminar airflow with a bunsen burner)). *S.pneumoniae* nosode 6CH, 9CH, 30CH, and 200CH were evaluated for antimicrobial efficacy on *S.pneumoniae (15)*.

Preparation of the discs

Filter paper (Whatman® no. 4) was used to prepare discs approximately 5 mm in diameter. These discs were placed in an aluminum foil and autoclaved at 15lbs for 15 minutes to ensure sterilization. Using sterile forceps, the discs were placed in sterile Petri dishes, and each disc was impregnated with an appropriate test substance (*S.pneumoniae* nosodes and 20% ethanol) using a double-impregnation technique. The first impregnation stage con-

sisted of 20 microlitres of the appropriate substance, the second consisted of 10 microlitres. Between each impregnation stage, the discs were dried at 37°C with the lids of each petri dish closed(16) .

Disc diffusion assay

The disc diffusion method for antimicrobial susceptibility testing was conducted according to the standard method by Bauer(17) to evaluate the potential presence of antibacterial activities of *Streptococcus pneumoniae* nosode. A 0.5 McFarland standard *Streptococcus pneumoniae* ATCC49619, was used to lawn Mueller Hinton agar supplemented with 5% sheep blood plates. The discs that had been impregnated with tested substances were applied on the center of the Mueller Hinton Agar surface. Each test plate comprised one disc. The tests were done in triplicate to ensure reliability and validity. The medicated disc included *S. pneumoniae* nosode 6CH, *S. pneumoniae* nosode 9CH, *S. pneumoniae* nosode 30CH, *S. pneumoniae* nosode 200CH, and 20% ethanol, and ceftriaxone 30μg. The positive control was Ceftriaxone 30μg discs obtained from JVL Lab Engineering and General Supplies Close Corporation, South Africa. The negative control was 20% ethanol obtained from Shalom laboratory suppliers, in South Africa.

The plates were then incubated at 37°C for 18-48 hours in an inverted position. The plates were observed at 18, 24, and 48 hours of incubation for zone inhibition(18-20). Zone diameters (mm) were determined after 18, 24, and 48 hours of incubation at 35°C and measured the point at which the total growth inhibition zone was noted. The assay was performed twice to ensure reliability. Ceftriaxone zone diameter was interpreted using Clinical Laboratory Standard Institute (CLSI) guidelines(21), where a zone diameter of ≥ 24mm is considered sensitive, while the absence of a zone indicated as (-) is considered resistant(21).

Minimum Inhibitory Concentration Determination

The minimum inhibitory concentration was determined by Epsilometer (E-test) method as per the manufacturer's instructions (Biomeriuex, South Africa). Twenty-four-hour *S. pneumoniae* colonies were suspended in a sterile 0.9% saline solution and adjusted to the McFarland turbidity standard of 0.5. After inoculating the agar plates with the standard inoculum, ceftriaxone E-test scripts were placed on the plates. The plates were incubated at 37°C in a dark incubator for 18-24 hours.

Results and Discussion

The results obtained from this research are presented in figures and tables below. Figures 1 and 2 show the antibacterial assay of *S. pneumoniae* nosode and controls by the Kirby Bauer method in *S. pneumoniae* for both dry and wet medicated discs. The MIC is shown in Figure 3.

The MIC assay results of ceftriaxone for antibacterial activity against *S. pneumoniae* was 2μg/ml. Antimicrobial susceptibility test showed that *S. pneumoniae* was resistant to *S. pneumoniae* nosode 6CH, *S. pneumoniae* nosode 9CH, *S. pneumoniae* nosode 30CH, *S. pneumoniae* nosode 200CH and 20% ethanol as there was an absence of zone of inhibition.

None of the tested substances, *S. pneumoniae* nosode 6CH, 9CH, 30CH, 200CH, and 20% ethanol demonstrated any zones of inhibition at 18, 24, and 48 hours of incubation. The positive control, ceftriaxone 30μg inhibited the growth of *S. pneumoniae.*

Figure 1. Antibacterial assay of *S. pneumoniae* nosode and controls by Kirby Bauer method in *S. pneumoniae* (dry medicated discs)

In Vitro effects of homoeopathic *Streptococcus pneumoniae* nosode on a
Streptococcus pneumoniae culture
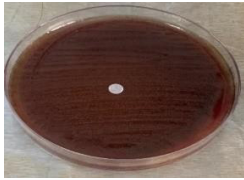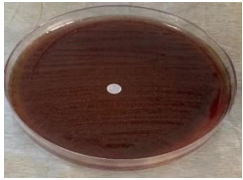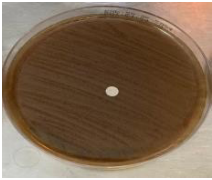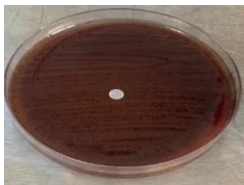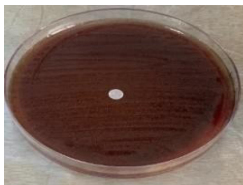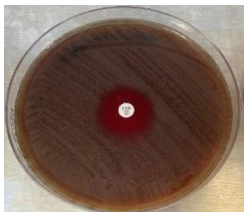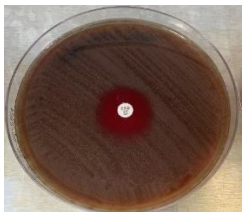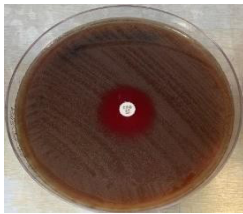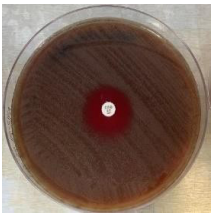
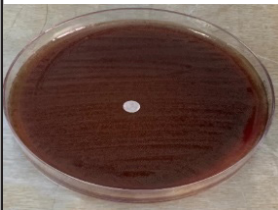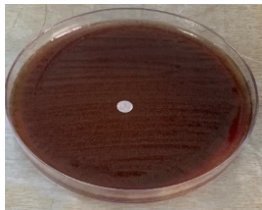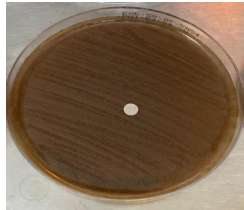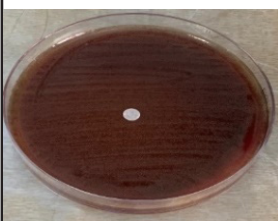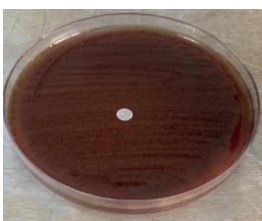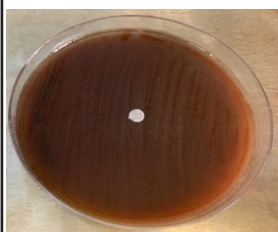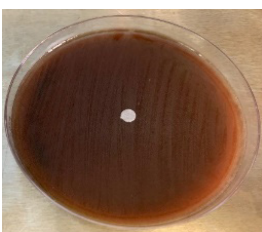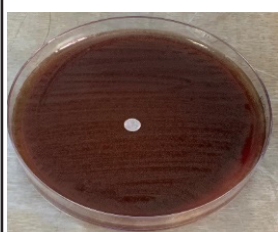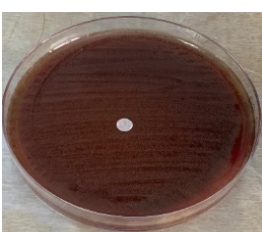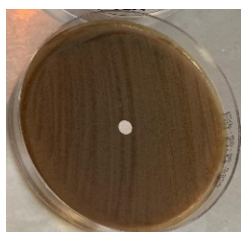| Tested substances	Time		
	18 hours	24 hours	48 hours
S.pneumoniae nosode 6CH Wet disc			
S.pneumoniae nosode 9CH Wet disc			
S.pneumoniae nosode 30CH Wet disc			
S.pneumoniae nosode 200CH Wet disc			
20% Ethanol Wet disc			

Figure 2: Antibacterial assay of *S.pneumoniae* nosode and controls using the Kirby Bauer method in *S.pneumoniae* (wet medicated discs)

Table 1: Antimicrobial susceptibility of *S.pneumoniae.*

Tested Substances	Concentration	Time (hours)	Zones Diameter (mm)
S. pneumoniae nosode	6CH	18	-
		24	-
		48	
S. pneumoniae nosode	9CH	18	-
		24	-
		48	-
S. pneumoniae nosode	30CH	18	-
		24	-
		48	-
S. pneumoniae nosode	200CH	18	-
		24	-
		48	-
Ethanol	20%	18	-
		24	-
		48	-
Ceftriaxone	30µg	18	20
		24	20
		48	24

The absence of zone diameter is interpreted as (-) and the presence of zone diameter is interpreted in (mm)

Table 1 shows the zone diameter measured from the *S.pneumoniae* nosode and controls after 18, 24, and 48 hours of incubation. The zone of diameter for ceftriaxone was interpreted using CLSI guidelines, where a zone diameter of ≥ 24mm is considered sensitive, while the absence of a zone indicated as (-) is considered resistant. Antimicrobial susceptibility test showed that *S.pneumoniae* was sensitive to ceftriaxone 30µg, with a zone diameter of 24mm which is within the expected zone diameter. *S.pneumoniae* nosode 6CH, 9CH, 30CH, and 200CH could not inhibit the growth of *S.pneumoniae* and this is shown by the absence of a zone of inhibition after incubation.
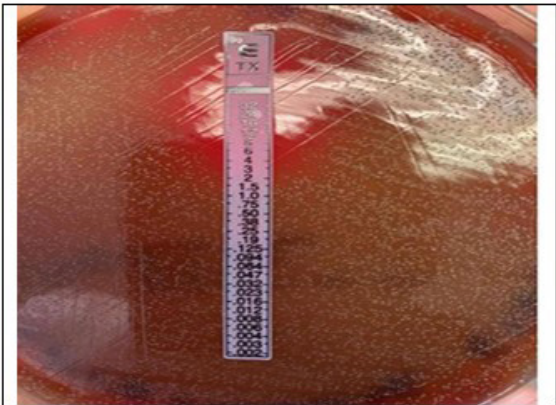

Figure 3: MIC for ceftriaxone using E-test

In Vitro effects of homoeopathic *Streptococcus pneumoniae* nosode on a *Streptococcus pneumoniae* culture

Discussion

The investigation into the direct microbicidal effects of potentized remedies, especially nosodes, in vitro, is relatively limited compared to the extensive homoeopathic clinical trials in medical research.

We were not able to demonstrate any significant effect of homoeopathic drugs in high potencies on *S.pneumoniae* growth in vitro. The hypothesis that *S.pneumoniae* nosode 6CH, 9CH, 30CH, and 200CH have an in vitro efficacy against *S.pneumoniae* bacteria was therefore rejected.

Only a few previous studies evaluated the in vitro effects of homoeopathic drugs on bacteria; the majority of these studies detected significant inhibition of bacterial growth. Passeti (22) examined the effects of Belladona (12CH and 30CH) and *S. pyogenes* (12CH and 30CH) on *S. pyogenes* strains. The results showed that both remedies inhibited bacterial growth in vitro. Additionally, the authors found that treating MRSA cultures with Belladonna or MRSA nosode (6CH and 30CH) reduced bacterial growth in vitro, decreased enzymatic activity, and increased bacterial susceptibility to antibiotic treatment(22).

The absence of a positive anti-microbial response against *S.pneumoniae* contradicts the findings of the study by Simi and Bencitha regarding the effectiveness of nosodes on microorganisms. Their study results showed that *Pytogrnium* 200CH, 1M, and A*nthracinum* 200CH have a significant antimicrobial effect against *methicillin-resistant Staphylococcus aureus* (MRSA)(23).

In contrast, the lack of growth inhibition in *S.pneumoniae* nosode 6CH, 9CH, 30CH, and 200CH on *S.pneumoniae* is consistent with the findings of Pareek and Jadhav(24). The study assessed whether Sulphur, Senega, Lobelia inflata, and *Klebsiella pneumoniae* nosode(6CH, 12CH, 30CH, 200CH, and 1M) possess antimicrobial effects against *Klebsiella pneumoniae*. According to the results, it was concluded Sulphur, Senega, and Lobelia inflata showed an inhibitory effect. However, no statistically significant results were demonstrated by *Klebsiella pneumoniae* nosode (24).

The study aimed to evaluate the efficacy of Apis mellifica, Graphites, Arsenicum album, and Pulsatilla against different diseases at the potencies of 30C and 200C. The tested homoeopathic remedies did not exhibit antimicrobial effects against *Staphylococcus spp* using the agar well diffusion method(10).

A study by Bruna(25) on the verification of antimicrobial activity of *S. sclerotiorum* nosode and sulphur on the mycelial growth of *S. sclerotiorum* indicated that neither *S. sclerotiorum* nosode nor sulphur reduced the growth of *S. sclerotiorum.*

An in vitro study analyzing the micro-sclera and mycelial growth of the fungi showed that the *M.phaseolina* nosode did not reduce the micro-sclerotia and mycelial growth(26).

Additionally, an in vitro study examined the antimicrobial activity of *Streptococcinum* nosode 6CH, 30CH, 200CH, 0/6, 0/30 and 0/60 LM potencies. It was found that *Streptococcinum* nosode in infinitesimal dilutions does not exhibit antimicrobial activity in either the broth dilution method or the disc diffusion method, however, it does exhibit promicrobial activity in both methods (27).

According to the study findings, the negative control ethanol 20% did not display an antibacterial effect against *S. pneumoniae.* Sauerbrei(28) indicate that the effective bactericidal concentrations of ethanol ranged from 60% to 85%, with required exposure times between ≤0.5 and ≥5 min. Ethanol concentrations of 30%–50% have significantly lower bactericidal activity, and the exposure times tested (5–30 min) are partly insufficient for a significant bactericidal effect(28, 29). Therefore, 20% ethanol is considered too low to produce a significant antibacterial effect. Centers for Disease Control and Prevention (CDC) recommends ethanol concentrations of 60% and 90% for disinfec-

tion(30).

A study on the efficacy of calendula offi-cinalis tincture 60% (v/v) against *Pseudomonas aeruginosa* found no significant difference be-tween the activity of calendula officinalis tincture 60% (v/v) ethanol and 60% ethanol on in vitro *Pseudomonas aeruginosa*. With mean activ-ities of 6.88 and 6.69mm, respectively. Based on these results, it can be concluded that the antibacterial properties of Calendula officinalis tincture 60% (v/v) ethanol are attributed to the 60% ethanol present in the tincture.

Conclusion

Nosodes face criticism and controversy as there is a lack of scientific evidence support-ing their efficacy. In the present study, no signifi-cant inhibitory effect of the diluted homoeopathic nosode samples was found against *Streptococ-cus pneumoniae* ATCC49619 Hence, the find-ing of the current study could not draw any supportive evidence for the in vitro antibacterial potential of the homoeopathic nosode sample. The outcomes also portray the need for further thorough in vitro investigation of homoeopathic nosodes in different diluted forms or conduct-ing several in vivo trials in model organisms to claim the potential effectiveness of homoeo-pathic remedies as a suitable therapeutic agent against pathogens.

Acknowledgment

Conflict of Interest

The authors declare no conflict of inter-est with respect to the authorship or publication of this paper.

Funding

References

1. Ugwu MC, Shariff, M., Beri, K., Okezie, U.M., Iroha, I.R., Esimone, C.O. Pheno-typic and Molecular Characterization of β-Lactamases among Enterobacterial Uro-pathogens in Southeastern Nigeria. The Canadian Journal of Infectious Diseases and Medical Microbiology. 2020;2020(1):1-9.

2. Nwobodo DC, Ugwu, M.C., Anie, C.O., Al-Ouqali, M.T.S., Ikem, J.C., Chigozie, U.V., Saki, M. Antibiotic resistance: The challenges and some emerging strategies for tackling a global menace. Journal of Clinical Laboratory Analysis. 2022;9(36):1-10.

3. Pereira C, Warsi, O.M., Andersson, D.I. Pervasive selection for clinically relevant resistance and media adaptive mutations at very low antibiotic concentrations. Mo-lecular Biology and Evolution. 2023;8(7):1-13.

4. WHO. World Health Organization [Inter-net]2019. [15 August 2024]. Available from: https://www.who.int/docs/default-source/ immunization/position_paper_documents/ pneumococcus/who-pp-pcv-2019-presen-tation.pdf.

5. Philips BJ, Redman, J., Brennan, A., Wood, D., Holliman, R., Baines, D., Baker, E.H. Glucose in bronchial aspirates increases the risk of respiratory MRSA in intubated patients. Thorax. 2005;60(9):709a-a.

6. Honert MSV, Gouws, P.A., Hoffman, L.C. Importance and implications of antibi-otic resistance development livestock and wildlife farming in South Africa: a re-view. South African Journals of Science. 2018;48(3):401-12.

7. Muller A, Kleynhans, J., Gouveia, L., Mei-ring, S., Cohen, C., Hathaway, L.J., Gott-berg, A.V. *Streptococcus pneumoniae* Serotypes Associated with Death South

Africa 2012-2018. *Emerging Infectious Diseases*. 2022;28(1):166-79.

8. Kato H, Hagihara, M., Hiramatsu,S.I., Suematsu, H., Nishiyama, N., Asai, N., Mikamo, H., Yamamoto, K., Iwamoto, T. Evaluating the antimicrobial efficacy of ceftriaxone regimens: 1 g twice daily versus 2 g once daily in a murine model of *Streptococcus pneumoniae* pneumonia. JAC- antimicrobial resistance. 2024;6(3):1-6.

9. Ram H, Sharma, R., Dewani, D., Singh, A. Differential Drivers of Antimicrobial Resistance across the World. Account for Chemical Research. 2019;52(4):916-24.

10. Kabir I, Ikram, A., Sikder,B., Tushar, H.H., Munshi, S.K. Determination of the Inhibitory Effects of Commercially Available Homoeopathic Drugs on Pathogenic Bacterial Growth. SVOA Microbiology. 2021:1-6.

11. Preena JJ, Kulsum, S.A.j., Amily, B., Nisha, G., Praveen, R.P., Gopukumar, S.T. A comprehensive Look at Nosode Remedies in Homoeopathic Medicines. International Neurourology Journal. 2023;27(4):326-30.

12. Munshi R, Talele, G., Shah, R. In vitro Evaluation of Antimicrobial Activities of Escherichia coli, Klebsiella pneumoniae, Salmonella typhi, Neisseria gonorrhoeae, and Candida ablicans Nosodes. *Homoeopathy*. 2022;111(1):42-8.

13. Benyunes S. German Homoeopathic Pharmacopoeia Supplement: Medpharm; 2005 3 December 2005.

14. Bibliothek D. German Homoeopathic Pharmacopoeia (GHP). publishers Ms, editor: Medpharm scientific publishers.2005. H5.2-H5.4 p.

15. Joshi S, Mukerjee, S., Vaidta, S., Talele, G., Chowdhary, A., Shah, R. Preparation, standardization and in vitro safety testing of Mycobacterium nosodes (Emtact-polyvalent nosode). Homoeopathy.

16. Prajapati S, Sharma, M., Gupta, P., Kumar, M., Dwivedi, B., Arya, B.S. Evaluation of antifungal activity of different homoeopathic mother tinctures against Candida albicans. Indian Journal of Research in Homoeopathy. 2017;11(4):237-43.

17. Bauer AW, Kirby, W.M.M., Sherris, J.C., Turck, M. Antibiotic Susceptibility Testing by a Standardized Single Disk Method. American Journal of Clinical Pathology. 1966;45(4):493-6.

18. Invernizzi JRR. A controlled in vitro study of the effectiveness of Tulbagia Violacea in herbal tincture and Homeopathic dilution (1X and 6X) against gram-positive and gram- negative bacteria. Durban Durban University of Technology; 2002.

19. Sikdar S, Saham S.K., Bukhsh, A.R.K. Relative Apoptosis-inducing Potential of Homeopathic Condurango 6C and 30C in H460 Lung Cancer Cells In vitro. Journal of Pharmacopunture. 2014;17(1):59-69.

20. Catarina A, Valle, V., Brunel, H.S.S., Malard, P.F., Villarroel, C.L., Andrade, R.V. Homeopathic Viscum Album at Potencies D3 and 200CH Presents Cytokine Modulatory Effect Produced by in vitro Culture of Mesenchymal Stem Cells. Current Research in Complementary and Alternative Medicine. 2022;6(155):1-7.

21. Institute CaLS. M100-Performance Standards for Antimicrobial Susceptibility Testing. 33 ed: Clinical and Laboratory Standard Institute; 2023.

22. Passeti TA, Manzoni, J.A., Ambrozino, L.G.P., Ferreira, M.L., Rodrigues, P.F.P., Bissoli, L.R., Diniz, S.N., Beltrame, R.L. Action of homeopathic medicines Arnica montana, Gelsemium sempervirens, Belladonna, Mercurius solubillis, and nosodium on the in vitro growth of the bacterium Streptococcus pyogenes / Action of

homeopathic medicines Arnica montana, Gelsemium sempervirens, Belladonna, Mercurius solubilis, and nosode in vitro growth of Streptococcus pyogenes. homeopathy. 2014;77(1/2):1-9.

23. Simi PS, Horrence, B.M., Priyashree, R., Maalolan, S., Rachana, M.R.S. Anti-bacterial activity of homoeopathic nosodes Anthracinum, Pyrogenium and Variolinum in 30CH, 200CH and 1M potencies against Methicillin-Resistant Staphylococcus Aureus- An in vitro study. Chettinad Health City Medical Journal. 2024;13(1):1-9.

24. Pareek S, Jadhav, A.B. In Vitro Evaluation of Antibacterial Activity of Homoeopathic Preparations on Klebsiella pneumoniae. International Journal of Health Sciences and Research. 2020;10(3):176-80.

25. Bruna BR, Jose, R.S., Sidiane, C.R., Omari, D.F.D.,Edilaine, D.V.G., Eloisa, L. . In vitro activity of homoeopathic medicines against Sclerotinia sclerotiorum. Scientia Agraria Pranaensis. 2016;15(3):1-18.

26. Lorenzetti E, Stangarlin, J.R., Treib, E.L., Heling, A.L., Roncato, S.C., Carvalho, J.C., Hoepers, L., Rissato, B.B., Coppo, J.C., Belmonte, C., Kuhn, O.J., Silva, I.F. Antimicrobial action against of Macrophomina phaseolina and action of the grey stem in soybean by homoeopathic remedies Nosode and sulphur. African Journal of Agriculture Research. 2016;11(36):3412-7.

27. Meneses NRA. Study of the effect of infinitesimal doses of streptococcinum nosode on the microbial activity of group a β-hemolytic streptococcus in an in vitro model. Microbiology. 2016.

28. Sauerbrei A. Bactericidal virucidal activity of ethanol and povidoneiodine. Microbiology Open. 2020;9(9):1-27.

29. Fallica F, Leonardi, C., Toscano, V., Santonocito, D., Toscano, V., Santonocito, Leornadi, P., Puglia. C. Assessment of Alcohol-Based Hand Sanitizers for Long-Term Use, Formulated with Addition of Natural Ingredients in Comparison to WHO Formulation. Pharmaceutics. 2021;13(4):1-16.

30. CDC. Centers for Disease Control and Prevention [Internet]: Centers for Disease Control and Prevention. 2024. Available from: Hand Sanitizer Guidelines and Recommendations | Clean Hands | CDC.

Chitosan: A Comprehensive Review of Structural Properties, Biological Activities, and Multidisciplinary Applications

Ebrahim Cheraghi [1,2] *, Zahra Cheraghi [3]

[1] Arthropod Borne-Diseases Research Center, Ardabil University of Medical Sciences, Ardabil, Iran.
[2] Department of Biology, Faculty of Sciences, University of Qom, Qom, Iran.
[3] Medical student, Faculty of Medicine, Qom University of Medical Sciences, Qom, Iran.

*Corresponding Author: cheraghi20@gmail.com

Abstract

Chitin deacetylation yields chitosan, a biopolymer gathered from different natural origins like animals and marine organisms. Chitosan quality is influenced by factors such as molecular weight, crystallinity, and degree of deacetylation, as well as purity parameters like ash content, protein content, and color. These inherent characteristics lead to biocompatibility, bio-adhesiveness, solubility, and its polycationic nature, making it suitable for a wide range of physical or chemical modifications. Despite its advantages, chitosan faces challenges such as seasonal and geographical availability, time-consuming extraction processes, and variability in quality due to different extraction methods. Technological advancements, such as genetic modification, hold promise for improving chitosan yield and expanding its applications. This review delves into the structure and properties of chitosan, exploring its extraction methods and emphasizing its diverse applications, including wound dressings, drug delivery systems, antimicrobial agents, wastewater treatment, and beyond. Finally, the discussion concludes with key challenges and future perspectives for chitosan research.

Keywords: Chitosan, Biological Properties, Applications.

Introduction

Chitosan is a biopolymer recovered from the exoskeletons of arthropods, cell walls of fungi, and other sources where chitin is abundantly present. It acts as a basis for many biological and industrial applications due to its unique characteristics, such as non-toxicity, antioxidative nature, biocompatibility, biodegradability, and renewability (1). Chitin, the precursor to chitosan, is the second most abundant biopolymer after cellulose, highlighting its wide occurrence in nature and potential use in various fields (2).

Chitosan which is a polysaccharide derived through deacetylation of chitin has various uses across several industries (3). Because of its non-toxicity, antioxidative nature, biocompatibility, biodegradability, and renewability (4), this substance finds use in several domains, including wound treatment (5), food science (6), agriculture (7), cosmetics (8), biotechnology (9), chelating agent (10), pharmaceutical and biomaterial purposes (11).

Chemical and biological methods can be used to extract chitosan from exoskeleton (12). Crabs (13), shrimp (14), desert locusts, honey bees (15, 16), beetles (17), crayfish, corals (18), fungi (19), and cockroaches (20, 21)

could be exploited for the commercial production of chitosan. The importance of chitosan and its derivatives spans a broad spectrum, from environmental sustainability to potential health benefits, making a chitosan review not just relevant but essential for understanding its multifaceted role (22).

This review aims to provide a comprehensive overview of chitosan's chemical structure, sources, and benefits, focusing on its biodegradability, biocompatibility, and environmental impact. By understanding the biodegradability, biocompatibility, and environmental impact of chitosan, alongside its industrial and biomedical applications, readers will gain comprehensive insights into why natural chitosan's and chitosan products are increasingly becoming a focus of scientific and commercial interest.

Historical background

The discovery and development of chitosan can be traced back over two centuries, marked by significant milestones that have shaped its current applications. The journey began in 1799 when Hatchett used mineral acids to decalcify shells of crabs, crayfish, lobsters, and prawns, observing the formation of a soft, plastic material. This laid the groundwork for future research into chitin and subsequently chitosan (23).

Early discoveries and nomenclature

The early discoveries of chitosan date back to 1799 when Hatchett first observed the formation of a unique material through the decalcification of crab shells using mineral acids. This discovery laid the foundation for further research into chitin and chitosan. In 1811, Braconnot identified chitin in fungi and coined the term "chitin." Later, in 1823, Odier isolated a hornlike material from cockchafer elytra treated with potassium hydroxide, further solidifying the understanding of chitin's structure and properties (23). In 1859-1894, Rouget manipulated chitin through chemical and temperature treatments to become soluble, leading to the naming of "chitosan" by Hoppe-Seyler (24).

Developmental phases of chitin and chitosan

The evolution of chitin into chitosan encompasses five distinct phases, each contributing uniquely to its understanding and utility:

1799-1894: Discovery phase initiated by Hatchett and expanded by subsequent researchers (25).

1894-1930: A period of confusion and controversy, where the properties and structure of chitin were debated (25).

1930-1950: Exploration phase, where the potential applications of chitin and chitosan began to be realized (25).

1950-1970: Doubt phase, characterized by skepticism over the practical uses of chitosan (25).

Post-1970: Application phase, seeing a surge in commercial and biomedical uses of chitosan (25).

Advancements and Modern Applications

Chitosan's journey from a curious derivative to a widely used biopolymer is marked by significant research milestones:

1950s: The structure of chitosan was further understood through x-ray analysis (24).

1960s: Studies revealed chitosan's potential as a hemostatic agent due to its ability to bind with red blood cells (26).

Recent decades: Chitosan has been popularized as a dietary supplement in Japan and Europe, and its production involves a series of chemical reactions starting from chitin, highlighting its versatility and the expanding scope of its applications (26).

This historical perspective not only highlights the scientific milestones that have defined the development of chitosan but also

underscores its evolving role across various sectors, driven by its unique properties and potential for innovation.

Major sources, chemical structure, and properties

Chitosan, a biopolymer derived from chitin, is primarily recovered from the exoskeletons of arthropods such as crabs and shrimp, as well as from fungal cell walls. Recent studies have highlighted its abundance in marine sources, with an estimated global production of chitin exceeding 10^{11} tons annually (22). Chitosan consists of copolymers of D-glucosamine and N-acetyl-D-glucosamine linked by β-(1-4) glycosidic bonds (27) (Figure 1). Its structure resembles cellulose, but the key distinction is the amino group at the C-2 position, giving chitosan a positive ionic charge (2). This positive charge enables chitosan to bind with negatively charged molecules, which is crucial for many of its applications (2).
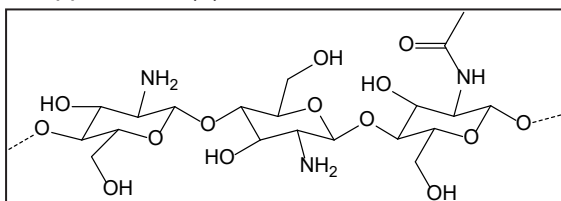

Figure 1. Structure of chitosan.

Key structural characteristics and modifications

Solubility and molecular weight

Chitosan's solubility is highly dependent on its degree of deacetylation (DD) and molecular weight (MW). Studies have shown that chitosan with a DD greater than 50% is soluble in acidic solutions (pH<6.5), while lower DD values result in reduced solubility (27). Additionally, chitosan oligomers with lower MW exhibit enhanced solubility across a broader pH range, making them suitable for various biomedical applications (28).

Degree of deacetylation (DD)

The DD significantly influences physicochemical properties of chitosan such as solubility and charge density. The degree of acetylation affects not only the solubility but also the biodegradability and biocompatibility of chitosan, making it suitable for various biomedical applications (2). Several techniques have been developed to measure the amount of DD found in insect chitosan and chitin. Infrared spectroscopy, UV spectroscopy, near-infrared spectroscopy, potentiometric titration, and magnetic resonance are a few of the analytical methods used to determine DD (29). Among them, the FT-IR, the conductometric, the acid-base, and the potentiometric titration methods are useful for completely soluble compounds.

Viscosity

Viscosity is a key factor in discovering the industrial usability of chitosan, with its dependency on the degree of deacetylation and the molecular weight of the compound. Viscosity increases with higher deacetylation levels and lower molecular weights. Additionally, it can vary based on the particle size and storage duration of chitosan (30). Temperature and concentration factors can affect the viscosity of chitosan solutions. The viscosity increases with decreasing temperature and increasing chitosan content. Due to depolymerization, the chitosan viscosity decreases with increasing demineralization time. The intrinsic viscosity of chitosan can be affected by physical factors (ultrasonic, milling, autoclaving, heating) and chemical (ozone) processes. Chitosan concentrated solutions with various levels of deacetylation differ in their viscosity and flow characteristics (31).

Crystallinity

One of the most important physical properties that determine the functionality of chitosan is its crystallinity. In the solid state, chitosan molecules often self-assemble into highly ordered crystallites within large amorphous domains. There are two primary crystal poly-

morphs of chitosan (32). The most prevalent polymorph is the hydrated "tendon chitosan" form, while the anhydrous crystal form is known as the "tempered polymorph". Both polymorphs consist of two antiparallel chitosan molecules in a double helix shape held together by hydrogen bonds to form the crystal cell. The inclusion of water molecules between these crystal cells stabilizes the structure via multiple hydrogen bonds, leading to distinctions between the polymorphs (33). X-ray diffraction (XRD) is used to measure the crystallinity of chitosan, which detects and analyzes the pattern created by X-ray diffraction through a dense atomic lattice in a crystal. One useful technique for visually verifying the shape and physical condition of the chitin surface is scanning electron microscopy. The surface shape of chitosan varies depending on the source species (20). Commercial chitosan not exhibited an apparent microfibrillar structure and has spherical in shape as indicated by the scanning electron micrograph (Figure 2).
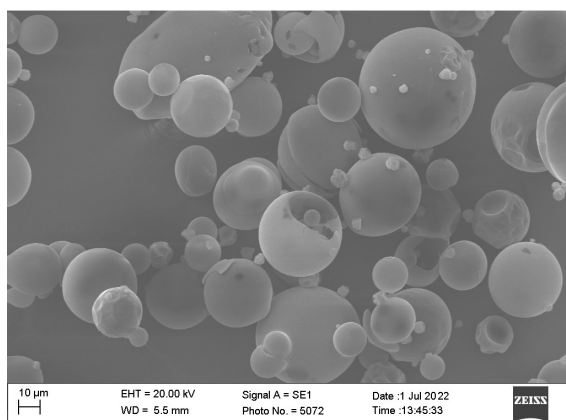

Figure 2. Scanning electron micrograph of commercial chitosan (20).

Chemical modifications

Chitosan, a versatile biopolymer, undergoes various chemical modifications to enhance its solubility, functionality, and application potential. These modifications include acylation, alkylation, carboxylation, and quaternization, each introducing specific functional groups that improve chitosan's water solubility and biolog-

ical compatibility (28). For instance, acylation and carboxylation significantly enhance chitosan's solubility in water (34), while alkylation introduces properties beneficial for medical applications such as coagulation and antibacterial effects. Furthermore, quaternary ammonium chitosan exhibits superior antibacterial, biocompatibility, and biodegradability characteristics (35).

Unique properties and environmental benefits
Non-toxic nature

Chitosan is inherently non-toxic, making it safe for a wide range of applications, from pharmaceuticals to food packaging (2).

Biodegradability

As a biodegradable material, chitosan breaks down into natural substances, reducing environmental pollution and supporting sustainable material cycles (2).

Adsorption capabilities

Its excellent adsorption properties enable the removal of contaminants like heavy metals and dyes from wastewater, contributing to cleaner and safer water sources (2).

Chitosan's role extends beyond biocompatibility to its significant environmental impact. Chitosan is the second most abundant biopolymer after cellulose. This abundance ensures a sustainable supply of raw materials for producing chitosan, which is crucial for its widespread application in environmentally sensitive areas (22). The biopolymer's ability to degrade naturally complements its applications in reducing pollution, particularly in agricultural and food industries where its use can lead to less reliance on synthetic materials (22).

Major sources

Among the various sources available for chitosan production (Figure 3), shrimp is one of the most promising and much discussed, and many other species, such as beetles and

insects, have also been used (36). Insects have emerged as a viable alternative supply of chitosan; nevertheless, this development has only occurred in recent times, and studies have only been conducted on a laboratory scale. Mollusks provide an additional source of chitosan. The use of species such as Sepia kobiensis, Sepia spp, Loligo lessoniana, and Loligo formosana has been seen in this regard. Compared to crustaceans, fungi are a source of chitosan and chitin that is not seasonal and not influenced by geographical factors. Chitin extraction from this source requires less use of chemicals, as there is usually no need for mineral removal and discoloration. In fungal chitin and chitosan, there are generally no heavy metal contaminants or allergenic proteins that can be found in marine sources (37).
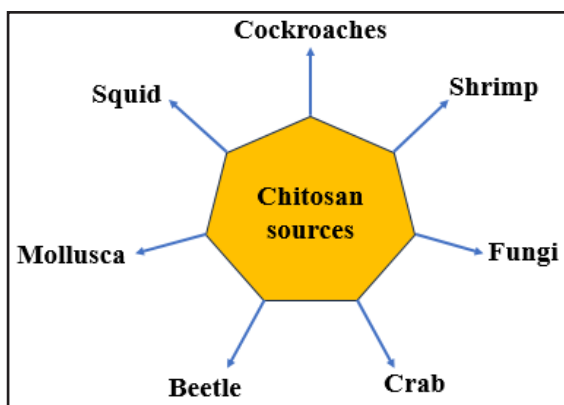

Figure 3. The most important sources of chitosan.

Industrial extraction and yield factors

The extraction of chitosan from chitin involves a deacetylation process using strong alkalis such as sodium hydroxide (NaOH), which is a critical step in determining the quality and yield of chitosan (2) (Figure 4). For instance, a study by Pacheco et al., demonstrated that treating chitin with 40% NaOH at 90°C for 4 hours resulted in chitosan with a DD of 85% (12). Alternative methods, such as enzymatic deacetylation using chitin deacetylase, have also been explored to achieve higher purity and controlled DD values (19). Factors such as temperature, alkali concentration, and reaction duration play significant roles in influencing the molecular weight and degree of deacetylation, thereby affecting the yield and purity of chitosan. The source of chitin, whether from animals, marine crustaceans or fungal biomass, along with the extraction method, impacts the final yield and quality of chitosan. Notably, solid-state fermentation of fungal biomass has been shown to produce higher yields of chitosan compared to submerged fermentation (2). Chemical and biological methods used to extract chitosan from exoskeleton of different sources are illustrated in Figure 3.
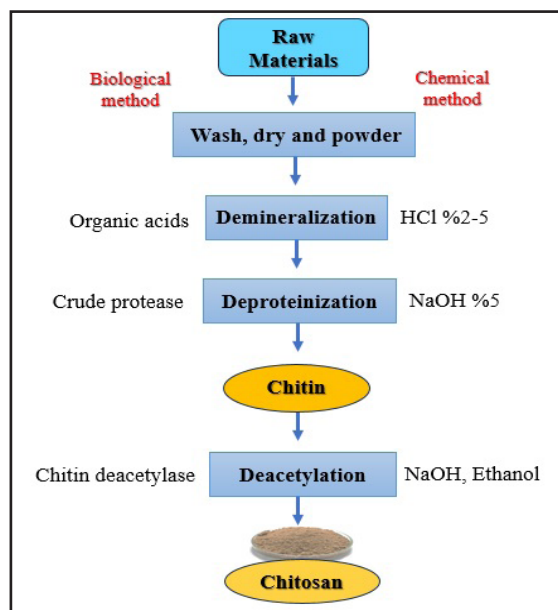

Figure 4. Scheme for the steps of chitosan preparation from raw materials (2) (Modified).

Applications of chitosan
Application in environmental fields

Chitosan's role in environmental management is particularly significant in water purification and waste treatment processes. It is employed in the development of water filtration membranes, where its ability to remove metal ions and heavy metals from industrial effluents is

highly valued (38). Additionally, chitosan-based nanocomposites are increasingly favored for their efficacy in eliminating hazardous contaminants like dyes and other pollutants during the water purification process (38). These capabilities not only enhance water quality but also support sustainable industrial practices.

Water and wastewater treatment

Chitosan's excellent adsorption capabilities allow it to remove harmful contaminants such as heavy metals, dyes, and pharmaceuticals from water, making it an invaluable component in water purification systems (39).

Biodegradable packaging

Chitosan-based films offer a sustainable alternative to conventional plastic packaging. These films degrade more rapidly in soil environments compared to commercial starch-based films, thereby reducing environmental pollution and aiding in waste management (40).

Greenhouse gas absorption

Chitosan contributes to sustainable development by absorbing greenhouse gases. This capability, coupled with its potential to adsorb heavy ions and organic matter, positions chitosan as a beneficial material in efforts to combat environmental pollution and climate change (41).

Application in biomedical fields

Chitosan's utility in the biomedical field is vast and varied, driven by its unique properties that include biodegradability, biocompatibility, and antimicrobial activity. Its applications span across drug delivery, tissue engineering, wound healing, and more, making it a critical material in modern medicine (39, 42).

Drug delivery and tissue engineering

Chitosan is extensively used in drug delivery systems due to its ability to protect drug molecules from the acidic environment of the stomach, facilitating targeted drug release. This property is crucial for administering medications for gastrointestinal, neurological, and chronic systemic diseases. Chitosan-based materials are also used in developing scaffolds for tissue engineering, mimicking the natural extracellular matrix which supports the growth and regeneration of tissues (42).

The development of chitosan-based materials continues to push the boundaries in drug delivery and material science. Chitosan-coated nanoparticles, for example, are utilized as efficient bio-imaging agents and in delivering anti-tumor agents like Paclitaxel, demonstrating the polymer's versatility and efficacy in medical applications (1). Additionally, the design of chitosan-based biomimetic materials, which mimic natural structures like lotus flowers and honeycomb, highlights the innovative approaches in enhancing material properties for specific applications (43). These advancements underscore chitosan's role in driving technological and medical innovations, further solidifying its importance in scientific research and industry applications.

Wound healing

In the realm of wound care, chitosan's hemostatic and antibacterial properties expedite the healing process, making it an invaluable component in wound dressings and antimicrobial coatings. The biopolymer is also employed in dental and orthopedic implants due to its ability to promote bone regeneration and reduce infection rates (38, 44). Chitosan's ability to accelerate wound healing has made it a subject of significant research. This wound-healing property stems from chitosan-based materials' capacity to: mobilize polymorphonuclear cells and fibroblasts, cause cytokines, facilitate migration of giant cells, and stimulate the formation of type IV collagen. Additionally, chitosan's susceptibility to degradation by enzymes like lysozyme in the body results in chito-oligomers, which stimulate macrophages and further accelerate collagen deposition, ultimately speeding up wound healing (45). Commercially accessible wound

dressings utilizing chitosan come in various forms, including non-wovens, hydrogels, films, and sponges (28, 46).

Biosensors and regenerative medicine

The development of chitosan-based biosensors illustrates the biopolymer's adaptability and effectiveness in medical diagnostics. These biosensors detect a wide array of substances, including glucose and cholesterol, essential for managing conditions like diabetes and cardiovascular diseases. Additionally, in regenerative medicine, chitosan is used to create innovative solutions such as bioimaging agents and cell encapsulation materials, which are fundamental in advanced therapeutic and diagnostic procedures (44).

Antimicrobial activity

Chitosan and its derivatives exhibit antibacterial activity against a wide range of microorganisms, such as bacteria, filamentous fungi, and yeast (47). The precise mechanism behind this antibacterial activity remains unclear. However, one offered mechanism suggests that chitosan disrupts cellular permeability, leading to leakage of intracellular components due to its interaction with the anionic components of the cell membrane, ultimately causing cell death. Another proposed mechanism involves chitosan penetrating the cell membrane and binding to DNA. This binding restrains DNA replication, ultimately leading to cell death (48). Several factors influence the antibacterial action of chitosan, including the degree of deacetylation, origin and level of polymerization, polymer viscosity, and particularly pH (49).

Chitosan has been suggested to operate on Gram-negative bacteria through two distinct mechanisms: chelation with divalent cations under acidic pH, diminishing membrane stability and nutrient uptake, and electrostatic interactions with lipopolysaccharides on the outer membrane, permitting chitosan to pass through the inner membrane and induce cell leakage (20, 50, 51). In contrast, the surface of Gram-positive bacteria is made up of peptidoglycans and teichoic acid, necessary for the function of various membrane-bound enzymes, ultimately leading to cell death (47, 52). The mechanism of chitosan's antifungal effect is similar to its antibacterial action and seems to be effective against fungi rich in polyunsaturated fatty acids (53).

Antioxidant activity

Chitosan and its derivatives exhibit potent antioxidant effects. They can reduce lipid oxidation by scavenging free radicals, due to their ability to bind metals. The antioxidant properties of chitosan and chitin are influenced by factors such as molecular weight, viscosity, and degree of deacetylation (DD). This free radical scavenging ability makes chitosan a potential therapeutic agent for oxidative stress and certain diseases (54).

Chitosan in nanomedicine

Chitosan nanoparticles hold significant promise in medical research as targeted delivery vehicles for drugs, adjuvants, and vaccines. They are particularly attractive as oral drug carriers for proteins because they can prevent enzymatic degradation in the gastrointestinal tract and facilitate muco-adhesion to the intestinal mucus layer (9, 55). This review highlights several applications of chitosan nanoparticles, including ocular-targeted drug delivery, delivery across the blood-brain barrier, targeted delivery of bioimaging markers, and vaccination by oral and intranasal application (56). Notably, a significant amount of research has been focused on chitosan nanoparticles in cancer medicine. These nanoparticles can encapsulate chemotherapeutic drugs, thereby reducing side effects, and can also increase the oral bioavailability of anti-cancer drugs (57).

Industrial and commercial applications

Chitosan's broad utility across various industries is underscored by its diverse applications ranging from agriculture to pharmaceu-

ticals and environmental sustainability. Its role in enhancing agricultural practices is particularly noteworthy, where it is used in the pre- and post-harvest treatments such as coating seeds, fruits, and vegetables to preserve them and improve their resistance to diseases and pests. Additionally, chitosan-based coatings are instrumental in the slow and sustained release of encapsulated agrochemicals, optimizing their effectiveness and reducing environmental impact (39).

Chitosan contributes significantly to the agriculture and food sectors. It is used in creating biopolymeric films for food packaging, which are favored for their biodegradability and the reduction of pollution in comparison to conventional materials (26, 58). Additionally, chitosan's properties as a natural biocide make it effective as a preservative, enhancing the shelf life and safety of food products. In agriculture, chitosan is applied for its ability to enhance plant growth and yield, making it a valuable component in sustainable farming practices (26).

In the pharmaceutical sector, chitosan contributes significantly to the production of various forms such as tablets and capsules. Its unique properties also make it a preferred material for drug delivery systems, enhancing the efficacy of pharmaceutical products by protecting active ingredients and controlling their release within the body. Moreover, chitosan's biocompatibility and non-toxic nature have paved its way into the food industry, where it is utilized as a food additive, preservative, and packaging material, contributing to food safety and longevity (1).

The table below summarizes the key applications of chitosan across different industries:

Industry	Applications of Chitosan
Agriculture	Seed coating, plant growth regulation, controlled release fertilizers
Pharmaceuticals	Production of tablets and capsules, drug delivery systems
Food	Additives, preservatives, packaging materials
Cosmetics	Skincare and haircare products
Textile and Paper	Sizing, finishing, wastewater treatment
Energy	Dye-sensitized solar cells, wastewater treatment

These applications not only highlight chitosan's versatility but also its contribution to sustainable practices across various sectors (1, 27). The most significant properties and recent applications of chitosan are highlighted in Figure 5.
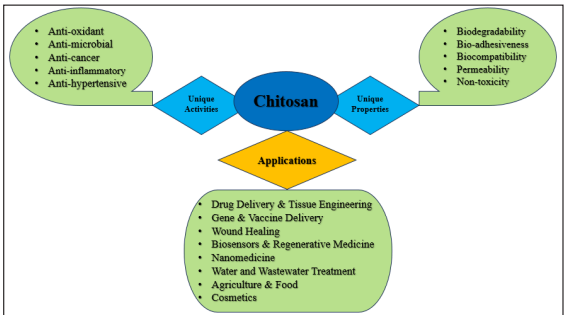

Figure 5. Unique Activities, Properties and Different applications of chitosan.

Recent advances in chitosan research

Technological enhancements and gene modification

Recent developments in chitosan research have focused on leveraging gene modification techniques to enhance the yield and functional properties of chitosan. This approach has opened new avenues for increasing the efficiency of chitosan production, which is crucial for its application across various industries. Technological advancements in genetic engineering provide a pathway to optimize the structural attributes of chitosan, thereby enhancing its solubility, biocompatibility, and overall effectiveness in industrial applications (2).

Biological properties and applications of chitosan

Breakthroughs in therapeutic applications and drug delivery

The potential of chitosan in therapeutic applications continues to grow with recent studies highlighting its efficacy in drug delivery systems. Research has shown that chitosan and its derivatives can be engineered to improve their therapeutic effects, offering targeted and controlled drug release mechanisms. These advancements are particularly significant in the development of non-invasive delivery systems for biologically active molecules, which can dramatically improve patient compliance and treatment outcomes (59).

Sustainable production and future directions

Combining traditional, biological, and alternative methods has proven to be the most effective strategy for the sustainable production of chitosan. This approach not only ensures high yields but also maintains the quality of chitosan, which is crucial for its application in various environmental and biomedical fields. The ongoing research and increasing number of publications related to chitosan highlight its growing importance and continuous development in sustainable practices (41).

Challenges and limitations

Chitosan, despite its widespread applications and benefits, faces several challenges and limitations that can impede its utility across various fields. These challenges stem primarily from its production process, physical and chemical properties, and the variability in its biological performance.

Production and standardization issues

Source and cost limitations: The primary raw materials for chitosan production are seasonal and localized, which can lead to supply inconsistencies and high production costs (60).

Extraction challenges: The extraction of chitosan is not only time-consuming but also cost-ly, involving the use of harsh chemicals that can impact the environment (2).

Quality variability: Due to differences in the source and extraction methods, the quality of chitosan can vary significantly, which affects its reliability in various applications (60).

Lack of standardization: There is a notable lack of standardization in the production and quality control of chitosan, making it difficult to ensure consistent performance across different batches and products (60).

Physical and chemical property variability

Solubility Issues: Chitosan's solubility is highly pH-dependent and it shows poor solubility in neutral and basic media, limiting its use in various applications (27).

Property Variations: The physical and chemical properties of chitosan, such as molecular weight and degree of deacetylation, can vary greatly. These variations can significantly impact its performance, further complicating the standardization of chitosan products (61).

Biological performance and safety concerns

Mechanisms of action: There is a limited understanding of the mechanisms by which chitosan interacts with cells and tissues, which can hinder its application in biomedicine and other fields (61).

Immunogenicity and toxicity: Although chitosan is generally considered safe, there are concerns regarding its potential immunogenicity and toxicity in some applications, which necessitate further studies to clarify these aspects (61).

Disputed biological properties: Some of the claimed biological properties of chitosan, such as its antimicrobial and biodegradability characteristics, are disputed, indicating a need for more comprehensive research to validate these properties (22).

These challenges underscore the ne-

cessity for ongoing research and technological improvements to enhance the yield, standardization, and application of chitosan, ensuring its sustainable and effective use in the future (2). This comprehensive analysis not only highlights the innovative uses of chitosan in emerging fields but also sets the stage for addressing the key challenges that lie ahead in fully realizing the potential of chitosan in both environmental and biomedical sectors.

Conclusion and future perspectives

Having traversed the expansive landscape of chitosan from its historical roots to its modern applications, one can appreciate the significant strides made in understanding and utilizing this versatile biopolymer. Its unique chemical structure facilitates a myriad of applications across various fields, especially in biomedical and environmental sectors, underscoring its potential to address contemporary challenges in sustainability and healthcare. The exploration of chitosan's properties, modifications, and the breadth of its applications reinforces its status as a material of crucial interest, poised for further innovation and wider adoption in the pursuit of a greener and more sustainable future.

Yet, as we delve into the future prospects of chitosan, it's evident that overcoming existing challenges related to production, standardization, and biological performance is paramount to unlocking its full potential. The call for further research and technological advancements is clear, aimed at enhancing chitosan's yield, functionality, and application efficiency. In drawing together the threads of chitosan's story, from historical curiosity to a beacon of biopolymer innovation, we are reminded of the continual need for inquiry, adaptation, and application of science for the betterment of society and the environment.

References

1. Thambiliyagodage C, Jayanetti M, Mendis A, Ekanayake G, Liyanaarachchi H, Vigneswaran S. (2023). Recent advances in chitosan-based applications—a review. Materials, 16(5):2073.

2. Alemu D, Getachew E, Mondal AK. (2023). Study on the Physicochemical Properties of Chitosan and their Applications in the Biomedical Sector. Int J Polym Sci, 2023(5):1-13.

3. Chauhan S, Das S, Baig FAH, Qadri SSH. (2022). APPLICATIONS OF CHITOSAN IN DENTISTRY-A REVIEW ARTICLE. J Pharm Negat Results, 13(10):1359-64.

4. Riaz Rajoka MS, Zhao L, Mehwish HM, Wu Y, Mahmood S. (2019). Chitosan and its derivatives: synthesis, biotechnological applications, and future challenges. Appl Microbiol Biotechnol 103:1557-71.

5. Madhumathi K, Sudheesh Kumar P, Abhilash S, Sreeja V, Tamura H, Manzoor K, Nair S, Jayakumar R. (2010). Development of novel chitin/nanosilver composite scaffolds for wound dressing applications. J Mater Sci: Mater Med, 21:807-13.

6. Zhang W, Zhang J, Jiang Q, Xia W. (2013). The hypolipidemic activity of chitosan nanopowder prepared by ultrafine milling. Carbohydr Polym, 95(1):487-91.

7. Minet EP, O'Carroll C, Rooney D, Breslin

C, McCarthy C, Gallagher L, Richards K. (2013). Slow delivery of a nitrification inhibitor (dicyandiamide) to soil using a biodegradable hydrogel of chitosan. Chemosphere, 93(11):2854-8.

8. Gomaa YA, El-Khordagui LK, Boraei NA, Darwish IA. (2010). Chitosan microparticles incorporating a hydrophilic sunscreen agent. Carbohydr Polym, 81(2):234-42.

9. Azmana M, Mahmood S, Hilles AR, Rahman A, Arifin MAB, Ahmed S. (2021). A review on chitosan and chitosan-based bionanocomposites: Promising material for combatting global issues and its applications. Int J Biol Macromol, 185:832-48.

10. Morin-Crini N, Lichtfouse E, Torri G, Crini G. Fundamentals and applications of chitosan. Sustainable agriculture reviews 35: chitin and chitosan: history, fundamentals and innovations2019. p. 49-123.

11. Yadollahi M, Farhoudian S, Namazi H. (2015). One-pot synthesis of antibacterial chitosan/silver bio-nanocomposite hydrogel beads as drug delivery systems. Int J Biol Macromol, 79:37-43.

12. Pacheco N, Garnica-Gonzalez M, Gimeno M, Bárzana E, Trombotto S, David L, Shirai K. (2011). Structural characterization of chitin and chitosan obtained by biological and chemical methods. Biomacromolecules, 12(9):3285-90.

13. Yen M-T, Yang J-H, Mau J-L. (2009). Physicochemical characterization of chitin and chitosan from crab shells. Carbohydr Polym, 75(1):15-21.

14. Badawy RM, Mohamed HI. (2015). Chitin extration, composition of different six insect species and their comparable characteristics with that of the shrimp. J Am Sci, 11(6):127-34.

15. Kaya M, Erdogan S, Mol A, Baran T. (2015). Comparison of chitin structures isolated from seven Orthoptera species. Int J Biol Macromol, 72:797-805.

16. Luo Q, Wang Y, Han Q, Ji L, Zhang H, Fei Z, Wang Y. (2019). Comparison of the physicochemical, rheological, and morphologic properties of chitosan from four insects. Carbohydr Polym, 209:266-75.

17. Shin C-S, Kim D-Y, Shin W-S. (2019). Characterization of chitosan extracted from Mealworm Beetle (Tenebrio molitor, Zophobas morio) and Rhinoceros Beetle (Allomyrina dichotoma) and their antibacterial activities. Int J Biol Macromol, 125:72-7.

18. Kaya M, Baran T, Mentes A, Asaroglu M, Sezen G, Tozak KO. (2014). Extraction and characterization of α-chitin and chitosan from six different aquatic invertebrates. Food Biophys, 9(2):145-57.

19. Chang AKT, Frias Jr RR, Alvarez LV, Bigol UG, Guzman JPMD. (2019). Comparative antibacterial activity of commercial chitosan and chitosan extracted from Auricularia sp. Biocatal Agric Biotechnol, 17:189-95.

20. Cheraghi E, Kababian M, Moradi-Asl E, Bafrouyi SMM, Saghafipour A. (2022). Structure and Antibacterial Activity of Chitosan from the American Cockroach, the German Cockroach and the Mealworm Beetle. Journal of Arthropod-Borne Diseases, 16(4):325-39.

21. Kaya M, Baran T. (2015). Description of a new surface morphology for chitin extracted from wings of cockroach (Periplaneta americana). Int J Biol Macromol, 75:7-12.

22. Aranaz I, Alcántara AR, Civera MC, Arias C, Elorza B, Heras Caballero A, Acosta N. (2021). Chitosan: An overview of its properties and applications. Polymers, 13(19):3256.

23. Crini G. (2019). Historical review on chitin and chitosan biopolymers. Environ Chem

Lett, 17(4):1623-43.

24. Qin Z, Zhao L. The history of chito/chitin oligosaccharides and its monomer. Oligosaccharides of Chitin and Chitosan: bio-manufacture and applications2019. p. 3-14.

25. Crini G. Historical landmarks in the discovery of chitin. Sustainable Agriculture Reviews 35: Chitin and Chitosan: History, Fundamentals and Innovations2019. p. 1-47.

26. Maliki S, Sharma G, Kumar A, Moral-Zamorano M, Moradi O, Baselga J, Stadler FJ, García-Peñas A. (2022). Chitosan as a tool for sustainable development: A mini review. Polymers, 14(7):1475.

27. Yadav M, Kaushik B, Rao GK, Srivastava CM, Vaya D. (2023). Advances and challenges in the use of chitosan and its derivatives in biomedical fields: A Review. Carbohydr Polym Technol Appl:100323.

28. Zhao D, Yu S, Sun B, Gao S, Guo S, Zhao K. (2018). Biomedical applications of chitosan and its derivative nanoparticles. Polymers, 10(4):462.

29. Fatima B. Quantitative Analysis by IR: Determination of Chitin/Chitosan DD. Modern spectroscopic techniques and applications. 1072020.

30. Chattopadhyay D, Inamdar MS. (2010). Aqueous behaviour of chitosan. Int J Polym Sci, 2010:939536.

31. Fenice M, Gorrasi S. (2021). Advances in chitin and chitosan science. Molecules, 26(6):1805.

32. Ogawa K. (2000). Crystalline behavior of chitosan. Molecules: Advances in Chitin Science, 4:324-9.

33. Kawada J, Yui T, Okuyama K, Ogawa K. (2001). Crystalline behavior of chitosan organic acid salts. Biosci Biotechnol Biochem, 65(11):2542-7.

34. Wang W, Meng Q, Li Q, Liu J, Zhou M, Jin Z, Zhao K. (2020). Chitosan derivatives and their application in biomedicine. Int J Mol Sci, 21(2):487.

35. Chen Q, Qi Y, Jiang Y, Quan W, Luo H, Wu K, Li S, Ouyang Q. (2022). Progress in research of chitosan chemical modification technologies and their applications. Mar Drugs, 20(8):536.

36. Iber BT, Kasan NA, Torsabo D, Omuwa JW. (2022). A review of various sources of chitin and chitosan in nature. J Renew Mater, 10(4):1097.

37. Hahn T, Roth A, Ji R, Schmitt E, Zibek S. (2020). Chitosan production with larval exoskeletons derived from the insect protein production. J Biotech, 310:62-7.

38. Hameed AZ, Raj SA, Kandasamy J, Baghdadi MA, Shahzad MA. (2022). Chitosan: a sustainable material for multifarious applications. Polymers, 14(12):2335.

39. Merzendorfer H, Cohen E. Chitin/chitosan: versatile ecological, industrial, and biomedical applications. Extracellular Sugar-Based Biopolymers Matrices2019. p. 541-624.

40. Matica A, Menghiu G, Ostafe V. (2017). Biodegradability of chitosan based products. New Front Chem, 26(1).

41. Lam WS, Lam WH, Lee PF. (2023). The Studies on Chitosan for Sustainable Development: A Bibliometric Analysis. Materials, 16(7):2857.

42. Ojeda-Hernández DD, Canales-Aguirre AA, Matias-Guiu J, Gomez-Pinedo U, Mateos-Díaz JC. (2020). Potential of chitosan and its derivatives for biomedical applications in the central nervous system. Front Bioeng Biotechnol, 8:389.

43. Piekarska K, Sikora M, Owczarek M,

Jóźwik-Pruska J, Wiśniewska-Wrona M. (2023). Chitin and chitosan as polymers of the future—obtaining, modification, life cycle assessment and main directions of application. Polymers, 15(4):793.

44. Budiarso IJ, Rini ND, Tsalsabila A, Birowosu-to MD, Wibowo A. (2023). Chitosan-based smart biomaterials for biomedical applications: Progress and perspectives. ACS Biomater Sci Eng, 9(6):3084-115.

45. Araújo D, Ferreira IC, Torres CA, Neves L, Freitas F. (2020). Chitinous polymers: extraction from fungal sources, characterization and processing towards value‑added applications. J Chem Technol Biotechnol, 95(5):1277-89.

46. Sharma S, Bhende M, Goel A. (2024). A review: polysaccharide-based hydrogels and their biomedical applications. Polym Bull:1-22.

47. Mondal A, Dhar AK, Banerjee S, Hasnain MS, Nayak AK. Antimicrobial uses of chitosan. Chitosan in Biomedical Applications: Elsevier; 2022. p. 13-36.

48. Kravanja G, Primožič M, Knez Ž, Leitgeb M. (2019). Chitosan-based (Nano) materials for novel biomedical applications. Molecules, 24(10):1960.

49. Gahruie HH, Niakousari M. (2017). Antioxidant, antimicrobial, cell viability and enzymatic inhibitory of antioxidant polymers as biological macromolecules. Int J Biol Macromol, 104:606-17.

50. Basseri H, Bakhtiyari R, Hashemi SJ, Baniardelani M, Shahraki H, Hosainpour L. (2019). Antibacterial/antifungal activity of extracted chitosan from American cockroach (Dictyoptera: Blattidae) and German cockroach (Blattodea: Blattellidae). J Med Entomol, 56(5):1208-14.

51. Kababian M, Cheraghi E, Asl EM, Saghafipour A, Nabizadeh Z. (2024). COMPARATIVE STUDY OF PHYSIOCHEMICAL AND ANTIMICROBIAL PROPERTIES OF ADULT COCKROACHES-EXTRACTED CHITOSAN. J Appl Biol Sci, 18(1):94-105.

52. Omura Y, Shigemoto M, Akiyama T, Saimoto H, Shigemasa Y, Nakamura I, Tsuchido T. (2003). Antimicrobial activity of chitosan with different degrees of acetylation and molecular weights. Biocontrol Sci, 8(1):25-30.

53. Kabanov VL, Novinyuk LV. (2020). Chitosan application in food technology: A review of rescent advances. Food Syst, 3(1):10-5.

54. Ivanova DG, Yaneva ZL. (2020). Antioxidant properties and redox-modulating activity of chitosan and its derivatives: Biomaterials with application in cancer therapy. BioResearch open access, 9(1):64-72.

55. Reshad RAI, Jishan TA, Chowdhury NN. (2021). Chitosan and its broad applications: A brief review. Available at SSRN 3842055.

56. Frigaard J, Jensen JL, Galtung HK, Hiorth M. (2022). The potential of chitosan in nanomedicine: An overview of the cytotoxicity of chitosan based nanoparticles. Front Pharmacol, 13:880377.

57. Khan MM, Madni A, Torchilin V, Filipczak N, Pan J, Tahir N, Shah H. (2019). Lipid-chitosan hybrid nanoparticles for controlled delivery of cisplatin. Drug Deliv, 26(1):765-72.

58. Shahbaz U, Basharat S, Javed U, Bibi A, Yu XB. (2023). Chitosan: A multipurpose polymer in food industry. Polym Bull, 80(4):3547-69.

59. Xia Y, Wang D, Liu D, Su J, Jin Y, Wang D, Han B, Jiang Z, Liu B. (2022). Applications of chitosan and its derivatives in skin and soft tissue diseases. Front Bioeng Biotechnol, 10:894667.

60. Mujeeb A, Miller AF. Peptide Bionanomaterials Global Market: The Future of Emerging Industry. Peptide Bionanomaterials: From Design to Application: Springer; 2023. p. 539-55.

61. Yu J, Wang D, Geetha N, Khawar KM, Jogaiah S, Mujtaba M. (2021). Current trends and challenges in the synthesis and applications of chitosan-based nanocomposites for plants: A review. Carbohydr Polym, 261:117904.